BUILDING INTEGRATED WIND ENERGY

A thesis submitted to The University of Manchester for the degree of
Doctor of Philosophy
in the Faculty of Engineering and Physical Science

2013

Jialin Wang

School of Mechanical, Aerospace and Civil Engineering

List of Contents

Final Word Count: 39,812

List of Figures

List of Tables

List of Symbols

a	induction factor	-
A	Weibull scale parameter	m/s
A_0	entrance area of control volume	m^2
A_C	cup swept area	m^2
Ae	exit area of control volume	m^2
A_H	horizontal area per roughness element	m^2
A_t	turbine rotor swept area	m^2
B_H	fraction of the total area occupied by roughness element	-
C_d	drag coefficient	-
C_P	conversion efficiency	-
d	displacement height	m
$\bar{d}$	mean difference	-
D_t	rotor diameter	m
E	wind power density	W/m^2
E_r	voltage record	$Volt$
f	frequency	-
f_e	eigen-frequency	Hz
f_{dir}	annual frequency of direction	-
f_{vel}	annual frequency of velocity	-
F_t	thrust force of a wind turbine	N
$F(u)$	cumulative Weibull distribution	-
g	length of gap in Hybrid-driven turbine	m
G_{ke}	the generation of turbulence kinetic energy due to the mean velocity gradients	-
h	height of the position at near building sites	m
h_b	internal boundary layer height	m
$h(u)$	failure rate of cumulative Weibull distribution	-
H	height of the roughness element (building or obstacle)	m
$\bar{H}$	average building height	m
I	turbulence intensity	-
I_{dir}	turbulence intensity in directions	-
k	Weibull shape parameter	-
k_e	turbulent kinetic energy	m^2/s^2
K	von Karman constant	-
l	distance between wind break	m
L	likelihood function	-
L_P	sound pressure level	dB
L_W	sound power level	dB
n	induced vibration	Hz
p	power per square meter	W/m^2
P	power in the wind	W
P_m	mechanical power at rotor axis	W
P_{obs}	porosity of the obstacle	-
Q	rotor torque	Nm
r	record	-

R_t	rotor radius	*m*
Re	Re number	-
R_1,R_2	empirical parameter for near obstacle position	-
S	cross-section facing the wind	m^2
T	time	*s*
u	instantaneous wind velocity	*m/s*
u_0	wind velocity at entrance of control volume	*m/s*
u_{cor}	mean wind velocity affected by shelter	*m/s*
u_e	wind velocity at exit of control volume	*m/s*
u_*	friction velocity	*m/s*
u'	turbulence velocity fluctuations	*m/s*
$\bar{u}$	mean velocity of wind	*m/s*
W_{vel}	energy output of each mean velocity	*W*
x	horizontal distance from obstacle to site	*m*
z	vertical distance from ground	*m*
z_0	roughness height	*m*

Subscripts

0	entrance of control volume
500	500 m height from ground
b	boundary layer
c	CFD results or cup
cou	country
CFD	CFD model
d	double-rotor part
dir	direction
e	exit of control volume
H	horizontal
i,j,k	one of the three axis directions of Cartesian coordinates
m	model
max	maximum
min	minimum
obs	obstacle
p	full-scale
P	pressure
r	record
ref	reference
rms	root mean square
t	turbine rotor or time
TUN	Tunnel model
vel	velocity
W	power
x	x-direction of Cartesian coordinates
y	y-direction of Cartesian coordinates
z	z-direction of Cartesian coordinates

Greek

α	exponent of power-law	-
δ	boundary layer thickness	m
$\delta_{i,j}$	Kronecker delta	-
ε	turbulent dissipation rate	m^2/s^3
θ	unknown parameter in probability density function	
λ	wind tunnel scale	-
ρ	density of air	kg/m^3
τ_{dir}	time scale of wind direction	s
τ_t	time scale of steam tube	s
τ_{turb}	time scale between average building height and velocity	s
μ	dynamic viscosity of the air	Ns/m^2
μ_t	turbulent viscosity	-
ω	angular velocity	rad/s

Building Integrated Wind energy

A thesis submitted to The University of Manchester for the degree of Doctor of Philosophy

Jialin Wang

2013

Abstract

In considering methods of reducing the emission of carbon dioxide; there is a growing interest for use of wind power at domestic building in U.K. But the technology of wind turbines development in building environment is more complicated than in open areas. Small wind turbines in suburban areas have been reported as having unsatisfactory energy output, but it is not clear whether this is due to insufficient wind resource or low turbine efficiency. The aim of this research is to discover whether the wind resource in suburban areas is large enough for small wind turbines to produce a useful energy output.

Historical wind data and manufacturers' turbine characteristics were used to estimate the hourly wind speed and energy output for different U.K. cities, terrain zones and turbines. It was found that for turbines at 10 m height in suburban areas and depending on city, the annual wind energy conversion efficiency ranged from about 20 to 40 %, while the number of turbines required to produce the annual average electricity consumption of a UK dwelling ranged from about 6 for the smallest turbine (5.3 m^2 rotor area) to about 1 for the largest (35.26 m^2 rotor area).

This analysis was based on average conditions, but the wind speed near buildings can vary considerably from one point to another. In order to predict the performance of wind turbines more accurately, the atmospheric boundary layer (ABL) of suburban areas was simulated in both CFD and wind tunnel models, and models of groups of semi-detached and terraced houses were set in this ABL. It was found that at 10 m height in the area of the houses, the turbulence intensity was too high for satisfactory operation of wind turbines (19 to 35 %) while the mean velocity at different points ranged from 86 to 108 % of the 10 m reference velocity. At 30 m height the turbulence intensity was satisfactory (less than 19 %), while the mean velocity ranged from 92 to 103 % of the 30 m reference velocity. It is concluded that for wind turbines in suburban areas, at 10 m height the wind speed is too low and the turbulence is too high for satisfactory performance, while at 30 m height the wind speed is much higher and the turbulence is low enough.

Keywords: urban flow characteristics, building environment, wind velocity, wind turbulence, CFD model, wind tunnel, AEP

Declaration

No portion of the work referred to in the thesis has been submitted in support of an application for another degree or qualification of this or any other university or other institute of learning.

Copyright Statement

i. The author of this thesis (including any appendices and/or schedules to this thesis) owns certain copyright or related rights in it (the "Copyright") and he has given The University of Manchester certain rights to use such Copyright, including for administrative purposes.

ii. Copies of this thesis, either in full or in extracts and whether in hard or electronic copy, may be made **only** in accordance with the Copyright, Designs and Patents Act 1988 (as amended) and regulations issued under it or, where appropriate, in accordance with licensing agreements which the University has from time to time. This page must form part of any such copies made.

iii. The ownership of certain Copyright, patents, designs, trademarks and other intellectual property (the "Intellectual Property") and any reproductions of copyright works in the thesis, for example graphs and tables ("Reproductions"), which may be described in this thesis, may not be owned by the author and may be owned by third parties. Such Intellectual Property and Reproductions cannot and must not be made available for use without the prior written permission of the owner(s) of the relevant Intellectual Property and/or Reproductions.

iv. Further information on the conditions under which disclosure, publication and commercialisation of this thesis, the Copyright and any Intellectual Property and/or Reproductions described in it may take place is available in the University IP Policy (see http://documents.manchester.ac.uk/DocuInfo.aspx?DocID=487), in any relevant Thesis restriction declarations deposited in the University Library, The University Library's regulations (see http://www.manchester.ac.uk/library/aboutus/regulations) and in The University's policy on Presentation of Theses

Acknowledgements

I would like to take this opportunity to express my gratitude to all who have helped me in the preparation of this thesis.

First of all I would like to acknowledge my parents, Yiduo Wang and Ying Xu, who have been very supportive throughout my life, especially these years in England.

I would like to gratefully acknowledge the discussions, comments and contributions made by my supervisors: Dr Jonathan Dewsbury and Professor Nickolas Jenkins, whose genuine passion for science is apparent to anybody fortunate enough to have them as teachers; I feel so lucky to have the opportunity to work with them these past years and I sincerely thanks for everything they have done for me. This dissertation would not have been possible without their kindly guidance.

Additionally I would like to thanks the people who helped me during my research time. Dr Tony Sung and Dr John B. Parkinson who helped me collecting the weather data; Mr Lee Ashton and Mr Paul Townsend who produced the house models for my experiment; and special thanks Dr Andrew Kennaugh, Mr Michael Carroll, Mr Mahyar Mahmoodilari who help me a lot during period of my wind tunnel experiments.

Finally and most importantly, I would like to thank Zhidi Du, my beloved wife, for all the support, assistant, advice and encouragement she exuded during this project. The past six years with you have been truly magical. You enrich my life and make me genuinely happy. This thesis is dedicated to you; I love you with all my heart.

CHAPTER 1

1 Introduction

In modern times, the greenhouse effect [1] is one of the most harmful environmental worldwide problems. In order to reduce the emission of carbon dioxide (CO2), which is the main greenhouse gas, and also to conserve energy, the U.K. government announced plans to reduce emissions in the household sector in December 2006. The zero-carbon homes plan is one of the new housing regulations. The Government's ambition is that, by 2016 all new homes will be 'zero-carbon', meeting the highest Code standard for energy efficiency [2]. To encourage this, in the Budget 2007 [3], the government announced a time-limited stamp duty exemption for the vast majority of new zero-carbon homes.

The zero-carbon building is also known as zero energy building (ZEB) or net-zero emissions building. One definition is: "A net-zero emissions building exports at least as much emissions-free renewable energy as it uses from emissions-producing energy sources" [4]. Obviously, it is impossible to rebuild all current buildings to be ZEB; a possible way to improve current buildings is to add some renewable energy systems into the buildings. This leads to two questions: which kinds of renewable energy sources could be used? And which building types should be considered

1.1 Climate of the United Kingdom

In order to find the renewable sources buildings could use to produce energy, the environment near the building should be considered. For current technology, the main renewable energy sources and their equipment are list as below:

- Water energy: hydro turbines
- Biomass energy: combustion or fuel cell
- Wind energy: wind turbines
- Solar energy: photovoltaic system, solar heating system
- Tide energy: tide turbines
- Wave energy: various mechanical to electrical devices.

Of the above sources, water, biomass, tide and wave are resources that are not available on sites for most building. Only wind and solar is feasible for most buildings to produce energy for themselves. As the power of these two sources has a close relationship with weather, the climate character of this country should be considered.

The climate characters of the U.K. cities could be found from the weather record. As the mainly possible renewable sources could be used are solar energy and wind energy, the sunshine and winds in some countries are reviewed below.

1.1.1 Sunshine

The cities in Great Britain do not have lots of sunshine compared with some important cities in other countries, **Table 1-1** shows the average annual sunshine hours of some important cities in world. Of all the area of United Kingdom, from 1971 to 2000, the average total sunshine is 1339.7 hours per year; this number is less than 30% of the maximum possible (approximately 4476 hours) [5]. The sunshine has different distributions for different geographical sites and seasons: the south and east counties have more sunshine than north and west; while the sunshine time in midyear (from April to September) is much longer than the rest months (from October to March).

Table 1-1 annual average sunshine hours of world cities [5]

city	New York	Los Angeles	London	Paris	Beijing	Tokyo	Mumbai	Sydney
Sunshine hours	2600	3200	1600	2100	2600	1600	3000	2300

For example, the annual average total sunshine hour is 1,750 for the countries of Dorset, Hampshire, Sussex and Kent in the south coast of England. This is a much large number than the number in northern and western counties; in some counties the average total sunshine hours are even less than 1,000. **Table 1-2** shows the four country average totals sunshine hours.

Table 1-2 country average total sunshine hours in U.K., 1971-2000 [5]

Country	Average total sunshine hours from 1971 to 2000 Month												Year
	Jan	**Feb**	**Mar**	**Apr**	**May**	**Jun**	**Jul**	**Aug**	**Sep**	**Oct**	**Nov**	**Dec**	
England	50.5	67.7	102.5	145.2	189.9	179.4	192.8	184.1	135.0	101.3	65.2	43.9	**1457.4**
Northern Ireland	41.0	60.1	90.0	140.8	175.9	150.9	139.6	138.0	113.1	85.5	52.8	31.9	**1219.7**
Scotland	30.8	58.1	87.6	128.2	173.2	153.2	145.0	137.5	104.4	74.5	43.2	24.7	**1160.4**
Wales	42.8	63.4	94.2	148.0	186.8	167.0	181.8	168.7	125.8	90.4	54.9	35.4	**1359.3**

From the data in the table above, for all the countries in U.K., England has the most sunshine. And different from the other three countries, the sunniest month in England is July; while for the other countries, May has the most sunshine.

The reason for these sunshine differences is the formation of cloud, mist and fog. Generally, cloud is made of vapor from the ocean; when vapor moves to the land, the cloud is made. However, as the prevailing wind in U.K. is from the south-west, the vapor is blow away from the south coast of England before it forms cloud. But the mountains and valley areas in north England, Scotland and Wales stop the vapor and bring cloud, fog and mist to these areas. In spring the sea is still cold, which made less evaporation than in summer, therefore there is less cloud. From March to June, sea fog may develop near the coast, while radiation fog develops in inland areas of U.K. from December to February. All these weather makes U.K. a less sunshine country [6].

1.1.2 Winds

The atmosphere could be considered as a large-scale circulation pattern system, wind is a main part of this system. Basically, this system is driven by the temperature differences between poles and tropics, the temperature differences between oceans

and land, and also by the planet's rotation. The wind follows some general rules, introduced below [7]:

- The higher up wind has a higher velocity than the wind near the ground; the wind on the ocean is stronger than on the land; the friction between the wind and the ground can explain all these differences.
- For diurnal variation, the wind near the ground is less strong in the night than in the daytime. This is because during the daytime, the sunlight heats the ground and lower layers air which therefore leads to rise, while during the night the ground and air are cooled. This rule only limits the wind below about 50 m from the ground, this is because the effect of heated ground decreases with the height from the ground, when the height is more than about 50 m, the ground heat will not affect the air flow.
- Obstacles will interrupt the wind and make turbulence in some considerable distance around the obstacles.
- The areas of high elevation have stronger wind than the low elevations areas.

Figure 1-1 is from the European Wind Atlas [8]; this map shows the mean wind velocity at 50 m height above the ground in Europe with 5 classes. From this map, it could be seen that compared with the other countries in Europe, U.K. has the largest wind energy source: as the wind class in this country is from C to E, this is quite high than the other countries.

The United Kingdom often experiences strong wind because it's geographical locality. This country is between the North Atlantic Ocean and the North Sea, and the latitude of this country is high. The prevailing wind in this country is from the south-west. Generally, in the counties near western coasts and exposed headlands, wind is stronger than the inland areas. The wind with velocities of 51 to 101 km/h is defined as gales. And Hebrides in west of Scotland has an average 35 days of gale a year while most other parts of U.K. receives less than 5 days [5].

Based on the above information, compared with other European countries, the United Kingdom is a less sunny and windier country. In this country, wind source could be

more widely used than the other renewable energy. Because of this, this research focuses on the analysis and application of wind source around U.K. buildings.

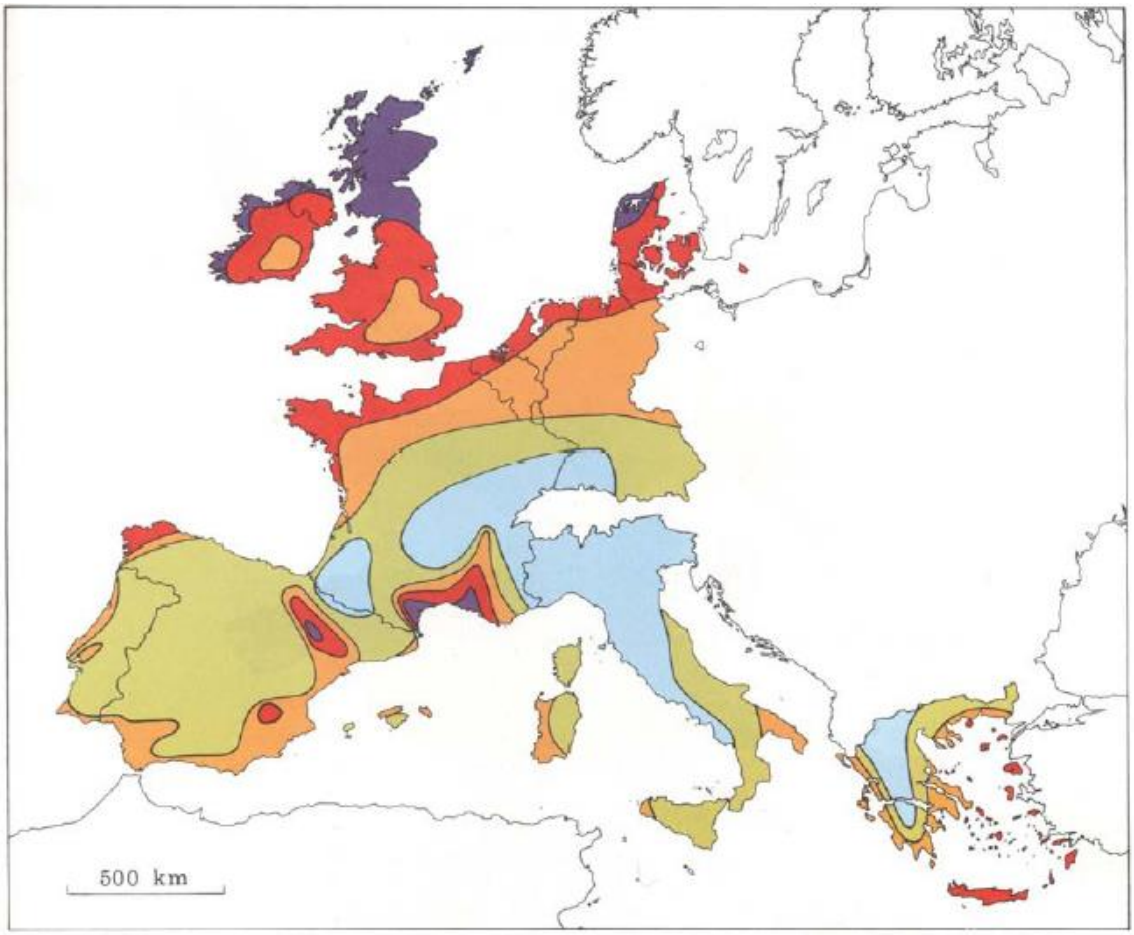

Wind resources[1] at 50 metres above ground level for five different topographic conditions

Wind Class	Sheltered terrain[2]		Open plain[3]		At a sea coast[4]		Open sea[5]		Hills and ridges[6]	
	m s^{-1}	Wm^{-2}	m s^{-1}	Wm^{-2}	m s^{-1}	Wm^{-2}	m s^{-1}	Wm^{-2}	m s^{-1}	Wm^{-2}
E	> 6.0	> 250	> 7.5	> 500	> 8.5	> 700	> 9.0	> 800	> 11.5	> 1800
D	5.0-6.0	150-250	6.5-7.5	300-500	7.0-8.5	400-700	8.0-9.0	600-800	10.0-11.5	1200-1800
C	4.5-5.0	100-150	5.5-6.5	200-300	6.0-7.0	250-400	7.0-8.0	400-600	8.5-10.0	700-1200
B	3.5-4.5	50-100	4.5-5.5	100-200	5.0-6.0	150-250	5.5-7.0	200-400	7.0-8.5	400-700
A	< 3.5	< 50	< 4.5	< 100	< 5.0	< 150	< 5.5	< 200	< 7.0	< 400

1. The resources refer to the power present in the wind. A wind turbine can utilize between 20 and 30% of the available resource. The resources are calculated for an air density of 1.23 kg m^{-3}, corresponding to standard sea level pressure and a temperature of 15°C. Air density decreases with height but up to 1000 m a.s.l. the resulting reduction of the power densities is less than 10%.
2. Urban districts, forest and farm land with many windbreaks (roughness class 3).
3. Open landscapes with few windbreaks (roughness class 1). In general, the most favourable inland sites on level land are found here.
4. The classes pertain to a straight coastline, a uniform wind rose and a land surface with few windbreaks (roughness class 1). Resources will be higher, and closer to open sea values, if winds from the sea occur more frequently, i.e. the wind rose is not uniform and/or the land protrudes into the sea. Conversely, resources will generally be smaller, and closer to land values, if winds from land occur more frequently.
5. More than 10 km offshore (roughness class 0).
6. The classes correspond to 50% overspeeding and were calculated for a site on the summit of a single axisymmetric hill with a height of 400 metres and a base diameter of 4 km. The overspeeding depends on the height, length and specific setting of the hill.

Figure 1-1 European mean wind velocity at 50 m [8]

1.2 Buildings in the United Kingdom

In order to find out which kind of building could make good use of wind energy, the energy consumption in buildings and building types should be considered. This section introduces the buildings in U.K. in these two ways.

1.2.1 Energy consumption in buildings

The building energy consumption can be separated into several systems. Of all these systems, some consume energy in high level while others consume energy in low level. It is not possible to include all energy consumption systems here, only the significant systems are discussed.

The major building energy consumption systems include:

- Lighting system
- Space temperature system: include radiator and air-condition
- Hot water system
- Kitchen heating system: include kitchen range, microwave oven, oven, etc.
- Home appliance system: include television, washing machine, refrigerator, etc.
- Office appliance system: include computer and other IT
- Motor systems: include fans and pumps
- Lift system: include lifts and escalators
- Security system: include fire alarm, CCTV, etc.
- Industry process system
- Laboratory equipment

As solar and wind energy are consider to provide energy for buildings, solar water heating could be used for hot water and space temperature system, while wind turbine and photovoltaic system could produce electricity for most energy consumption systems.

Of all the systems above, security system and laboratory equipment cost less energy than the other systems [9]. But undoubtedly, not all the buildings have the same energy distributions of the above systems. The system consumes large energy in one building might be a small consumer in another building. And these differences have a connection with the purpose of the buildings. Generally, there are four kinds of buildings: domestic, commercial, public and industrial.

1.2.1.1 Domestic building

The domestic building is the building for people to live in. For such building, the main energy consumers include: space temperature system, hot water system, kitchen heating system, lighting system, and home appliance system. The space and water heating consume most of the energy [9]. As DU.K.ES 2011 [9] shows, in the year 2010, 30% of the total U.K. energy is consumed by such kind of building.

1.2.1.2 Commercial building

Commercial building includes offices, emporiums, hotels, etc. The main energy consumers of such building include: lighting system, office appliance system, lift system, hot water system and security system [9]. Compared with the domestic building, this kind of building cost less energy for heating, and cost more for lighting and office appliance. The energy consumption of this kind of building accounted for around 6% of the total U.K. energy in 2010 [9].

1.2.1.3 Public administration building

Such building includes government buildings, NHS, etc. The main energy consumers of such building include: lighting system, office appliance system, motor system, lift system, security system and laboratory equipment [9]. The energy consumption of this kind of building accounted for less than 4% of the total U.K. energy in 2010 [9].

1.2.1.4 Industrial building

The industrial building is mainly the workshop or factory. The main energy consumers of such building include: Industry process system, lighting system and motor system [9]. The energy consumption of this kind of building accounted for around 17% of the total U.K. energy in 2010 [9].

The main sources of the energy consumed by the above buildings include gas, electricity, petroleum, coal, and some other fuels which include manufactured fuel, heat, renewable and waste. For different kinds of buildings, the energy consumption source is different. **Figure 1-2** shows the energy consumptions of these buildings.

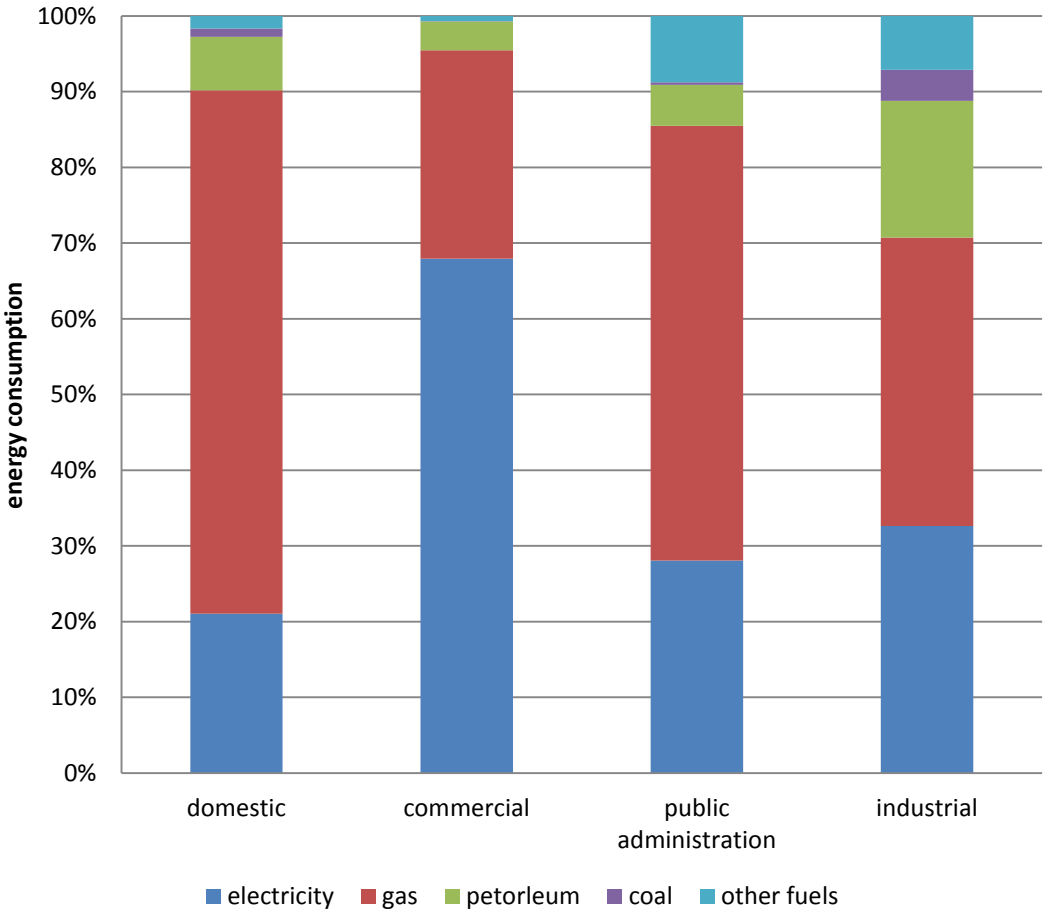

Figure 1-2 energy consumption of different kinds of buildings [9]

However, the above introduction just gives a brief idea about building energy consumption; for an individual building, the assessing and devise of its energy consumption should base on its own data. This data could be accurately determined

by using several kinds of instrumentations and meters, such as gas, water and electricity meters, etc. And also, some other criteria within the building should be considered for the design of the building energy system, which include: space temperature, space humidity, illumination levels, noise levels, indoor air quality (IAQ) [11]. With a view to these criteria, some of the energy consumption systems should be added into the building.

This research focuses on the possibility of improving the domestic building. There are two reasons for this selection: firstly, of all above different purpose buildings, the domestic building takes the largest percentage of the total U.K. energy consumption. Secondly, as the wind turbines are used to produce electricity for the buildings, the electricity consumptions of different building types are compared with each other. Of all above building types, the electricity consumption of domestic building is the largest, which account for 36% of the total U.K. electricity in 2010 [9].

1.2.2 Common building types in U.K.

As this research focuses on the domestic buildings in U.K., the common used domestic building types should be set as the subject. In U.K., there are three house types which are most common used: Semi-detached, Terrace and Detached [11]. More than 85% of these houses are sited in city or town zones in U.K. cities, and appear as building groups [11]. In this research, the site designs of the houses are based on some policy about house extensions [12] and some satellite images from the Google Earth [10].

Semi-detached house is defined as a house joined with another one on one side; more than 32% of all U.K. homes are such kind [13]. While detached house is a house type which is not connected to any other buildings, accounting for 21% of U.K. homes [13]. **Figure 1-3** shows the view of such two kinds of houses. From the satellite images, Semi-detached and Detached house often sites in the same area and mixed together, and the building density of these two house types are similar to each other [11]. Thus, in this research, these two kinds of houses are modelled with the model of semi-detached house.

Terrace house is the second popular house type in U.K., which could be defined as streets of house joined together in rows [11], 27% of all U.K. houses are this kind [13]. Compared with the other two house type, the size of building and area around the building is less, which leads to a larger building density [11]. This kind of building is modelled as another model to compare with the Semi-detached model. **Figure 1-3** also shows the view of such building.

Figure 1-3 Common building types in U.K. [11]

Another common domestic building type in U.K. is flat, which is part of a bigger building. Such building only appears in cities or large towns; the view of such building is as shown in **Figure 1-3**. This kind of building makes up about 20% of U.K. houses [13], and the shape and size of such buildings could be changed in large range. Therefore, in this research, such building is not considered.

1.3 Integrated building wind energy systems

The technology of integrating wind energy system into building design is investigated in worldwide. Based on the size of the building, the technology could be divided into two kinds: the wind energy system on high-rise building, and the wind energy system on low-rise housing. The following sections introduce these two kinds of technology and the limitation of them.

1.3.1 High-rise buildings

A building with more than 5 floors may be defined as high-rise building [14]. A marked characteristic of such building is that high-rise buildings always have elevator system; beside buildings with facilities for disabled, most buildings in U.K. with less than 5 floors do not have lifts inside [13]. For high-rise buildings, besides the buildings with special shapes, the wind energy system is always fixed on the top or sides of such kind of building. Some examples of this wind energy system could be found in the research reports from CPP [15] and some other research group across the globe. Generally, their researches are some cases about a given building, which is restricted by the location, climate, and some other factors of the building. The input wind data of the system comes from the analysis of the historical wind data and the modelling experiment. And the output energy of the system could be calculated with this input data and the energy output curve of the wind turbine used in the system.

1.3.2 Low-rise buildings

For low-rise house with generally up to 4 floors, a prominent example of the technology of integrating wind energy system is the Beddington Zero Energy Development (BedZED) [14] in U.K. The view of this design is as shown in **Figure.1-4**.

The site design of BedZED includes workspace, office park, daycare, and athletic facilities [14], which could be used as domestic building or public administration building. In energy system area, the BedZED generates its own energy from

renewable sources, which include the woodchips from its own trees, the solar energy and wind energy [14]. As a whole, this case is a technical Zero Energy Building. In this design, wind cowl ventilation system is designed to use the low velocity wind close to the house. A small wind turbine is used to produce energy from the wind above the roof of the buildings. This energy is used to deliver preheated fresh air and extract vitiated air in each room of the house. As a performance of this design, the spacing heating requirement of each household of BedZED is 88% less than the U.K. average level [16].

Figure 1-4 the view of BedZED [16]

Besides the design of BedZED, the wind energy system integrated in low-rise buildings always shows as small wind turbines sited outside the buildings. In 2007 and 2008, Encraft [81] initiated a project about small wind turbines near different buildings in U.K. (Warwick Wind Trial). With wind turbines at 26 different sites across U.K., the research group collected both wind velocity and output energy data around buildings in different regions in U.K. From the final report of this trial [81], 15 of all 26 sites used in this project are sited at 10 m height around low-rise buildings in suburban zones. The annual actual average energy generated in these 15 sites is 59.3 kWh, while the predicted output energy from the manufacturers gives an annual

average 190.1 kWh among these sites. The actual energy output value is about 31% of the predicted output energy from the manufacturers. The final report explain this different as the result of power production tailing off at higher wind velocities: the wind turbines' output power in actual conditions are close to the power output curve at low wind velocity (less than 8 m/s), for wind velocity more than 8 m/s, there is a tailing off trend in power production at high wind velocities [81]. This tailing off trend makes the actual hourly energy output of the wind turbines less than the output data of same hourly mean velocity supplied by the manufacturer. The main reason of this tailing off is that the method manufacturer used to forecast the output power is different from the real case. The manufacturer supplied data is based on the power curve and 10 minutes mean wind velocity; during the 10 minutes, the wind velocity is considered to be steady and has same value as the mean velocity, which is different from the actual conditions. In actual environment around low-rise house, the wind flow is fluctuant during the 10 minutes measured time: during the time when wind velocity is lower than the mean wind velocity, the output power of the turbines would be less than the expect value; as a result of these low output power, the actual total output energy of the turbines during the measured time is lower than the manufacturer supplied value, show as tailing off at higher wind velocity. Beside this, turbulence might be another reason of this tailing off: the manufacturer's data is for a low-turbulence environment, which is not similar to the real environments near buildings. In real environment with higher-turbulence, due to the turbulence, the turbines cannot work as well as the laboratory environment where the power curves are measured; this makes the power product by the turbines lower than the expect value from the power curve.

Besides the common used wind turbines, there are also several patents about integrating small wind turbines in to the building energy systems. For example, placing wind-driven turbines in vortices close to the edge of buildings [93] or using turbines with special design [94]. These designs always require special working environments; due to the lack of trial and industrial production, these patents are not widely used till now. In this project, such patents are not taken into consideration.

1.3.3 The limitation of related work

However, both above two kinds of technology have some limitations. For the tall buildings, the wind energy systems are always different among different cases; a widely used system is not designed. This means engineers should design different models and experiments for different cases, which consume lots of time and fund. While the function of the tall building makes the energy require a fluctuant curve during a day, there will be some peak time at which more energy are required. This fluctuant energy requiring curve might lead to an invalidation of the energy system. At the peak time, the energy output of the system might not meet the required energy value of the building, and at other times, the generated energy might be wasted.

The limitation of wind energy system on low-rise building is a little different from the high-rise building. Besides the problem of the fluctuant energy requirement, the size of the building makes it hard to be used in the city zone with large population density. Moreover, the turbulences and low-velocity wind on the surface of the city area will reduce the efficiency of such design.

1.4 Aim of the present work

Generally, the aim of this research is to find some characters about wind flow around individual houses in U.K. These characters are used to calculate the energy output of wind turbines which are used in the wind energy system of the buildings. Comparing this energy output with the energy requirement data of the houses, it can be found whether the house could obtain a significant amount of wind energy.

The wind characters include two kinds of work: historical weather record analysis and experimental simulations.

The historical weather record analysis work is based on the record of weather stations around several U.K. cities; these cities distribute in different areas in U.K. and can shows the climate of areas around them. For a single city weather record, the analysis

includes frequency of different mean wind velocity and frequency of different wind direction. Combining these analysis results with the experimental simulation results and wind turbine parameters, the energy output of the wind turbines could be found out.

CFD and wind tunnel experiments model the environments around groups of houses; the results of these experiments should include two parts:

- Wind velocity at different heights and positions, this result shows the velocity parameters of several positions at common used wind turbine setting heights. The result could be used to calculate the energy output of different wind turbines. The velocity parameters include the mean velocity and its component vectors in Cartesian coordinate system. For each height, the contours plot of mean velocity magnitude is given.
- Wind turbulence intensity at positions around buildings. This result is used to decide the setting position of the wind turbines and also to amend the energy output of the wind turbines.

In this work, “buildings” include semi-detached and terrace house which are differentiated from each other with their size and building density. The details about the house models are introduced in Chapter 4.

1.5 Experimental approach

In the experimental part of this research, two methods are used: Computational Fluid Dynamics (CFD) and Wind tunnel experiment.

The experimental of CFD simulation solves and analyzes the air flow around buildings with computer and relevant numerical techniques. By the use of different CFD models, the wind direction vectors are calculated. These vectors are different from each other with site position, upwind direction and input wind velocity, building type and building density.

Wind tunnel experiment is another experimental simulation used in this research. The wind tunnel experiments were performed with two purposes: firstly, to check the velocity results obtained from CFD simulation; secondly, to obtain and check the turbulence data which was not available from the CFD report. A small wind tunnel is used to give the result. The wind tunnel is set to simulate the similar external environment with the CFD models; the results of this simulation are collected with hot-wire transducer and compared with relevant CFD results to conform each other.

Compared with the above two research method, there is another way to do such research, which is measuring the wind data around real buildings. However, in this research such measurements are not used. This is due to such method requires more funding and time, which is much higher than the research provider level.

1.6 Outline

This thesis is organized as follows: Chapter 2 introduces the historical wind record analysis and theory of topographical characteristic used for this study, Chapter 3 shows the results about historical wind record analysis. The setting details about the CFD experiments used in this research can be found in Chapter 4. Then Chapter 5 covers the setting of wind tunnel experiment and the way to calculate the experiment results. Chapter 6 exhibits and compares the wind velocity and turbulence results in both CFD and wind tunnel experiments. Chapter 7 shows the energy output results based on the results in Chapter 3 and Chapter6. The finally conclusions are reached in Chapter 8.

CHAPTER 2

2 Historical Wind Record Analysis

In this chapter, some descriptions about how to analyze the U.K. historical wind record are included. First, the information about U.K. regions and weather stations analyzed in this research is introduced in Section 2.1, followed by building wind turbines information used in this research in Section 2.2. Then, Section 2.3 is about the methods to transform the wind record; and finally Section 2.4 includes some theories and parameters of topographical characteristic. The analysis results about historical wind record in several U.K. cities are introduced in Chapter 3.

2.1 Selected regions and weather sites

In climatology area, U.K has some standard areas (regions) which has similar climate. Based on this, U.K. Met office [5] divided the country into several parts when the climatology of these regions is generated. In each region, there are several weather stations with weather records which show the climatic character of the region. Of all these regions, the density of population in some regions is obviously larger than the others; there are always one or more large cities in such regions. And as introduced in Chapter 1, this research focused on domestic buildings which are built in or round the cities, thus, the characteristics of the cities should be analysed. For the cities with no original weather records for themselves, the weather record from weather stations most close to the city centre is used. This section shows some information about 7 selected regions and the main cities in these regions. **Figure 2-1** shows these regions on U.K. map [5]. The geographical positions of large cities are also shown in this plot, which are marked as red points.

Figure 2-1 U.K. climatology regions map with cities and weather sites [5]

2.1.1 Character of 7 regions

In this research, U.K. is divided into 7 regions; this division is based on the following rules:

- Climate: Each region is set as standard area used by U.K. Met office when generating climatology.
- Population: in each region, there is a large city.
- Weather stations: each region includes more than one weather station.

Table 2-1 the list of select regions [17]

Location	Main City	City Population in 2011	Annual sunshine *[hours]*	10 m height mean wind velocity *[m/s]* in main city
SE & South England	London	*7,825,200*	1579.7	4.24
South Wales & SW England	Bristol	*421,300*	1522.7	4.61
Midland England	Birmingham	*1,081,800*	1398.3	4.64
North Wales & NW England	Manchester	*483,000*	1394.5	4.47
NE & East England	Leeds	*487,600*	1474.6	4.54
East Scotland	Edinburgh	*486,000*	1405.8	5.54
West Scotland	Glasgow	*692,500*	1239.6	5.39

Table 2-1 shows some detail about these regions, which includes the location, main city, city population in 2011, annual total sunshine and hourly mean-wind velocity at 10 m height from ground of the main cities. The annual sunshine hour and mean wind velocity in this table are based on 30 year of weather data, covering the period 1971~2000. The hourly wind velocity at 10 m height in urban area of each city is averaged and marked as the mean wind velocity of the city; these mean wind velocities are only used to compare the level of the wind in these cities in this section.

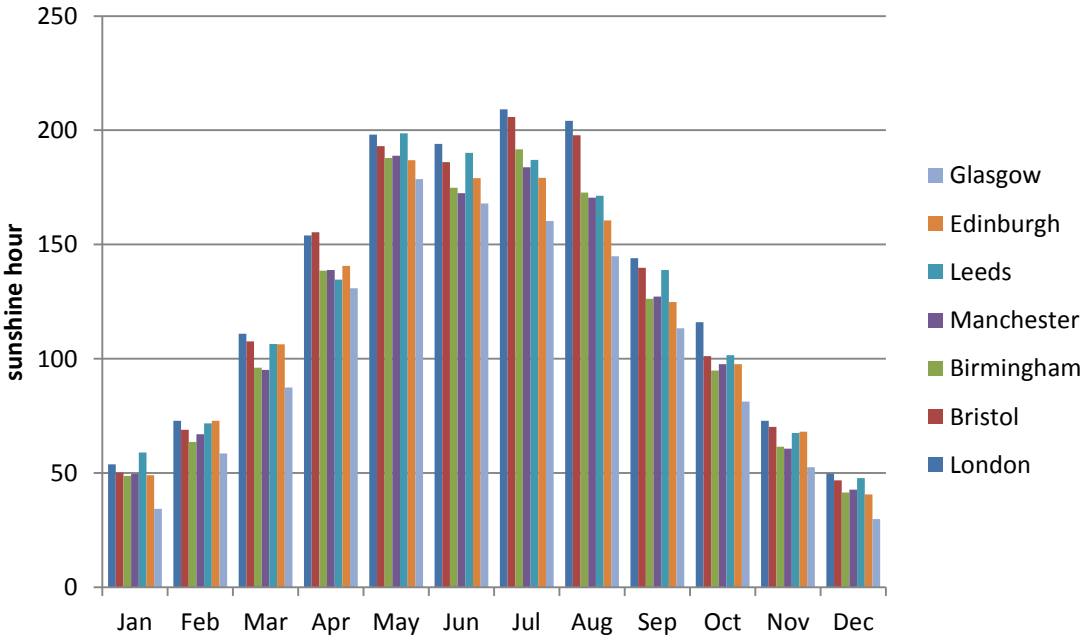

Figure 2-2 monthly average sunshine hour of different regions (1971-2000) [5]

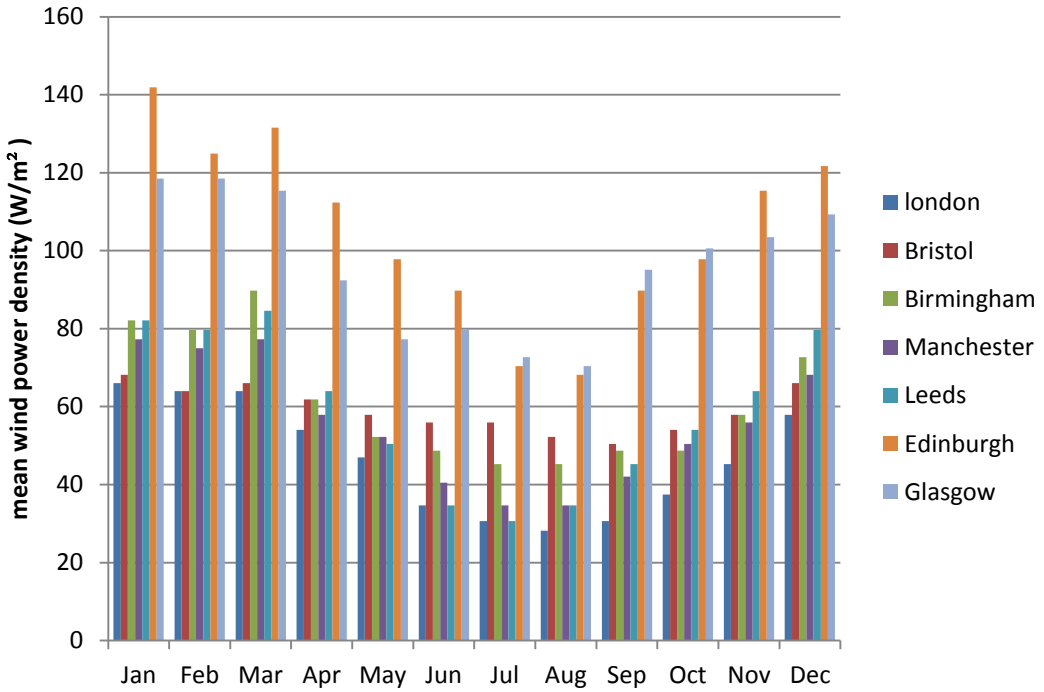

Figure 2-3 average wind power density at 10 m height of different cities (1971-2000) [5]

The monthly average sunshine hour of the regions is shown in **Figure 2-2**, and **Figure 2-3** shows the monthly mean wind power density in main cities of each region. In following section, the solar and wind resource in the main cities of these regions are introduced, and in following Chapter 3 and Chapter 7, these cities are used to show the wind record analysis results and energy output results in correlative regions. This is because the wind is variable for different terrains; it is not possible and meaningless to analysis the wind in large areas. This research focuses on different roughness zones close to the main cities.

- **London (SE & S England)**

London is situated in the south of England. The Greater London includes City of London and other 32 London Boroughs [18]. Although the temperature of the city area is higher than the surrounding areas due to the "urban heat island" effect [19], the average data of sunshine and wind in this city could shows the characters in southern and south-east of England. In these areas, the annual average total sunshine reaches 1,579.4 hours [5]. **Figure 2-2** shows the monthly average sunshine hour in London Heathrow from 1971 to 2000. In London, the mensal sunshine time increases from

January to May, and is steady for about 4 months, then decreases till the end of the year; compared with other cities, London has the largest annual sunshine hours. While the monthly average wind power density in London could be found in **Figure 2-3**, it could be found that the wind have a nearly same strength during the year, but weaker in the middle of the year. For this project, it means that, in south-east & south England, the solar source could produce more energy in summer while the wind energy is more powerful from November to May.

- **Bristol (S Wales & SW England)**

Bristol is the largest city in South Wales & South-west England. Base on the weather record from 1971 to 2000 **[5]**, the average sunshine hour is 1522.7, and the average wind at 10m is 4.61 m/s in the centre of this city (postcode zone BS1). From **Figure 2-2**, the monthly curve is quite similar to the record of SE & S England, and the sunshine hour in this region is in second place of all regions, which means this region has good solar source. Comparing to the other regions, the wind source in this region is also good: just weaker than Scotland and Midland England. **Figure2-3** shows the monthly mean wind power density in Bristol, it could be found that the mean wind velocity is nearly the same during the whole year, which means the wind energy is uniform during the whole year.

- **Birmingham (Midland England)**

Birmingham is a city with the second largest population in U.K., and in this description, it is the only midland city. As a large city, Birmingham has the same "urban heat island effect" **[19]** as London. In this city, from 1971 to 2000, the average sunshine hour is 1398.3; and the average wind velocity at 10m in city centre (postcode zone B1) is 4.64 m/s **[5]**. From the sunshine hours in **Figure 2-2**, the sunshine in Birmingham follows almost the same rule as the others, but there is a decrease in June; the total sunshine hour in this region is similar with north Wales & north-west England: more than west Scotland but less than other areas in U.K. **Figure 2-3** shows the mean wind power density in this city, during the whole year, this region has the

strongest wind in England and Wales, but weaker than Scotland. For the region itself, wind is weaker from May to November than rest of the year.

- **Manchester (N Wales & NW England)**

Manchester is also called "Capital of the North". This is a typical northern England city; the average sunshine hour is 1394.5 from 1970 to 2000; with an average wind 4.47 m/s at city centre (postcode zone M1) [5]. The sunshine hour and curve in this region is similar with midland, the sunshine hour increases from January to May and decrease from August to December; and there is a decrease in June. The wind velocity in Manchester follows the same rule with the midland but more even, and the wind source in this region is in the second weak place of all regions, just stronger than the S & SE England.

- **Leeds (NE & E England)**

Leeds is a north-east England city. From **Figure 2-2**, the sunshine in this region in less than south England and south Wales, but stronger than other regions. And the wind source in this region is similar with the wind in Midland from September to May, but turns weak in June, July and August.

- **Edinburgh (East Scotland)**

Edinburgh is the capital city of Scotland. Generally, compared with England and Wales, Scotland regions have more wind but less sunshine; this could be found in **Figure 2-2** and **Figure 2-3**. In this region, the monthly sunshine hour increase from January and reaches the peak in May, then decrease till the end of the year. The total sunshine hour is close to midland and north-west England: more than west Scotland but less than other regions. As shown in **Figure 2-3**, the mean wind power density in this region is close to west Scotland and much stronger than England and Wales regions during the whole year. The annual mean wind velocity at 10 m height in city centre (postcode zone EH2) reaches 5.54 m/s based on the historical record.

- **Glasgow (West Scotland)**

Glasgow is the largest city in Scotland. This region has the least sunshine of all regions; as shown in **Figure 2-2**, in May the sunshine hour reach the peak in this region. Compared with the weak solar source, the wind source in this region is strong: close to the east Scotland and larger than other regions.

In general, the difference of sunshine hour between these regions is smaller than the variations from different time of the year. Of all above regions, the annual sunshine hour in SE & S England (the region with most annual sunshine hour) is only about 1.27 times of the sunshine hour in West Scotland (the region with least sunshine hour). While for each region, the sunshine hour in mid-summer (peak time of the year) is more than 4 times of the sunshine hour in mid-winter (trough of the year). Thus, the research about solar energy should pay more attention on the sunshine variations during different periods of the year.

For wind source, the variations of energy in wind from city to city are much larger than variations from different time periods of the year. As shown in **Figure 2-3**, in each city, although the wind power density is somewhat less in summer than winter, the difference is not large. While the wind power density difference between Scotland and England & Wales is large: the wind power density in the two Scotland cities is almost two times of that in England & Wales cities. Because of this, this research focuses on the wind energy analysis in all above cities.

The location of all U.K. buildings could be found in one of above regions. After analysing the climate of a city, the energy consumption in buildings should be considered.

2.1.2 Data sources and data modelling

Hourly wind velocity data has been recorded by the U.K. Met Office [5]. This data will be used to estimate the energy output of 14 different wind turbines. This part gives a

main introduce about the U.K. weather sites and the energy output models used in this research.

2.1.2.1 Wind velocity data sources

The U.K. Met Office records the weather data of 66 U.K. sites. In order to get the data of energy outputted by the wind turbines, frequency distribution of hourly mean wind velocity is required. However, not all the sites observed hourly wind velocity data. On the basis of the length and completeness of the hourly wind velocity record, the data used in this research comes from weather sites closest to centre of above U.K. cities, with time range between 1970 and 2004. The locations of these cities are as shown in **Figure 2-1**. The data from the Met Office gives the wind speed and direction to the nearest 1 m/s and 10 degrees respectively.

As introduced above, the wind data used in this research comes from weather sites close to the city centre; since wind is affected by nearby local obstacles, the environments close to the weather site and anemometers which are used to measure the wind data should be considered. **Table 2-2** shows the details of weather sites used in this research, which includes location kind, name, terrain surface characteristics, data time range of these sites, and the sites' location from the nearby city centre.

Table 2-2 details of the weather sites

Name	Nearby city	Terrain characteristic	location from city centre	Time range
Birmingham	Birmingham	Airport runway area	7 km ESE	1970-1981, 1993-2004
Heathrow	London	Airport area with building and trees	28 km W	1970-1996, 2000-2002
Horfield	Bristol	Suburbs	6 km N	1970-1996, 2000-2002
Ringway	Manchester	Airport runway area	16 km S	1970-1992, 2000-2004
Turnhouse	Edinburgh	Airport runway area	13 km W	1970-1993, 2000-2002
Church Fenton	Leeds	Farmland with open appearance	26 km E	1970-1992, 1999-2004
Abbotsinch	Glasgow	Airport area with building and trees	16km W	1977-1988; 1999-2003

Generally, the historical wind data from the above weather sites shows the state of wind in the position where the anemometers are sited; and the wind data would be different for different terrain surface characteristic. The method about transform the wind data between different terrain roughness levels is introduced in Section 2.3.

Attention should be paid on these wind records that some of them are error shows as "-999". For this kind of records, the author deleted the data and did not calculate them.

2.1.2.2 Energy output modelling

The energy output of wind turbines is calculated by a model based on the published power curve data for different kinds of wind turbines. In this research, the hourly wind velocity data is inputted into the model and converted into the hourly energy output of each wind turbine. The wind turbines considered in this chapter have blade diameters from 3 meters (Kestrel 1000) to 6.7 meters (Aerostar 6). They have been selected as turbines which were available on the market and small enough to be installed near houses. The manufacturer and name of the turbines are as below:

- **SouthWest Wind Power (USA)** [20]: Whisper 200, Whisper 500, and Skystream 3.7;
- **Proven energy** [22]: Proven WT2500 and Proven 6kW;
- **Westwind** [23]: Westwind 3kW, Westwind 5.5kW, and Westwind 10kW;
- **Turby B.V.** [24]: Turby VAWT;
- **Kestrel Wind Turbines** [25]: Kestrel 1000;
- **Samrey Ltd.** [26]: Samrey Merline;
- **Quiet Revolution** [27]: Quite Revolution;
- **Eoltec** [28]: Scirocco 6kW;
- **Aerostar** [29]: Aerostar 6.

Table 2-3 shows the data of these turbines from the design reports of the manufacturers; which include the type, rotor area, rated output power, price, cut-in velocity, rated velocity, and cut-out velocity. The price in this table is just for the turbine only, and might be changed in different market. The typical install price which includes mast,

cable and other fittings are not included. **Figure 2-4** shows the appearance and power output curve [20] of Whisper 200 as an example, the appearance and power output curve of all turbines are shown in Appendix A. For each power curve used in this research, measured 10 minutes average wind speed is used to produce the power curves, which is recommended by British Standard BS EN 61400-12-1:2006 [92].

Table 2-3 the wind turbine data

Name	Type	Rotor area *[m^2]*	Rated power *[W]*	Price *[£]*	Cut-in velocity *[m/s]*	Rated velocity *[m/s]*	Cut-out velocity *[m/s]*
Whisper 200	HAWT	7.55	1,000	2,000	4	11.6	N/A
Whisper 500	HAWT	15.9	3,000	5,200	4	10.5	N/A
Proven WT2500	HAWT	9.62	2,500	11,000	4	13	N/A
Proven 6kW	HAWT	23.76	6,000	19,200	4	13	N/A
Westwind 3kW	HAWT	10.75	3,000	6,400	4	14	N/A
Westwind 5.5kW	HAWT	20.43	5,500	10,200	3	14	N/A
Westwind 10kW	HAWT	30.19	10,000	18,200	3	14	N/A
Turby	VAWT	5.3	2,500	6,940	4	14	14
Kestrel 1000	HAWT	7.07	1,000	4,500	3	9.5.	N/A
Samrey Merline	HAWT	9.62	1,150	4,800-6,000	3	9	N/A
Skystream 3.7	HAWT	10.87	2,400	6,000-7,500	3.5	13	N/A
Quiet Revolution	VAWT	13.6	6,000	25,000	4.5	14	16
Scirocco 6kW	HAWT	24.63	6,000	19,000-27,000	3	11.5	N/A
Aerostar 6	HAWT	35.26	7,000	10,000	3.5	12.5	N/A

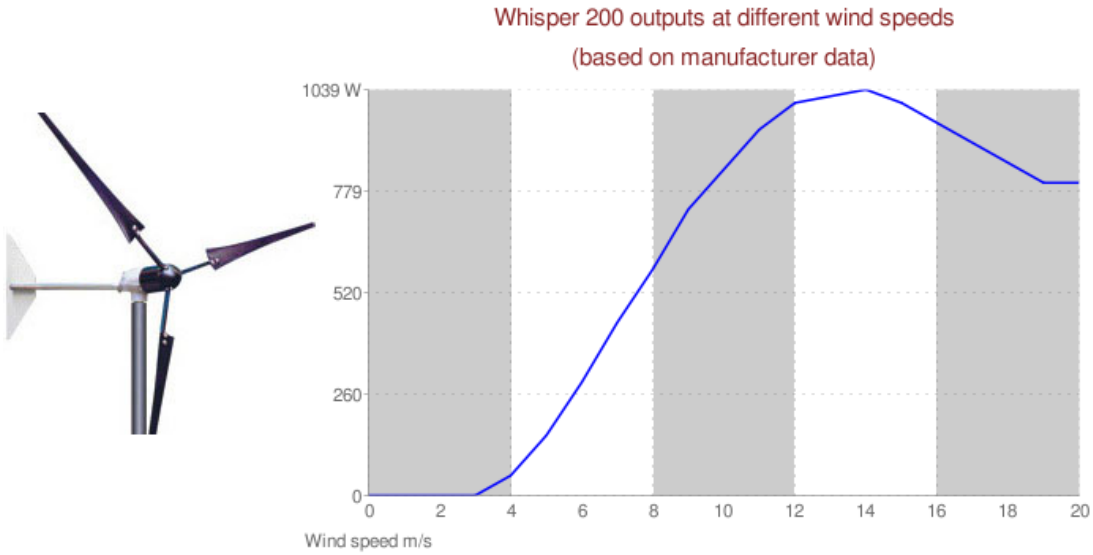

Figure 2-4 the appearance and power output curve of Whisper 200[20]

For each wind turbine, the power transform data could be got from the above power output curves, the output energy analysis of the wind turbines are based on these data. These power output curves comers from the manufacturers of wind turbines, and

show the relationship between wind velocity and output energy of each wind turbine. In this research, hourly mean wind velocity is used as the velocity parameter of this curve and then gets the power output prediction result [8]. It should be mentioned that such prediction method shows an approximate value of the hourly energy output, for real case, the result might be different.

In this project, due to the lack of funding and support, the analysis of wind velocity is based on the CFD and wind tunnel experiment results, and the energy output analysis is based on the output curves supplied by the manufacturers. Due to the lack of trials in actual environment, the energy output result in this report is predicted from historical hourly mean wind velocity and power curve, the output power different between power curve and real case is not included. Because of this, the output energy in real case could be less than the values in this report. Chapter 3, Chapter 6 and Chapter 7 show the analysis results at different height in U.K. regions.

2.2 Building wind turbines

In most wind farms, modern wind turbine appears as three blades and a horizontal axis rotor on the top of a high tower. The different rotor diameter (27m to 80m) leads to quite different electrical output (225kW to 2500kW) [30]. However, although the wind turbine used near house is much smaller than the ones used in wind farms, they operate according to the same principles. The theory of wind turbines and some qualifications about setting small wind turbines close to buildings are introduced in this section.

2.2.1 Theory of small wind turbines

There are mainly two steps for the energy conversion of wind turbine: first, the wind energy is converted into mechanical power in the rotor axis; second, the dynamo produces electricity with the mechanical power [31]. For the first step, there are two concepts to achieve this conversion: drag-driven and lift-driven; and with these

concepts, three kinds of wind turbine are designed: drag-driven wind turbine, lift-driven wind turbine and hybrid-driven wind turbine, which is a combination of the above two [32]. The conversion efficiencies [32] of these three kinds of turbine is introduced and compared below, this efficiency is signed as C_P and defined as:

$$C_P = \frac{P_m}{P} \quad \text{(Eq.2-1)}$$

In this equation, P_m is the mechanical power at the rotor axis and P is the power in the wind defined as:

$$P = \frac{1}{2}\rho \cdot u^3 \cdot A_t \quad \text{(Eq.2-2)}$$

In this equation, ρ is the around air density; u is the wind velocity, and A_t is the swept area of the wind turbine [31].

From the above equation, the amount of power of a wind turbine has a directly proportional relationship with the efficiency factor, the air density, the swept area of the turbine and the cube of the wind velocity. Of all these conditions, the air density is fixed by natural forces, the efficiency factor and the swept area of the wind turbine is depending on the design of turbine; and the wind velocity could be affected by the surface roughness of the building zones. The theory of topographical characteristic is introduced in Section 2.4 below.

2.2.1.1 Drag-driven wind turbine

A drag-driven is as shown in **Figure 2-5a**, it contains a vertical axis and some cups. When wind blows on these cups, the drag of each cup is different, and this difference makes the cups rotating around the axis. The schematic configuration is shown in **Figure 2-5b**. In this configuration, cup A has a lower drag than cup B, and the turbine rotating in counter-clockwise, which produces power.

The conversion efficiency of this wind turbine could be got out from **Figure 2-5b**. In this plot, $C_{d,A}$ is the drag coefficient of cup A, while $C_{d,B}$ is the drag coefficient of cup B; the wind velocity is u, the spin velocity is ω; the radius of the rotor is R_t; and set the swept area of each cup as A_c.

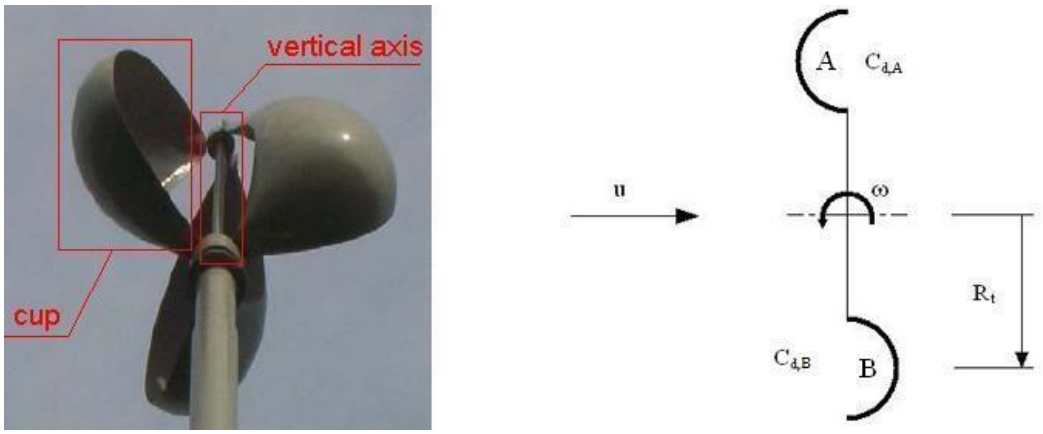

Figure 2-5 a.Drag-driven wind turbine (example); b. Schematic configuration (drag-driven) [32]

As Sander Mertens [32] mentioned, the torque Q of the rotor should be:

$$Q = C_{d,B} \cdot \frac{1}{2} \cdot \rho \cdot (u - \omega R_t)^2 \cdot R_t \cdot A_c - C_{d,A} \cdot \frac{1}{2} \cdot \rho \cdot (u + \omega R_t)^2 \cdot R_t \cdot A_c \quad \text{(Eq.2-3)}$$

In the equation above, the power of the rotor assumed to be a pure translation from the cups. And it is also assumed that the velocity of cup A is constant u - ω R_t, while the velocity of cup B is constant u + ω R_t. Then, from P_m=Q ω, the mechanical power at the rotor axis P_m is defined as:

$$P_m = \frac{1}{2} \cdot \rho \cdot R_t \cdot \omega \cdot A_c \cdot \left[C_{d,B} \cdot (u - \omega R_t)^2 - C_{d,A} \cdot (u + \omega R_t)^2 \right] \quad \text{(Eq.2-4)}$$

Then set $\lambda = \omega R_t / u$, which shows the ratio of tip velocity (ωR_t) and the wind velocity (u_o), take this ratio into Eq.2-4, it can get that:

$$P_m = \lambda \cdot \frac{1}{2} \cdot \rho \cdot u^3 \cdot A_c \cdot [C_{d,B} \cdot (1 - \lambda)^2 - C_{d,A} \cdot (1 + \lambda)^2] \quad \text{(Eq.2-5)}$$

Connect Eq.2-5 with Eq.2-1, for Eq.2-1, $A_t = 2A_c$. It gives that:

$$C_P = \frac{1}{2} \lambda \cdot [C_{d,B} \cdot (1 - \lambda)^2 - C_{d,A} \cdot (1 + \lambda)^2] \quad \text{(Eq.2-6)}$$

Actually, because of the cups in this turbine move rotationally, the average torque these cups device is lower than Eq.2-3 shows, which means for this kind of turbine, Eq.2-6 gives an upper value of C_p. And if neglect the drag on cup A, Eq.2-6 changes to:

$$C_P = \frac{1}{2} \lambda \cdot (1 - \lambda)^2 \cdot C_{d,B} \quad \text{(Eq.2-7)}$$

Optimizing this equation, it gives that at λ_{opt}=1/3, the equation gives the maximum, which is:

$$C_{P,\max} = \frac{2}{27} C_{d,B} \qquad \text{(Eq.2-8)}$$

Hoerner gives $C_{d,B} \approx 1.5$ [32], which gives $C_{P\,max} \approx 3/27 \approx 0.11$. This means that the drag-driven wind turbine could convert at most 11% of the wind power into mechanical power at the rotor axis.

2.2.1.2 Lift-driven wind turbine

There are two kinds of lift-driven wind turbine used now: Vertical Axis Wind Turbine (VAWT, **Figure 2-6 Left**) and Horizontal Axis Wind Turbine (HAWT, **Figure 2-6 Right**). However, the theory of these two kinds of wind turbines is the same. The schematic configuration is shown in **Figure 2-7.**

Figure 2-6 Lift-driven wind turbines: VAWT and HAWT (Example)

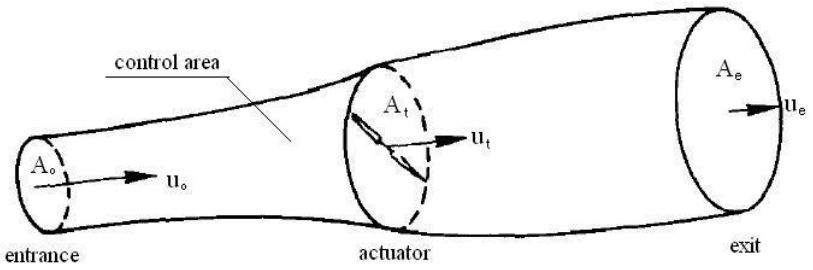

Figure 2-7 Schematic configuration (lift-driven) [32]

In this case, Froude [32] introduced an actuator concept to get the $C_{P,max}$. "This actuator is defined as an energy- extracting disk or plane of infinite small axial size with a

normal force on the surface that decelerates the normal velocity through the disk or plane" [32]. As shows in **Figure 2-7**, the actuator is in a control volume. This area is assumed that the flow in it is rotational and divergence-free, the entrance and exit of this area is infinitely far away from the actuator; at the entrance, the wind velocity is u_0, with area A_0; the wind velocity and area through the actuator is u_t and A_t; while at the exit, wind velocity is u_e, area is A_e. Thoma and Glauert [32] show that the thrust force F_t on the actuator is:

$$F_t = \rho \cdot {u_0}^2 \cdot A_0 - \rho \cdot {u_e}^2 \cdot A_e \quad \text{(Eq.2-9)}$$

As in the control area, the air follows the mass conservation law: $\rho u_0 A_0 = \rho u_t A_t = \rho u_e A_e$ then it gives:

$$F_t = \rho \cdot A_t \cdot u_t \cdot (u_0 - u_e) \quad \text{(Eq.2-10)}$$

With Bernoulli's theorem [33], the thrust force is like:

$$F_t = \frac{1}{2} \cdot \rho \cdot A_t \cdot (u_0^2 - u_e^2) \quad \text{(Eq.2-11)}$$

From Eq.2-10 and Eq.2-11, it gives:

$$u_t = \frac{1}{2} \cdot (u_0 + u_e) \quad \text{(Eq.2-12)}$$

Take an induction factor "a" to show how much the wind is decelerated, defined as: $u_t = u_0 (1-a)$. From Eq.2-12, gives: $u_e = u_0 (1-2a)$. This shows that the wind velocity around the actuator is the mean of the wind velocitys at the entrance and exit, known as "bar actuator wake expansion" [32].

The absorbed power is the difference between the inlet and out let wind power:

$$P_m = \frac{1}{2} \cdot \rho \cdot u_0^3 \cdot A_0 - \frac{1}{2} \cdot \rho \cdot u_e^3 \cdot A_e \quad \text{(Eq.2-13)}$$

With the mass conservation law, Eq.2-13 changes to:

$$P_m = \frac{1}{2} \cdot \rho \cdot u_t \cdot A_t \cdot (u_0^2 - u_e^2) \quad \text{(Eq.2-14)}$$

Connect Eq.2-14 with Eq.2-1, gives:

$$C_P = \frac{u_t \cdot (u_0^2 - u_e^2)}{u_0^3} \quad \text{(Eq.2-15)}$$

Connect Eq.2-15 with Eq.2-12, gives:

$$C_P = \frac{1}{2} \cdot \left(1 - \frac{u_e}{u_0}\right) \cdot \left(1 + \frac{u_e}{u_0}\right)^2 \quad \text{(Eq.2-16)}$$

Optimizing this equation, it gives that at $\frac{u_{e,opt}}{u_0}$=1/3, the equation gives the maximum C_p, which is 16/27 ≈ 0.59. This means that the lift-driven wind turbine could convert at most 59% of the wind power into mechanical power at the rotor axis.

2.2.1.3 Hybrid-driven wind turbine

The hybrid-driven wind turbine is evolved from the drag-driven wind turbine. **Figure 2-8** shows the view and Schematic configuration of this turbine. Because there is a gap (*g* in the figure), this wind turbine is driven by drag and lift. This makes the turbine has a higher $C_{P,max}$ than a pure drag-driven turbine. Paraschivoiu [31] shows that $C_{P,max}$ ≈ 0.24 at λ ≈ 0.9, with a gap of g/D_t = 0.10-0.15.

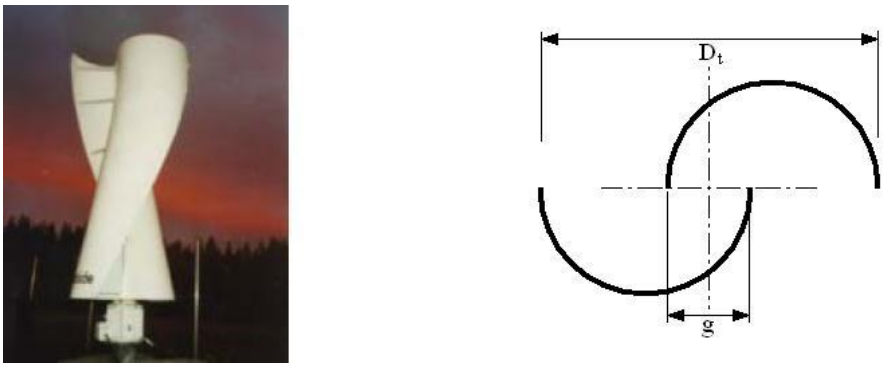

Figure 2-8 a Hybrid-driven turbine (left) and its schematic configuration (right) [31]

2.2.1.4 Comparison

With the introduction above, these wind turbines should be compared in two aspects: cost and efficiency. **Table 2-4** shows this comparison:

Table 2-4 comparison of different kinds of wind turbine

Driven kind	Drag-driven	Hybrid-driven	Lift-driven
Cost per kW	High	High	Low
Max efficiency	11%	24%	59%

For a given power output, 20% of the wind turbines cost is spent on the material of the blades [32]. From the views of the wind turbines it is easy to find that the drag-driven and hybrid-driven wind turbine have much larger blades. This makes these two wind turbines more costly than the lift-driven one. The max efficiency of these wind turbines have been introduced above, the lift-driven one has a much higher than the other two. Thus, lift-driven wind turbine should be used, unless the other types have some other advantages that offset their lower efficiency and high cost.

2.2.2 Limitations of small wind turbine

Considering the influences between wind turbine and built environment, the mainly qualifications of small wind turbine include: size, yawed direction, safety and Re number effects [32].

2.2.2.1 Size

As above sections introduce, the small wind turbine is different from the one used in wind farm. This is mainly because the wind is affected by the surface roughness of city/town zones. For small wind turbines with rotor height close to the building height, the average building height $\overline{H}$ [32] should be considered as an important characteristic. When the wind flows around buildings, the nearby buildings would change the direction of the wind with a time scale τ_{turb} [32]. This time scale could be calculated with the average building height and wind velocity u, which is defined as:

$$\tau_{turb} = \frac{\overline{H}}{u} \qquad \text{(Eq.2-17)}$$

Sander [32] gives that "for a virtual stream tube, the length of the stream tube is approximately 6 times the diameter of the rotor (D_t)". This gives another time scale τ_t:

$$\tau_t = \frac{6D_t}{u} \qquad \text{(Eq.2-18)}$$

In a steady wind tube, during the time scale τ_t, the input wind direction should be steady; which means the building should affect the wind with a longer time than the time scale of the stream tube. In other words, τ_{turb} should be larger than τ_t, with Eq.2-17 and Eq.2-18, the result is:

$$D_t < \frac{\overline{H}}{6} \quad \text{(Eq.2-19)}$$

And this is the limit for the size of the wind turbine [32]. However, this limit mainly affects the turbine selection for high-rise buildings inside the city. The wind turbines are fixed on the top of the tall buildings and the wind directions are always changed by nearby mansions. For town or country zones with low average building height, the turbines are sited on the top of their own tower. The height of the turbine would be much higher than the average building height and the nearby buildings would not affect the wind directions a lot. For such case, Eq.2-19 should not be used to limit the turbine size.

2.2.2.2 Yawed flow

Yawed flow is a constraint for HAWTs only. The yaw comes from the change of wind direction, as there is a time scale τ_{dir}, "the HAWT needs to yaw at least every τ_{dir}" [32]. But due to the inertia, the HAWT might not achieve this yawing.

Because of this problem, most small HAWTs have a yaw system based on vane. However, this gives HAWT another problem: the vane force yaw the wind turbines towards the direction of wind, while the inertia of the yaw axis obstructs this movement. As a result of these two forces, Eigen-frequency appears. If this Eigen-frequency is close to the winds' frequency [32] ($f_{turb} = 1/\tau_{turb}$), there will be a resonance. This resonance would damage the turbine and need to be avoided.

Compared with HAWT, the VAWT is not affected by the yaw problem. As a result of this yawed flow, the average output power of HAWT is lower than same size VAWT. Another result of the yawed flow is the frequent load change to HAWT, which leads to an increased fatigue load [32].

2.2.2.3 Safety

Safety is another boundary condition for turbines. As these small wind turbines operate near buildings, malfunction probability of these turbines should be very small.

Beside the system malfunction, there is another hidden trouble: the blade rip-off. As above introduced, the wind turbine has an increased fatigue load, which acts on the blades, the blades are possible to rip-off. In order to avoid this accident, Steel cage may be added to cover the rotor and more serviceable blades are used [32]. However, steel cage is not an attractive way to solve the safety problem, as the cage would affect the wind through turbines and thus reduce the wind velocity and produce more turbulence. The lower wind velocity and higher turbulence would reduce the output energy produced by the turbines. The designers of the turbines should consider more about serviceable blades.

2.2.2.4 Re number effects

The Reynolds Number is a non-dimensional parameter defined by the ratio of momentum and shearing forces [34]. The Re number could be used to characterize different kinds of flows: a lower Re number (less than 2000) shows the flow is a laminar one, in this flow the viscous forces are dominant, its character is the "smooth, constant fluid motion" [34]; while a high Re number (more than 3000) shows the flow is a turbulent one, in which the inertial forces are dominant, the character of this flow is "random eddies, vortices and other flow fluctuations" [34]. It should be mentioned that the above Re number is set for flow in pipes and similar flow; for this project, the Re number could be defined as:

$$R_e = \frac{\rho \cdot u \cdot D_t}{\mu} \qquad \text{(Eq.2-20)}$$

For the wind turbine used in ZEB, the small size of the rotor and the lower wind velocity make the Re number smaller than the wind farm turbines. Compared with the larger Re number, the drag of blades is increased (due to the shear forces) and the lift of blades is decreased (due to the momentum forces), these force changes decrease the output power of the wind turbine, which results in a distinct decrease of C_p. In 2002, Mertens finished some experiment on the blades of the Turby (a kind of VAWT). From his report, the relationship between $C_{P,max}$ and average Re number is as shown in **Figure 2-9** [32]. In his project, the wind turbine is designed with D_t = 1.5 m and λ =3. The maximum C_P at wind velocity 10 m/s is 0.3, as shown in **Figure 2-9**. And it's also

found that the design of the wind turbine should also limited by a lower ratio of tip velocity and free stream wind velocity λ (2~4) because of the noise emission, this limit is for a better material usage, power coefficient and noise emission [32].

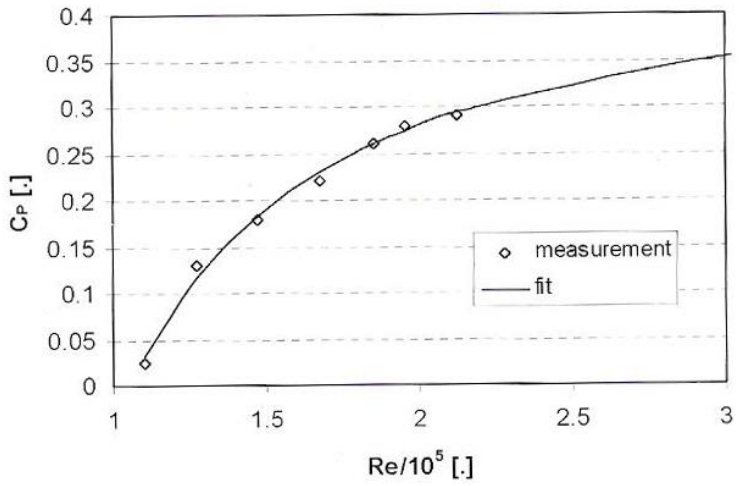

Figure 2-9 $C_{P,max}$ from measurements as a function of the Re number on the blades of the Turby prorotype see Mertens [32]

With the above boundary conditions, the promising wind turbine for ZEB should have the following characteristic: small size; lift-driven turbine; and the ratio of tip velocity and free stream wind velocity should between 2 and 4. Some appropriate wind turbines are introduced in the Subsection 2.1.2.2.

2.2.3 Limitations of building and built environment

As attached equipment to the building, wind turbine brings many influences besides more energy. Some of these influences might affect the comfort of the built environment like peace or sunshine; while the others might affect the original structure of the building.

2.2.3.1 Noise

The Environmental Protection Act (1990) [35] ordains that for a building, the total noise level outside the buildings should stay below some maximum allowable noise levels. Of all these maximum allowable noise levels, the lowest is for the homes

during nights, which is 50 *dB (A)* in U.K. The wind turbine must design to fulfil this claim. The Wind Energy Handbook [36] shows that, for noise emission, the following three aspects should be considered: the noise source, the distance from the source, and the amount of noise source.

The noise source is from the moving blades and the air around them. Burton et al. [36] states there is an approximately proportional relationship between the noise emission of HAWT and fifth-power of its tip velocity. Based on this relationship, the wind turbine's noise emission could be reduced by limit the tip velocity of the rotor. The noise of the air comes from the velocity and pressure differences of the wind, which shows as vortexes around the blades. The noise emission could be reduced by avoiding these vortexes.

It is proverbial that the sound turns lower with distance from the sound source. The sound level equation [36] is given as:

$$L_P = L_W - 10 \cdot \log_{10}\left(4\pi r^2\right) \quad \text{(Eq.2-21)}$$

This equation shows the sound pressure level L_P, which is away from the sound source that has a sound power level L_W with a distance r. It could be educed from this equation that when the distance doubled, the sound pressure level will decrease 6 *dB*. The total sound pressure of n sound sources could be calculated with the following equation [36]:

$$L_{P,n} = 10 \cdot \log_{10} \sum_{j=1}^{j=n} 10^{0.1 L_{P(j)}} \quad \text{(Eq.2-22)}$$

Attentions should be paid that there are two sound pressure level units in this section: *dB* and *dB (A)*. The unit *dB (A)* is frequency weighted to adjust *dB* for the typical frequency response of the human ear. Thus, sound levels denoted by *dB* and *dB (A)* are usually different, depending on the frequency spectrum of the sound.

2.2.3.2 Sunray

The wind turbine might affect the sunshine of building in two ways: the moving blades will make a flickering shadow if its location is in the direct path of the sunray;

and the sunray might reflect from the surface of the blades [32]. The first issue is especially harmful to the eye if the frequency of the wind turbine is below 20 *Hz* [36]; which is a usual frequency for HAWT. Thus, the frequency of HAWT should be designed more than 20*Hz* if it is in the sunray path. The second issue could be avoided by using dull paint on the blades.

2.2.3.3 Vibrations & Resonance

Because of the mass unbalance and the differences of load on the blades, the wind turbine produces an induced vibration at the rotational frequency *n* [32]. For a single turbulent structure whose velocity is different from the average velocity, the *B* blades induce a frequency *Bn*. And if the amount of turbulent structures increases to *i*, the higher frequency *iBn* will be induced [32]. Attention should be paid that there in the same environment; the frequency of VAWT is twice of the frequency of HAWT. This is because the blades of VAWT cut the turbulent structure twice: at the upwind and downwind side of the VAWT. Also, there are periodic thrusts on the blades of VAWT when they are turning, these thrusts induce vibrations on the turbine.

The Eigen-frequency f_e of the building is given as a function of the building height *H* [37]. The large amount of data fit: $f_e = 46/H$.

The frequencies of wind turbine should avoid the Eigen frequencies of the building structure (i.e. roof, wall, mast, etc.). If the frequencies of the wind turbine are close to the eigen-frequencies of the building, vibrations will affect the wind turbine, and resonance will affect the building or parts of the building. These disadvantages could be avoided by select the wind turbine with different frequencies from the eigen-frequencies of the building and building parts.

2.3 Transform wind record.

In order to estimate the energy output of wind turbines at different terrain locations, the historical wind records of the locations are needed. In most U.K. area, the

historical wind record could be found on the website of U.K. Met office [5]; most of these records are based on the weather data from nearby weather sites. For some area without reliable weather record close to it, the meso-scale modelling should be used to determine the wind record [38]. Most of the weather sites are some distance away from the cities; even in the same city, the different surface roughness environment affects the wind. Because of this, the wind climate data should be transferred and then used in the modelling. This section shows the idea of transform the wind record, the correlative topographical theory is described in Section 2.4. Generally, the transformation of wind data includes two parts: velocity and direction [38].

2.3.1 Wind velocity

In order to transform wind velocity between terrains with different roughness levels, the most common method is based on Deaves and Harris' work [39] and the approach codified by ESDU [40]. There are two steps for this method.

In the first step, the wind velocity records are extended to a gradient height. This gradient height might be different for different atmosphere stabilities; for common atmosphere boundary layer in U.K., the gradient height is about 200m to 600m above ground [40]. It could be considered that the wind velocity is not affected by the local terrain at this height; which means at this horizontal height, the wind velocity in city zone and the close suburban zones could be consider the same. Two functions could be used to achieve the extension of wind velocity: the Power-law proposed by Deaves and Harris and the Logarithmic-law proposed by Oke [56] [57]. For the height lower than 150 m from the ground, both functions show the similar results; while power-law shows more accurate predictions of the wind profile with height more than 150 from the ground [42]. The details of these two functions are introduced in Section 3.1 and Section 4.2, respectively.

In the second step, the extended wind velocities from above step are transferred down to the height of the buildings in group. There are two ways to achieve this step: by using the Power-law or Logarithmic-law with a site specific exponent [38], or by setting the extended wind velocity as a boundary condition of an experiment.

Figure.2-10 could be used to explain the above two steps, which is a part of a research in Houston, USA.

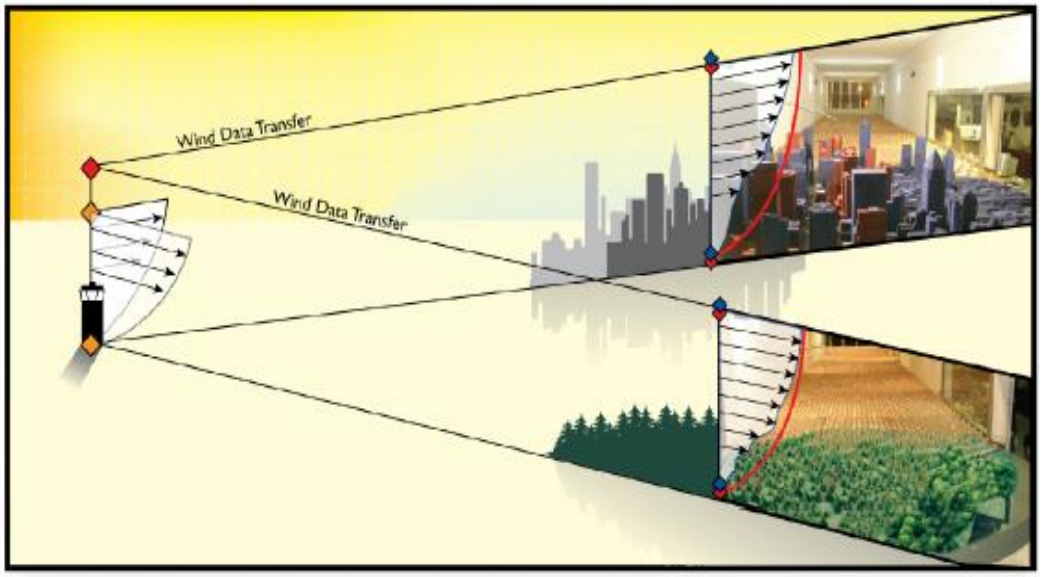

Figure 2-10 Transfer of wind velocity from suburb to city zone [38]

The department of wind energy at the Technical University of Denmark **[41]** has developed a PC program WAsP (Wind Atlas Analysis and Application Program) which could be used to predict the wind climate in different terrain surface zones. This program includes several models which can simulate the terrain environment of real cases and air flow above these areas. This program is widely used by the Met office and gives wind data for different terrain zones close to the sites.

In this research, both Power-law and Logarithmic-law are used to do the velocity transformation. This is because at the research height of this project (10 m and 30 m from the ground), compare to the power law, the Logarithmic law shows a better wind velocity result; while power law is used to transform hourly mean wind data between different terrain zones (introduced in Section 3.1) and to obtain some characteristic parameters used in the Logarithmic law.

Generally, in this research, the experiment results from the wind tunnel experiment is compared with Power-law and gives some characteristic parameters for the atmospheric boundary layer around suburban areas; these parameters are used in the

Logarithmic-law function and gives the velocity result at different height. These velocity results are compared with the wind tunnel experiment results and then used to set the input wind velocity of the CFD models.

2.3.2 Wind direction

The direction of wind is another important parameter which is considered in this research. For each topographical location, the wind blows from some directions have more frequency than the other directions; and the frequencies of each input wind directions are different in different U.K. regions. This different frequency will lead to different energy output for wind turbines used around the houses in these cities. At same position around same houses, the velocity the wind are different when wind blows from different directions; as the hourly output energy of the turbine is based on the hourly mean velocity in the position, when the wind blowing from different directions, the hourly output energy of the turbine is different. The annual energy production (AEP) of the turbine in each position is the sum total of the turbine's hourly output energy in the position, thus, the frequency of input wind affects the output energy directly. Chapter 3 and Chapter 7 give some results about the wind direction analysis.

The wind direction could be confirmed by the weather data statistics. In this research, as selected wind sites are quite close to the centre of nearby cities (distance less than 28 km), the wind direction record from the weather site is used as the wind direction of suburban area of the city directly.

2.4 Theory of topographical characteristic

As mentioned above, the wind record from different topographical zones should be transformed to analysis the wind energy in different zones. This section shows some literature review about how to estimate the wind energy resource at locations with no historical wind records.

2.4.1 Topographical characteristic

Before introduce the estimation of the wind energy at the locations, the topographical characteristic of the location should be described. In general, there are 3 main topography effects on the wind: roughness, shelter, and orography [8]. For each effect, there is one or more parameters show the grades of the effect and could be used in further analysis, introduced below:

2.4.1.1 Roughness

The roughness of the location is determined by several factors, which mainly includes the size of the area, the elements contained in the area, etc. for land surface, the possible factors include vegetation, houses and soil surface. A length scale called "roughness length z_0" [36] shows the level of the roughness element, defined as:

$$z_0 = 0.5 \cdot \frac{H \cdot S}{A_H} \quad \text{(Eq.2-23)}$$

In Eq.2-23, H is the height of the roughness element, S is the cross-section facing the wind, and A_H is the horizontal area per roughness element.

For the case of windbreaks with no porosity (e.g. a row of houses), the equation could be changed by letting $S \sim H \cdot L$ and $A_H \sim l \cdot L$. Thus, Eq.2-23 changes to:

$$z_0 = 0.5 \cdot \frac{H^2}{l} \quad \text{(Eq.2-24)}$$

In the area of wind resource, the roughness length has relevant relationship with the characteristics of the terrain surface; and based on this relationship, the terrain areas could be divided into 4 roughness classes. As an approximation, the roughness length is between 1/10 and 1/30 of the typical height of roughness element on the ground [36]. **Figure 2-11** shows the details of these classes [8].

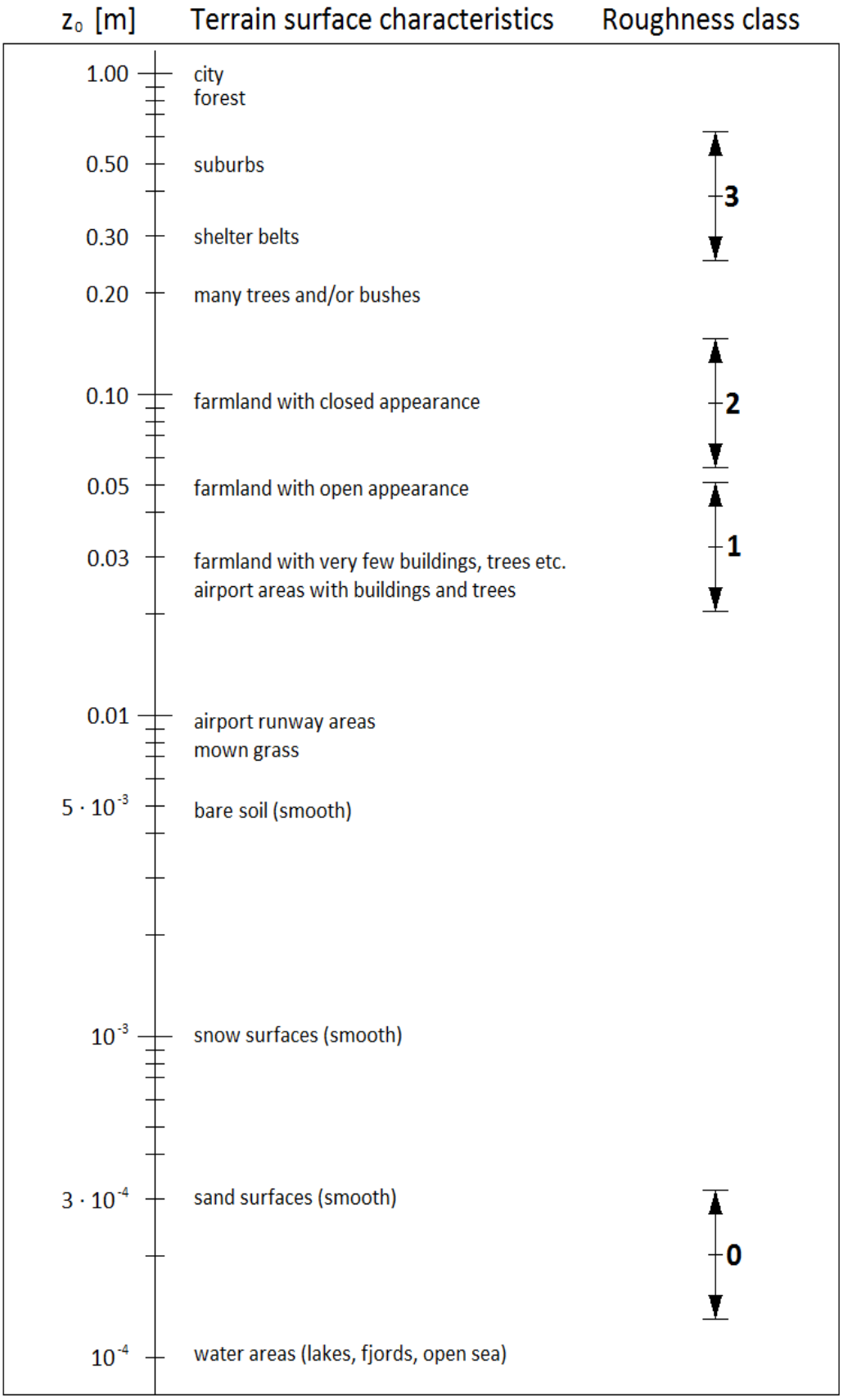

Figure 2-11 roughness class for different terraon surface [8]

Attention should be paid that for some area with very large z_0 (e.g. city centre terrain), a displacement height d needs to be used. This is because; when the windbreaks are close together, these windbreaks could be considered as a whole and the flow is lifted over them. Based on ESDU 82026 [40], the displacement height is the height above ground at which wind velocity is achieved zero. In the area where d is used, the vertical roughness height should be $d+z_0$.

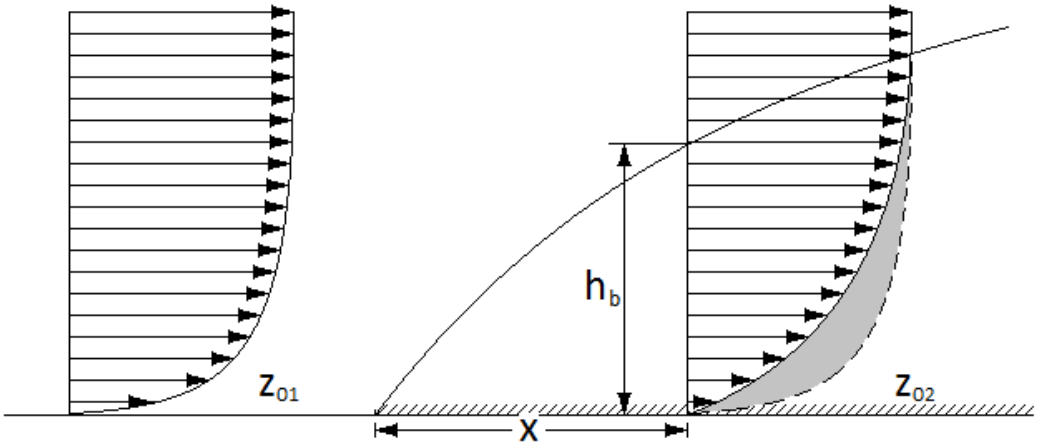

Figure 2-12 change of wind flow on different roughness terrace [8]

It should also be mentioned that the roughness class of a site depends on the sectors around it, for most of the time, the sectors around the site should not be consider as homogeneous because there might have some roughness change in the sector [8]; **Figure 2-12** shows the wind flow change on different roughness class. In this plot, z_{01} is the roughness length before the roughness change, and z_{02} is the roughness length after the change. The effect of the roughness to the wind velocity decreases with increasing height from the ground. At or above a certain height at any particular distance downstream of a roughness change, the effect of the change is not felt. The height is known as internal boundary layer height h_b. Similarly, the wind velocity below h_b depends on the roughness with in the distance x, but not on the roughness further away.

The confirmation of the boundary layer height h_b and distance x is very important in the analysis of roughness, because above the height h_b, the roughness with distance less than x does not need to be considered; only the roughness farther than x affects the wind above height h_b.

$$\frac{h_b}{z_0'}\left(\ln\frac{h_b}{z_0'}-1\right)=0.9\frac{x}{z_0'} \qquad \text{(Eq.2-25)}$$

Eq.2-25 gives the relationship between x, h_b and roughness lengths of the change [8]. In this equation, z_0' is the larger one of the two roughness length before and after the change. For the four roughness classes (0 to 3), there is a plot shows the relationship between x and h_b, as shown in **Figure 2-13** [8].

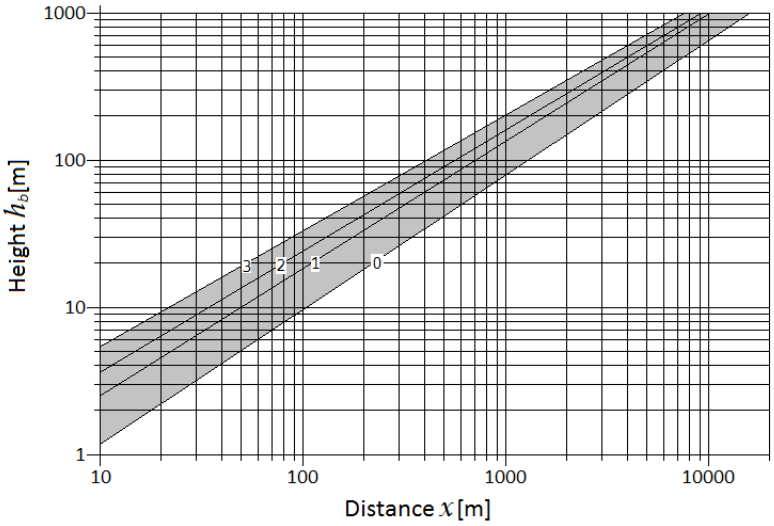

Figure 2-13 h_b vs x for different roughness class [8]

2.4.1.2 Shelter

In the area behind house or other obstacles in a terrain, the velocity of the wind would be decreased; and this relative is defined as shelter. There are several factors affect the relationship between the obstacle and the position close to it, as shown in **Figure 2-14**, which includes:

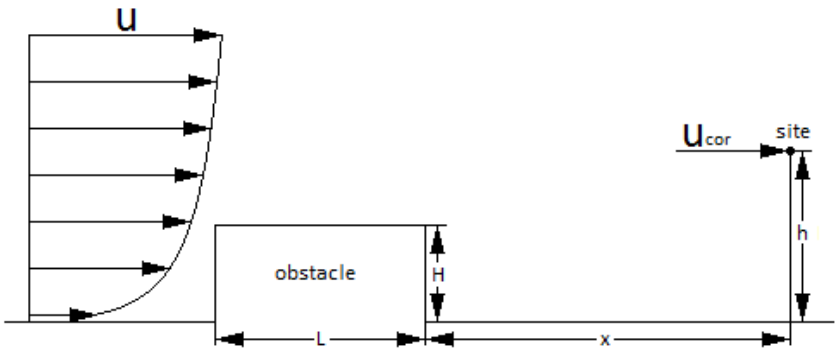

Figure 2-14 factors between obstacles and nearby sites

The distance from the obstacle to the site (x);

The height of the obstacle (H);

The height of the point at the site (h);

The length of the obstacle (L);

The porosity of the obstacle (P_{obs})

Table 2-5 setting of obstacle porosity [8]

Appearance	Porosity of obstacle
Solid (wall)	0
Very dense	≦0.35
Dense	0.35 – 0.50
Open	0.50 – 1.00

Generally, the porosity of the obstacle shows how dense the windbreaks are. The setting of this parameter could be changed with the class of the windbreaks, i.e. building could be set equal to 0 and trees could be set as 0.5, while for a house row with space between them of one third the length of a building is set as 0.33. **Table 2-5** shows the setting of this parameter for different appearances.

In **Figure 2-14**, the mean wind velocity at the site which is affected by the shelter is shown as u_{cor}, and the following equation shows the relationship between u_{cor} and the mean wind velocity before the shelter (u):

$$u_{cor} = u \cdot \left(1 - R_2 \cdot R_1 \cdot \left(1 - P\right)\right) \qquad \text{(Eq.2-26)}$$

In Eq.2-26, R_1 and R_2 are two empirical parameters decided by the position of the site from the obstacle, given by Perera in 1981 [43]. R_1 is defined in percent as shown in **Figure 2-15**, and R_2 is defined with the following equation:

$$R_2 = \left(1 + 0.2\frac{x}{L}\right)^{-1} \text{ for } \frac{L}{x} \geq 0.3\text{; and } R_2 = 2\frac{L}{x} \text{ for } \frac{L}{x} \leq 0.3 \qquad \text{(Eq.2-27)}$$

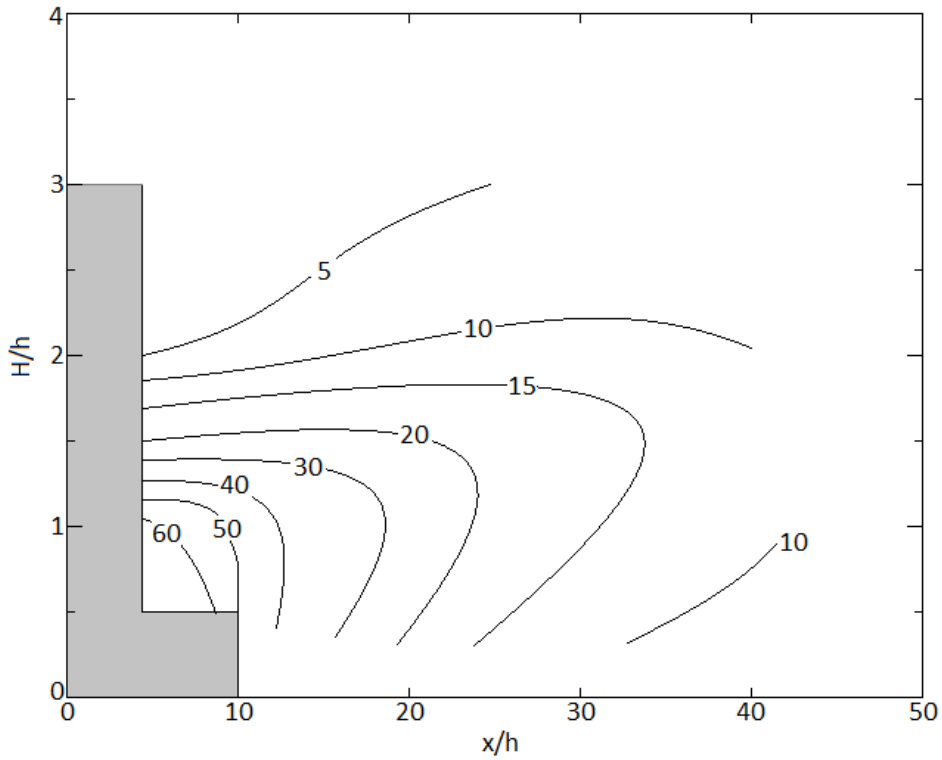

Figure 2-15 empirical parameter for near obstacle site position [43]

2.4.1.3 Orography

Orography is another topographical characteristic which affects the flow of the wind, which includes the landform around the site, e.g. hills, cliffs, etc. The experiment of Taylor and Teunissen, 1987 [44] gives some relationship between the height and shape of the hill and the wind flow around it; the wind velocity would increase at the top of the hill and decelerate near the foot. However, for different positions, it is often difficult or impossible to determine the wind resource with simple equations. In this research, the effect of the orography is not included.

2.4.2 Weibull parameters

Based on the historical wind records from the weather stations, the frequency of annual hourly mean wind velocity are distributed according to the Weibull

distribution [45]. In this theory, *f(u)*, the frequency of wind velocity u follows the following equation:

$$f(u)=\frac{k}{A}\left(\frac{u}{A}\right)^{k-1}e^{-\left(\frac{u}{A}\right)^{k}} \qquad \text{(Eq.2-28)}$$

From this equation, two Weibull parameters are defined as scale parameter *A* and the shape parameter *k*: *A* is related to the mean value of the wind velocity and *k* is determined by the shape of the Weibull curve. Some more details about this relationship can be found in Subsection 3.1.3.

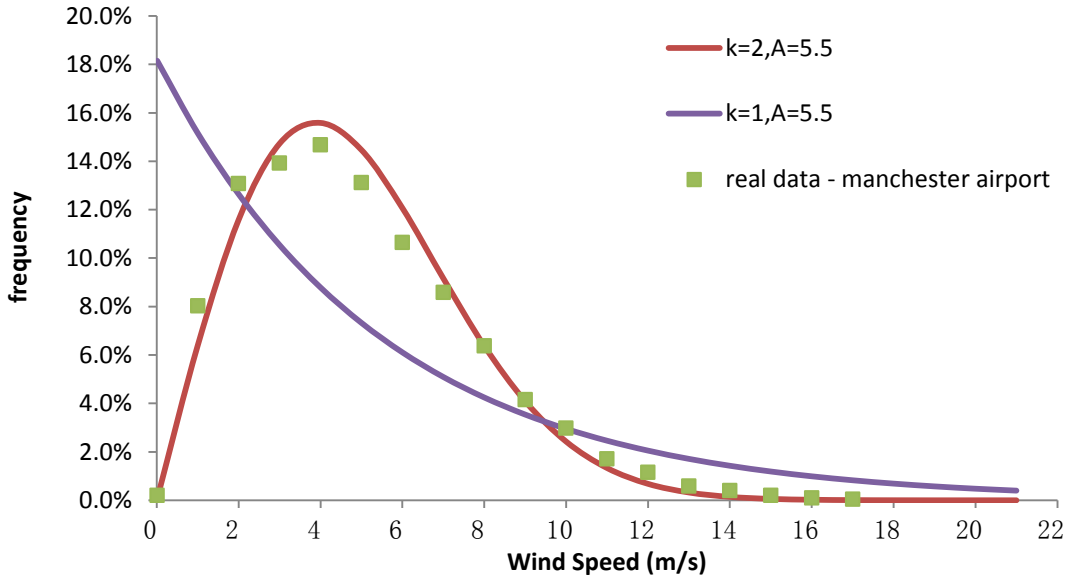

Figure 2-16 Weibull curve with different *k*

Figure 2-16 shows three Weibull curve with different *k* values. Of these curves, the curve with *k*=2 is known as "Rayleigh distribution" and most common used to describe the frequency of wind data [8]. The green cubes in this plot are the annual frequencies of different hourly mean wind velocities in Ringway airport (Manchester), and the two solid Weibull curves have same mean wind velocity value (*A*) but different *k* values (1 and 2). From the plot it could be found that the real data is between the two solid curves and more close to the curve of *k*=2, which means the value of k is between 1 and 2 and around 2. The detail of calculating the Weibull could be found in Section 3.1.2. After calculation, the Weibull parameter in Manchester airport is A=5.1, k=1.86; it should be mentioned that the Weibull curve is a trend line, it can't show all the details of the record. In records from weather stations,

more than one group of such parameter may be given to show the wind frequency in different heights, directions and roughness class. In following Chapter 3, the Weibull parameter in different cities is given as a result of historical wind record analysis.

The Weibull parameter of different weather stations and airport in U.K. could be found in their wind records, which includes several groups with different roughness level.

CHAPTER 3

3 Historical Wind Record Analysis Result

This chapter describes the historical data analysis results about the hourly mean wind velocity and direction in the main cities of 7 regions at 10 m height above the ground. The selection of this height is because most of the small wind turbines would be in or near this height if they are fixed on top of the U.K. buildings [47]. By integrating the data of these cities, the velocity, direction and energy of the wind in these regions are showed as several charts and tables. Due to the length limit of the chapter, these charts and tables are set as the appendixes of this report for further check.

In order to show more intuitionistic results, in this chapter, the terrain roughness class of building area is shown as 3 classes: town (class 3, z_0=0.3 m, d=5 m, α= 0.23), country with closed appearance (class 2, z_0=0.1 m, d=0 m, α= 0.2), and airport (class 1, z_0=0.02 m, d=0, α= 0.16), the setting of these parameter is based on the report of ESDU 85020 [71]. The data source and city locations are as Section 2.1 shows, all historical wind records for different terrain class used in this research are based on the data sources from the U.K. Met Office sites [5].

3.1 Wind Velocity and Direction Analysis

As mentioned in Section 2.3, for different terrain zones, the wind data are different. The historical data from the weather sites only shows the climate of wind at same terrain surface zones close to the sites. In order to get the wind data for different roughness classes close to the cities, some data transformations from weather sites to the three roughness class zones need to be finished. **Table 3-1** shows the value of

roughness parameters z_0 of weather sites used in this research. These data could be found from the homepage of U.K. Met office [5].

Table 3-1 roughness parameter of selected weather sites

Nearby city	Weather site	z_0 [m]	d [m]	α
Birmingham	Birmingham	0.01	0	0.16
London	Heathrow	0.02	0	0.16
Bristol	Horfield	0.3	5	0.23
Manchester	Ringway	0.01	0	0.16
Edinburgh	Turnhouse	0.01	0	0.16
Leeds	Church Fenton	0.05	0	0.17
Glasgow	Abbotsinch	0.02	0	0.16

The method of transform wind data is introduced in Section 2.3. In this project, Power-law is used to finish the wind velocity transformation between terrain roughness classes. This is because of the wind record should be extended to height higher than gradient height, and for large cities the predicted gradient height is 457 m from the ground [82]. In this project, the wind record are extended to 500 m height, at this height, Power-law shows a more accurate result than Logarithmic-law.

Based on the wind profile Power-law, the mean wind velocity at height z from the ground could be calculated with this function [60]:

$$\bar{u}_z = \bar{u}_{ref} \cdot \left(\frac{z-d}{z_{ref}-d} \right)^{\alpha} \qquad \text{(Eq.3-1)}$$

In this function, $\bar{u}_{ref}$ is the mean wind velocity from the weather site record, z_{ref} is the height of the anemometers used by the weather site (10 m from the ground); the exponent value of the Power-law (α) is different for different roughness levels, and the relationship between roughness length and α could be found in ESDU 72026 [70]. The exponent value of the Power-law used in this research is as above shown. With Eq.3-1, the hourly mean wind velocity in different roughness classes could be calculated.

For example, the mean wind velocity at 500 m height from ground in Horfield is

$$\bar{u}_{500} = \bar{u}_{ref} \cdot \left(\frac{500-5}{10-5} \right)^{0.23} \qquad \text{(Eq.3-2)}$$

While the mean wind velocity at 500 m height from ground in country zone (class 2) close to Bristol is

$$\bar{u}_{500} = \bar{u}_{cou} \cdot \left(\frac{500-0}{10-0} \right)^{0.2} \quad \text{(Eq.3-3)}$$

Together with these two equations, it gives:

$$\bar{u}_{cou} = \bar{u}_{ref} \cdot \frac{\left(\frac{500-5}{10-5} \right)^{0.23}}{\left(\frac{500-0}{10-0} \right)^{0.2}} \approx 1.32 \cdot \bar{u}_{ref} \quad \text{(Eq.3-4)}$$

In above equation, $\bar{u}_{cou}$ is the mean wind velocity at 10 m height from ground in country zone (roughness class 2) close to Bristol.

For each terrain zones in the 7 U.K. cities, the hourly mean wind velocity is transformed from the sites' historical weather records. After the transformation, the hourly mean wind velocities in each roughness class are sorted and counted with the value of the velocity; the result of the count is then averaged to get the annual average hour count of each wind velocity in that terrain zone.

Three kinds of charts are given to show the characteristic of hourly mean wind velocity and directions in those cities. Of all 7 cities, Bristol has the medium annual average wind velocity; the charts of this city are shown as example. Appendix B shows the charts for all the 7 cities.

3.1.1 Frequency of hourly mean wind velocity

In each terrain zone, the annual average hour of each wind velocity is divided by the annual total hour count; the result shows the annual frequency of each velocity. In this project, these frequencies are marked as several percentage values. The chart of hourly mean wind velocity frequency is made by setting the hourly mean wind velocity as the X axis value and frequency as Y axis value, respectively. **Figure 3-1** shows the chart of frequency of hourly mean wind velocity in Bristol as an example. In this chart, the frequency of different hourly mean wind velocity in different terrain

zones are marked with 3 kinds of point markers; around each group of markers, there are also three Weibull distribution curves which show the relationship between hourly mean wind velocity and the frequency of each wind velocity. **Table 3-2** shows the Weibull parameter for different zones in all 7 cities.

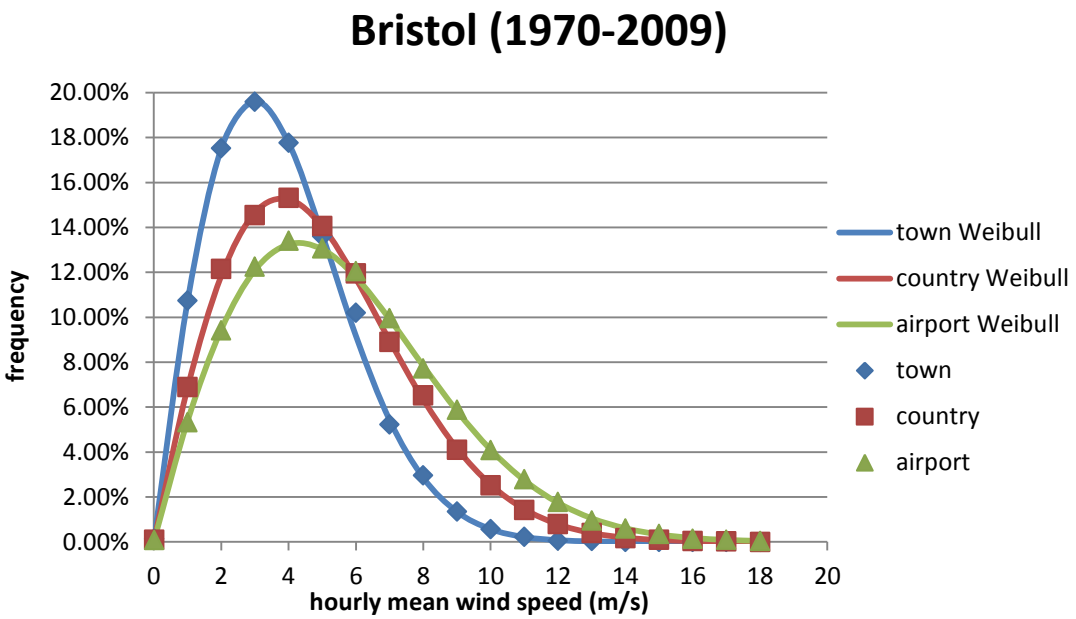

Figure 3-1: frequency of 10 m height hourly mean wind velocity in Bristol (1970-2009)

Table 3-2 Weibull parameter of different zones in 7 cities

City	town zone	country zone	airport zone
London	A=3.4, k=1.88	A=4.3, k=1.88	A=4.9, k=1.88
Bristol	A=4.3, k=1.95	A=5.5, k=1.94	A=6.3, k=1.93
Birmingham	A=3.8, k=1.83	A=4.9, k=1.83	A=5.6, k=1.83
Manchester	A=3.8, k=1.80	A=4.8, k=1.79	A=5.5, k=1.79
Leeds	A=3.8, k=1.82	A=4.8, k=1.82	A=5.5, k=1.82
Edinburgh	A=4.5, k=1.48	A=5.7, k=1.47	A=6.5, k=1.47
Glasgow	A=4.0, k=1.56	A=5.1, k=1.56	A=5.8, k=1.54

It could be found that for each city, the shape parameter *k* in different terrain zones are almost the same, and the scale parameter *A* is changed. Take the city of Bristol for example, as shown in **Figure 3-1**, all three curves have the same basic shapes, but different in the value of wind velocity in peak frequency; the zone more close to the city centre has a lower wind velocity. This difference is due to the terrain difference of these zones, as the zone more close to the centre of the city, there are more buildings and other obstacles, which will depress the velocity of the wind. In **Figure 3-1**, these depress show as higher frequency of small mean wind velocity.

Due of some mistake of the wind data record, for most of the case, the annual hour count is less than 8760 (365×24).

3.1.2 Cumulative frequency of hourly mean wind velocity

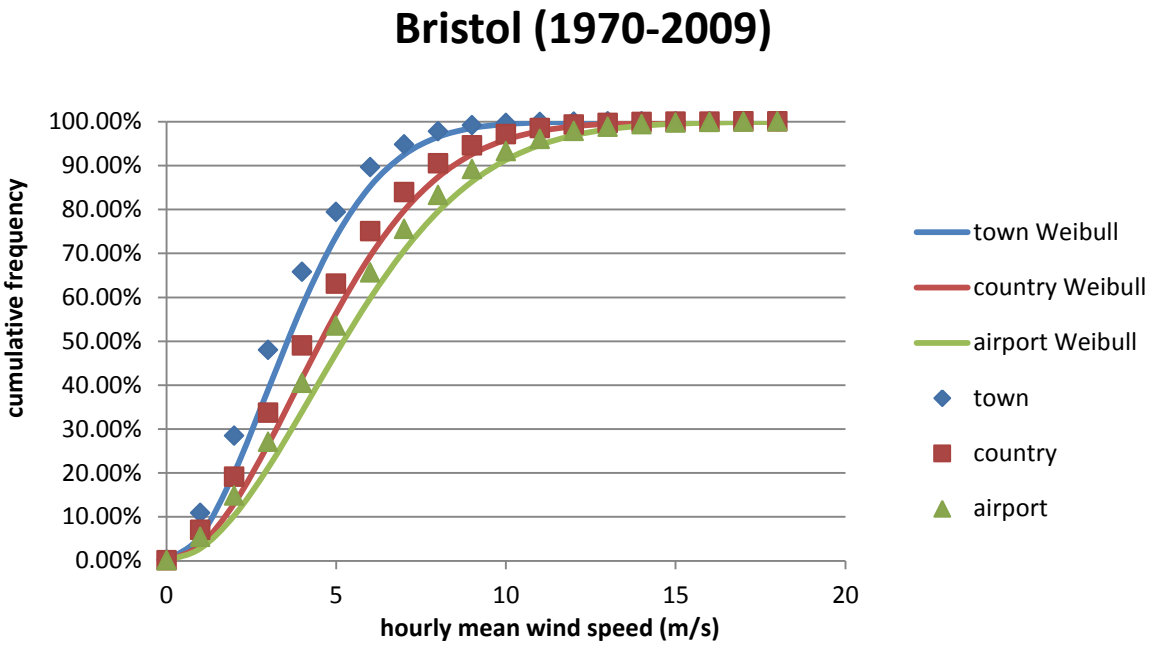

Figure 3-2: Cumulative frequency of 10 m height hourly mean wind velocity in Bristol (1970-2009)

This kind of chart is made based on the frequency of hourly mean wind velocity. In this chart, the series value on Y axis is the cumulative frequency of wind velocity equal or lower than corresponding velocity values on X axis. Which means the percentage value on Y axis shows the frequency of wind velocity no more than each velocity on X axis. **Figure 3-2** shows the chart for cumulative frequency of hourly mean wind velocity (point markers) in different terrain zones near Bristol. This chart could be used to show the percentage of time for which wind turbines will operate. Alternatively, the small turbines have cut-in speeds of 3 m/s to 4 m/s, as **Table 2-3** shows; based on this, the cumulative frequency value correspond to 3 m/s on X axis shows the percentage of time for which small wind turbines will not operate. **Table 3-3** shows the stop time percentage for wind turbines in different zones in the cities.

Table 3-3 stop time percentage of small wind turbines for different zones in the cities

City	town zone	country zone	airport zone
London	65.02%	48.73%	40.64%
Bristol	47.99%	33.69%	27.07%
Birmingham	57.02%	41.74%	33.72%
Manchester	57.17%	42.36%	35.25%
Leeds	57.36%	42.70%	34.63%
Edinburgh	48.46%	37.26%	32.60%
Glasgow	54.71%	41.54%	36.03%

From **Table 3-3**, in town zone of each city, small wind turbines will not operate for more than half of the time; this is due to the low wind velocity at 10 m height in this terrain. In country and airport zones, the operate time for wind turbines is longer than town zones (51% to 64% in country, and 59% to 72% in airport). However, although the larger wind velocity takes less percentage of the time, it does not means the energy in these time periods is small. Subsection 3.2.1 compares the cumulative frequency of wind velocity and energy in the wind.

Weibull parameters are also used to show the cumulative frequency, the cumulative Weibull distribution F **[45]** is given as:

$$F(u) = 1 - e^{-\left(\frac{u}{A}\right)^k} \qquad \text{(Eq.3-5)}$$

In **Figure 3-2**, the cumulative Weibull distribution curves are shown as solid lines, which give the probability of wind velocity not exceeding corresponding value. Compared with the cumulative frequency record (point marker), the cumulative Weibull distribution curves show lower value. This is because although the Weibull parameters were calculated as best fitting to the frequency distribution of hourly mean velocity (as shown in **Figure 3-1**), there are still some different between the real data (point marker) and Weibull curve. When the Weibull parameters are applied to the cumulative frequency distribution (shown in **Figure 3-2**), the difference would also be cumulated, shown as the error between the point markers and the Weibull curve.

Based on Eq.3-5, the wind data could be fit to the cumulative Weibull distribution and then determine the two Weibull parameters. Eq.3-5 can be changed to:

$$-\ln(1 - F(u)) = \left(\frac{u}{A}\right)^k \qquad \text{(Eq.3-6)}$$

Take the natural logarithm (ln) value on both side of Eq.3-6, it gives:

$$\ln(-\ln(1-F(u))) = k\ln u - k\ln A \qquad \text{(Eq.3-7)}$$

Setting ln(-ln(1-$F(u)$)) as the Y axis value and ln$u$ as the X axis value, Eq.3-7 could be consider as a linear function; taking the wind data into Eq.3-7, it shown as Weibull probability plot [49]. **Figure 3-3** shows the Weibull probability plot of Bristol as an example.

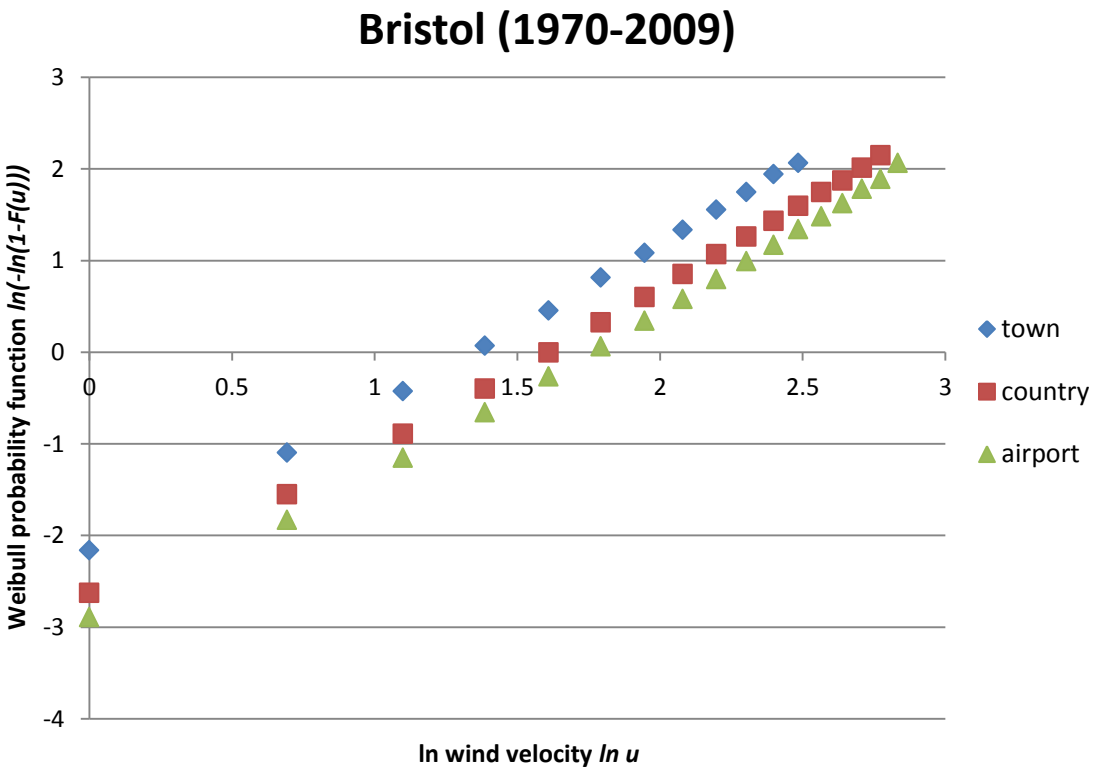

Figure 3-3 Weibull probability plot for Bristol (1970-2009)

Based on this plot, Weibull parameters could be calculated by ordinary least squares linear regression. This kind of graphical method is named "Weibull Probability Plotting" [84] and is one of the main graphical methods used to estimate the Weibull parameters.

Although the graphical method above could be used to estimate the Weibull parameters, the probability of error in the results is high because the parameter estimation is done with functions of wind speed and probability, not with the actual data. A better method to estimate Weibull parameter is "Maximum Likelihood Estimator (MLE)" [83]. For a random sample of size n, x_1, x_2 … x_n are the individuals

of this sample. The probability density function of this sample is $f_x(x;\theta)$ in which θ is a unknow parameter

The joint density of the n random variables is a function of θ, this function is named likelihood function [83], shown as:

$$L = \prod_{i-1}^{n} f_{x_i}(x_i;\theta) \quad \text{(Eq.3-8)}$$

The Maximum Likelihood Estimator value of θ (θ_{MLE}) is the value of θ that maximizes L. Because of the logarithm function is a kind of monotone increasing function, the value of θ that maximizes $Log\ L$ is the same as θ_{MLE}; comparing to get the maxima of L, it is easier to get the maxima of a logarithm function. Often, but not always, θ_{MLE} is a solution of

$$\frac{dLogL}{d\theta} = 0 \quad \text{(Eq.3-9)}$$

Applying the MLE to estimate the Weibull parameters, with Weibull distribution function (Eq.3-5), Eq.3-8 would be changed to:

$$L(u_1, u_2, ..., u_n, k, A) = \prod_{i=1}^{n} \left(\frac{k}{A}\right)\left(\frac{u_i}{A}\right)^{k-1} e^{-\left(\frac{u_i}{A}\right)^k} \quad \text{(Eq.3-10)}$$

The maxima of k and A could be got with following functions:

$$\frac{\partial \ln L}{\partial k} = \frac{n}{k} + \sum_{i=1}^{n} \ln u_i - \frac{1}{A}\sum_{i=1}^{n} u_i^k \ln u_i = 0 \quad \text{(Eq.3-11)}$$

$$\frac{\partial \ln L}{\partial A} = \frac{-n}{A} + \frac{1}{A^2}\sum_{i=1}^{n} u_i^k = 0 \quad \text{(Eq.3-12)}$$

On combining these two above equations and eliminating A, it gives:

$$\frac{\sum_{i=1}^{n} u_i^k \ln u_i}{\sum_{i=1}^{n} u_i^k} - \frac{1}{k} - \frac{1}{n}\sum_{i=1}^{n} \ln u_i = 0 \quad \text{(Eq.3-13)}$$

This equation could be solved and get the value of k. Once the value of k is determined, the value of A could be calculated with Eq.3-12 as:

$$A = \frac{\sum_{i=1}^{n} x_i^k}{n} \quad \text{(Eq.3-14)}$$

3.1.3 Analysis about wind direction of the cities

The wind record from the weather station used in this project includes the direction details of the hourly mean wind. Generally, there is no information available about difference in wind direction between the weather station and the town. Thus, the hourly mean directions of the wind in the city/town zone are considered to be the same as the wind at weather station close the city. In each historical weather record, the direction of the hourly wind is divided into 36 sectors, each sector includes 10 °; this classification is also used in this project, north is set as 0 °, east is 90 °, etc. And for each sector, the hourly mean velocities of the wind are classified with their values, there are three grades: less than 4 m/s (wind turbines stop), 4 ~ 14 m/s (turbines operating), and more than 14 m/s (cut out speed for some turbines). **Figure 3-4** shows the wind frequency distribution at different zones in Bristol.

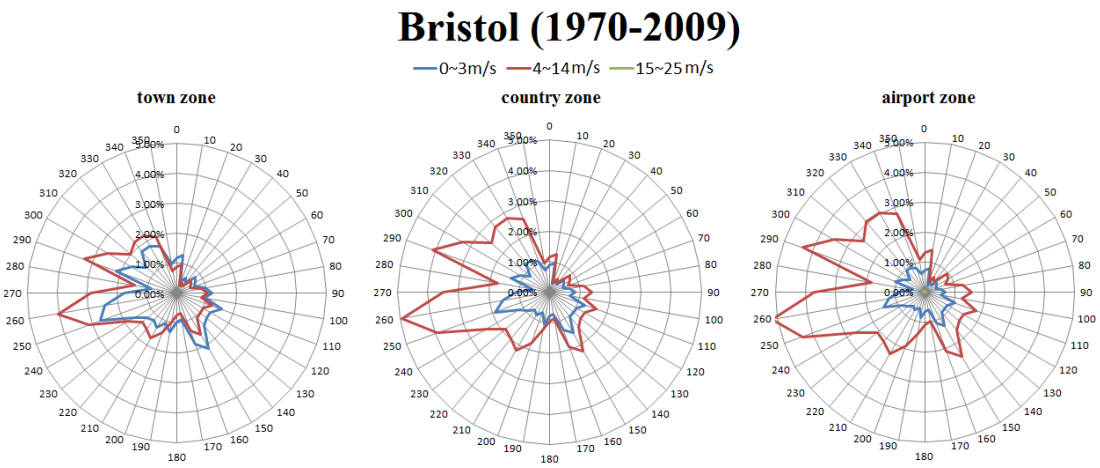

Figure 3-4: Wind frequency distribution in Bristol (1970-2009)

It could be found that for each city, the shape of wind frequency distribution is nearly the same between different zones; and the size of each velocity grade changes with the zones. The size of 1 ~ 3 m/s grade reduces with the distance from the centre of the city, while the 4 ~ 14 m/s grade increases its size with the same distance. And for all cities, the frequency of 15 ~ 25 m/s grade is always too small to be plot. The plots of all the 7 cities are list as Appendix C.

3.2 Potential Wind Energy

In considering how to estimate how much energy could be produced by the wind turbines, the wind resource at the 7 cities need to be identified. As the work of the wind turbines is to extract kinetic energy from the wind, transform it to mechanical energy and then to electrical energy. The power (P) and power density (E) are used to show the power level of the wind. The power in wind is defined as Eq.2-2, and the mean power density of the wind shows the average energy flux per unit area of the flow [8], given as:

$$E = \frac{1}{2}\rho u^3 \qquad \text{(Eq.3-15)}$$

For each terrain zone in each city, the hourly mean wind power density should be defined. This is achieved by applying Eq.3-15 to different hourly mean wind velocity through the years. **Table 3-4** shows the wind power density for different wind velocity. With these result, the energy in the wind could be analysed in three ways: cumulative frequency plot, average wind energy density, and wind power density frequency distribution plot.

Table 3-4 wind power density for different wind velocity

Wind velocity (m/s)	1	2	3	4	5	6	7	8	9
Power density (W/m^2)	0.602	4.816	16.26	38.53	75.26	130.0	206.5	308.3	438.9
Wind velocity (m/s)	10	11	12	13	14	15	16	17	18
Power density (W/m^2)	602.1	801.3	1040	1323	1652	2032	2466	2958	3511

3.2.1 Cumulative frequency of wind energy density

In different terrain zones of each city, the power density of each wind velocity is timed with the annual average hours ($f(u) \times 8760$), the result is the energy density in the wind. After all wind energy densities are calculated, the total wind energy density is given. The energy density for each velocity is divided by this total value and gives the energy density frequency of each u value.

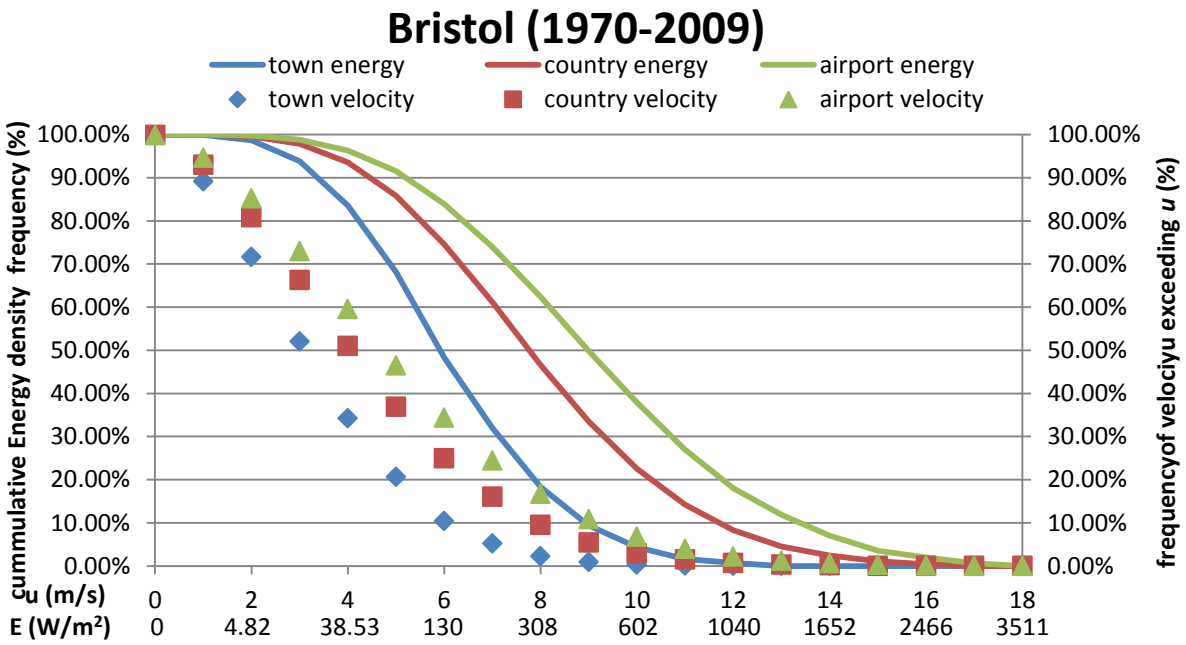

Figure 3-5: Cumulative frequency of wind energy density in Bristol (1970-2009)

The cumulative frequency of wind energy density gives the probability of the wind energy density exceeding the value *u* with power density *E*; the result for different zones near Bristol is shown in **Figure 3-5** (solid lines). The probability of wind velocity exceeding the value u is also shown in this figure (point markers); the value 1 minus the cumulative velocity frequency gives this value.

It should be mentioned that there is a limitation to analyse the wind power with the hourly mean wind velocity, as the mean wind velocity during an hour might not give correct mean power. This is because the instantaneous wind power varies with the cube of the instantaneous wind velocity; for different wind records, even though the hourly mean wind velocities are the same, the instantaneous wind velocity during the hour might be different, and these differences would lead to a different output wind power. And also, in environments with different temperature and air density, the output power of the wind turbine would be different. The wind turbine power curves should attempt to deal with these factors with some corrections. In this research, these factors are ignored.

Compare the two kinds of markers in **Figure 3-5**. It could be found that the wind power density affects the energy in the wind more than the operating time. For example, in town zone of Bristol, the wind velocity exceeds 4 m/s for only 34% of the total time,

but this period of time represents 84% of the energy in the wind. The range of wind velocity represents majority of wind energy could be found out based on this plot.

Table 3-5 Principal energy produced wind velocity and wind power density in U.K. cities

City	Town zone		Country zone		Airport zone	
	u **(m/s)**	***E*** **(W/m^2)**	***u*** **(m/s)**	***E*** **(W/m^2)**	***u*** **(m/s)**	***E*** **(W/m^2)**
London	2.58 ~ 7.33	10~237	3.42 ~ 9.39	24~498	4.04 ~ 10.8	40~758
Bristol	3.37 ~ 8.93	23~429	4.46 ~ 11.7	53~964	5.20 ~ 13.4	85~1449
Birmingham	3.06 ~ 8.52	17~372	4.09 ~ 11.1	41~823	4.71 ~ 12.7	63~1233
Manchester	3.09 ~ 8.68	18~394	4.05 ~11.1	40~823	4.67 ~ 12.8	61~1263
Leeds	3.07 ~ 8.57	17~379	4.02 ~ 10.9	39~780	4.62 ~ 12.5	59~1176
Edinburgh	4.31 ~ 13.2	48~1385	5.50 ~ 15.5	100~2242	6.18 ~ 16.2	142~2560
Glasgow	3.60 ~ 12.0	28~1040	4.73 ~ 13.8	64~1582	5.43 ~ 15.2	96~2114

Table 3-5 shows the result of this analysis in different zones of the cities, these wind velocities shown correspond to 10% and 90% of the energy in the wind, which means 80% of the wind energy is contained in the velocity range shown in this table; the wind power density ranges of these velocities are also included in this table. The range of wind power density in this table is used in Subsection 3.2.3 to grade the power density direction distribution plots. For further work, these wind velocity results will give some suggestions to the wind turbine selection in these areas.

3.2.2 Average wind power density

For each terrain, the average wind power density reveals the hourly potential wind energy in the site; it is calculated by averaging all the hourly wind power density. The results for all the zones of the 7 U.K. cities are listed in **Table 3-6**.

Table 3-6: historical wind power density of U.K. cities at 10 m height

City	Town zone	Country zone	Airport zone
London	34 Wm^{-2}	68 Wm^{-2}	101 Wm^{-2}
Bristol	67 Wm^{-2}	138 Wm^{-2}	206 Wm^{-2}
Birmingham	49 Wm^{-2}	104 Wm^{-2}	155 Wm^{-2}
Manchester	50 Wm^{-2}	101 Wm^{-2}	151 Wm^{-2}
Leeds	49 Wm^{-2}	99 Wm^{-2}	148 Wm^{-2}
Edinburgh	111 Wm^{-2}	212 Wm^{-2}	288 Wm^{-2}
Glasgow	72 Wm^{-2}	146 Wm^{-2}	211 Wm^{-2}

As **Table 3-6** shows, although there is some different, the values of historical wind power density of the cities at 10 m height are poor, especially in the town zone; this is due to the low wind velocity at that height in the city centre zone. However, these results only shows the average level of the wind power in the sites, the energy output of the wind turbines is not based on these data.

3.2.3 Plot of wind power density direction distribution

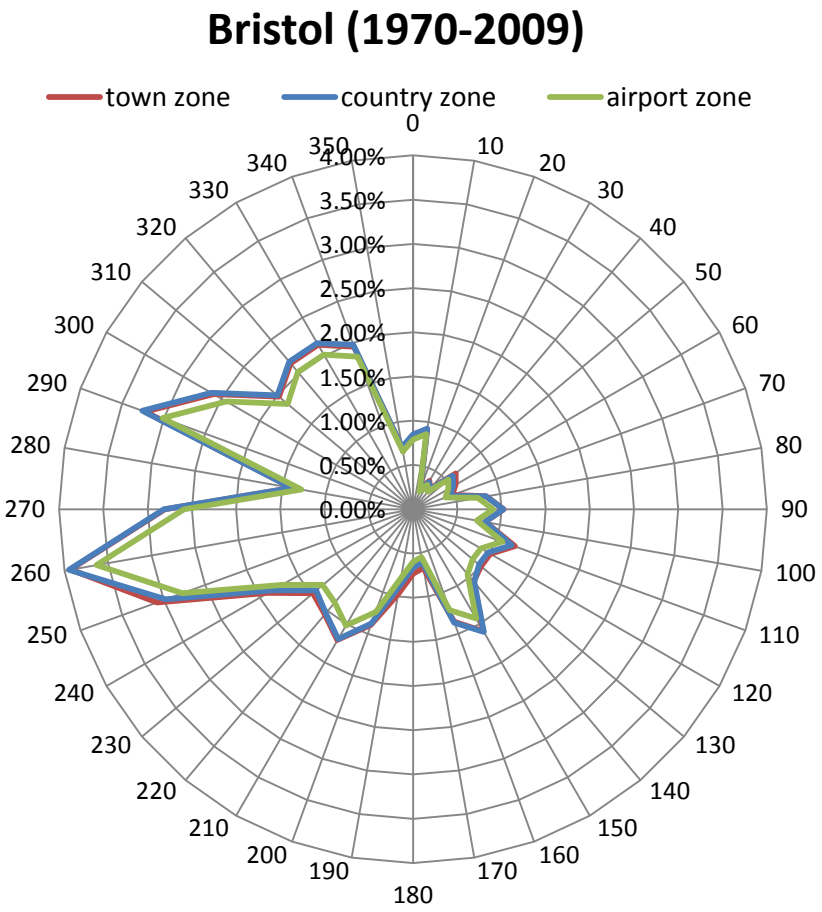

Figure 3-6: wind power density frequency distribution in Bristol (1970 - 2009)

The wind power density direction distribution plot is almost the same as the wind direction distribution plot; the only different is that the analysed data is the hourly wind power density rather than the velocity of the wind. Based on **Table 3-5**, the values could be divided counted in 3 grades: power density with less than 10% of energy in wind, 10% ~ 90% of energy in wind (majority part), and more than 90% of energy in

wind. Of these three bands, the first one (less than 10 %) contains too small energy which is hard to be used by the turbines, while the hour count for the last one (more than 90%) is small, which leads to a small energy output. Most of the wind energy is included in the majority part. **Figure 3-6** shows the majority part plot in different zones in Bristol as an example.

From the plots of each city, the wind energy direction distribution is quite close to the shape of wind direction distribution for turbines' operating grade (4 ~ 14 m/s) in **Figure 3-4**. In Chapter 6, the frequency of different input wind directions are used as one of the factors that affect the energy output of wind turbines in different fixed positions. Based on these two kinds of plots, the main wind direction and energy direction could be found out, which could help to confirm and optimize the working positions of the wind turbines. Appendix D includes the plots of all the 7 cities.

3.3 Wind Turbine Output Energy Analysis

In order to determine the annual energy production of different wind turbines, the above wind calculations results were combined with the published power curves of some selected wind turbines. In this thesis, 14 wind turbines which could be used in environment around buildings are calculated. **Table 2-3** shows the information of these turbines.

Of all these wind turbines, Turby and Quiet Revolution are vertical axis wind turbines (VAWT), while the others are horizontal axis wind turbine (HAWT). Comparing these two kinds, the VAWTs are more used in the wind system of high buildings; because of they have a better chance of withstanding the strong wind shear predicted to exist on the roof of the building **[24]**; but HAWTs are cheaper. The advantages of both kinds of wind turbines should be considered in the selection.

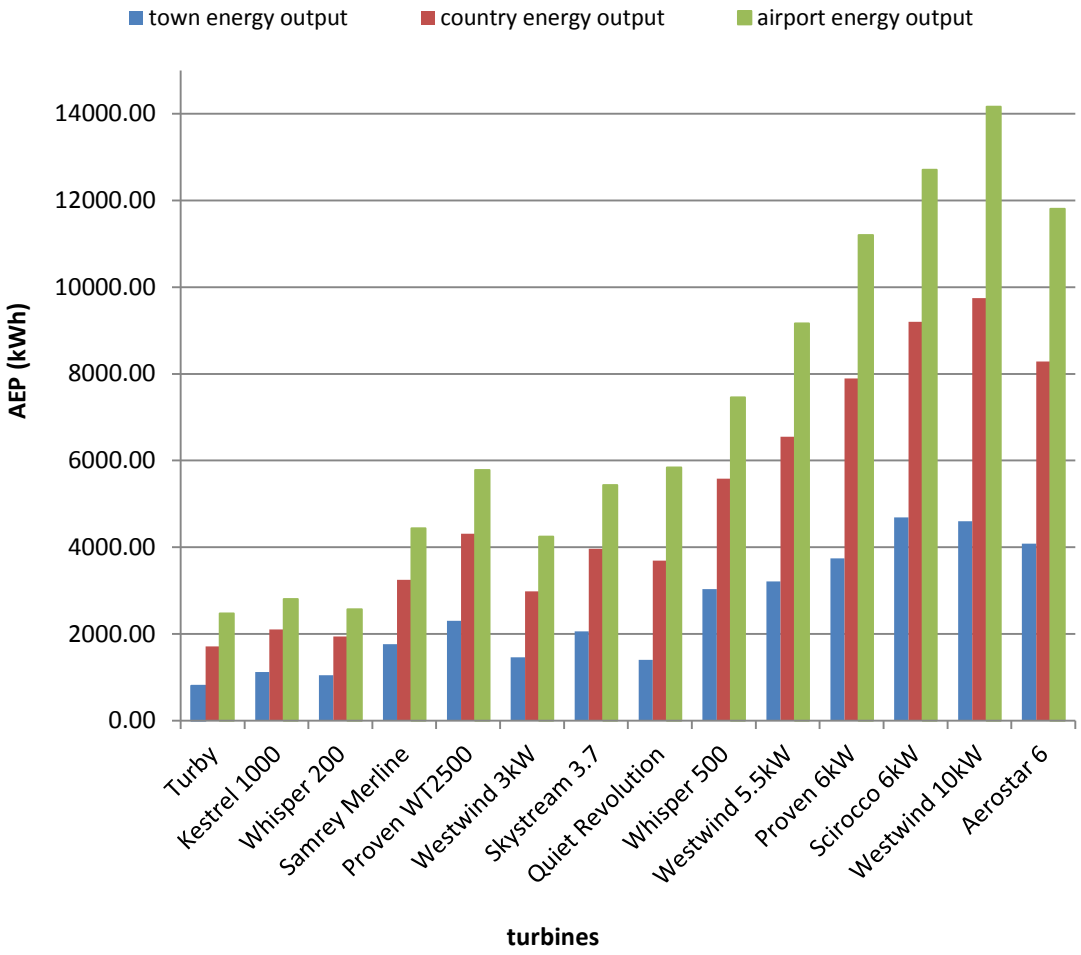

Figure 3-7: AEP of turbines at 10 m height in Bristol (1970-2009)

Figure 3-7 shows the expected annual energy production (AEP) values of each wind turbine at different terrain zones in U.K. based on the data value above. It could be found that the town AEP values shown in **Figure 3-7** is much larger than the actual average AEP of wind turbines used in Warwick wind trial (59.3 kWh) and predicted average AEP of wind turbines used in same trial (190.1kWh) [81] . The main reason of this different is that the wind turbines used in Warwick wind trial (includes Ampair 600 230, StealthGen D400 etc. [81]) are small turbines with rated power less than 1000 W, which are smaller than the turbines used in this project. The lower rated power makes the total AEP in Warwick wind trial less than the values in **Figure 3-7**. However, till now there are no wind trials results for the turbines of same size and type used in this project; in further research, the expected AEP of turbines could be improved if trial results of same type of turbines are given.

The turbines in **Figure 3-7** are list according to their swept area (shown in **Table 3-7**). Dividing these AEP values with the swept area of each turbine respectively and working hours (24×365), the hourly mean power in each square meter (p) of these wind turbines could be got. The result in different zones in Bristol is as **Table 3-7** shows.

Dividing the rated power of selected wind turbines with the rotor area of each turbine, the rated power in each square meter (p_{rat}) of these wind turbines could be calculated; results shown in **Table 3-7**. Compared with the rated value, the p values of all the three roughness zones are small. Also, the expected AEP results shown in **Figure 3-7** are based on the hourly mean wind velocity and power curve only, some other factors (e.g. turbulence, yaw performance, wind shading etc.) which might decrease the output power are not considered; the result should be even worth if these factors are taken into consideration. Based on this performance, all selected wind turbines cannot work on well with the wind source at 10 m height in Bristol.

Table 3-7 hourly mean power in each square of turbines in Bristol

Wind Turbine	Rotor area $[m^2]$	p_{rat} $[W/m^2]$	Town $[W/m^2]$	Country $[W/m^2]$	Airport $[W/m^2]$
Turby	5.3	471.70	17.33	36.90	53.37
Kestrel 1000	7.07	176.24	18.11	33.94	45.35
Whisper 200	7.55	137.62	15.84	29.35	38.86
Samrey Merline	9.62	282.12	20.99	38.59	52.69
Proven WT2500	9.62	332.64	27.34	51.22	68.69
Westwind 3kW	10.75	294.42	15.57	31.72	45.11
Skystream 3.7	10.87	248.39	21.67	41.66	57.16
Quiet Revolution	13.6	465.44	11.76	31.01	49.05
Whisper 500	15.9	208.36	21.79	40.11	53.59
Westwind 5.5kW	20.43	255.51	17.98	36.63	51.28
Proven 6kW	24.63	243.61	17.36	36.61	51.97
Scirocco 6kW	23.76	252.53	22.54	44.25	61.12
Westwind 10kW	30.19	337.86	17.41	36.90	53.61
Aerostar 6	35.26	283.61	13.23	26.86	38.28

After the AEP of each wind turbine is calculated, the result was compared with the annual electricity consumption of a household. This shows how many wind turbines are required to support enough electricity used by the household. It could be found that the U.K. annual average domestic electricity consumption is 4,831 kW per household [9]. Base on this data, the numbers of wind turbines required by each household in Bristol are list in **Table 3-8.** Appendix E keeps all the results.

Table 3-8: required turbine number at Bristol

Wind Turbine	Town zone	Country zone	Airport zone
Turby	6.0	2.8	2.0
Kestrel 1000	4.3	2.3	1.7
Whisper 200	4.6	2.5	1.9
Samrey Merline	2.7	1.5	1.1
Proven WT2500	2.1	1.1	0.8
Westwind 3kW	3.3	1.6	1.1
Skystream 3.7	2.3	1.2	0.9
Quiet Revolution	3.5	1.3	0.8
Whisper 500	1.6	0.9	0.6
Westwind 5.5kW	1.5	0.7	0.5
Proven 6kW	1.3	0.6	0.4
Scirocco 6kW	1.0	0.5	0.4
Westwind 10kW	1.0	0.5	0.3
Aerostar 6	1.2	0.6	0.4

It could be found that in town and country zones, more than one small wind turbines are required to produce enough energy for a household; this gives a problem because the area around each house is limited and it is not possible to set so many wind turbines in area around houses. However, all the turbines could produce more energy if there is more wind power; a possible way is to heighten their fixed position, which will upgrade the AEP of the turbines and thus reduces the required number.

Based on the Domestic energy consumption by fuel and end use 2010 [51] and the CO_2 emission factor of each fuel [51], the annual CO_2 emission of a household could be calculated; as **Table 3-9** shows. This is also the carbon emission reduction of a household if the house changed to a ZEB. From this table, electricity is a large CO_2 emitter of all fuels used in house. So wind turbine could have important impact on CO_2 if it produces significant amount of electricity.

Table 3-9 annual CO2 emission of a household

Domestic CO_2 emissions 2010 (kg per household)

End use	Gas	Oil	Solid fuel	Electricity	total
Space heating	2058.42	298.66	85.25	309.35	2751.67
Water heating	882.44	105.41	24.98	357.83	1370.66
Cookinf/Catering	67.60	0.58	0.50	151.25	219.92
Lighting and Appliances	0.32	0	0	1727.51	1727.83
Total	3008.79	404.64	110.72	2545.94	6070.08

The economic and carbon payback time of the wind turbines should be considered before selecting a wind turbine system. The cost of the system is divided by the cost of electricity it produced, and the result is the economic payback time. Due to the new

F.I.T scheme announced by the U.K. government, from April 2010, the mainly payback times of wind turbines are as **Table 3-10** shows [9].

Table 3-10: Expect payback time of wind turbines [50]

Turbine type	AEP (kWh)	Economic payback time (Year)	Carbon payback time (Year)
3 kW	5460 - 9800	5 - 11	0.4 – 0.7
5kW	10920 - 21100	4 - 10	0.2 – 0.4
10 kW	18200 - 41800	3 - 9	0.1 – 0.2

The carbon payback time of a wind turbine is the amount of CO_2 emissions in its manufacture, and the length of time it takes for the wind turbine to save that [50]. The carbon emissions of different wind turbines (include the tower and other fittings) are different, but all of them are under 2 tonnes of CO_2 [50]. In U.K., the CO_2 emission factor of electricity is 0.53 kg/kWh [51], and the AEP of wind turbines are list in **Table 3-9**; the annual saved CO_2 could be calculated by multiplying the two data. The CO_2 emission of manufactures the turbine (2 tonnes) is then divided by the result to get the carbon payback time; as **Table 3-10** shows.

Comparing the AEP value in **Table 3-10** and the chart in **Figure 3-7**, it could be found that the AEP in **Table 3-10** is much larger than the AEP of corresponding wind turbines in **Figure 3-7**. This is because the AEP value in **Figure 3-7** is based on the wind record at 10 m height from ground, while **Table 3-10** is based on some laboratory record from the manufacturers of the turbines, the C_p of the wind turbines is low that reduces the AEP value. If some of the above wind turbines are selected to be used in the wind energy system, the fix position would have to be higher than 10 m, to achieve AEP values close to those shown in **Table 3-10.**

It should be mentioned that the CO_2 emissions include the manufacture of both turbine and the fittings, as the life of the fittings would be much longer than the turbines (about 2 or 3 times), the carbon payback time of the wind turbines themselves would be even shorter.

Based on the historical wind data analysis in U.K., for a single small wind turbine, the wind power at 10 m height above the ground is not strong enough to produce enough electricity for the consumption of a typical household. The main reason for this

situation is the small wind turbine size and the low wind velocity at most locations. Because of this, large wind turbines at higher level should be considered to be added into the wind energy system. However, the fee of installing and preserving large turbines is always too much for a single householder, and the energy output is always more than the energy requirement of a house. Thus, sharing large wind turbines between several houses appeared to be a good idea. Alternatively, getting the locations with enhanced wind velocity suitable for small wind turbines around the house groups can be considered.

As Section 2.4 mentions, the air flow around the houses will be affected by the house and other obstacles. As a result of this effect, compared with other locations, some areas around the houses may have higher wind velocity and less turbulence intensity, which is more suitable for the setting of wind turbines. The aim of this project is to find these locations around different type of house in U.K., if they exist. However, the analysis till now only shows the hourly mean wind velocity in large area (more than 1 km^2) **[5]**, no more detail analysis about the area around different house groups is given. The following chapters shows the CFD and wind tunnel experiments about wind flow around house groups; with the result of these experiments, the optimal positions around different house groups would be given, which could optimize the wind turbine energy output results.

CHAPTER 4

4 CFD Analysis

Computational Fluid Dynamics (CFD) is used to model the wind around the buildings because it is easier and quicker than measuring the wind flow in reality or in a wind tunnel model. Simply, it is about the solving and analysing of fluid flow problems with numerical techniques. In this project, by setting wind velocity as the input data on the inlet plane, the model would give the distributions of airflow around the buildings, and the results would change with different velocity and direction of the input wind. After that, the results could be integrated with the wind character in different areas around U.K., and then the optimum position near the building in these areas could be found.

This Chapter describes the CFD method used in this research. Section 4.1 introduces the typical houses used as the prototype of the CFD model, and Section 4.2 shows the setting of the CFD models. Finally Section 4.3 shows the methods to analysis the CFD results. The results of the CFD models are shown and analysed in Chapter 6.

4.1 The design of the model

In this section, some element about the design of the CFD model used in this research is introduced. The CFD models used in this project have similar geometry appearances with the U.K. house in full-scale. Three facets are included: the size of the house used in this model, the range of the house group, and the selection of CFD software.

4.1.1 Size of house model

The model is intended to be applicable in different areas around U.K., the base type of the house modelled should be the most popular ones. As Section 1.2 shows, the most popular house in U.K. is Semi-detached (two houses joined together), followed by Terrace (streets of house joined together in lows) and Detached (a house that is not connected to any other building). In this experiment, the site designs of the houses are based on policy about house extensions [12] and some satellite images from the Google Earth [10]. From the satellite images, Semi-detached and Detached houses are often situated in the same area and mixed together, and the building density of these two house types are similar to each other. Thus, in this simulation, only semi-detached house and terrace house are used in the model.

For different case, the sizes of the houses are always different from each other. The size of the house models in this research are based on the normal size of the houses in U.K. In this model, Semi-detached house is a 2 storey house designed for 2 households, with 6 m height and 96 m^2 floor spaces (8 m $\times$ 12 m); and terrace house is a line of 2 storey house designed for 20 households, the size of each household is 6 m height and 48 m^2 floor spaces (12 m $\times$ 4 m).

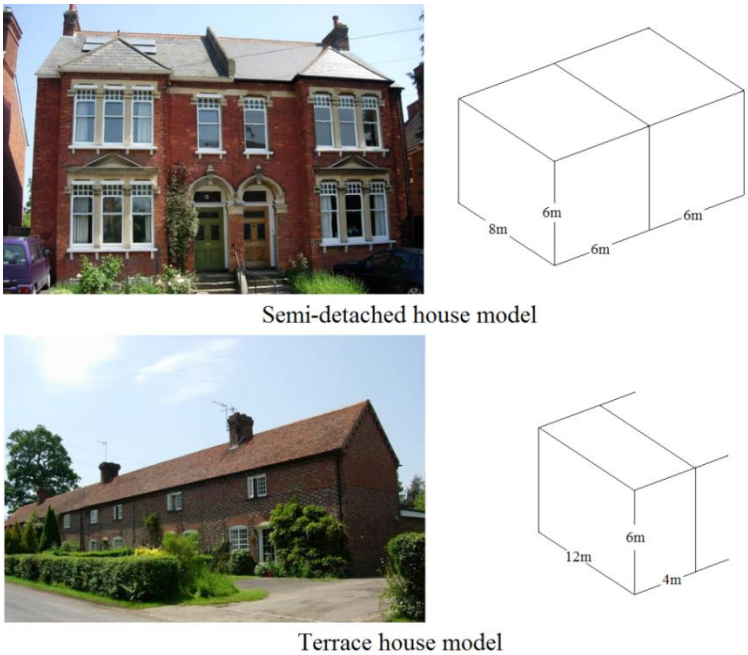

Figure 4-1 the view and dimensions of the house and model

Figure 4-1 shows the view of the house and the size of the model for each house type. For both semi-detached house model and terrace house model, the houses are reduced to square blocks.

It should be mentioned that the models do not show all details of the houses. The main different between the square block models used in this project and the real houses in U.K. is the shape of the roof: most of the real U.K. houses have pitched roofs and/or chimneys; while the models in this project are square blocks which make the roof flattop. These roofs may have different size and inclinations, the height to eaves might be lower than 6 m and to ridge might be higher than 6 m. In this project, 6 m is selected to show the approximate height of the houses. The length and width of the models are selected in similar way.

In this project, the different roof shapes would not affect the results of CFD and wind tunnel experiments. Base on the wind tunnel research from S.Rafailidis [85] and CFD report from G.Theodoridis & N.Moussiopoulos [86]; compared with flat-roof building, building with pitched roof would generate an additional vortex at roof level. The comparison of wind flow around pitched-roof building and flat-roof building is as shown in **Figure 4-2**. The scale and intensity of the vortex is different for different slopes of the roofs; in vertical profile, this vortex would not be higher than 2 times of the roof height [85].

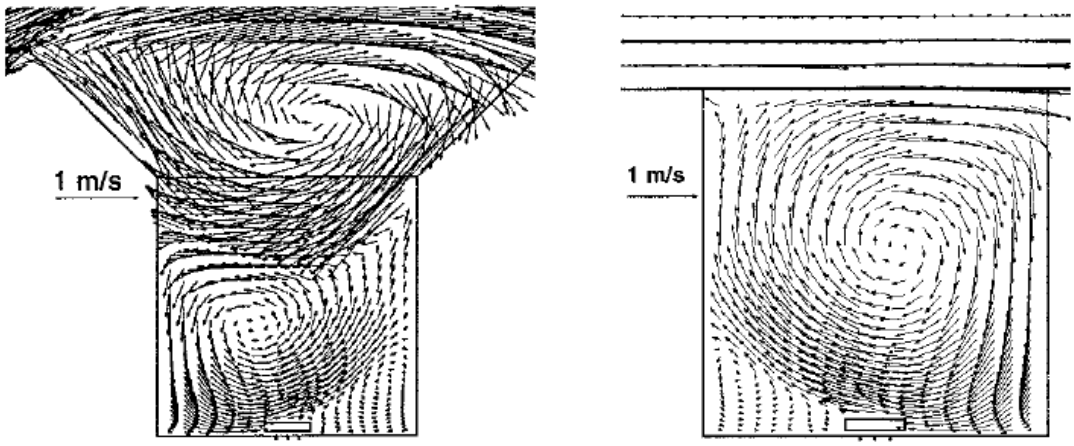

Figure 4-2 air flow around pitched- roof building and flat-roof building [86]

For most 2 story houses in U.K., the roof height would be less than 1.5 m [14]; which means the vertical scale of the vortex would be less than 3 m. Adding this scale to the average height of the model. The wind above building is influenced by the presence of pitched roof only within 9 m above the ground. In this research, the measured height of the wind vector is 10 m and 30 m height from the ground; at these heights, the shape of roof would not affect the vector results.

From the research of T.Kubota [87] and J.Kim [88], the flow in urban area is mainly affected by the building density .Because of this the aim of this experiment is to find the wind flow around different house groups with different building density: the models are intended to represent a small part of a large urban area of similar houses. The detail parts which are different between different actual houses are neglected in the model.

Besides the shape of the house, there always have some plants or other articles as small obstacles (e.g. shrubbery, outbuildings, garden fences, etc.) in the courtyard of the house. Because of the height of such obstacles are always lower than the half of the building height (3m), all these differences are not taken into account. For a zone with more obstacles, the roughness level should turn higher with the calculation introduced in Section 2.4.

4.1.2 Arrangement of the houses

For most of the time, the arrangement of the houses is related to the relief feature around them. For the design of house sites, the following three rules should be complied **[12]**:

- The communication of the houses should be fine: this means for each house, there should be at least one road connected with it.
- There should be enough personal space for each household: the house should have its own courtyard for parking etc.

- The relationship of each house should be suitable: this is mainly about the spaces between the houses. The distance between houses should not be too close for a better privacy, and not too far to keep down the cost of the land.

With these rules, the road in the models is designed as two-lane road with a 6 m width, and the width of the verge and footpath is set as 3 m [53]. The detailed design of area around semi-detached house is shown in **Figure 4-3**, and **Figure 4-4** shows the detail design of area around terrace house:

As shown in **Figure 4-3**, the area around each semi-detached house include a parking area in front of the house (5m), a garden at the back of the house (14m), and some space by the side of the house (2m). For Terrace house, there is often no parking area in front of the house and no space by the sides. Two house lines stand back-to back as a group. There is a one lane road between the two house lines in each group; the width of the one lane road is set as 3 m. two-lane roads are used to separate the house groups in the model

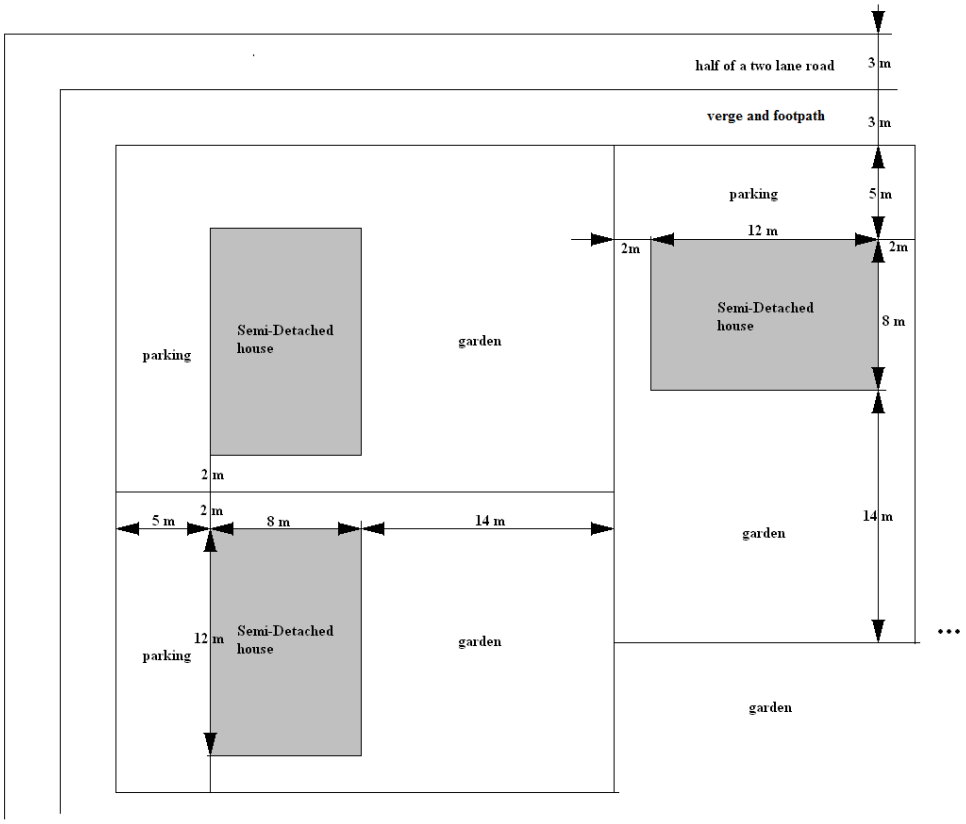

Figure 4-3 area around semi-detached house

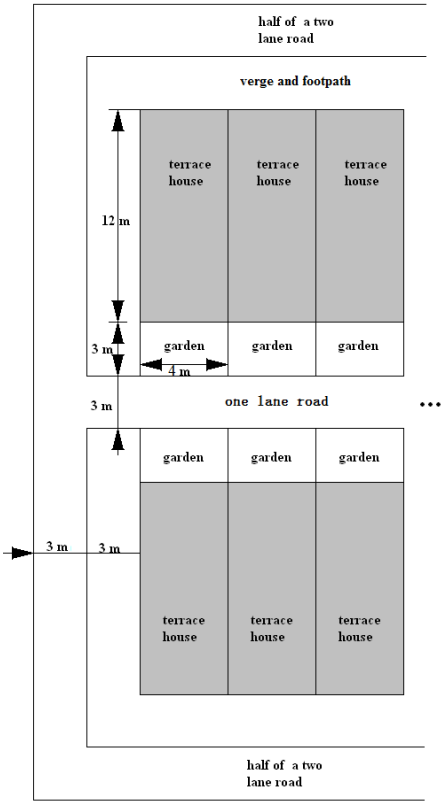

Figure 4-4 area around terrace house

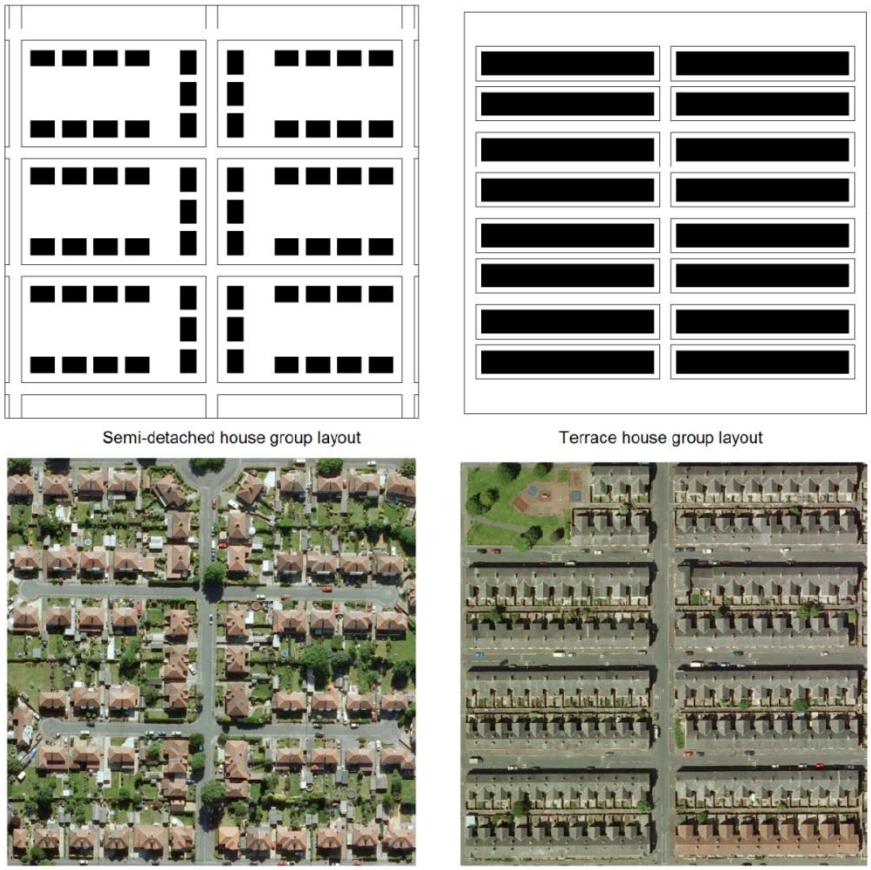

Figure 4-5 layout of house groups in this research

Figure 4-5 shows the layout of the houses as group, left plot for semi-detached house and right plot for terrace house. The houses are shown as some black squares, and separated with different groups by the road around them. The aerial photos of real house layouts are shown below each house type: left for the semi-detached house groups at Sale (53° 24′ 31.79″ N, 2° 20′ 25.68″ W) and right for terrace houses near Salford (53° 27′ 18.52″ N, 2° 14′ 29.08″ W). It could be found that the layouts of the models are similar to real layout of houses.

4.1.3 Selection of CFD software

There is lots of software used for CFD analysis, till now, the common used ones include PHOENICS, CFX, STAR-CD, FLUENT, etc. introduces as followed:

PHOENICS is the first commercial CFD package; CHAM is the developer. The name is the abbreviation of "Parabolic Hyperbolic or Elliptic Numerical Integration Code Series". This software could be used for the calculation of flow and heat transfer. Some more information and computed example of this software could be found from http://www.cham.co.U.K. and http://www.phoenics.co.U.K. .

CFX is the first commercial CFD package who passed the ISO9001. The developer is ANSYS. This software is developed to solve the industrial practical problem, based on this intention; exact results, abundant physical models and consumer expansibility are regarded as the basic requirement of CFX's development, which are also claimed to be the strongpoint of this software. Further information could be found on the website of this software http://www.ansys.com/Products/cfx .

STAR-CD is developed by CD-adapco. Initially, it is invented by professors from Imperial College, which is a computational programme for non-structured gradient; then, after reinforced by experts around the world in the areas of discontinuous gradient, slip gradient and gradient repair, STAR-CD is claimed to be one of the best

CFD software in gradient adaptability, steady account and convergence. Web address: http://www.cd-adapco.com .

FLUENT is another common used CFD software. The developer is Fluent, web address: http://www.fluent.com. With CFD software package, this software could simulate different kinds of fluid from incompressible flow to high-pressure flow. Basic on the technology of multi-computing methods and multi-mesh accelerate convergence; FLUENT is claimed to have good convergence rate and precision. The basic technologies of FLUENT include unstructured grid (e.g. Quad, Tri, Hex, Tet, Wedge, and Hybrid), self-adaption grid and physical model. All these make FLUENT widely used in nearly all areas of CFD.

As a whole, all the above software could be used to analysis the airflow around the buildings. In this research, FLUENT is used as the analysing tool. The reason of this selection includes 4 points as claimed below.

- Function and applicability: This software could model required situation.
- Good earlier-stage system and import data interface: FLUENT provides special software with the name GAMBIT, which could produce model and meshes easily. The data interface of FLUENT is also multifunctional, which could read the files from several kinds of software (e.g. AutoCAD, Pro/ENGINEER, etc.)
- Fault tolerance: If the value of the computing result is out of the normal limit, the software gives a warning and some possible reasons about the problem, which would help the user to improve the program.
- Applicability in different system environments: FLUENT is applicable to most kinds of operating system used now (UNIX, Windows, Mac, etc.)

4.2 The setting of the model

This section is mainly about the setting and running steps of the FLUENT model. For each house type, the model includes the model area as shown in **Figure 4-5**. With a consider that the analysis of the wind flow includes 36 directions (each 10 degrees in

a circle) and the buildings are symmetrical in x and y directions, the author gives 20 models to analysis all the case, each model expresses the instance of 2 opposite directions. These models are divided into 2 kinds: symmetry (0 ºand 90 º) and periodic (all the other directions).

4.2.1 Computational area

In this project, all the models are made with original size of the building groups. For each model, the computational domain should include 3 parts: upstream, central and downstream parts [54]. The inlet flow is changed in the upstream part, and can be defined as inlet flow (flow defined by the inlet function), approach flow (flow traveling from the inlet plane to the building models), and incident flow (flow at the same position of the buildings in an empty computational domain) [54]. **Figure 4-6** shows these flows and domain parts.

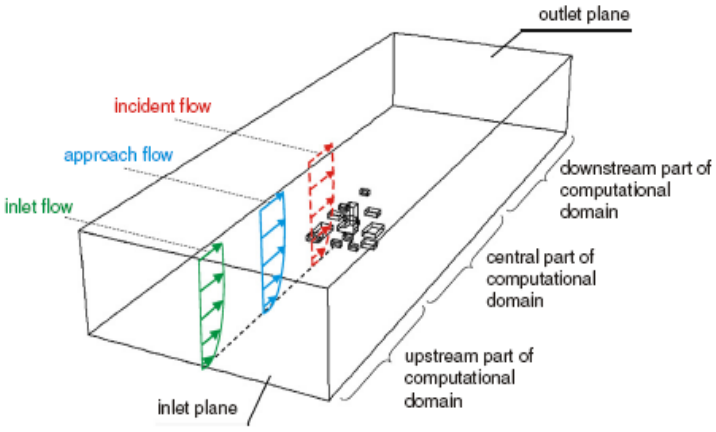

Figure 4-6 flow and indication at different parts in the computational domain for CFD atmosphere boundary layer simulation [54].

The necessary size of the computational domain depends on the size of the models. Generally, the position of inlet plane and outlet plane should be set with distance far enough from the models to give enough space for the upstream and downstream parts. In principle, the distance between the outlet plane and the last wall of the building group should be at least 10 times of the height of that building [48]. In this case, as the height of the building is 6 m, the distance should be more than 60 m. In this simulation, because some of the rotated models have different input wind direction, the inlet plane and outlet plane is set 100 m from the building.

For the central part of computational domain, which includes the models of the house groups, the flow around downstream houses are affected by the upstream houses. As Section 2.4 shows, for a position more than height *h* from the ground, there is a distance limit *x*; only terrains more than distance x away from the position affect the flow. The aim of this research is to find the flow of wind around buildings which is affected by same building types upstream with same building density. If the size of the central part is not large enough, the solved result at measured position with height *h* from the ground would not show the air flow affected by the upstream houses, but affected by the area before the building models. Due to this, for each height *h*, the model area should be large enough to make sure the distance from the upstream houses to the downstream houses is more than this limit *x* [8]. In this project, the research focus on the flow at height 10 m and 30 m from the ground, which is the normal setting height for small and middle size wind turbine could be used in suburban zones. Because of this, the distance limit is 20 m and 90 m for these heights, respectively. This means the flow at 10 and 30 m height is mainly affected by the roughness change at upwind 20 and 90 m distance away from it, respectively. In order to get the correct airflow result affected by similar house groups, the first row of house (start position of roughness change) should be at least 90 m away from the first measure position in the model. Based on this distance limit and the layout of the houses, the minimum size of representative domain of the house groups is given in **Figure 5-1**.

For symmetry models (0 ºand 90 º), the side face planes of the computational domain are set as symmetry face. This is like put the model between two mirrors; the models are intended to represent a small part of a large area of similar house. For each model, the distance between two symmetry faces should be enough for the house models.

For models with input wind direction from 10 ºto 80 º, the computational domain side face planes are set as periodic face. In such faces, the physical parameters at same position in different face are circularly repeated. Take velocity vector for example, the output velocity on one side face is assumed to be the input velocity on the other side face at same position. With such setting, the modelled house group is repeated with

same layout and airflow environment, and one of the repeated parts is shown in the model.

For both symmetry and periodic models, the side face is set at the centre of two-lane road by side of the models. For semi-detached and terrace house, the distance is 66 m and 45 m, respectively.

4.2.2 Mesh setting

After the computational area is set up, the whole area needs to be separated into lots of small cells; FLUENT would calculate the flows value on each cell based on the physical values of boundary conditions introduced in Subsection 4.2.4 and some model functions shown in Subsection 4.2.3. The results in all cells show the details of flow in the whole computational area. These small parts are named “mesh” in Gambit.

For a selected computational area, Gambit could build the mesh in Operation/Grid/ Volume. Scheme and Spacing should be set to finish the mesh building part.

The Scheme of the mesh includes mesh element and mesh type. For 3D model, 4 mesh cells are used, as shown in **Figure 4-7**, which are **(a)** tetrahedron or “tet”; **(b)** hexahedron or “hex”, prism with quadrilateral base; **(c)** wedge, prism with triangular base; and **(d)** pyramid. These cells are used to build the mesh area used in the CFD. In each model, one or more kinds of mesh cells are used. To different models, Gambit would build the mesh area with 3 mesh elements and 4 mesh types [55], introduced below:

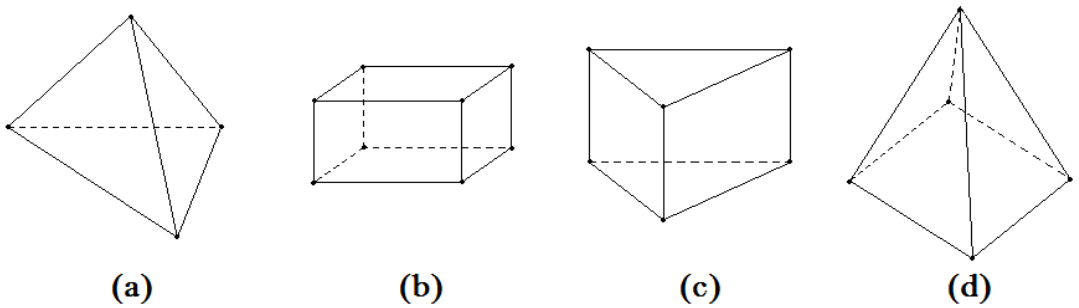

Figure 4-7 cells of 3D mesh in Gambit

Mesh element

- Hex: the mesh only includes hexahedron;
- Hex/Wedge: the mesh includes hexahedron and a spot of wedge;
- Tet/Hybrid: most of the meshes are tetrahedron, and the other three mesh cells are used if needed.

Mesh type

- Map: the mesh is built by regular structured grids, which utilizes regular hexahedron as mesh cell. Hex is used only in this type of mesh;
- Submap: the computational area is divided into several parts, each part is set as Map, and Hex is used only;
- Cooper: the mesh is built by unstructured grids, the nodes of the grid are irregularly distributes in the computational area. Hex and Hex/Wedge is used in this mesh type;
- TGrid: the mesh is built by blend grids, and the mesh element used in this type is Tet/Hybrid. This mesh type is always used in complicated model.

All these mesh types have their advantage and disadvantage. For different model, one of these 4 mesh types would be more suitable than the other. Explain below:

Map start with basic geometry. The cells in this kind of mesh are generated with similar size. Compared with other mesh types, the advantages of Map is their simplicity. For models with simple structure, the build of this type of mesh requires the least computation time. However, simplicity is also a disadvantage of this mesh type. First of all, due to the cells in this mesh have similar size; there are no areas with dense grids in this kind of mesh. In order to get more accurate result, the grids should be small enough in all mesh areas. As a result, for same model with same minimum grid size, there are more cells in Map than other mesh. This means more computing time is required for FLUENT to solve the result. Secondly, this mesh type is only suitable for simple models. For complicated models, the Map is hard to be generated.

Submap is an upgraded mesh of Map. In this mesh type, there are several Map meshes with different grid size. Compared with Map, some areas in Submap has more dense grids than the others; which means FLUENT could give more accurate results in the areas with dense grids. This mesh type saves more solve time than Map due to the simplified calculation in the areas with larger grid size. This mesh type also has some advantage: first, similar as Map, Submap is also suitable for models with simple structures only. Secondly, the mesh needs to be separated into several parts with different grid size; this zoning work requires more skilled operation and modelling time.

Cooper is a kind of unstructured mesh. Due to the cells in this mesh includes hexahedron and wedge, models with complicated structure could be made with this mesh type. This mesh could be easily generated by Gambit because it requires small user input and is well suitable to inexperienced users. The disadvantage of this mesh is that it requires more computing time and internal memory to finish the mesh. Also, the generation of this mesh might not be successful for some complicated models. This is because there might be some mistake when the computer finishes the mesh, sometimes it is not possible to solve these mistakes due to the low user input required.

TGrid is designed with both structured and unstructured grid and has the advantage of both grids. In inner regions of the model, the mesh is made of unstructured grid, while structured mesh is used in areas close to wall surface of the model. As a result of this, area close to wall surface is made of structured grid with good density, which made the air flow result close to wall surface more actually. While for the rest domain of the model, unstructured cells (most are tetrahedron) is used to build the mesh which made TGrid suitable for complicated models. The disadvantage of this mesh is that it is difficult to make and requires CFD expertise in setting the mesh properties to obtain the best result.

The Spacing of the mesh is used to decide the length of the edges of each grid, which affects the volume of each 3D grid. Gambit gives 3 ways to set the spacing:

- Interval Count: setup the count of interval in each edge of the volume, the mesh will be dense on small face and thin on large face;

- Interval Size: setup the size of the interval in each edge, all the grids would be the similar size;
- Shortest Edge %: select a percentage of the shortest edge as the length of the interval, and build the mesh with this length.

For this model, the element is set as Tet/Hybrid, and the mesh type is TGrid. The spacing is interval size with value 0.3 m, the volume of the tetrahedron mesh is about 0.045 m^3. This mesh volume is suitable for this model: not too larger which leads to error result, and not too small which cost too long computer time. With these setting, the computational area is separated into several millions of mesh cells, these cells are saved as mesh file. During the calculating part, the wind flow in these cell areas is calculated with FLUENT; and the results of mesh cells on selected positions are used to show the wind flow parameter at these positions.

4.2.3 Parameter definition

After read the mesh file, several parameters should be defined to run the model with FLUENT; which includes the solver type, the operating condition, the material, model selection, etc. the setting of these parameters rests with the condition of the model. In this case, the modelled fluid is air, and the flow could be considered as incompressible; flow and turbulence equations are used during the solution. The parameter is defined as **Table 4-1** shows; this table also explain the reason of these setting.

Table 4-1 defined parameter

Define/Models/Solver		**Explain [46]**
Solver	Segregated	Suitable for velocity less than 340 m/s
Space	3D	For 3D model
Time	Steady	Calculating till a steady-state solution is given
Velocity formulation	Absolute	For flow in most of the domain is not rotating
Gradient option	Cell-Based	Show the value in mesh cell centre
Define/Models/Viscous		
Model	k-epsilon (2 eqn)	Common used 2 equation turbulence model [64]
k-epsilon Model	Realizable	For normal stress, turbulence flows [64]
Near-Wall Treatment	Standard Wall Functions	For near wall area with low-Re number
Define/Materials		
Material Type	Fluid	the material in the calculating area
Fluent Fluid Materials	Air	Set the physical parameter of fluid as air

Based on the setting of similar simulation in ABL (atmospheric boundary layer) of urban areas [54], for the parameters not appear in **Table 4-1**, the default value of FLUENT is suitable for this case.

Of all the models in **Table 4-1**, the viscous models are the basic solve method used by FLUENT in this research. The mesh area of the house models simulates the air flow outside the houses. In general, there are two kinds of flow in this area: turbulence flow in most domains and laminar flow close to the wall of the building and ground. "Realizable k-epsilon Model" [90] and "Wall Function" are used by FLUENT to simulate the two kind of flow respectively.

"Realizable k-epsilon Model" is a viscous model with two functions about turbulent kinetic energy k_e and turbulent dissipation rate ε respectively [89]. This model is based on the Boussinesq hypothesis [33] which related the Reynolds stress to the mean velocity gradients as:

$$-\rho\overline{u_i' u_j'} = \mu_t\left(\frac{\partial u_i}{\partial x_j}+\frac{\partial u_j}{\partial x_i}\right)-\frac{2}{3}\left(\rho k_e+\mu_t\frac{\partial u_i}{\partial x_i}\right)\delta_{ij} \qquad \text{(Eq.4-1)}$$

In Eq.4-1, i or j shows the one of the three axis direction of Cartesian coordinates, which should be selected from (x, y, z); δ_{ij} is "Kronecker delta" (if $i=j$, $\delta_{ij}=1$; if $i\neq j$, $\delta_{ij}=0$); μ_t is the turbulent viscosity depends on the condition of the flow, defined as [89]:

$$\mu_t = \rho C_\mu \frac{{k_e}^2}{\varepsilon} \qquad \text{(Eq.4-2)}$$

In "Realizable k-epsilon Model", the transport equations about k_e and ε are [90]:

$$\frac{\partial(\rho k_e)}{\partial t}+\frac{\partial(\rho k_e u_i)}{\partial x_i}=\frac{\partial}{\partial x_j}\left[\left(\mu+\frac{\mu_t}{\sigma_{k_e}}\right)\frac{\partial k_e}{\partial x_j}\right]+G_{k_e}-\rho\varepsilon \qquad \text{(Eq.4-3)}$$

$$\frac{\partial(\rho\varepsilon)}{\partial t}+\frac{\partial(\rho\varepsilon u_i)}{\partial x_i}=\frac{\partial}{\partial x_j}\left[\left(\mu+\frac{\mu_t}{\sigma_\varepsilon}\right)\frac{\partial\varepsilon}{\partial x_j}\right]+\rho C_1 E\varepsilon-\rho C_2\frac{\varepsilon^2}{k_e+\sqrt{\nu\varepsilon}} \qquad \text{(Eq.4-4)}$$

In Eq.4-3, $\sigma_{ke} = 1.0$ [90]; G_{ke} is the generation of turbulence kinetic energy due to the mean velocity gradients [89], calculated as:

$$G_{k_e}=\mu_t\left(\frac{\partial u_i}{\partial x_j}+\frac{\partial u_j}{\partial x_i}\right)\frac{\partial u_i}{\partial x_j} \qquad \text{(Eq.4-5)}$$

In Eq.4-4, $\sigma_\varepsilon = 1.2$, $C_2 = 1.9$, C_1 could be calculated as [90]:

$$C_1 = \max\left(0.43, \frac{\eta}{\eta+5}\right), \text{ where } \eta = \left(2E_{ij}\cdot E_{ij}\right)^{1/2}\frac{k_e}{\varepsilon},\ E_{ij} = \frac{1}{2}\left(\frac{\partial u_i}{\partial x_j}+\frac{\partial u_j}{\partial x_i}\right) \quad \text{(Eq.4-6)}$$

In Eq.4-2, C_μ is computed from [90]:

$$C_\mu = \frac{1}{A_0 + A_S\frac{U^* k_e}{\varepsilon}} \quad \text{(Eq.4-7)}$$

$$A_0 = 4.04$$

$$A_S = \sqrt{6}\cos\phi$$

$$\phi = \frac{1}{3}\cos^{-1}\left(\sqrt{6}W\right)$$

$$\text{where } W = \frac{E_{ij}E_{jk}E_{ki}}{\left(E_{ij}E_{ij}\right)^{1/2}} \quad \text{(Eq.4-8)}$$

$$U^* = \sqrt{E_{ij}E_{ij} + \tilde{\Omega}_{ij}\tilde{\Omega}_{ij}}$$

$$\tilde{\Omega}_{ij} = \Omega_{ij} - 2\varepsilon_{ijk}\omega_k$$

$$\Omega_{ij} = \overline{\Omega}_{ij} - \varepsilon_{ijk}\omega_k$$

and $\overline{\Omega}_{ij}$ is the mean rate-of-rotation tensor viewed in a rotating reference frame with the angular velocity ω_k [50], this parameter shows the effect of rotating in this model.

"Wall Function" is a group of semi-empirical functions and formulas [91]. In the CFD model, the air flow of the cells close to the wall surface is affected by the viscosity force from the wall and the effect of turbulence is weak. Thus, the flow close to the wall surface should be considered as laminar flow. The "Standard Wall Function" in FLUENT is based on the research from Launder and Spalding [91] and widely used in industrial flows. Some layers of cells close to the wall surface of the model are named as transition layer; in this area, the air flow is considered as a transition from laminar to turbulence. It is assumed that the physical parameter on the bottom layer (which is closest to the wall) is same as the boundary condition of the wall, while the physical parameter on the top of the transition layer is same as the turbulence flow solved by realizable k-epsilon model. The wall function is used to relate the physical parameter of the top and bottom layers with each other, and thus give the physical parameter of the cells inside the transition layer [91]. Functions about momentum, energy and turbulence are included in the wall functions, and they are provided as default option in FLUENT.

4.2.4 Boundary condition

For different zone types in the model, the physical character is different; the boundary condition of the model is used to define these physical characters. For this case, the boundary conditions are linked to the main faces of the model shown in **Figure 4-6,** with following details.

- Air zone: fluid. This zone includes all account area of the model, the physical characters of the fluid depends on the material. For this case, the fluid is air.
- Solid-face (ground and building): wall. These faces are used to define the boundary of fluid and solid. It is considered that the fluid does not move on these faces.
- Ceiling-face (top plane): wall. This plane is setting to be a moving wall. The velocity of this wall is same as the top value of the inlet plane with the same moving direction. This set is used to make sure the air will not leak from the top of the model, and represents air moving horizontally at the top of the boundary layer which makes the model closer to the real case.
- Windward-face (inlet plane): velocity inlet. On this plane, the velocity of the fluid is known, which alters with the height from the ground. As the input velocity is not a constant, a function about the relationship between the input velocity and the height is used in this setting, which is defined in the following part.
- Leeward-face (outlet plane): outflow. On these faces, the velocity and pressure of the fluid is unknown.
- Side-face for 0 °and 90 °models (side face plane): symmetry. The fluid is mirror symmetry on each side of the face.
- Side-face for 10 °to 80 °models (side face plane): periodic. The fluid is circularly repeated at same position on each side of the face.

User-Defined Functions (UDF) is used to describe some complicated boundary conditions. For this case, the height of the CFD models is lower than the ABL thickness (from ground surface to more than 1000 m height) [66]. There are two reasons for this setting: lower height will reduce the volume of the computational area

which saves computer memory and computer time, and profile velocity functions shows good result at lower height of the ABL (shown in Subsection 2.3.1). Based on the research of Richard and Hoxey [56], the profile of the mean wind velocity on the inlet plane follows the Logarithmic-law in surface conditions of town zone [57], shows as:

$$\bar{u}_z = \left(\frac{u_*}{K}\right)\ln\left(\frac{z-d}{z_0}\right) \quad \text{(Eq.4-9)}$$

In this equation, $\bar{u}$ is the mean velocity of wind at height z, K is the von Karman constant, setting as 0.4 in this case; the friction velocity u_* is 1.37 m/s, the roughness length z_0 is 0.26 m, and the displacement height d is 3.75 m; these parameters are calculated with the result from wind tunnel experiment, introduced in Section 6.1.

Based on Eq.4-9, at same height, the friction velocity u_* is changed depends on the value of $\bar{u}$. Thus, for a fixed mean wind velocity $\bar{u}_{ref}$ at height z_{ref}, the value of u_* could be calculated as:

$$u_* = \frac{\bar{u}_{ref}\cdot K}{\ln\left(\frac{z_{ref}-d}{z_0}\right)} \quad \text{(Eq.4-10)}$$

Thus, Eq.4-9 could be changed as:

$$\bar{u}_z = \frac{\ln\left(\frac{z-d}{z_0}\right)}{\ln\left(\frac{z_{ref}-d}{z_0}\right)}\cdot\bar{u}_{ref} \quad \text{(Eq.4-11)}$$

In this simulation, set z_{ref} as 10 m, and set $\bar{u}_{ref}$ as a constant. This setting is because most of the wind velocity records from the Met office are for the flow at 10 m height from the ground. The mean wind velocity at different height from the ground in the model could be calculated with Eq.4-11.

For CFD models with different input wind directions, the mean velocity vectors are multiplied by the sine and cosine values of each input wind angle, the results show the velocity values on x and y direction of the inlet plane respectively. Different UDF files which show x-velocity and y-velocity are defined and used in FLUENT,

respectively. The setting of boundary condition and UDF of this case is as **Table 4-2** shows below:

Table 4-2 defined boundary conditions

Define/Boundary Conditions	
Zone: air/Type: fluid	
Zone: building/Type: wall	
Zone: default-interior/Type: interior	
Zone: ground/Type: wall	
Zone: inlet/Type: Velocity-inlet	velocity Magnitude(m/s)/udf
Zone: outflow/Type: outflow	Flow Rate Weighting/1
Define/User-Defined/Functions/Interpreted/Interpret	

The source code of the UDF is written in C language. **Figure 4-8** shows the source code of UDF used in one of the CFD models as an example. This UDF is used to calculate the wind velocity of vertical profile on the inlet plane of model. The model simulates wind blowing from north of the house in town zones. The function of the profile is Eq.4-11 with parameters shown above, with $\bar{u}_{ref}$ = 10 m/s. explain below:

```
/************************************************************************/
/* town.c*/
/* UDF for specifying steady-state velocity profile boundary condition*/
/************************************************************************/
#include "udf.h"
#define va 10
DEFINE_PROFILE(inlet_y_velocity,thread,index)
{
 real y[ND_ND];
 real z;
 face_t f;
 begin_f_loop(f,thread)
 {
  F_CENTROID(y,f,thread);
  z=y[1];
  {
   F_PROFILE(f,thread,index)=log((z-3.75)/0.26)*va/log((10-3.75)/0.26);
  }
 }
 end_f_loop(f,thread)
}
```

Figure 4-8 source code of UDF (example)

- "#define va 10" means va is the value of $\bar{u}_{ref}$, defined as 10 m/s, this value could be changed by set the value in code "#define va XX";

- "DEFINE_PROFILE" means the following code provides profile boundary information to FLUENT;
- "inlet_y_velocity, thread, index" is used to define the inlet velocity in y direction of the zone appoint by "thread"; "thread" is defined by setting the zone of boundary conditions in FLUENT, "index" is defined by "begin_f_loop". In this UDF, as the wind blows from the north of the city, y direction is the main wind direction; the velocity vector on y direction is much larger than other two axis directions. The velocity in x and z directions are ignored. For models with different main wind direction, the profiled velocity in Eq. 4-11 should be timed with sine and cosine of the input wind angle, which gives the profiled velocity in x and y direction respectively.
- "begin_f_loop" is used to loop on all the face cell of inlet plane;
- "F_CENTROID" coordinates the centre of each cell on the inlet plane;
- "F_PROFILE" defines the y-velocity the cells with different height z, these codes calculate the result with Eq.4-11

There are 5 macros used in this source code, which are "DEFINE_PROFILE", "begin_f_loop", "F_CENTROID", "F_PROFILE", and "end_f_loop"; these macros are defined by FLUENT and more macros are introduced in Fluent User Defined Function Manual [55].

4.2.5 Solve setting

After finish the above setting, FLUENT could start the calculating, however, the following setting is used to control the process of the calculating, as **Table 4-3** shows.

Of these setting, solution includes the equations used in this model process; and the discretization parameter is used to setting the Equations. In this CFD experiment, flow and turbulence functions are used to calculate the air flow inside the mesh area of the model, explain in above Subsections. The discretization is set as "second order upwind" for momentum and turbulence, this means for each mesh cell, the result is computed based on the two cells adjacent to it, with a multidimensional linear

reconstruction approach [65]. With this setting, the result in each cell will be limited by the cells close to it, and thus reduce the error during the computation.

Table 4-3 solve setting

Solve/Controls/Solution	
Equations	Flow, Turbulence
Discretization Pressure	Standard
Discretization Momentum	Second Order Upwind
Discretization Turbulence Kinetic Energy	Second Order Upwind
Discretization Turbulence Dissipation Rate	Second Order Upwind
Solve/Monitors	
Options	Print, Plot
Normalization	Normalize Scale
Solve/Initialize/Initialize	
Compute From	inlet
Solve/Iterate	
Number of Iterations	5000

The initialize sets the guess result of the fluid. By setting an appropriate value, the calculating time would be reduced greatly. For this case, the result is computed from the value of inlet wind velocity.

The monitors setting is used to survey the calculating process. From the option part, the monitor shows as plot and print; and by setting the normalize scale, the monitor show normalize results. **Figure 4-9** show the plot monitor of residual as an example.

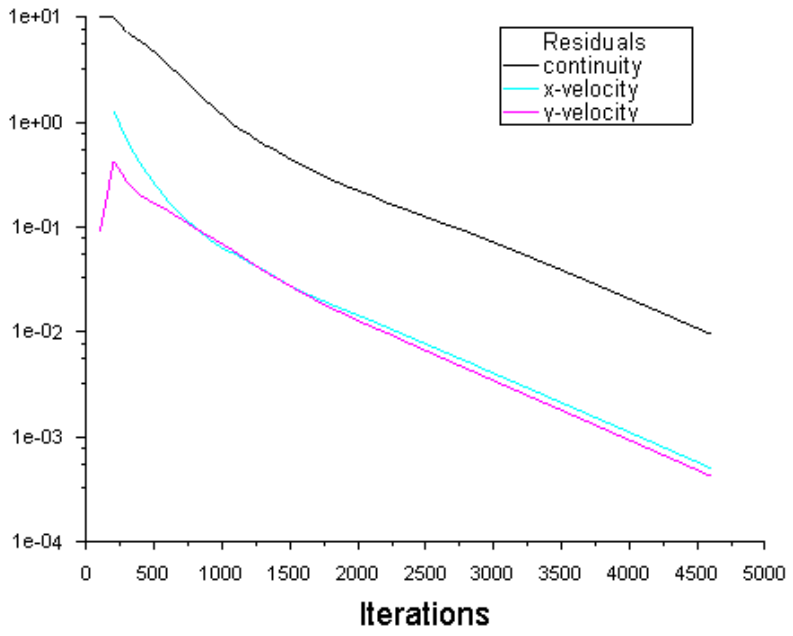

Figure 4-9 plot monitor of residual (example)

FLUENT start calculating after setting the number of iterations, for this case, the result appears suitable mainly after 4000 times of calculating. An example is shown in **Figure 4-9**. This monitor plot shows the residual value of different physical parameters. If this value is small, the difference between calculated results of each iteration solves would be small. In **Figure 4-9**, the residual values of x-velocity and y-velocity are both less than 0.001 after 4500 times of iteration solves, the result shows to be convergent. However, different model in this case need different iteration number, for general, the number is set 5000.

4.3 Way to analysis the CFD results

In this simulation, several models are used to analysis the relationship between different input wind velocities. These include the 0 °(wind blow from N), 30 °(wind blow from NNE), 60 °(wind blow from NEE), and 90 °(wind blow from E) models for both semi-detach and terrace house groups. For each model, $\bar{u}_{set}$ is set as 4 m/s, 8 m/s, and 12 m/s and got different results respectively. From these results, it was found that the velocity of wind at same positions in the model change in proportion with $\bar{u}_{set}$, as expected. Thus, for the other models, set $\bar{u}_{set}$ as 10 m/s and the results are used for following research.

For each house group, because the input wind comes from different direction, 10 CFD models with different wind input angle are simulated. In these models, the wind direction on the inlet plane rotates each 10 degrees. The cases for other input wind directions could be found by do some symmetric treatment to these models.

The CFD simulation results could be displayed in several ways with the software FLUENT. For this research, the analysis of the result focused on the velocity of the wind flow and turbulence around the last downstream building group. After the analysis, for each model, there would be several locations with more powerful wind energy than the others, the method about post processing is also introduced in this part.

4.3.1 Wind velocity

For the wind velocity, FLUENT could show the result as profile plot and velocity vector plot. As the computational domain is in 3D, several planes could be build inside the computational domain and show the results on these planes. **Figure 4-10** shows part of the velocity vector plot for 10 m height plant of semi-detached houses with wind input direction from 90 º (east) as an example. This velocity vector plot shows the situation of air flow around house groups directly. In this plot, the velocity vector at 10 m height from the ground is shown as several small arrows: these arrows point to the direction of the velocity vector, while the value of the velocity is marked with different arrow colour. The black panes in the plot show the position of the semi-detached houses.

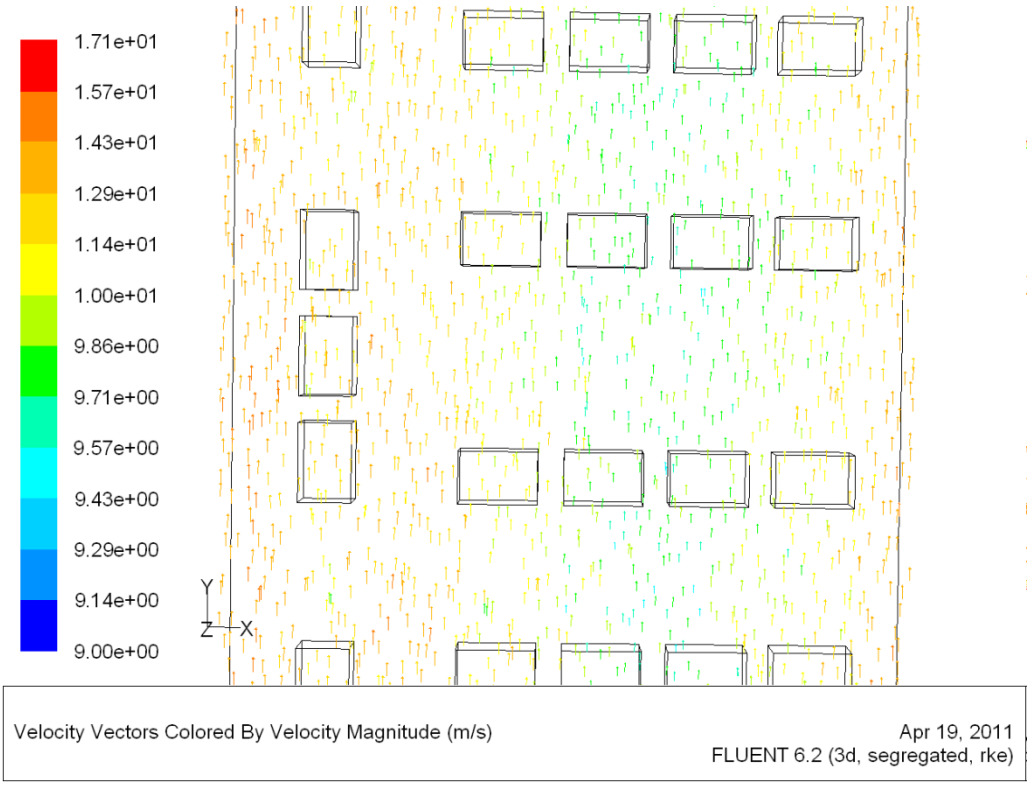

Figure 4-10 velocity vectors of flow (example)

In this project, the wind flow in lateral direction of each model is periodically repeated due to the boundary layer setting on the side faces of computational domain.

The air flow in longitudinal direction (also direction of the flow) should also be checked. If the velocity vectors in same position around different house row shows the similar result, it could be considered that the wind in these positions are affected by same upwind roughness and give same flow result. And at same positions around leeward houses, the air flow is considered same as this repeated result. For both semi-detached and terrace house groups, the 0 º and 90 º models are used to check the air flow in longitudinal direction.

5 groups of both semi-detached and terrace houses are modelled in 0 º and 90 º models respectively. From the velocity vectors plots, the airflow around third, fourth and fifth of the leeward semi-detach house groups show similar results in same position close to the house; while for the terrace house, the repeated velocity vector appears in area around the fourth and fifth leeward house group. **Table 4-4** shows the velocity result of same position around semi-detached house (position 1_L in Appendix F3) and terrace house (position 1_L in Appendix F4) as example.

Table 4-4 velocity at same position of different house row

House type		Velocity [m/s]			
		$\bar{u}_x$	$\bar{u}_y$	$\bar{u}_z$	$\bar{u}$
Semi-detached	**Row 1**	0.22	10.02	0.44	10.03
	Row 2	0.09	9.87	0.32	9.87
	Row 3	0.07	9.43	0.09	9.43
	Row 4	0.06	9.42	0.09	9.42
	Row 5	0.07	9.43	0.08	9.43
Terrace	**Row 1**	1.83	8.06	0.17	8.45
	Row 2	1.65	9.56	0.19	9.89
	Row 3	1.87	8.15	1.49	8.51
	Row 4	1.45	8.94	2.15	9.32
	Row 5	1.46	8.93	2.15	9.32

With above result, for both CFD and wind tunnel experiment, 3 row of semi-detached house group and 4 row of terrace house are modelled respectively. Only the flow velocity result around the last leeward group is used in the analysis part. This result is considered to be periodic repeated in large area with same house groups.

Besides the vectors plot, FLUENT can also show the velocity vectors in any area inside the computational domain with reports. With these report, the magnitude and directions at 10 m and 30 m height of the area around the building groups could be find out. For each simulation, the locations near the buildings with the largest wind

velocity are recorded for further analysis. These records include the coordinates, wind magnitude and direction of each location. Section 6.1 shows the velocity result of CFD simulation.

4.3.2 Turbulence

After the wind velocity vectors at 10 m and 30 m height near the house group is calculated, the turbulence intensity (*I*) around both kinds of house group should be find out. For positions with same mean wind velocity, the position with less turbulence intensity will produce more energy. FLUENT could show the turbulence intensity with profile plots, and these plots are based on a function for fully developed pipe flow. In this case, the flow in CFD domain could not be considered as pipe flow, as the side face of the computing area is set as symmetry and top face as moving wall. This means the turbulence intensity profile plots can't show the real turbulence in this case. For each location, the turbulence intensity is calculated with the define function [58].

$$I \equiv \frac{\sqrt{\overline{u_x'^2} + \overline{u_y'^2} + \overline{u_z'^2}}}{\bar{u}} \qquad \text{(Eq.4-12)}$$

where u_x' u_y' and u_z' are the turbulence velocity fluctuations in three axes directions, respectively; and $\bar{u}$ is the mean velocity for the location. All these parameters could be reported by FLUENT. Section 6.2 shows the turbulence intensity around both house groups based on the CFD models.

4.3.3 Post processing

After the velocity and turbulence analysis, for each model with different input wind direction, the wind velocity and power varies at different positions around the house. The post processing is based on this result and the historical wind records from the U.K. Met office. The historical wind record in different cities around U.K. is analysed and shown as wind rose for different wind velocity magnitude level, which is shown in Chapter 3. For each input wind direction, the wind velocity of the each position is multiplied with the annual amount of each velocity level and the wind turbines'

output power stage of the velocity level, which gives the AEP of each wind turbines in the wind direction. The summation of all directions gives the total AEP of the wind turbines.

Chapter 7 shows the energy output result based on the CFD models. Some more details about the energy analysis method are also introduced in that Chapter.

CHAPTER 5

5 Wind Tunnel Experiment

Wind tunnel experiments are made in order to find the wind vectors at different position around two kinds of building group models. The building models are fixed in wind tunnel which models the airflow environment of suburban zones in U.K. (roughness class 3 [8]). For each measurement point, the results of the experiment included the wind velocity vector in 3-axis directions and wind turbulence. And these results are compared with the CFD modelling in same position to test the CFD model. With the analysis of both the wind tunnel and CFD results, the velocity and turbulence intensity around both semi-detach and terrace house groups could be found out.

This Chapter introduces all the details of the wind tunnel experiment, which includes the setting of the models and other apparatuses used in this wind tunnel experiment, the technique of transform the recorded parameter to wind vectors, and the result analysis of both wind velocity and turbulences at the measurement points.

5.1 Model scale

The boundary layer tunnel at MACE is used for this wind tunnel experiment. The cross-section of the tunnel is 0.92 m × 0.92m, which limits the size of the model. In this experiment, the model should be able to be rotated to different directions in the tunnel, based on size of the tunnel; the length of a side should be less than 900 mm for a square model plane.

In real case, the roughness class of a site depends on the sectors around it, and the building at the windward position changes the wind flow. The effect of this change decreases with increasing height from the ground. Generally, at a height *h* from the ground, the roughness changes in an area within distance *x* upwind do not affect the wind flow above height *h* [8]. The details of this theory are shown in Section 2.4.

Based on this theory, in order to measure the wind flow affected by different kinds of building group with different building density, the distance from the measurement point to the boundary of the building group should be longer than the distance *x* for different height. In this experiment, two height levels are used to measure the flow of the wind at the site: 10 m and 30 m, these heights are the common heights for small and middle wind turbines used in the urban area; based on the class 3 curve of **Figure 2-13**, the relevant distance of these two heights are 20m and 90 m.

Another decisive factor of the scale is the outline of the buildings. In this experiment, several same type building models are listed as group, and spread on the plan to represent a typical residential area in a town or city. All the measurement points are around the last house group in the leeward position. In order to measure the wind flow affected by the buildings, there should be at least one row of buildings sited outside the distance x from the windward boundary of the last buildings. The outline plans for different building types is as next section shows.

The scale of the model is also decided by the size of the model. A smaller scale means more buildings are included in the model, which leads to a more actual boundary layer; but the size of each house would be smaller, which means the measurement result is less accurate due to the size of the measuring instrument (in this experiment hotwire anemometer is used). The setting of the scale should consider both the veracity of the boundary layer and the size of the buildings.

In consideration of all the above factors, the model plane is set as 800 mm $\times$ 800 mm, and the scale of the model is set as 1/250, this scale shows the relationship between the size of model and full-scale building, and it is named as length scale (λ_L). With this length scale, each model represented the area of 200 m $\times$ 200 m space in real case. **Figure 5-1** shows the size and max relevant distance (90 m) of 90° model in real case.

It could be find that for both semi-detached and terrace house, the first windward house group is further than 90 m from the last leeward house group. This means the measurement point at 120 mm (30 m in real case) would measure the wind flow affected by the first windward house group. For the models with different input wind directions, this distance rule is also obeyed. And the hotwire anemometer used in this experiment has a swept area (area between the wires) 3.14 mm^2; with this length scale, the swept area is 7.84e^{-4} m^2 in full scale. This size is less than the swept area of the wind turbines used in this project and thus acceptable for the measurement.

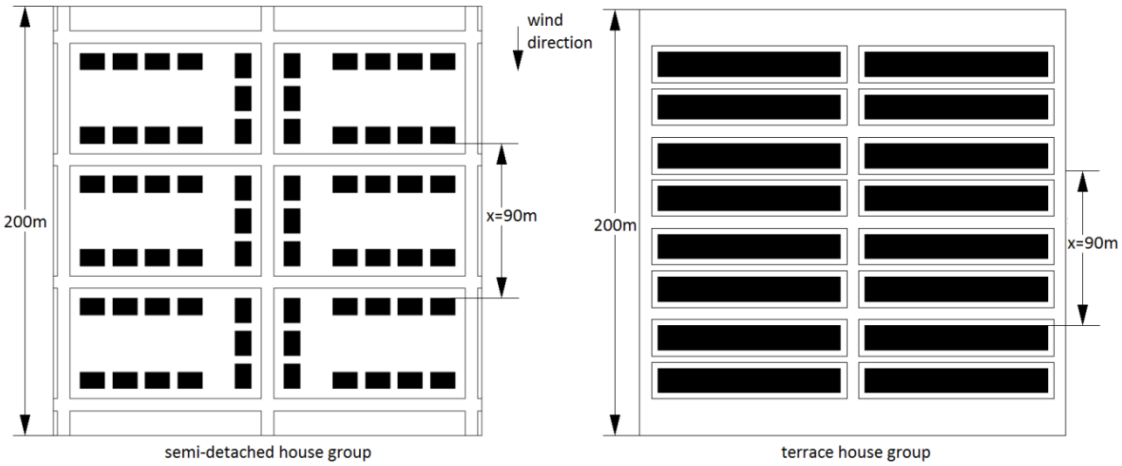

Figure 5-1 model size in full-scale.

Reynold number (*Re*) is another similarity parameter for the flow simulation in wind tunnel. This parameter is defined as [59]:

$$\mathrm{Re} = \frac{\rho u L}{\mu} \qquad \text{(Eq.5-1)}$$

In this experiment, it is not possible to simulate same *Re* value in tunnel as the full-scale buildings. This is because the field used in tunnel is air, which has same ρ and μ values as the air of full-scale environment; and the length scale in this experiment is 1/250, which means in order to get the same *Re* value as full-scale environment, the velocity inside the tunnel should be 250 times of actual wind velocity. It is not possible to get such velocity in the tunnel. However, the difference between wind *Re* value in wind tunnel and full-scale does not affect the experiment result; as this

experiment simulates the air flow around low ABL environment with large *Re* value, for such simulation, it is not necessary to make the *Re* values in tunnel and full-scale buildings similar to each other [80].

Besides the above length scale, another two scales need to be set. In this experiment, each measure takes 30s (the working frequency of the hotwire anemometer is 300 *Hz*, in this period of time the anemometer measured 9000 groups of wind data which are recorded for the turbulence analysis), and the result of each measurement is used to compare with the hourly mean wind velocity (which is also used in weather sites). This gives the temporal scale (λ_T), in this experiment, this scale is defined as:

$$\lambda_T = \frac{T_m}{T_p} = \frac{30s}{3600s} = \frac{1}{120} \quad \text{(Eq.5-2)}$$

And based on the velocity equation ($u=L/T$), for this experiment, the velocity scale could be defined as:

$$\lambda_u = \frac{u_m}{u_p} = \frac{L_m / T_m}{L_p / T_p} = \frac{\lambda_L}{\lambda_T} = 0.48 \quad \text{(Eq.5-3)}$$

Because the CFD models used in this project has the same size as the full-scale building, the velocity results from the wind tunnel experiment need to be transformed to do the comparison. The above three scales are used for such transformation. In Chapter 6, scaled wind velocities are used as the wind tunnel velocity results.

5.2 Model size and layout

The building model used in this experiment follows the same size and layout as the CFD model shows in Section 4.1. This section shows the size and layout of the wood models used in this experiment.

In consideration of the accurate geometric size, LEGO blocks were first used to build the model. Totally 2038 pieces of LEGO bricks and plates were used to make the semi-detached and terrace models. These models had perfect geometric shape but not successful to be used in this experiment: the LEGO model was lifting up from the bottom of the tunnel due to the wind force in the tunnel, which might damage the wind tunnel and the measured results were incorrect due to this displacement. In view of safety and to get correct records, the models used in this experiment were made of wood and attached to the bottom of tunnel with screws

5.2.1 Semi-detached house

The simulated semi-detached house is set as a two floor house, 6 m height, 12 m length and 8 m width, with scale 1/250, the tested model size is 24 mm height, 48 mm length, and 32 mm width. **Figure 5-2** shows the view of semi-detached house model in real (left) and experiment (right) scale.

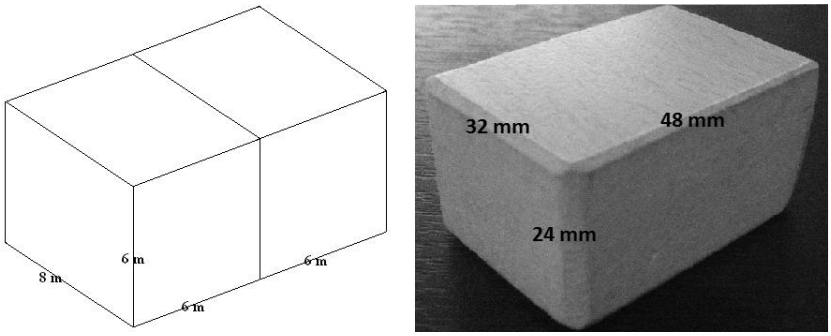

Figure 5-2 size and view of semi-detached house model

The layout of semi-detached house model is introduced in Section 4.1, with scale 1/250, 66 wood blocks as shown in **Figure 5-2** right were fixed on a 800 mm × 800 mm wooden plane. **Figure 5-3** shows the photo of the model plane (left) and the aerial photograph of such layout (right) as in previous **Figure 4-5**. The houses are separated with different groups by the road around them. Each house group includes 11 houses and there are 6 groups in this model. The outline of the house model is educed from such distribution.

Figure 5-3 model photo and aerial photograph of semi-detached house[1]

5.2.2 Terrace house

In this experiment, the size of each terrace house is set as: 6m height, 4m length and 12 m width, and 20 houses joined together as a house line. With scale 1/250, the size of each model house line is 24 mm height, 48 mm width, and 320 mm length. **Figure 5-4** shows the view of single terrace house (left) and house line (right)

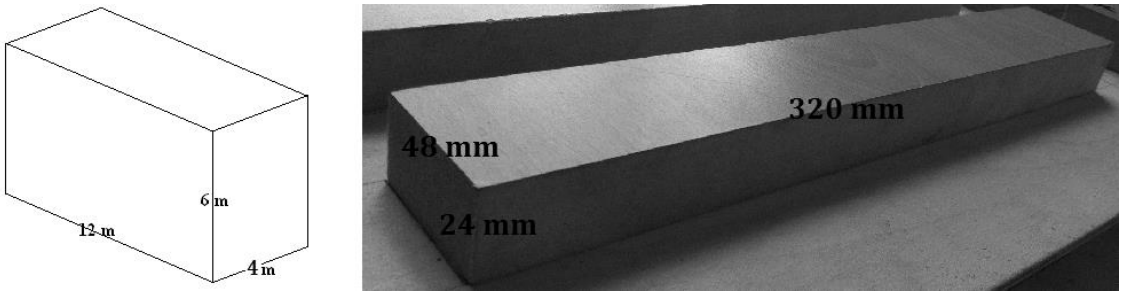

Figure 5-4 size and view of terrace house model

With the layout as Section 4.1 shows, 16 wooden house line models are fixed on a wooden plane with same size of the semi-detached model. Two house lines joined as a group and there are 8 groups of houses in the model as in previous **Figure 4-5. Figure 5-5** shows the view of model photo (left) and aerial photograph (right) of terrace house groups.

Figure 5-5 model photo and aerial photograph of terrace house

5.3 Measurement points setting

The aim of this experiment is to find the wind flow at two heights around different building densities. As mentioned above, the effect of the obstacle array react on each height with distance x away from the obstacle. In consideration of this distance, the measure position should fasten on the leeward house groups. Also, as both of the models have axes of symmetry, only one side of each model need to be measured.

In this experiment, 2-axis hot wire is used to measure the velocity of the wind at height 10 m and 30 m from the ground. In consideration of the scale of the model, the measure height of the model should be 40 mm and 120 mm from the floor. Only one hot wire anemometer was available to be used in this experiment; the velocity at the measurement points is measured one by one. **Figure 5-6** shows the 2-axis hot wire anemometer used in this experiment, there are 4 pins at the top of the transducer, the hot wires are fixed on each two pins at different angles. A constant electric current is passed through each hot wire, generating heat. When the velocity of the air flow change, the temperature of the hotwire will be changed, which will change its resistance and therefore the voltage drop through it. The value of the voltage through the hotwire is measured and saved by the logging system of the computer used in this

experiment, which reports the output voltage results as some ‘txt.’ file. The technique of transform the output voltage into velocity values is introduced in Section 5.5.

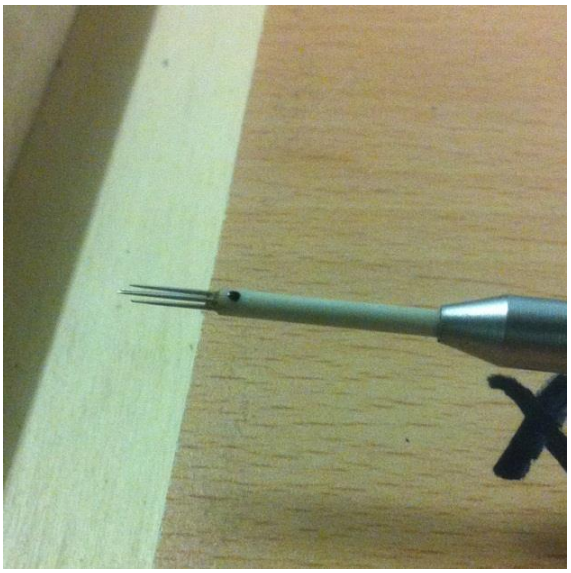

Figure 5-6 2-axis hot wire anemometer

For each measurement, the 2-axis hot wire could measure the velocity vector in two axis directions at the same time; however, for each measurement point, the velocity axis vector in 3 directions are needed. In order to measure all the axis vectors, the hot wire needs to be rotated 90 degrees during the measuring period. The x-y and x-z records are calculated respectively to give the velocity vectors in these 3 axis directions.

In this experiment, there are limited measurement position could be used. This is because of the hot wire transducer is fixed on a metallic pole which comes down from the ceiling of the cross-section area; and the pole could only move through several travelling gaps in the ceiling. Because of this, the measurement points could only be set along the track of these gaps. The positions and length of these gaps are as shown in **Figure 5-7**.

During the experiment, measurements with input wind velocity from different directions of the models were done. The house group models were fixed towards different directions to make the input wind blowing from different directions. It requires more space to fix the models when the input wind direction is closer to 45°.

Due to the space of the wind tunnel is not large enough for the setting of all input directions, only 7 such directions were done, which include 0 °, 5 °, 90 ° for semi-detached house group, and 0 °, 5 °, 85 °, 90 ° for terrace house group. All measurement positions relative to models sides are recorded in Appendix F.

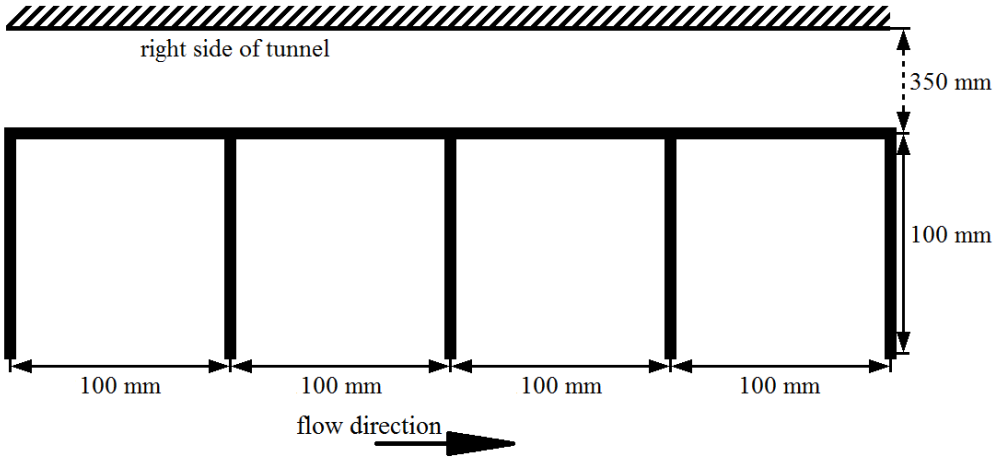

Figure 5-7 travelled gaps in the ceiling of the wind tunnel cross-section area

5.4 Details of the apparatus

In order to simulate the wind flow around urban zones, the augmented growth method [60] [61] is used to set the ABL inside the wind tunnel. In general, the air flow in a boundary layer thickness (δ), the mean wind velocity profile at different height follows the power-law [60]; and as Section 2.3 shows, the logarithmic-law [56] [57] shows similar results at height up to 150 m. The power-law is used to represent the mean velocity at different height *z*, show as:

$$\frac{\bar{u}_z}{\bar{u}_{ref}} = \left(\frac{z-d}{z_{ref}-d} \right)^{\alpha} \qquad \text{(Eq.5-4)}$$

And logarithmic-law is as Eq.4-9 shows, shows the relationship between mean wind velocity at height *z* and the friction velocity.

The apparatus used in the augmented growth method include turbulence grid, trip wall and roughness blocks: the turbulence grid is used to generate turbulences, while trip

wall and roughness blocks are used to modify the boundary layer for different roughness classes. **Figure 5-8** shows the schematic of the wind tunnel setting. And **Figure 5-9** is the photo of the apparatus used in this experiment.

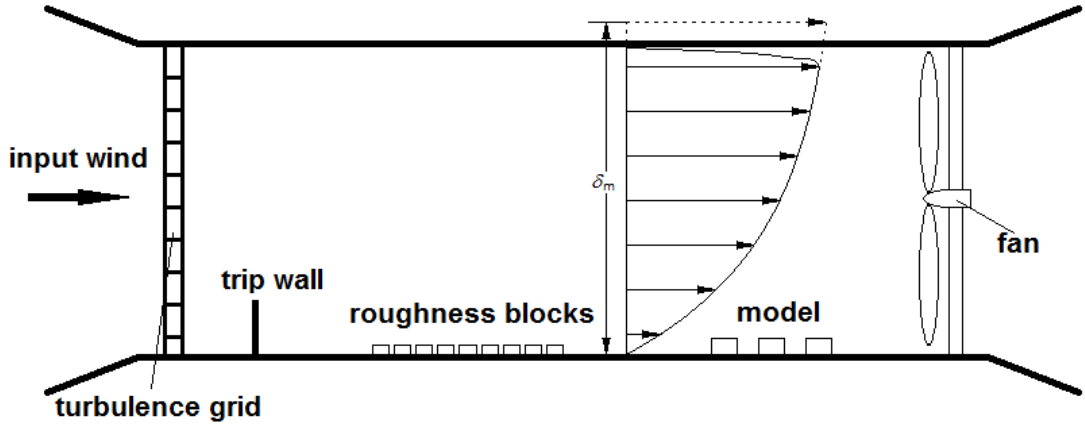

Figure 5-8 longitudinal schematic of wind tunnel setting

Figure 5-9 apparatus used in the wind tunnel experiment

As shown in **Figure 5-8**, the wind tunnel can't simulate the ABL in whole. Based on the research of Counihan [67] a full-scale ABL for urban zones should be around 400 m, in this 1/250 simulation, the ABL thickness should be around 1.6 m in the tunnel. This height is larger than the wind tunnel's test section height. As a result, the wind velocity at the top of the test section is slowed down because of the friction force from

the roof of the test section. However, for this project, this part-depth simulated ABL does not affect the result, due to the measurement points are fixed at 40 mm and 120 mm from the wind tunnel floor, the friction force from top of the tunnel will not affect the air flow at these two heights. Similarly, the measurement positions are close to the centre of the tunnel; as shown in **Figure 5-7**, the closest measure position is more than 350 mm away from the side of the tunnel. Thus, it is acceptable that the tunnel sides do not affect the measurement results. Research from Kozmar **[68]** shows the similar result.

As introduced above, the main apparatuses used in this experiment includes the turbulence grid, the trip wall and roughness blocks. Beside these apparatus, there is a velocity sensor fixed on the top of the wind tunnel, the mean velocity inside the wind tunnel could be read from this sensor, which helps control the input velocity. This section focused on the details of the three main apparatuses.

Generally, the size of the turbulence grids used in this wind tunnel experiment are set based on the literatures and the actual circumstances of the wind tunnel used in this experiment. The tunnel has a cross-section of 0.92 m $\times$ 0.92m with length of 5.52 m; based on the research of Mohsen & John **[62]**, the distance of the position with suitable turbulence should be more than 40 times the side length of each single mesh. In this experiment, the measurement position is set by the end of cross-section area; and the closest position is 4.684 m away from the start section of the cross-section area where the grid is fixed. Due to this, the mesh size of the grid is set as 100 mm.

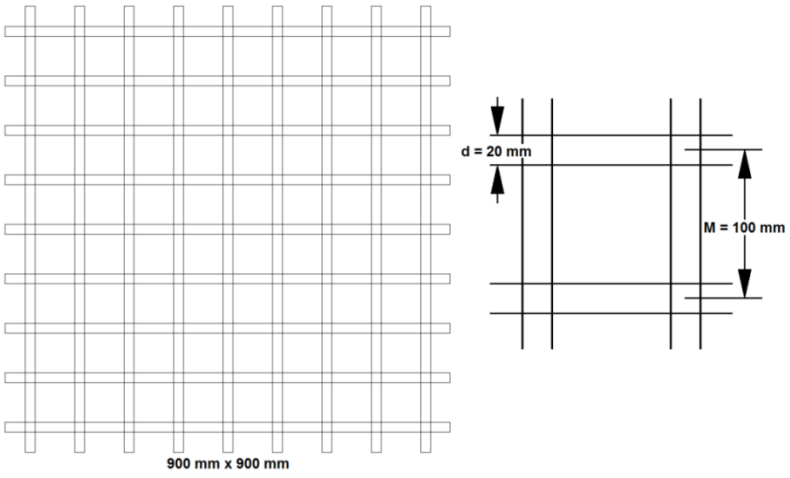

Figure 5-10 size of turbulence grid and single mesh

Figure 5-10 shows the size of the turbulence grid and each mesh. As this figure shows, the turbulence grid is made with 18 metallic rods in this experiment; the diameter of the rods (d) depends on the size of the mesh (M). In order to generate suitable turbulence, M/d should be close to 5 [63], due to this, the diameter of the rods is set as 20 mm.

The trip wall is used to reduce the wind velocity by the bottom of the wind tunnel. Based on the work of Cook [60] which simulates the same boundary layer as this experiment, the wall is 900 mm length with 100 mm height, and set 600 mm away from the turbulence grid. **Figure 5-11** shows the size of this trip wall.

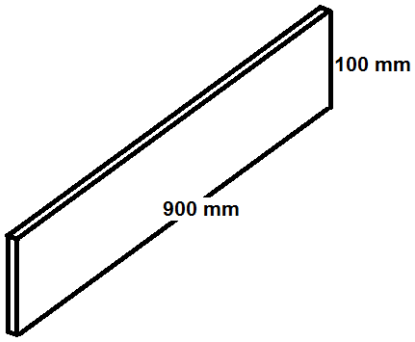

Figure 5-11 size of trip wall

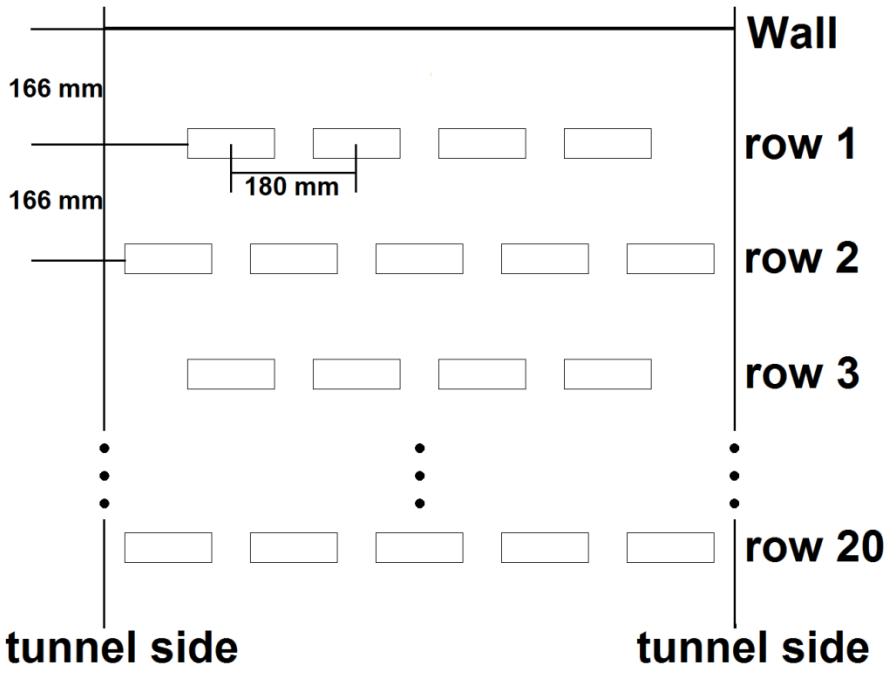

Figure 5-12 layouts of roughness blocks

Roughness blocks are set at the lee wind direction of the trip wall. These blocks are set to simulate the roughness environment of town zones in U.K. Based on Cook's work on 1973 [61] and 1978 [60], in order to simulation the roughness environment of suburban areas, the blocks should occupy about 15% of the total area; and these roughness blocks should appears dense (obstacle porosity 0.35 ~ 0.5 in **Table 2-5**) with a mean height close to the average building height. In this experiment, 90 blocks with size 125 mm × 42 mm × 42 mm are used to cover the area from trip wall to model (3.15 m^2); it could be calculated that the roughness blocks covered 15% of the surface in this area, which is up to the research of Cook. The length between two blocks in same row is 55 mm, which is 44% of the block length (125 mm), as **Table 2-5** shows, the appearance of this obstacle porosity is dense. The height of the blocks is 42 mm; the full-size of this height is close to the average building height in U.K. towns. **Figure 5-12** shows the layout of these roughness blocks.

5.5 Calibration of the records

For each wind tunnel experiment, some calibration works need to be finish before or after the measurement. The aim of these works is to find the relationship between measured records and the wind flow vectors at the measurement points. These works could also find and reduce the errors comes from different experiment environments and hot-wire styles. As the experiment are finished in two different period of time, two different hot wire anemometers are used for the two models in this experiment, the calibration work should be finished twice.

Based on the work of Browne, Antonia & Chua [52], the calibration work is finished on a test desk with a turntable with marked scale on it. The hotwire used in the wind tunnel experiment is fixed on the turntable and set towards a nozzle which connects with a press-air pipe. With a valve on the pipe and the turntable, the velocity and direction of the airflow towards the hotwire could be changed. With the same computer used in the wind tunnel experiment, some records from the hotwire could be recorded for different wind velocities and effective directions.

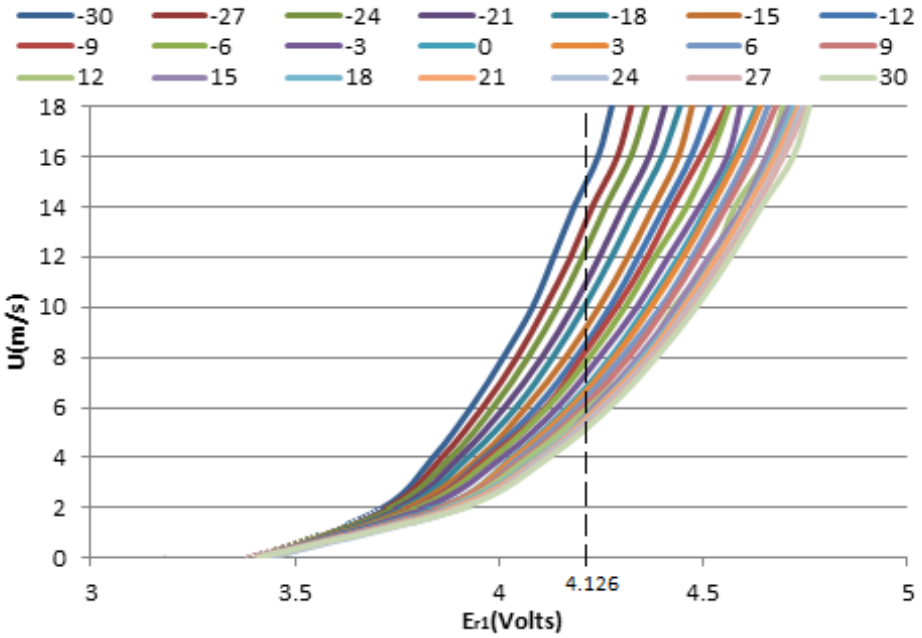

Figure 5-13 velocity vs. yaw angle calibration results for one wire of the semi-detached model

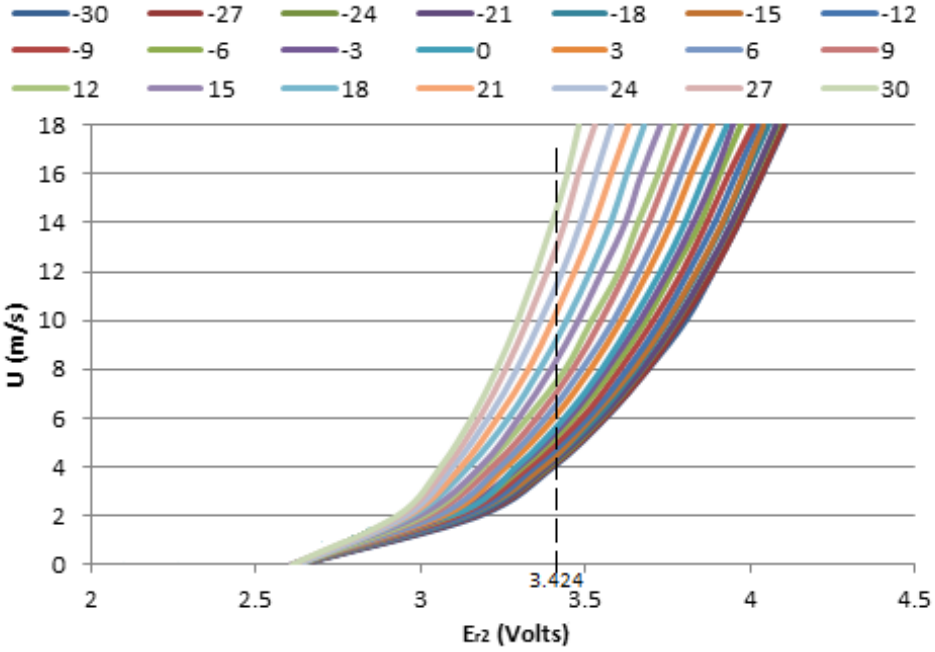

Figure 5-14 velocity vs. yaw angle calibration results for the other wire of the semi-detached model

For a fixed effective angle from the wind flow to the hotwires, the velocity of the wind (u) and voltage record (E_r) has the following relationship [52]:

$$u = a_1 + a_2 E_r + a_3 E_r^{\,2} + a_4 E_r^{\,3} + a_5 E_r^{\,4} \qquad \text{(Eq.5-4)}$$

In this equation, a_1, a_2, a_3, a_4 and a_5 are constants which being determined in different case. In this experiment, the calibration is taken from -30° to 30°, every 3 degrees. As

the hotwire transducer used in this experiment has two wires in it, each measure should include two records, named as E_{r1} and E_{r2}. Thus, there are 42 equations for this hotwire in total for each model. **Figure 5-13** shows the calibration results for one of the two wires in semi-detached model; and **Figure 5-14** shows the results for the other wire in semi-detached model.

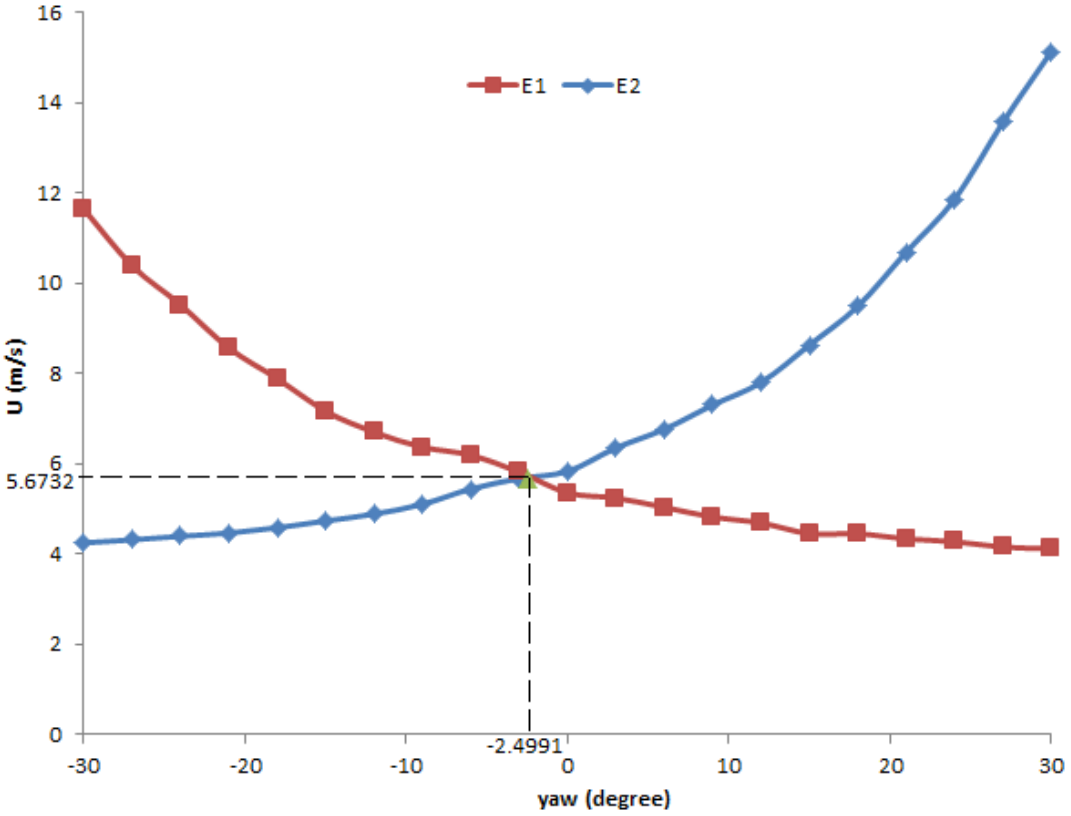

Figure 5-15 curves of velocity vs. yaw angle of two wires

For each measured record, E_{r1} and E_{r2} show the voltage of the two wires. Using these records and the curves from **Figure 5-12** and **Figure 5-13**, U can be found for each angle. With a third order polynomial fitted with these data, curves of velocity vs. yaw angle could be obtained. **Figure 5-14** shows an example of these curves. The record at one of the point is: E_{r1}=4.216, E_{r2}=3.424. In **Figure 5-13**, the line of E_{r1}=4.216 cuts different yaw angle curves at different U value, these U values and the yaw angle of each value are used to make curve E_1 in **Figure 5-15**; similar the curve E_2 is get. The intersection point of these two curves shows the velocity and yaw-angle of the wind vector which fits both E_{r1} and E_{r2} from the record, and this wind vector is the measure result at the

measurement position. In this example, the velocity is 5.67 m/s and the yaw angle is -2.5 °.

After the velocity and yaw angle of the wind flow is got out, the wind vector in two axis directions could be calculated with trigonometric functions. At each measure position, two measurements are finished which give the flow vectors in XY and XZ directions, respectively. These results are used in the wind velocity and turbulence analysis.

5.6 Calculation of the results

With above calculation, the voltage records at each measurement point were transformed to wind vector. In the environment with mean wind velocity 10 m/s, the hot-wire anemometer used in this experiment gives good response with working frequency up to 10 *kHz* [52], and the time period of each measure should be longer enough to get reliable wind flow data for following analysis. At each measurement point, the hot-wire anemometer measured the wind velocity for 30 seconds with a frequency 300 Hz, which gives 9000 records for wind vectors in 3 Cartesian coordinates axis directions severally. This section shows the way to calculation these vectors in each measurement positions.

For wind velocity analysis, the mean velocitys of the flow in these measurement positions are required. Each record shows the instantaneous velocity in 3 Cartesian coordinate axis, shows as $u_x\,(t)$, $u_y\,(t)$ and $u_z\,(t)$; the mean velocity of these axis are marked as $\bar{u}_x$, $\bar{u}_y$ and $\bar{u}_z$ The vector sum of $\bar{u}_x$, $\bar{u}_y$ and $\bar{u}_z$ is marked as $\bar{u}$, defined as:

$$\bar{u} = \sqrt{\bar{u}_x^{\,2} + \bar{u}_y^{\,2} + \bar{u}_z^{\,2}} \qquad \text{(Eq.5-5)}$$

where

$$\bar{u}_x = \frac{1}{T}\int_0^T u_x(t)dt\,,\ \bar{u}_y = \frac{1}{T}\int_0^T u_y(t)dt \text{ and } \bar{u}_z = \frac{1}{T}\int_0^T u_z(t)dt \qquad \text{(Eq.5-6)}$$

Another parameter which needs to calculate is the turbulence intensity (I) [57]. This parameter shows the level of turbulence in each measurement position. Eq.5-7 shows

the definition of turbulence intensity in x direction (I_x), y direction (I_y) and z direction (I_z).

$$I_x = \frac{\sqrt{\overline{u_x'^2}}}{\bar{u}},\ I_y = \frac{\sqrt{\overline{u_y'^2}}}{\bar{u}}\ \ I_z = \frac{\sqrt{\overline{u_z'^2}}}{\bar{u}} \quad \text{(Eq.5-7)}$$

where

$$u_x(t) = \bar{u}_x + u_x'(t),\ u_y(t) = \bar{u}_y + u_y'(t),\ u_z(t) = \bar{u}_z + u_z'(t) \quad \text{(Eq.5-8)}$$

The overall turbulence intensity for the measurement position is defined as Eq.4-12 shows.

The calculation results of the wind tunnel experiment were compared with the CFD results in same position which is showed in Chapter 6.

CHAPTER 6

6 Experiment Results

This chapter shows the velocity and turbulence results of both wind tunnel experiment and CFD results. Two main parts are included in this chapter: Section 6.1 shows the mean velocity result in both CFD and wind tunnel experiments, and Section 6.2 shows the turbulence result in both experiments. In each of these two sections, the results from CFD and tunnel experiment are compared with each other and checked with some functions from literatures to conform the results are acceptable. Some velocity and turbulence intensity profiles which show the air flow around house groups are also included in each section. Finally, Section 6.3 wraps up this chapter with a short summary.

6.1 Wind velocity results

As a physical parameter, mean wind velocity is common used in power output curves of different wind turbines to calculate the output power. In this section, the mean wind velocity at different positions around the house models in both CFD and wind tunnel experiments are measured and analysed. Subsection 6.1.1 shows the characteristic parameter value of ABL simulation based on the result of the wind tunnel experiment; while Subsection 6.1.2 introduces the selected measurement points and wind velocity result for both CFD and wind tunnel experiments at these points, the results of both experiments are compared in this part; and Subsection 6.1.3 shows the optimal velocity positions based on the CFD results.

6.1.1 Characteristic parameters of tunnel experiment

As introduced in Section 2.4, there are some parameters which show the topographical characteristic of different terrains. In wind tunnel experiment, the values of these parameters depend on the setting of wind tunnel apparatus before the model. In this experiment, these parameters are calculated before measure the wind velocity at measurement points. There are two reasons to doing this calculation: first, these parameters are used to check the roughness level in the wind tunnel environment; second, these parameters are used in the CFD simulation to make sure the CFD has same ABL setting with wind tunnel.

In order to calculate the characteristic parameters, the mean wind velocity in a vertical line in the middle of the tunnel with 4 m distance away from the turbulence grid is measured. The height of the measurement points changes from 40 mm to 800 mm, each 40 mm in a line; totally there are 20 points. As δ_m in **Figure 5-8** shows, the area close to top of the wind tunnel is affected by the roof; thus, this measurement only cover the area from wind tunnel floor to 800 mm height.

As mentioned in Section 5.4, the measured mean velocity at different height follows the power-law or logarithmic law. Due to this, the characteristics parameters can be obtained by fitting the measured mean wind velocity to the power-law or logarithmic-law functions, as Eq.4-9 and Eq.5-4 show.

In these two equations, the reference height z_{ref} and the mean wind velocity at this height $\bar{u}_{ref}$ need to be confirmed. Generally, for building height less than twice of the average height of surrounding buildings, this reference height could be set around the building height **[69]**. For this project, the height of roughness blocks is 42 mm, thus, 40 mm in model scale is set as reference height, this height is 10 m for full-scale, this height is also the common equipment height for small wind turbines.

Figure 6-1 compares the recorded mean wind velocity at different height with the power-law curve with exponent =0.21. In this chart, at each height *z*, the mean wind

velocity $\bar{u}_z$ is normalized with the mean wind velocity $\bar{u}_{ref}$ at height z_{ref}. With this normalized value, **Figure 6-1** could be used for both model-scale and full-scale.

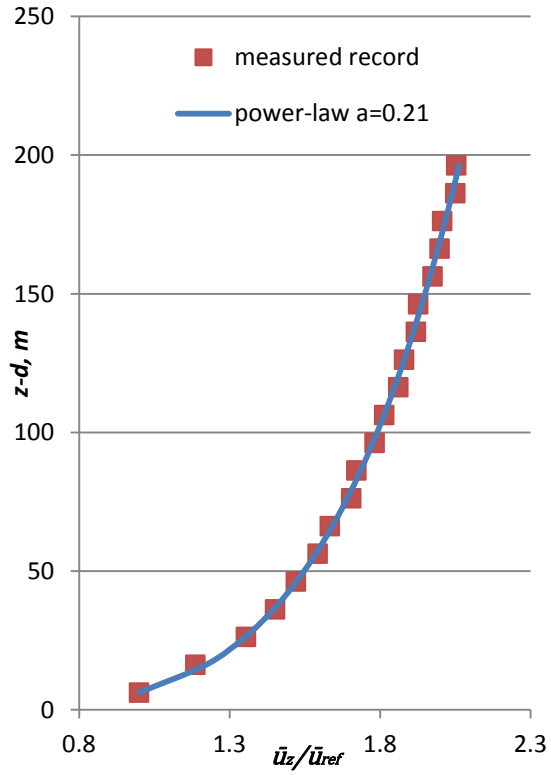

Figure 6-1 profile of mean velocity in wind tunnel experiment vs. power law

From **Figure 6-1**, the experiment results agree well with the power-law with exponent 0.21. Based on ESDU 72026 [70], for aerodynamic roughness length (z_{0p}) from 0.1 m to 0.3 m (roughness level 2 and 3 in **Figure 2-24**), the power-law exponent should between 0.20 and 0.23. Because of this, it can be accepted that the wind tunnel setting represents the ABL developing above town zones.

Based on **Figure 6-1**, 0.21 is set as the exponent value of power law; take 40 mm as z_{ref} (10 m in full-scale) and 120 mm as z (30 m in full scale), the experiment gives $\bar{u}_{ref}$ = 5.6 m/s and $\bar{u}_z$ = 7.59 m/s. take these data into Eq.5-4, which gives:

$$\frac{7.59}{5.6} = \left(\frac{120 - d_m}{40 - d_m}\right)^{0.21} \qquad \text{(Eq.6-1)}$$

Solving this equation and it gives d_m = 15mm.

Take all above values into Eq.4-11, it gives:

$$\frac{7.59}{5.6} = \frac{\ln\left(\frac{120-15}{z_{0m}}\right)}{\ln\left(\frac{40-15}{z_{0m}}\right)} \qquad \text{(Eq.6-2)}$$

The result of this equation is z_{0m} = 1.05 mm.

Then take these values into Eq.4-10, u_{*m} is given as:

$$u_{*m} = \frac{5.6 \times 0.4}{\ln\left(\frac{40-15}{1.05}\right)} = 0.66\,(\text{m/s})$$

Table 6-1 shows the value of characteristic parameters in the wind tunnel experiment, these parameters are also used in the CFD simulation as the input boundary layer setting. In this table, the values of z_{0m}, d_m and u_{*m} are calculated as above, while the values of z_{0p}, d_p and u_{*p} are scale-up from model parameters with length scale 1/250 and velocity scale 0.48.

Table 6-1 ABL characteristic parameters in wind tunnel experiment

α_m=α_p	z_{0m}	z_{0p}	d_m	d_p	u_{*m}	u_{*p}
0.21	1.05 mm	0.26 m	15 mm	3.75 m	0.66 m/s	1.37 m/s

Based on the report of ESDU 85020 [71], for small towns or suburb of large town and cities, the roughness length should be between 0.1 m and 0.3m, the displacement height could be between 2 m to 10 m. From the research of Holmes [72], for same terrain, the roughness length is from 0.1 m to 0.5 m; and Simiu & Scanlan [73] suggest the roughness length should be between 0.2 m and 0.4 m for suburban area. In this experiment, the roughness length is 0.26 m in full-scale, and the displacement distance is 3.75 m in full-scale; both of these two parameters agree well with all references.

The friction velocity is calculated and used in the logarithmic-law. For full-scale, Dyrbye and Hansen [74] report the range of this parameter from 1 m/s to 2 m/s, in this experiment, u_{*p} is 1.37 m/s which agrees with this report. **Figure 6-2** shows the

comparison of wind records and logarithmic-law in this project. In this chart, the measured record agree well with the logarithmic-law from 0 to about 150 m height, for the height more than 150 m, the record value of $\bar{u}_z/u_*$ is larger than the logarithmic-law value. This result agrees with the research from Sockel [75] which mentioned the logarithmic-law can only successful applied in the height less than 150 m height. For this experiment the heights of measurement points are 40 mm and 120 mm; all of these measurement positions are under 100 m height in full-scale, the logarithmic-law still applied the result well.

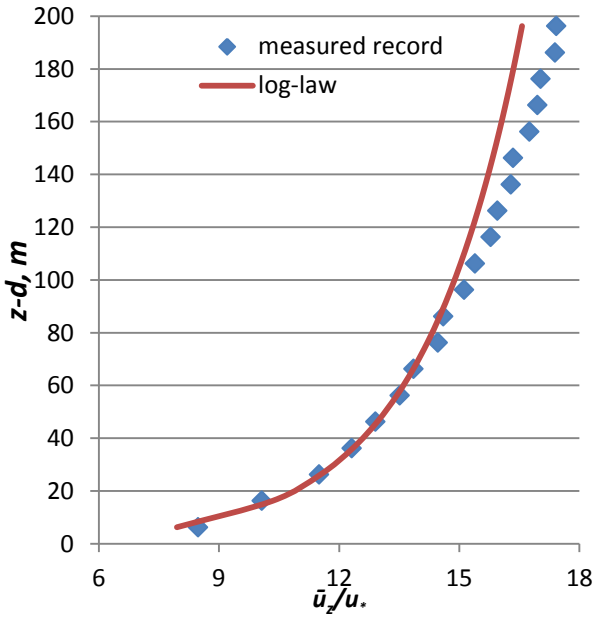

Figure 6-2 profile of mean velocity in wind tunnel experiment vs. logarithmic-law

The characteristic parameters in this experiment agree well with all above range, it could be considered that the ABL in town zone is successful generated in this experiment.

6.1.2 Wind tunnel velocity results

As mentioned in Section 5.3, the measurement position of the wind tunnel experiment is limited by the size and ceiling of the wind tunnel cross-section area; thus, the wind tunnel velocity results are grouped with different house type and input wind directions. Totally 7 such groups are given (0 °, 5 °, 90 ° for semi-detached houses and 0 °, 5 °, 85 °, 90 ° for terrace houses); and in each group, following 3 parts are included:

- **Group description**: shows the house type and input wind direction of the model;
- **Position plot**: marks the measurement points' position on the top view of the models, positions with different height are marked with different number; the Cartesian coordinates and its origin which are used to show the positions are also shown in this plot;
- **Detail table**: shows the detail result of each measurement point, includes the mark, coordinate, mean velocity in 3 coordinate axis directions, and horizontal mean wind velocity.

Appendix F shows the velocity results of all directions.

Attention should be paid that the mean velocities shown in these tables are measured and then scaled value from the wind tunnel; in order to compare with the value from CFD model, these data are transformed to dimensionless quantity by dividing by a reference velocity. In this project, the mean wind velocity at 40 mm height in wind tunnel and 10 m height in CFD model are used to do the transformation, respectively. The record result of these wind tunnel experiments are compared with mean velocity value at corresponding position in CFD models, **Figure 6-3** and **Figure 6-4** show these value comparison.

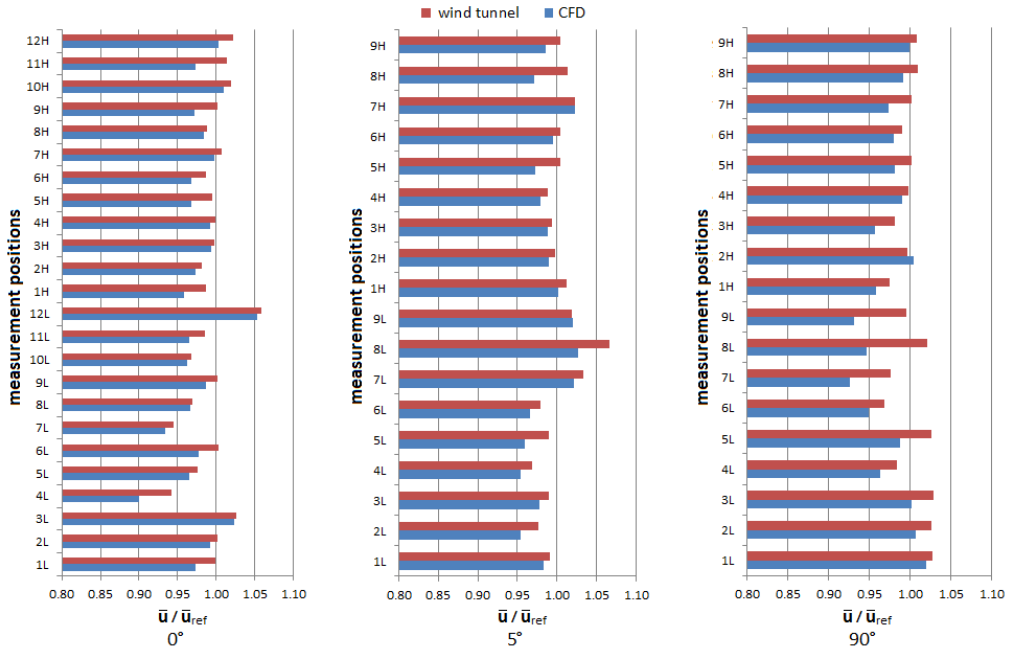

Figure 6-3 comparison of mean wind velocity at measurement points in tunnel and CFD, semi-detached

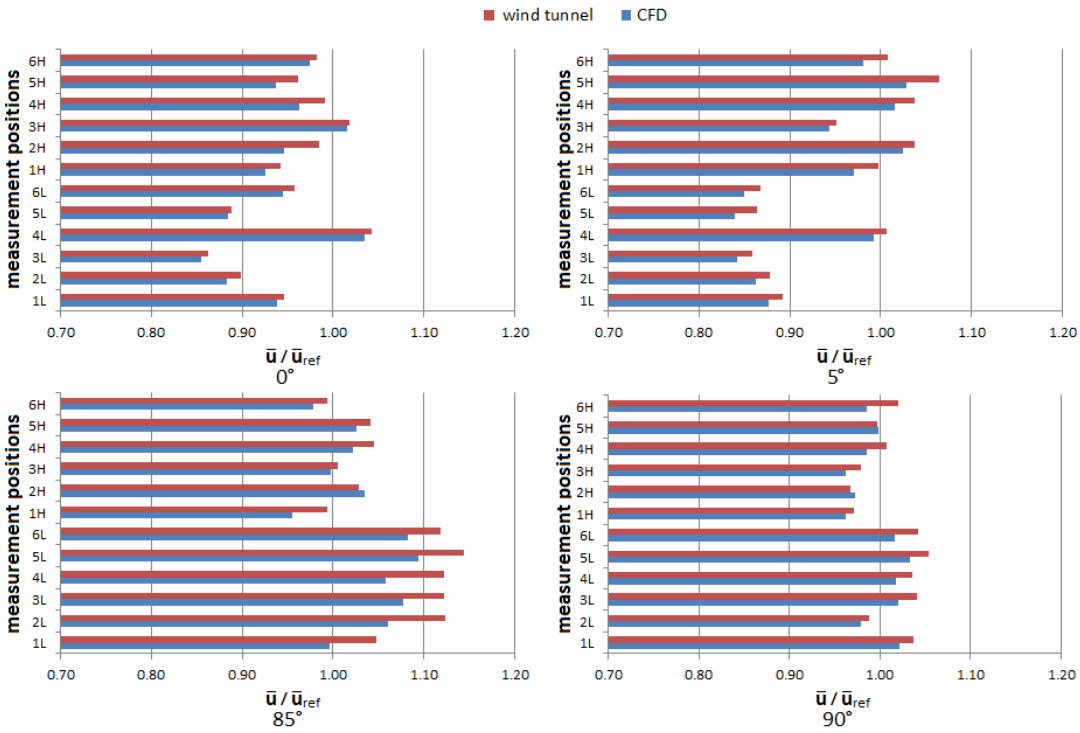

Figure 6-4 comparison of mean wind velocity at measurement points in tunnel and CFD, terrace

In **Figure 6-3** and **Figure 6-4** above, in order to compare the measured velocity result of CFD and tunnel experiments clearly, $\bar{u}_{ref}$ is defined with different value. In general, $\bar{u}_{ref}$ is the suburban wind velocity at windward direction of the house groups. In wind tunnel experiment, $\bar{u}_{ref}$ is the wind velocity at the start plane of the house models: $\bar{u}_{ref}$ =5.29 m/s at 40 mm model height (height of low measurement points) and $\bar{u}_{ref}$ = 7.59 m/s at 120 mm model height (height of high measurement points). These two reference velocity values are the average measured results of 5 measured positions in the reference plane across the tunnel, 40mm and 120 mm model height respectively. In CFD results, $\bar{u}_{ref}$ is the velocity at the start plane of the CFD house models: $\bar{u}_{ref}$ = 10 m/s at 10 m height (height of low measurement points) and $\bar{u}_{ref}$ = 14.5 m/s at 30 m height (height of high measurement points). The reference planes for both wind tunnel and CFD are at the same position and this reference plane is used for all tunnel results.

For both semi-detached house group and terrace groups, the mean velocity result from wind tunnel is larger than the CFD model in same measurement positions. There are two reasons for this difference: the first of all, environment settings of the CFD and tunnel experiments are different. CFD model is set to simulate a limitless area with

same house groups; while in wind tunnel experiment, the amount of model is limited by the size of the tunnel. In wind tunnel experiment, the area between model and two sides of the tunnel is empty; this makes the tunnel models have fewer obstacles than the CFD models. Due to this difference, at same position the wind record in tunnel experiments shows a larger mean wind velocity. The second, there are some measurement errors during the tunnel experiment. In the tunnel experiments, the anemometer is fixed through the ceiling of the tunnel with a control stick, the wind flow in the tunnel makes the anemometer slightly quivers during the experiment. Because of this, the measured result should be a small area around the measurement point but not the exact position, which makes the tunnel results different from the CFD results.

The average difference and average root mean square (rms) difference between the mean wind velocity at measurement points in tunnel and CFD models are shown in **Table 6-2**. The average difference between tunnel and CFD is measured with Eq.6-3; and the average rms difference is measured with Eq.6-4.

$$\bar{d} = \frac{1}{n}\sum_{i=1}^{n}\left|r_{TUN} - r_{CFD}\right| \qquad \text{(Eq.6-3)}$$

$$\bar{d}_{rms} = \sqrt{\frac{1}{n}\sum_{i=1}^{n}\left(r_{TUN} - r_{CFD}\right)^2} \qquad \text{(Eq.6-4)}$$

Table 6-2 average difference and average rms difference between Tunnel and CFD

model	semi-detached			terrace			
	0°	5°	90°	0°	5°	85°	90°
average velocity difference	1.61E-02	1.60E-02	2.59E-02	1.47E-02	2.00E-02	3.48E-02	2.52E-02
average velocity rms difference	1.98E-02	1.99E-02	3.21E-02	1.80E-02	2.14E-02	4.01E-02	2.99E-02

In **Table 6-2**, both average difference and average rms difference in 90 ° semi-detached model and 85 ° terrace model are larger than other models. Comparing the results in **Figure 6-3** and **Figure 6-4**, the differences come from the error at lower measurement points; especially position 7L, 8L, 9L in 90 ° semi-detached model and 4L, 5L, 6L in 85 ° terrace model. The position of these measurement points are as shown in **Figure 6-**

5. From this figure, all these points are close to the leeward edge of the model; some screws which are used to stay the model are close to these points. Compared with other points, these measurement points would be affected by these screws and the tunnel record would be different from the CFD simulation. For tunnel record at higher measurement points, the effect from these screws is less and the difference between the tunnel record and CFD simulation is less.

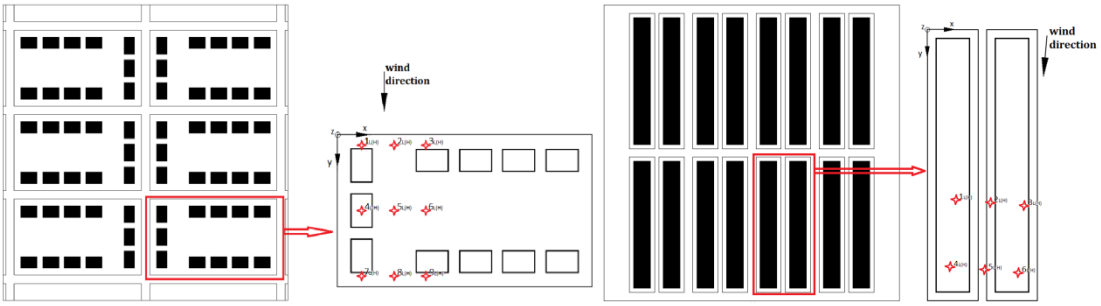

Figure 6-5 Tunnel measurement points with larger error

Anyway, in general, for both semi-detach and terrace model, the CFD and wind tunnel fit each other well. As shown in **Figure6-3** and **Figure 6-4**, in same position, the value different of $\bar{u}_z/\bar{u}_{ref}$ between the tunnel model and CFD model is less than 0.1. These results prove that the CFD setting in this project successfully modelled the air flow around both kind of building groups. In following sections of this chapter, the results from CFD models are used to analysis the velocity of wind around two building groups.

6.1.3 CFD velocity result

As mentioned in Section 4.3, FLUENT can show the velocity result as profiles and vectors. In such plots, there are more than 3000 velocity vector values in each cubic meter area of the model. In order to compare the velocity in different area close to the houses, these values are separated into several cubes with their positions. In each cube, the mean velocity vector sum ($\bar{u}_c$) is used to show the level of the wind velocity, which is defined as:

$$\bar{u}_c = \sqrt{\bar{u}_x^2 + \bar{u}_y^2 + \bar{u}_z^2} \qquad \text{(Eq.6-5)}$$

where

$$\bar{u}_x = \frac{1}{n}\sum_{1}^{n} u_x \,, \bar{u}_y = \frac{1}{n}\sum_{1}^{n} u_y \,, \bar{u}_z = \frac{1}{n}\sum_{1}^{n} u_z \qquad \text{(Eq.6-6)}$$

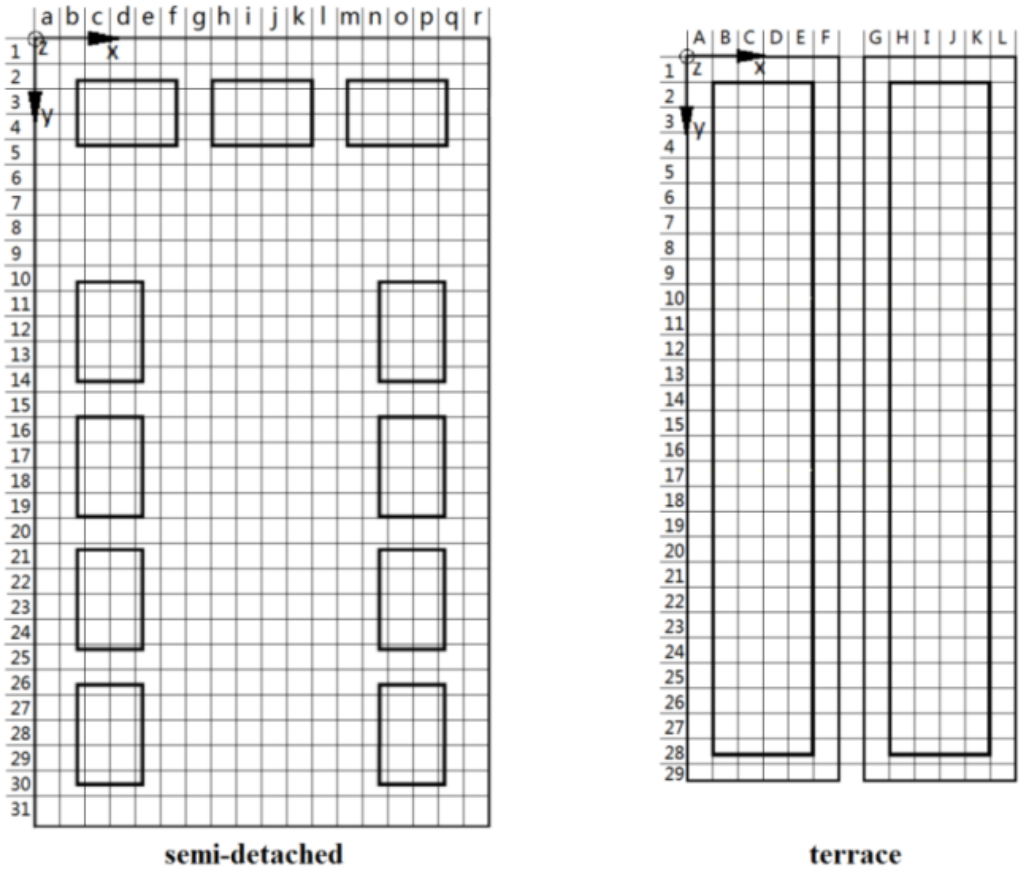

Figure 6-6 region division of areas around house groups

The size of each cube depends on the rotor area dimension of the wind turbines. As introduced in Section 2.1, the diameter size of the smallest wind turbine used in this project is 3 m (Kestrel 1000), thus, 3 m is set as the side length of the cube. **Figure 6-6** shows the vertical view of the area around semi-detached and terrace house groups.

In **Figure 6-6**, some letters and numbers are used to show the different cube area around the houses. These cubes only cover the house and garden area of the house group, the road around the house where wind turbines should not be fixed is not included. In this project, as the research focused on the height of 10 m and 30 m where wind turbines could be fixed in, two layers of cube with central core fixed at these two heights are used to show the CFD result.

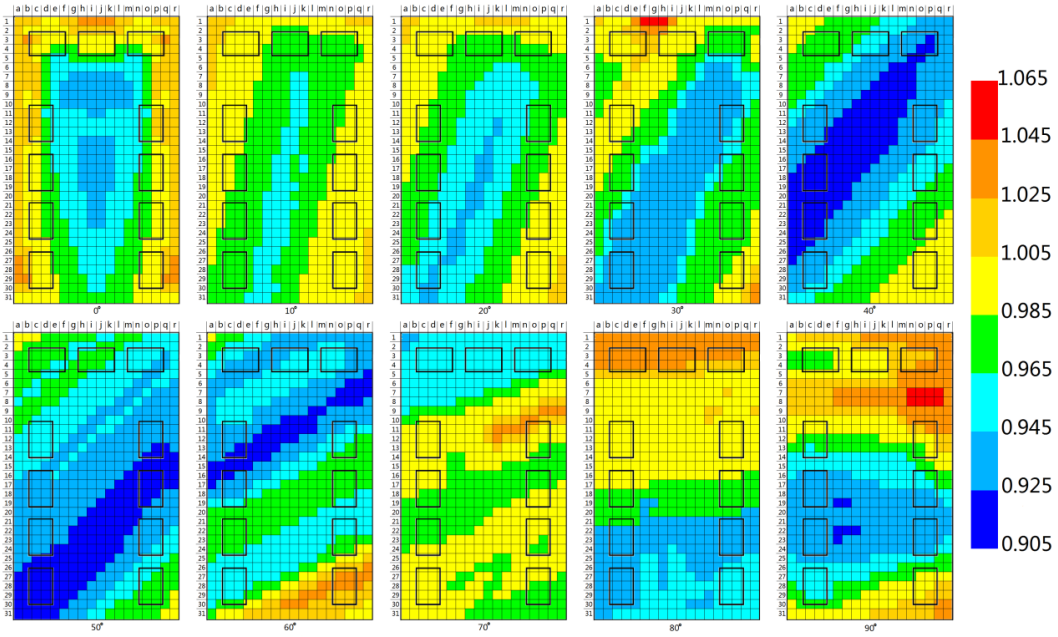

Figure 6-7 10 m height wind velocity around semi-detached house groups, $\bar{u}_{ref}$ = 10.22 m/s

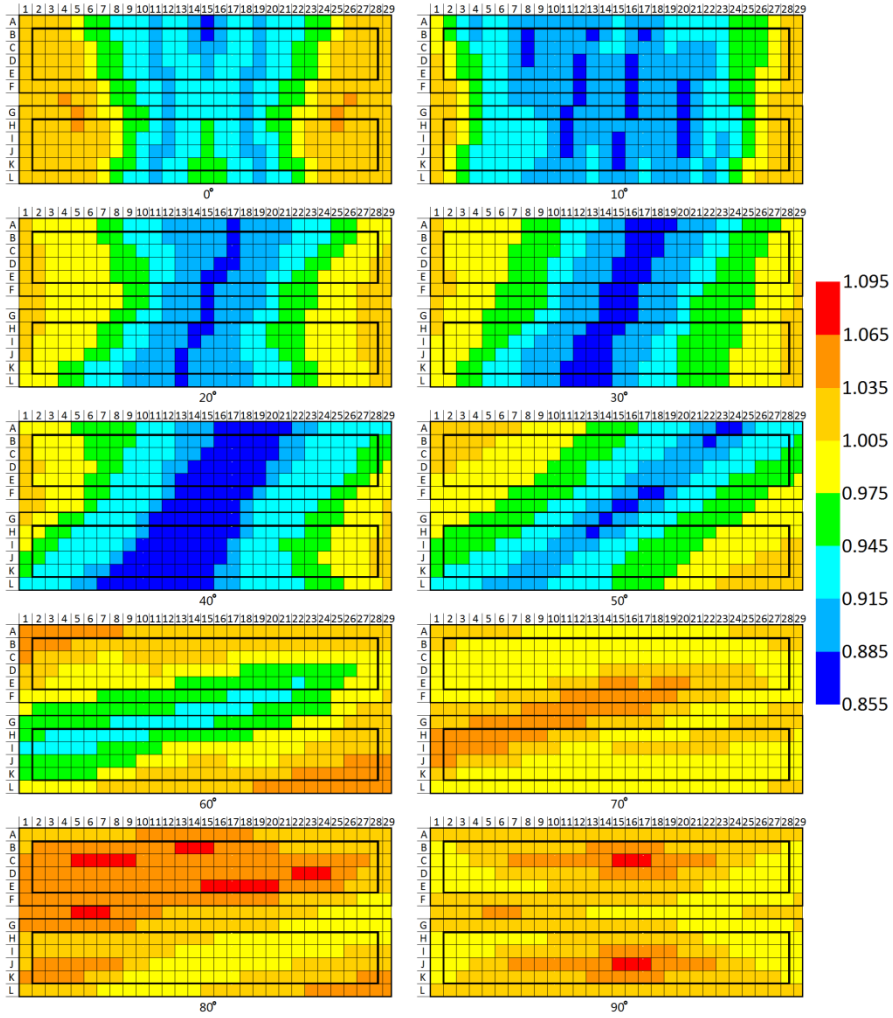

Figure 6-8 10 m height wind velocity around terrace house groups, $\bar{u}_{ref}$ = 10.03 m/s

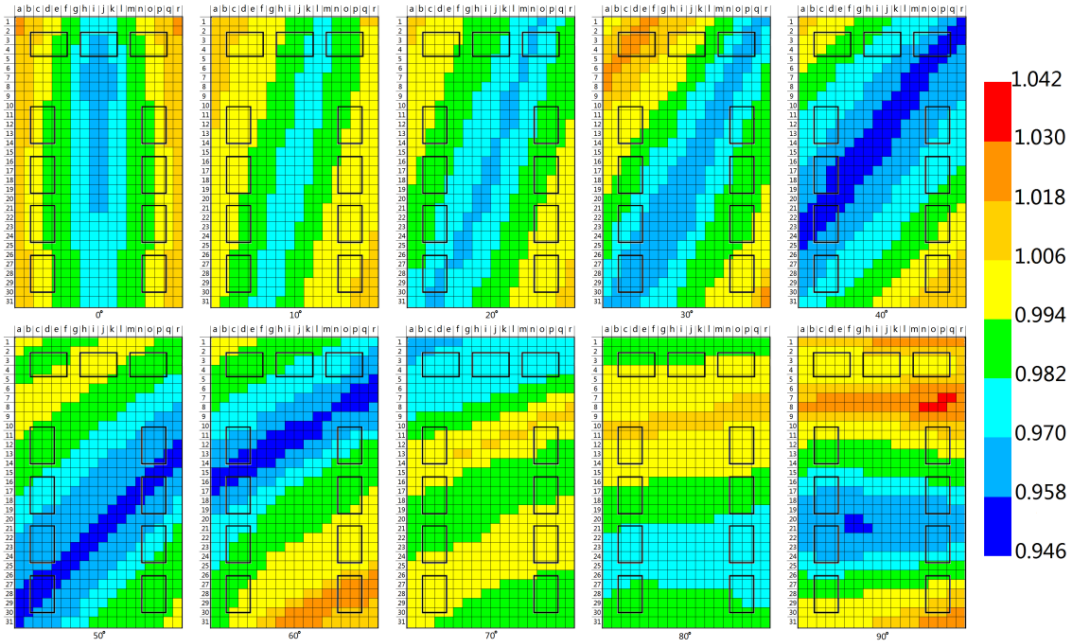

Figure 6-9 30 m height wind velocity around semi-detached house groups, $\bar{u}_{ref}$ = 14.79 m/s

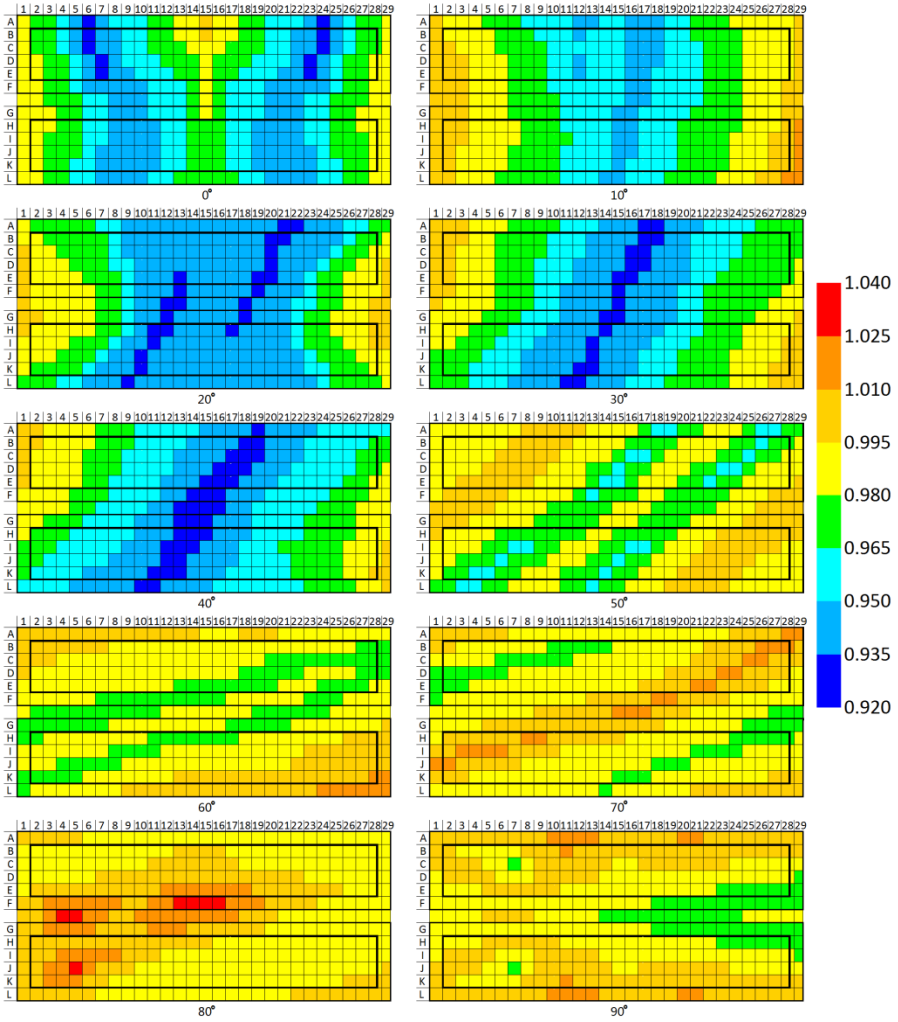

Figure 6-10 30 m height wind velocity around terrace house groups, $\bar{u}_{ref}$ = 14.46 m/s

Figure 6-7 and **Figure 6-9** shows the wind velocity result from the CFD semi-detached model as an example. In this plot, the average velocity vector sum of each cube is divided by the mean wind velocity at reference height (10 m and 30 m respectively); and the result is shown as different colour meshes in each vertical view plots. These plots show the velocity level of zones around semi-detached house group with different input wind direction, respectively. **Figure 6-8** and **Figure 6-10** show the velocity result for terrace houses group.

Attention should be paid that the values of $\bar{u}_{ref}$ shown in above figures are not the same as the $\bar{u}_{ref}$ value in **Figure 6-3** and **Figure 6-4.** In **Figure 6-3** and **Figure 6-4**, in order to compare the results with tunnel, the $\bar{u}_{ref}$ shows the mean wind velocity at 10 m and 30 m height at the same positions of the tunnel reference plane (start plane of the CFD house models), which is set as 10 m/s and 14.5 m/s respectively. From **Figure 6-7** to **Figure 6-10**, the aim of the reference velocity setting is to show the wind velocity level of area around the house groups more clearly; the values of $\bar{u}_{ref}$ are identified by the mean velocity around the models. For example, the reference wind velocity in **Figure 6-7** is 10.22 m/s; this value is the average wind velocity of the area around the 10 models shown in this figure. The reference velocity from **Figure 6-8** to **Figure 6-10** is identified in similar way. From these velocity values, the velocity levels at 10 m and 30m height around semi-detached and terrace houses are given. For different house group types, the area around semi-detached house group has stronger mean wind velocity than the area close to terrace house groups; at 10 m height, the differences of $\bar{u}_c/\ \bar{u}_{ref}$ between two house types is larger than the one at 30 m height. Based on the result from CFD models, the range of velocity at area close to the house groups at 10 m and 30 m height is as **Table 6-3** shown.

Table 6-3 range of wind velocity around the house groups

House type	10 m height		30 m height	
	min $\bar{u}_c/\bar{u}_{ref}$	max $\bar{u}_c/\bar{u}_{ref}$	min $\bar{u}_c/\bar{u}_{ref}$	max $\bar{u}_c/\bar{u}_{ref}$
Semi-detached	0.91	1.05	0.95	1.03
Terrace	0.86	1.08	0.92	1.03

With the CFD results show above, the hourly mean wind velocity at positions outside the building groups have following characteristics:

- The profile direction of velocity level is same as the input wind direction. In above plots, the area around house groups is divided into several levels which different wind velocities; shown as different colour zones in the plot. It is shown that these zones have clear directions which are same as the input wind direction of the model.
- Wind velocity at position with fewer obstacles is larger than the other positions. Of all the models above, the position with fewer houses at windward direction shows larger mean wind velocity. For most models, the positions with stronger flow are grouped mainly on the street side.
- The range of wind velocity increases with the building intensity. At 10 m height, the mean velocity at different points around semi-detached house group (building density 15.5%) ranged from 91% to 105% of the reference velocity; while for terrace house group (building density 46.4%) the range is from 86% to 108%. Comparing these two models, the building group with larger building intensity has larger velocity range than the building group with less building intensity.
- With the increasing height, the effect of building on the wind flow would decreases gradually. For both semi-detached and terrace house models, the velocity profiles at 10 m and 30 m height shows the similar plots. The main difference is the range of $\bar{u}_c/\bar{u}_{ref}$: at 30 m height the mean velocity ranged from 92% to 103% of the 30 m reference velocity, this range is much smaller than the range of 10 m height around same model. Also, the meshes with extreme velocity level (red or dark blue) at 30 m height are much less than 10 m height. As a result, the wind velocity in the whole area at 30 m height is more close to the reference velocity than the 10 m height.
- The wind velocity increases with the height from ground. The hourly mean wind velocity at 30 m height is larger than the mean velocity at 10 m height. The minimum velocity at 30 m height around semi-detached model is 14.05 m/s, which is larger than the maximum velocity at 10 m height around same model (10.83 m/s); while for terrace models, the minimum velocity at 30 m height is 13.3 m/s, which is also larger than the maximum velocity at 10 m height (10.79 m/s).

Based on the CFD result from **Figure 6-7** to **Figure 6-10**, the area around buildings with larger wind velocity could be found. In Section 6.2, the turbulence intensity results of these areas are used to select the suitable position for the wind turbines.

6.2 Turbulence results

The study about characteristics of turbulence around house groups is based on the result from wind tunnel and CFD models. Generally, both CFD and tunnel experiments gives some instantaneous velocity value in x,y and z directions, marked as $u_x(t)$, $u_y(t)$ and $u_z(t)$; during the process of measuring, the mean wind velocity and turbulence velocity fluctuations on these directions could be calculated with Eq.5-6 and Eq.5-8. For each measurement points, these values are calculated with Eq.5-7 and give the turbulence intensity values in 3 directions. Eq.4-12 is also used in this study which gives the main turbulence intensity of the position.

In this section, the turbulence intensity profile in wind tunnel is checked with some literature functions in Subsection 6.2.1; followed by the comparing of wind tunnel results and CFD results in Subsection 6.2.2; and finally, based on CFD results, Subsection 6.2.3 gives the profile of turbulence intensity around house groups.

6.2.1 Turbulence intensity profile in wind tunnel

Similar with the analysis of wind velocity, for turbulence analysis, the turbulence intensity profiles in wind tunnel experiment are checked before calculate the turbulence intensity at measurement points. **Figure 6-11** shows the turbulence intensity profiles $I_{x,}$ I_y and I_z in the wind tunnel experiment.

The turbulence intensities in **Figure 6-11** have following relationship:

$$I_x : I_y : I_z = 1 : 0.78 : 0.55 \qquad \text{(Eq.6-7)}$$

This form agrees well with the equation suggested by Couniham **[76]** and Holmes **[77]**, who proposed the value as 1: 0.75: 0.5 and 1: 0.88: 0.55.

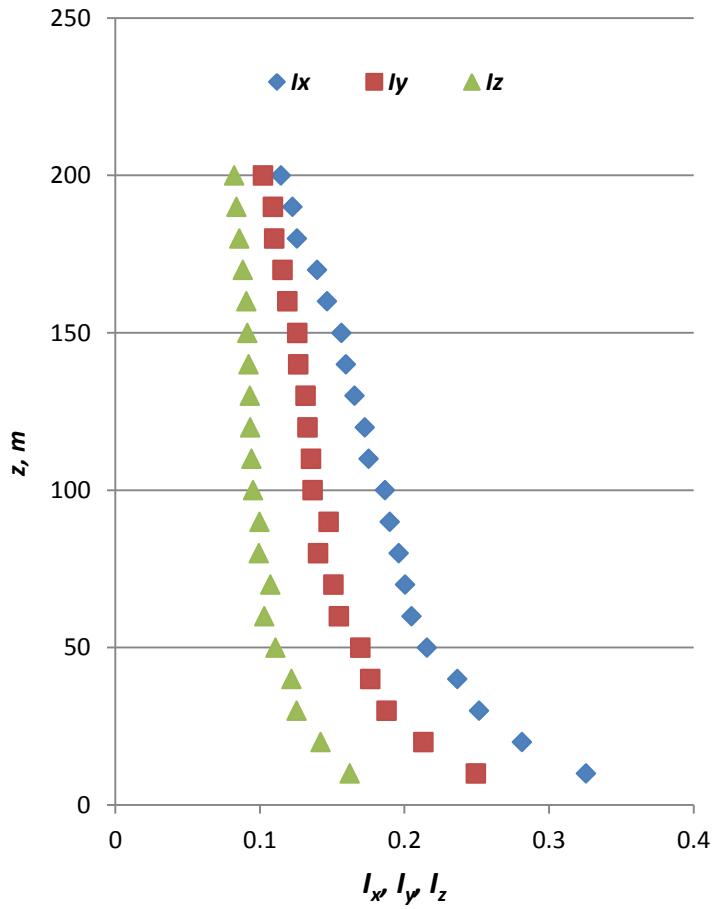

Figure 6-11 turbulence intensity profiles I_x,I_y and I_z in wind tunnel experiment

The turbulence intensities could also be checked with function:

$$I_x = \frac{1}{\ln\left(\frac{z}{z_0}\right)} \qquad \text{(Eq.6-8)}$$

This function is used to calculate the full-scale turbulence I_x in ESDU 85020 [71]. Based on this literature, a tolerance range of ±20% is acceptable for practical purposes. In this project, the roughness height z_0 is 0.26 m in full-scale, **Figure 6-12**, **Figure 6-13** and **Figure 6-14** compares turbulence intensity profiles with the acceptable range of I_x, I_y and I_z respectively. The "limit +" curve shows the 120% value of I_x, I_y and I_z, while "limit -" curve shows the 80% value of I_x, I_y and I_z. The basic value of I_x is calculated with Eq.6-8 with z_0 =0.26 m, the basic value of I_y and I_z is 88% and 55% of I_x, respectively.

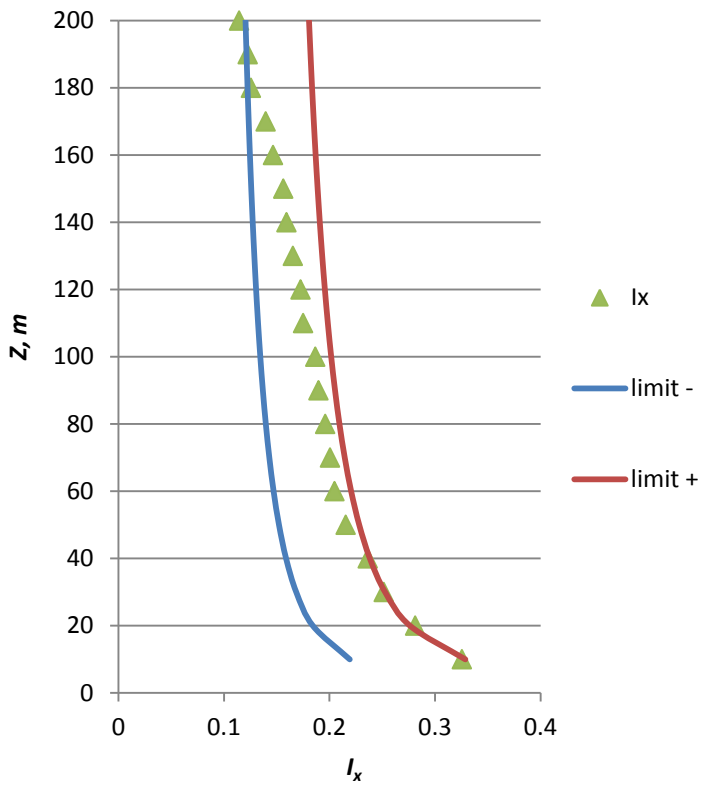

Figure 6-12 profile of longitudinal turbulence intensity in wind tunnel experiment

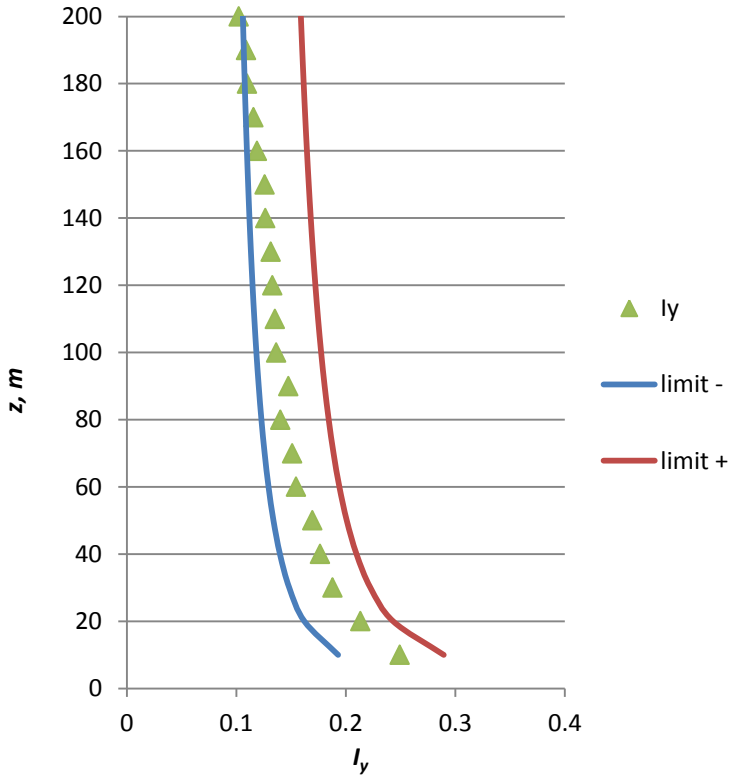

Figure 6-13 profile of lateral turbulence intensity in wind tunnel experiment

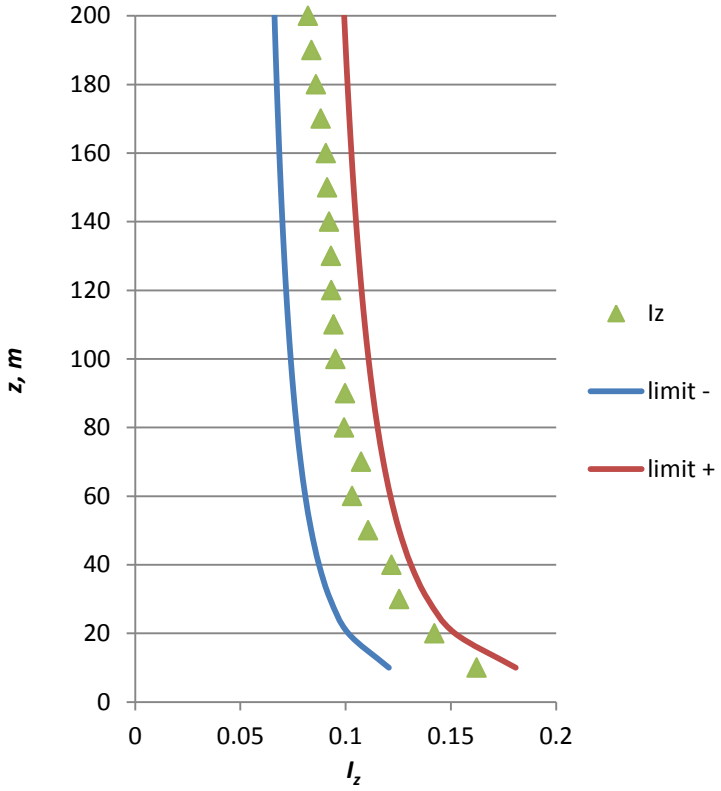

Figure 6-14 profile of vertical turbulence intensity in wind tunnel experiment

From the turbulence intensity profiles, the turbulence intensity in 3 directions shows good agreement with the calculated value. For all directions, the turbulence intensity value at lower height from the ground is larger and close to the "limit +" curve. This is due to the effect of roughness blocks on ground of the tunnel increase the turbulence. In general, the turbulence setting in wind tunnel experiment successfully simulates the ABL of suburban terrain in this project.

6.2.2 Wind tunnel turbulence results

The turbulence results from the wind tunnel experiment are calculated from the velocity result from the experiment records. In each measurement position, 9000 records are taken during the experiment. Each record includes the velocity value in 3 directions, marked as $u_x\,(t)$, $u_y\,(t)$ and $u_z\,(t)$. With Eq.5-5, Eq.5-8 and Eq.4-12, the mean turbulence intensity in the measurement point could be calculated.

Similar as the velocity analysis part, the turbulence intensity value from the wind tunnel experiment need to be compared with the CFD results in same positions. As mentioned in Section 4.3, the turbulence intensity function used in FLUENT is for full developed pipe flow, which is not suitable for this project. Because of this, the turbulence intensity profile plots from FLUENT are not used in this project. Instead of the turbulence intensity profile, the CFD turbulence intensity results of each cube in this report are calculated with the definition function (Eq.4-12), the turbulence velocity fluctuations and mean velocity of each cube could be gain from FLUENT result list.

Figure 6-15 and **Figure 6-16** compare the turbulence intensity value in same position from CFD and wind tunnel experiments. It could be found that the wind tunnel results have a larger value than CFD results. Besides the reasons analyzed in the velocity parts, the control stick and anemometer used in the tunnel experiment affect the flow and make the turbulence intensity value larger than the value at same positions in CFD models.

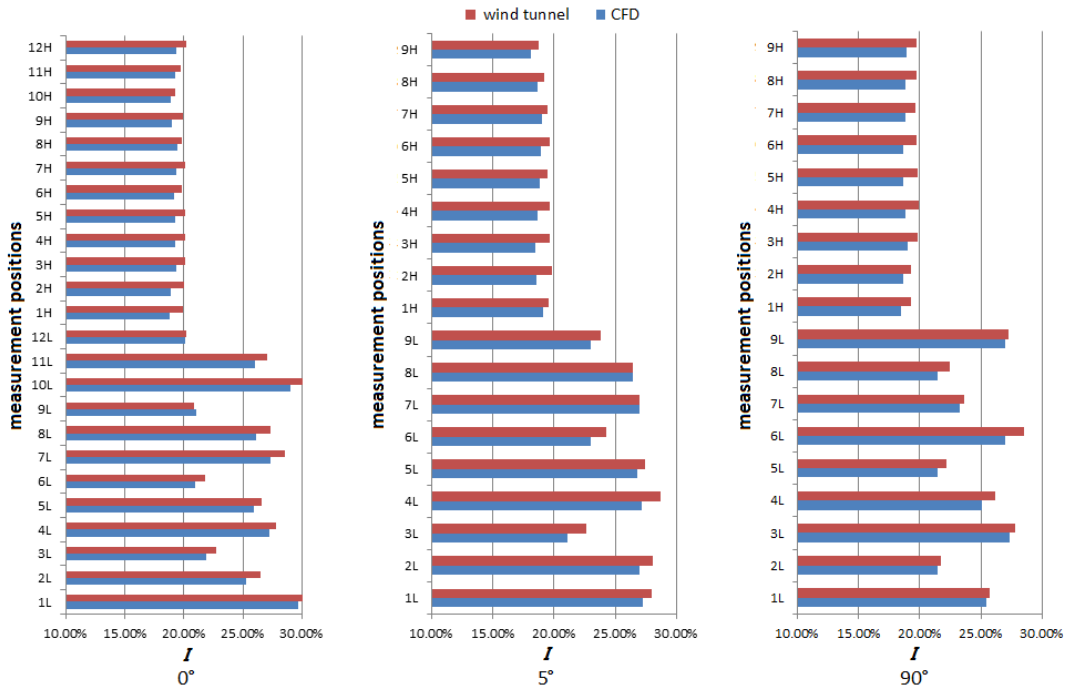

Figure 6-15 comparison of turbulence intensity at measurement points in tunnel and CFD, semi-detached

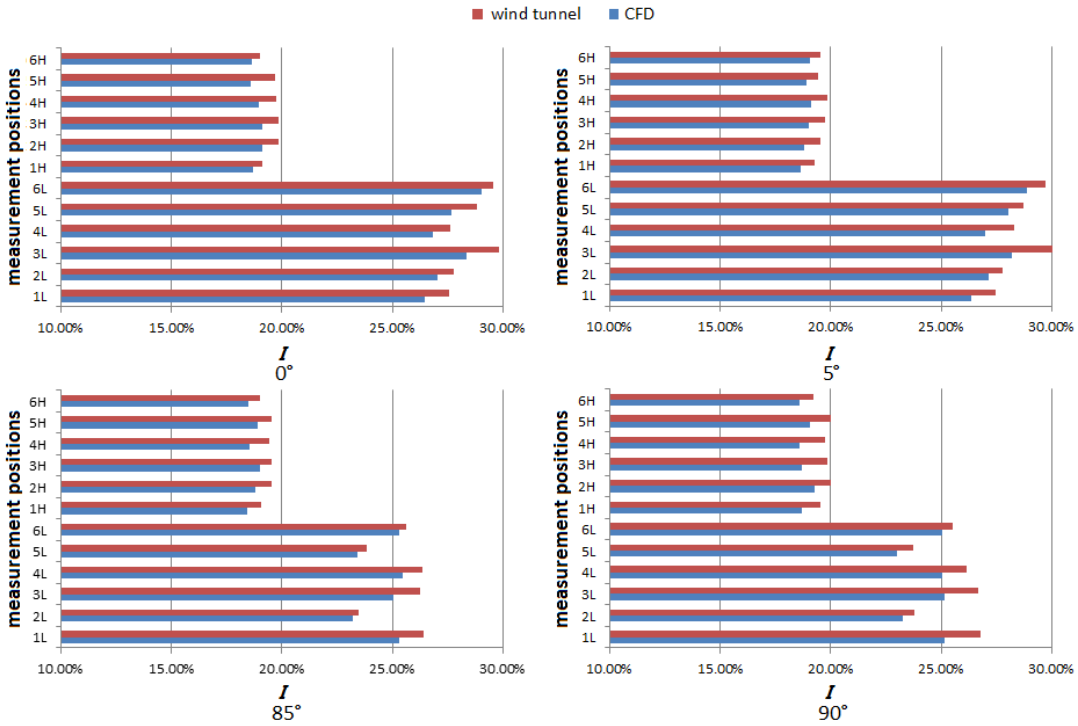

Figure 6-16 comparison of turbulence intensity at measurement points in tunnel and CFD, terrace

Generally, the turbulence intensity different between the CFD models and tunnel experiment is less than ±2%. It is accepted that FLUENT successfully modelled the turbulence of the wind tunnel experiments. **Table 6-4** shows the turbulence intensity range of area around different house types in CFD models.

Table 6-4 range of turbulence intensity around the house groups

House type	10 m height		30 m height	
	min *I*	max *I*	min *I*	max *I*
Semi-detached	19%	33%	16%	18%
Terrace	24%	35%	16%	19%

6.2.3 CFD turbulence results

In this part, the turbulence intensity results from the CFD model are shown in same way as the velocity analysis part in Subsection 6.1.3. In each cube area, the velocity vector results during the last 500 iterative calculations are calculated with Eq.5-5, Eq.5-8 and Eq.4-12, which gives the mean turbulence intensity result of that cube area. **Figure 6-17** shows the turbulence result around semi-detached house at 10 m height as an example.

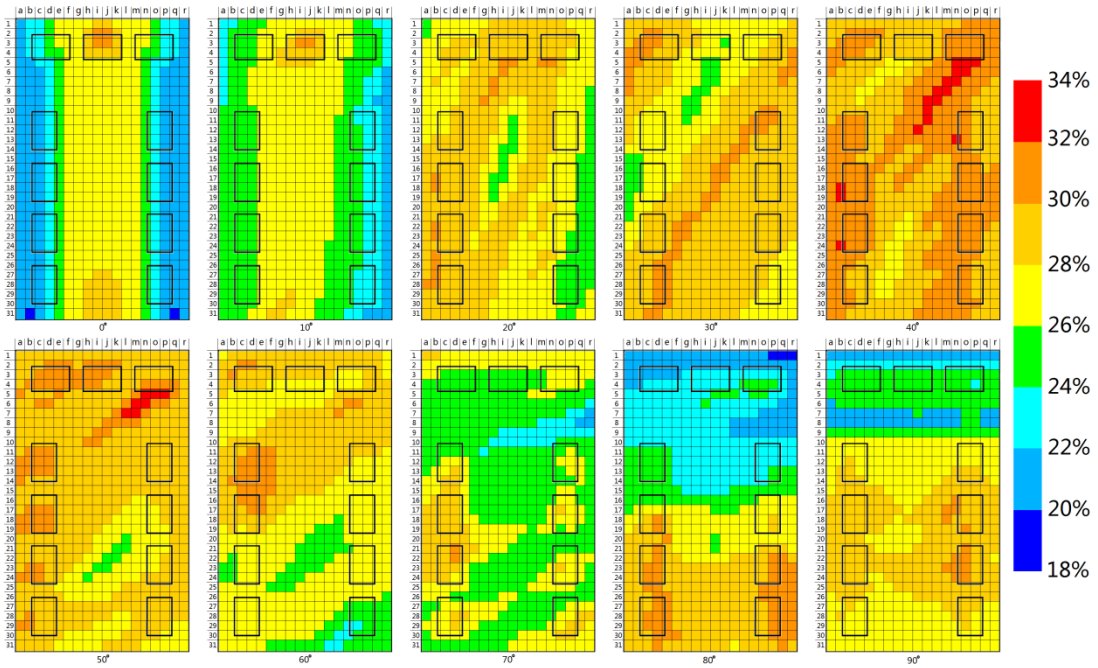

Figure 6-17 10 m height turbulence intensity around semi-detached house groups

These turbulence plots show the turbulence level in areas close to the houses. For wind turbines, because of the high turbulence intensity leads to a stronger fatigue load on turbines, which will reduce the service life of the wind turbines; the area with less turbulence intensity is more suitable than the ones with larger values for the setting of wind turbines. Based on IEC 61400 [78], the turbulence intensity class for wind turbines is between 16% (Class B) and 18% (Class A), which means nearly all areas at 10 m height close to the house have larger turbulence intensity than the effective turbulence intensity of the turbines. Based on the CFD results, the turbulence intensity of area at 30 m height is from 16.8% to 18.7%, which is close to turbulence intensity Class A; for both types of house group, 30 m height is more suitable for the setting of wind turbines.

6.3 Summary of experiment results

In general, both wind velocity and turbulence intensity results are analyzed in three steps in this chapter. First of all, the tunnel profile result at vertical line in the middle of the wind tunnel is calculated, which gives some characteristic parameters of the

ABL simulated by the wind tunnel. These characteristic parameters are checked with some literature functions and proved that the ABL of suburban terrain is successful modeled by the tunnel. These parameters are also used to set the boundary condition of the CFD models.

Secondly, the tunnel results at measurement positions are calculated and compared with CFD results in same positions. Both CFD and tunnel results at these positions fit each other well, and it is acceptable that the CFD and tunnel models successful modeled the air flow around the house groups.

Finally, based on the result from the CFD models, the condition of air flow around house groups is given. Fitted profiles are used to show both wind velocity and turbulence intensity results. These plots show the flow in area close to the houses, and listed with different input wind directions. Based on these plots, the wind is more affected by the houses at 10 m height than 30 m height; the environment at 10 m height show larger turbulence intensity and smaller wind velocity than the one at 30 m height. And the wind resource at same height around the semi-detached house group is better than the one around terrace house group.

Generally, the wind at 10 m height in suburban areas is not suitable for the setting of wind turbines. There are mainly two reasons for this conclusion: first, the velocity at this height is not large. From the velocity plots of area around the houses, although there do have some positions which increase the velocity of the wind, but the increased wind velocity is still not large enough to support enough energy. And also, the areas which increase the wind velocity are few and limited by the input wind direction; at most of the area around the house, the wind velocity is equal or even lower than the mean value. Secondly, the turbulence intensity of nearly all areas close to the houses at 10 m height is larger than the turbulence intensity class A of most wind turbines. This means the service life of the turbines will be reduced if they are fixed at these positions. Based on the result from this research, the turbines are suggested to be fixed at height greater than or equal to 30 m from the ground. In following Chapter 7, only the results from 30 m height is used to analysis the energy output at areas around house groups.

CHAPTER 7

7 Energy Output Analysis

This chapter focused on the energy output of areas around house group at 30 m height, the experiment results from chapter 6 are combined with the historical wind records in chapter 3. Section 7.1 introduces the method of select the optimal area around house groups, which is based on the CFD results in Chapter 6 and the wind direction frequency data in Chapter3, some functions used in this research to calculate the energy output for different wind turbines are also introduced in this section. While Section 7.2 shows the energy output results of different wind turbines in different regions around U.K., which includes the optimal area and total energy output for different wind turbines. The economic and carbon payback time of these wind turbines which are used to find the most suitable turbines are also included in this section.

7.1 Research method of energy output

As shown in Section 2.1, for all wind turbines, the energy output of the turbines has direct relationship with the velocity of the wind. Thus, optimal area which can support better wind energy should have larger wind velocity than the other areas. Besides the velocity, turbulence is another factor need to be considered; as larger turbulence intensity means less service life of wind turbines, the area with lower turbulence intensity shown to be better position for the setting of wind turbines. The velocity and turbulence level of the areas around house groups is as Chapter 6 shows

Based on the velocity and turbulence plots, the velocity and turbulence level of a select position are variable for different input wind directions; thus, the frequency of

input wind direction should be considered in the selection of optimal areas around house groups. And also, the rated velocity are different for different wind turbines, in order to comparing the energy output, the frequency of different mean velocity should be included in the calculation.

The energy output calculation of areas around house should include all above factors. As the frequency of input wind direction and mean wind velocity is different for different regions in U.K.; for each region, the optimal area should be calculated respectively.

The mean wind velocity at 30 m height is calculated based on the historical record at 10 m height in town area; Eq.4-11 is used to do this calculation, with characteristic parameters shown in **Table 6-1**, the mean wind velocity at 30 m height and 10 m height has following relationship:

$$\bar{u}_{30} \approx 1.45\bar{u}_{10} \qquad \text{(Eq.7-1)}$$

For different input directions, the mean wind velocity at 30 m height is timed with the value of $\bar{u}/\bar{u}_{30}$ shown in **Figure 6-9** which gives the mean velocity in each area around the houses. And the mean velocity in each cube area near the house is

$$\bar{u} = \frac{\bar{u}}{\bar{u}_{30}} \cdot 1.45\bar{u}_{10} \qquad \text{(Eq.7-2)}$$

In each area around buildings, for a selected wind turbine in a selected region, the energy output in each input wind direction is calculated with following function:

$$AEP = \sum_{dir=0}^{350} \sum_{vel=v_{in}}^{v_{out}} 8760 \cdot f_{dir} f_{vel} W_{vel} \qquad \text{(Eq.7-3)}$$

where f_{dir} is the annual frequency of each input direction in the region, f_{vel} is the frequency of each wind velocity, v_{in} is the cut-in velocity, v_{out} is the cut-out velocity, and W_{vel} is the energy output of each velocity from the power output curve of the wind tunnel, respectively.

For example, at suburban area close to Bristol, in area a1 around semi-detached house. As shown in **Figure 6-9**, in $0\,°$ input wind direction, the value of $\bar{u}/\bar{u}_{30}$ is 1.02. The hourly mean velocity 3m/s at 10 m height is transformed to $\bar{u}$ =4.44 m/s in this area.

From the historical weather record, 0.32% of the annual hours have this velocity in this direction, which is 28 hours. Based on the power output curve of Whisper 200 (shown in **Figure 2-4**), the output power of 4.44 m/s is 101 W, the annual energy output of Whisper 200 in this area with $0°$ input direction and mean velocity 4.44 m/s is 101W times 28hour, which equal to 2.83 kWh. Similar, annual energy output with different input velocity and direction are calculated, and the summation of these values is marked as the annual output energy of Whisper 200 in this cube area.

The mean turbulence intensity in each cube area is calculated as:

$$I = \sum_{dir=0}^{350} f_{dir} I_{dir} \qquad \text{(Eq.7-4)}$$

Similar as the distribution profile of mean wind velocity around house groups, because of the annual frequency of input direction is different in different U.K. regions, the distribution of turbulence around house groups are different in different cities. In general, the turbulence intensity in each cube is checked with the turbulence intensity class of wind turbines; only the cube area with mean turbulence intensity less than 18% is suitable for the setting of wind turbines.

Another restriction for the layout of wind turbine is the space between turbines. Based on IEC 61440-1 **[79]**, the distance between each two wind turbines should be at least 5 times of the turbines' blade diameter. The reason of this distance requirement is that the wind through wind turbines will be affected by the turbines, and some produce turbulence in the downstream direction of each turbulence. Because of this, the distance between optimal setting positions is at least 5 times of the blade diameter of each wind turbine.

7.2 Energy output

For selected region and selected wind turbines, the *AEP* value in each cube area (calculated with Eq.7-3) shows the annual energy output of one wind turbine if it is set in that cube area. After the *AEP* in all cube areas are calculated, these values are compared with each other, the cube area with larger *AEP* values are select as the

optimal area. The selection of optimal area is also limited by the turbulence level of the position and space between each other, as introduced in Section 7.1.

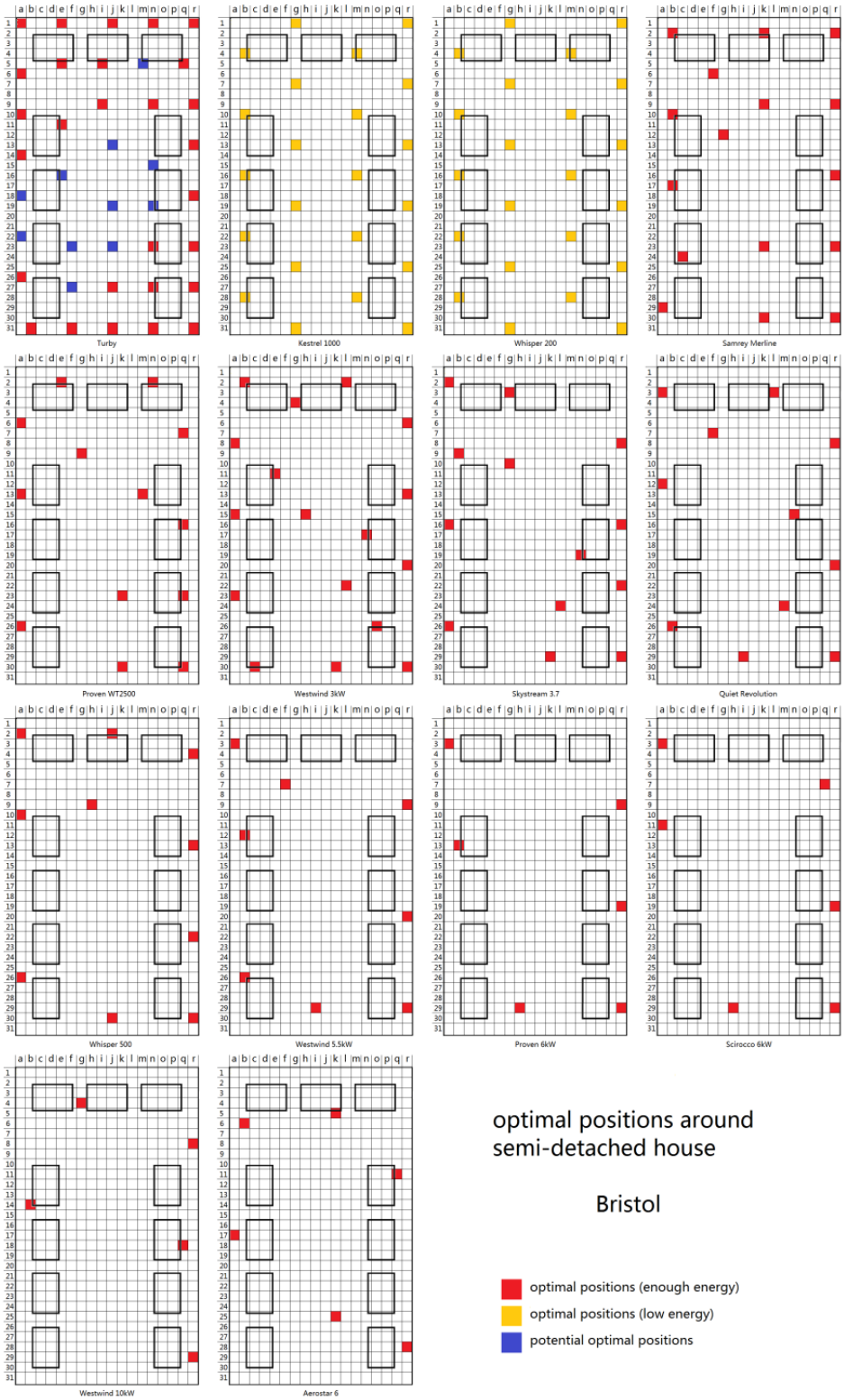

Figure 7-1 optimal positions around semi-detached house groups in Bristol

Figure 7-1 shows the optimal areas for different wind turbines around semi-detached house group in Bristol as an example. The total AEP of each wind turbines in Bristol are listed in **Table 7-1**.

In this project, the output energy of wind turbines should be compared with the annual electricity consumption of the household. As mentioned in Section 3.3, the annual electricity consumption of one household is 4,831 kWh [9], and in this model, 22 households are included in each semi-detached house group; which means the electricity consumption of the households is 106,282 kWh per year.

The cube areas close to the house groups are sorted by their AEP value and give the optimal positions. The total AEP value of the selected optimal positions is compared with 106,282 kWh. This comparing shows two kind of result: The total AEP of the optimal positions is larger than 106,282 kWh which means the wind turbines can produce enough energy; or the total AEP is less than the annual electricity consumption of the households, which means the AEP is not enough for the houses. These optimal positions in these two circumstances are marked with different colour in **Figure 7-1**: red points shows the optimal positions with enough output energy, and yellow points shows the optimal positions with low energy output. For the plot of Turby, as the blade diameter of this wind turbine is the smallest of all turbines used in this analysis, there are more positions to be selected; a third kind of mark, the blue points, is used to show the potential positions around the houses. Comparing to the AEP in red positions, the output energy in blue position is just a little less. If some of the red positions are not suitable for the setting of wind turbine, Turby could be set at these blue positions.

The optimal positions shown in **Figure 7-1** give the siting position of different wind turbines. The selection of these positions has direct relationship with the frequency of windward direction and frequency of hourly mean wind velocity. In different U.K. regions, these two frequencies are different; thus, the optimal sitting positions in different U.K. regions are different. However, there are still some general rules which could help find the positions with larger AEP, shown below:

- The positions with fewer obstacles have larger wind energy output. From the analysis result of all U.K. regions, the wind turbines sited at positions which

are surrounded by obstacles have fewer energy outputs; while the wind turbines sited at positions closer to the street side have larger energy output. For example, at 30 m height from ground around semi-detached house groups in Bristol, the average AEP of Whisper 500 sited by the street side is 11,158 kWh, while the average AEP of same wind turbine sited at the area surround by the houses is 10,324 kWh. The energy output at the street side is about 108% of the energy output at positions surround by houses. The AEP of other wind turbines in other cities shows similar results. This is because there are fewer obstacles on the street, which lead to a higher wind velocity at these positions and thus a higher energy output.

- The building group with less building density is more suitable for the siting of wind turbines. Based on the AEP analysis result of the turbines sited at 30 m height around semi-detached house group and terrace house group, the average AEP of each wind turbine is larger when it is sited around semi-detached houses. Take Bristol for example, the average AEP of Whisper 500 around semi-detached houses is 10,480 kWh; this value is larger than the average AEP of same turbine sited around terrace houses (10,334 kWh). From the analysis result, for most U.K. regions, the total output energy of most wind turbines sited at all possible position at 30 m height around terrace house group is less than the electricity requirement of households (193,240 kWh); it is not possible to select optimal positions around terrace houses. There are three reasons for this result. First, the size of area around semi-detached house group is larger than the area around terrace house group; as a result, there are more positions to be selected around the semi-detached house. Secondly, the mean velocity at same height around semi-detached houses is larger than the mean velocity around terrace houses, the turbine output energy at each position around semi-detached house is larger. Thirdly, there are more households in terrace house group than the semi-detached house groups. The annual energy requirement of the terrace group is larger than semi-detached group; the required amount of wind turbines in terrace house group is larger than the one in semi-detached house groups. As a result, at 30 m height, there are always not enough site positions suitable for the wind turbines to produce enough energy for the requirement of terrace households.

Table 7-1 expectant payback time of turbines used in semi-detached house group, Bristol

Turbine name	Require amount	Total AEP (kWh)	AEP per turbine (kWh)	Economic payback time (year)	Carbon payback time (year)
Turby	27	107,257	3,972	14.6	1.0
Kestrel 1000	22	83,765	3,808	9.9	1.0
Whisper 200	22	79,679	3,622	4.6	1.0
Samrey Merline	16	108,456	6,779	6.7	0.6
Proven WT2500	13	109,640	8,434	10.9	0.4
Westwind 3kW	17	111,453	6,556	9.0	0.6
Skystream 3.7	13	106,989	8,230	8.2	0.5
Quiet Revolution	11	112,576	10,234	20.4	0.4
Whisper 500	10	108,573	10,857	4.0	0.3
Westwind 5.5kW	8	112,387	14,048	6.1	0.3
Proven 6kW	6	106,668	17,778	9.0	0.2
Scirocco 6kW	6	117,128	19,521	9.8	0.2
Westwind 10kW	5	115,995	23,199	6.6	0.2
Aerostar 6	6	116,968	19,495	4.3	0.2

Table 7-2 expectant payback time of turbines used in terrace house group, Bristol

Turbine name	Require amount	Total AEP (kWh)	AEP per turbine (kWh)	Economic payback time (year)	Carbon payback time (year)
Turby	51	193,660	3,797	14.0	1.0
Kestrel 1000	23	85,108	3,700	9.6	1.0
Whisper 200	23	77,498	3,369	4.3	1.1
Samrey Merline	16	105,390	6,587	6.5	0.6
Proven WT2500	16	130,527	8,158	10.5	0.5
Westwind 3kW	16	101,713	6,357	8.7	0.6
Skystream 3.7	16	126,991	7,937	7.9	0.5
Quiet Revolution	9	89,599	9,955	19.8	0.4
Whisper 500	13	136,128	10,471	3.9	0.4
Westwind 5.5kW	9	122,474	13,608	5.9	0.3
Proven 6kW	9	153,227	17,025	8.6	0.2
Scirocco 6kW	9	169,693	18,855	9.5	0.2
Westwind 10kW	9	201,427	22,381	6.4	0.2
Aerostar 6	9	170,630	18,959	4.2	0.2

Table 7-1 shows the total AEP produced by different wind turbines fixed in the optimal positions around semi-detached house group in Bristol. **Table 7-2** shows the total AEP produced by different wind turbines fixed in the possible positions around terrace house group in Bristol. These values are divided by the amount of turbines and give the average AEP of each turbine. With the method introduced in Section 3.3, the economic payback time and carbon payback time of each wind turbine is given. From **Table 7-1**, Whisper 500 has the shortest economic payback time, while Aerostar 6 has the shortest carbon payback time. Based on different targets (saving economic payback time or saving carbon payback time), these two kinds of turbines could be selected as the optimal wind turbine for semi-detached house group close to Bristol.

For other regions, the optimal positions and most suitable wind turbines could be select in similar way. The selected wind turbines and their optimal fixed position for semi-detached and terrace house for all U.K. regions are shown in Appendix G.

Table 7-3 the amount of turbines sited positions around semi-detached house groups

	Edinburgh	Bristol	Glasgow	Birmingham	Manchester	Leeds	London
Turby	29	27	32	34	35	35	46
Kestrel 1000	-	-	-	-	-	-	-
Whisper 200	-	-	-	-	-	-	-
Samrey Merline	16	16	18	20	20	20	-
Proven WT2500	13	13	15	16	16	16	20
Westwind 3kW	17	17	19	21	21	22	-
Skystream 3.7	13	13	15	16	17	17	21
Quiet Revolution	11	11	12	-	-	-	-
Whisper 500	11	10	12	12	13	13	16
Westwind 5.5kW	8	8	9	10	10	10	-
Proven 6kW	7	6	7	8	8	8	11
Scirocco 6kW	6	6	7	7	7	7	9
Westwind 10kW	5	5	6	6	6	6	8
Aerostar 6	6	6	6	7	-	-	-

The amount of sited positions of each wind turbines around semi-detached houses in each region are shown in **Table 7-3.** In this project, some turbines could not produce enough energy for the households even they are sited at all possible positions around the houses; such situation is shown as "-" in this table.

Based on the analysis results above, the key results about optimal choice of wind turbines in different U.K. regions are as following:

- Small turbines are not suitable to be used in both house groups. From the analysis result, at 30 m height around semi-detached house groups, the wind turbines with rate power less than 2,500 W (Kestrel 1000 and Whisper 200) could not produce enough energy. Due to the low output power from each small turbine is low; the amount of small wind turbines should be large enough to ensure the turbines produce large enough energy for the use of households. However, the size of area around house group limits the amount

of turbines; as a result, none of the turbines with rate power less than 2500 W is suitable for the house groups.

- Medium turbines could produce enough energy for semi-detached house groups. In general, at 30 m height, most of the wind turbines with rate power between 2500 W and 6,000 W works well, which gives a good economic and carbon payback time. For wind turbines with rate power larger than 6,000 W, the wind is not strong enough that the turbines cannot work in high efficiency. In suburban zones around U.K., the wind turbines with rate power larger than 6,000 W is suggested to be fixed at height higher than 30 m from the ground, which would reduce the total amount, economic and carbon payback time as well.
- HAWTs have better economic payback time than VAWTs. In this project, two VAWTs (Turby and Quiet Revolution) are compared with HAWTs. Due to the prices of VAWTs are larger than HAWTs, the economic payback time of these two turbines are much larger than the other turbines. VAWT is not suggested to be used in house groups.
- Turbines with larger rate power are more suitable for suburban zones with larger building density. The rate power of turbines used at 30 m height around terrace house groups should be larger than 10,000 W; turbines with rate power less than 10,000 W could not produce enough energy. There are three reasons for this conclusion. Firstly, due to the fewer site space, the amount of turbines sited around terrace house groups is less than the turbine amount around semi-detached house groups. The fewer amount would reduce the total AEP of the turbines. Secondly, the mean wind velocity around terrace house groups is less than the velocity around semi-detached house groups; this makes the AEP per turbine around terrace house groups less than the one around semi-detached house groups. Thirdly, there are more households in each terrace group (40 households) than the households in each semi-detached group (22 households). The required electricity consumption of each terrace group is larger thus more total AEP from the turbines are needed. However, for most U.K. regions, 30 m height around terrace house groups is still not good enough for the setting of wind turbines; the selected wind turbine should be set at height higher than 30 m to prove the energy production is enough.

- There are more turbines suitable for the building group wind energy system at regions with larger Weibull scale parameter. At same height of suburban area in each region, the required amount of each wind turbine is different. Due to the space limit around house groups, there are not enough site positions for some wind turbines to produce enough energy from the wind; such turbines are not suitable for the wind energy system around buildings. For semi-detached house groups, Edinburgh has the most kinds of turbine which could produce enough energy, and the require amount of each turbine is the smallest of all regions; followed by Bristol, Glasgow, Birmingham, Manchester, Leeds, and then London. At 30 m height around terrace house groups, only the wind turbines sited in Edinburgh and Bristol could produce enough energy for the terrace households. In general, the above sequence of cities shows the wind energy intensity order of these cities, from strong to weak. Compared with the Weibull parameter in **Table 3-2**, the Weibull scale parameter (*A*) of the town zone in these cities follows same sequence: Edinburgh has the largest *A* value and London has the smallest *A* value. Also, at 30 m height around terrace house groups, the Weibull scale parameter should be larger than 4.0 to make sure the turbines in this research could produce enough energy. For regions with scale parameter less or equal to 4.0, larger wind turbines which are sited at higher positions should be selected.

Attention should be paid that the output energy calculated in this project is based on the power curve supplied by the manufacturers of the turbines; this power curves show the net output power of wind turbines. In real case, electricity is required for the operating of wind turbines. For wind turbines used in this project, electricity is used in following equipment **[31]**:

- Yaw mechanism: to keep the turbine blades perpendicular to the wind direction;
- Hydraulic brake: lock the blades to prevent damage if the wind velocity is too high;
- Output conversion: to produce a stable voltage and AC frequency;
- Blade-pitch control: to keep the rotors regularly spinning;

- Start the rotor: to help the blades start to turn when the wind is low;
- Communication, sensors, data collections, etc.

Although the manufacturers' data allow for all of the above power consumptions when the turbines are operating; these equipment consumes power even if the turbines are stopped. During the period the turbines are not operating, the energy consumed by above equipment should be subtracted from the AEP of the turbines; this could make a significant difference to the AEP. Besides this energy consumption, as mentioned in Section 2.1, there is a tailing off trend in power production under real operating conditions compared to manufacturers' data at wind velocity more than 8 m/s; all these make the actual energy output less than the predicted value shown in this Chapter.

CHAPTER 8

8 Conclusions and Recommendations

From the policy of U.K. government, the new domestic buildings should be zero-carbon by the year 2016. In consideration of the climate in U.K., for most U.K. buildings, solar and wind are the primary renewable sources available to be used in the house energy system. Comparing these two kinds of energy sources, wind is dominant in most area because U.K. is a windy and cloudy country. Thus, the potential wind energy close to domestic buildings in U.K. is investigated. As most of the domestic buildings lie in suburban areas in U.K.; this study focuses on terrain corresponding of roughness class 3 which includes town and village zones around U.K.

The results of this study have shed more light on the subject of wind flow around different domestic buildings. The most common domestic building types in U.K. (semi-detached and terraced houses) are modelled in CFD and wind tunnel experiments, the velocity vector results of these two models show the airflow in different areas close to the houses. In order to make sure the airflows are correctly modelled, these CFD and wind tunnel results are compared and checked with each other and some literatures. The airflow result from the models are combined with historical wind records around U.K. regions to predictive the annual energy production of different wind turbines in suburban areas. Section 8.1 relates to the main process and achievements of this research, which includes historical weather record analysis, CFD & wind tunnel modelling and oval all conclusions; while in Section 8.2, some outlook for further research are given.

8.1 Conclusions

8.1.1 Historical weather record analysis

The historical wind record at 10 m height in different zones close to main city is analysed. In order to generate wind energy around the individual houses, the individual turbines for each household need to be small and at low height. The size of the turbine is limited to about 1.5 m; while the setting height is limit by town planning restrictions and the economic status of the household because it is not possible for individual small houses to have tall masts. Based on the analysis results, the energy output from small wind turbines (less than 1.5 m diameter) at low level (10 m) near an individual house is less than 1000 kWh per year, which is not enough to support the electricity requirement of a household (typically 4831 kWh per year). The reason of low energy output is the small turbine size and low wind velocity at the height in urban areas and normal countryside.

Therefore, in order to produce more energy from the wind, large turbines at higher level shared between multiple buildings should be considered. There are mainly two benefits for such shared wind system: first, the larger wind velocity at higher level makes better use of turbines, which lead to a higher energy output. Secondly, depend on different market models, the peak and troughs on energy demand could be evened out in the sharing system; so reduce the peak power required and wastage of generated energy at periods of low demand. And also, if the group is mixed with buildings in different purpose (residential and commercial for example), the energy development would have even better characteristics (more smooth peak and troughs curve) due to different demand patterns in different purpose buildings.

8.1.2 CFD and wind tunnel modelling

For single or shared turbines system, the air flow around group of house is modelled and analysed. The aim of this analysis is to find the positions with larger wind velocity and small turbulence intensity, which is more suitable for the fix of wind

turbines. The wind flows at both low (10 m) and high (30 m) height level are included in this analysis, for the setting of different size turbines respectively. Semi-detached and terrace house groups, which are most common used in U.K. as domestic buildings are modelled; the velocity and turbulence level around each house are shown respectively. Based on the results, the area at low height (10 m) around both kinds of house groups is not suitable for the setting of wind turbines because the low wind velocity and high turbulence intensity. And at high height level (30 m), the optimal positions for each wind turbines analysed in this project are given.

8.1.3 Overall conclusions

Compared with related works about building wind energy systems, the achievement of this project mainly shown in following aspects:

First of all, the air flow at positions around semi-detached and terrace houses in suburban area are successful modelled in both wind tunnel and CFD. In CFD and wind tunnel experiment, the atmosphere boundary layer (ABL) of suburban area with roughness length 0.26 m is successful modelled, this ABL environment agrees well with ESDU 85020 [71] and several other references. The models of semi-detached houses (building density 15.5%) and terrace houses (building density 46.4%) are sited in this ABL environment and the dimensionless measured velocity and turbulence results from 108 measurement points around these models agrees well with each other with average root mean square difference less than 4.01E-02.

Secondly, it has been shown by detailed investigation using CFD and wind tunnel modelling that the wind environment at low (10m) height in suburban areas is unsuitable for wind turbines. This result agrees well with the finding from the Warwick Field Trials in 2008 [81]. There are two main reasons for this conclusion: the low wind speed and high turbulence.

At 10 m height in the area around semi-detached houses in suburban zones, the wind velocity range from 91 to 105 % of the 10 m reference velocity (average velocity in suburban area around low-rise houses); while at same height around terrace houses,

the range of wind velocity is between 86 to 108%. The historical wind records at different regions from U.K. Met office show that the 10 m reference velocity mainly follows the Weibull distribution, and the Weibull parameters of different regions in U.K. agree the work from Warwick Field Trials (Weibull shape parameter less than 2) [81]. Based on the historical wind record, the wind flow at this height is not strong enough for small and medium wind turbines (1,000 W to 10,000 W wind turbines) to support the electricity requirement of the households. Besides the low wind velocity, turbulence is another problem for the site of wind turbines at this height in suburban areas. The turbulence intensity at 10 m height around semi-detached houses varied from 19 to 33%, while at 10 m height around terrace houses, the range of turbulence intensity is between 24% and 35%; these turbulence intensity values are too high for satisfactory operation of wind turbines.

Thirdly, the analysis about wind velocity, turbulence intensity and energy output of different wind turbines at 30 m height in suburban area in U.K. regions are given in this project. At this height, the turbulence intensity is lower than 18% at area around semi-detached houses and most area around terrace groups, while the wind velocity ranges from 95 to 103 % of the mean velocity at 30 m height for semi-detached houses environment and 92 to 103% for terrace houses environments. The relationship between mean wind velocity at 30 m and 10 m height follows the Logarithmic-law which makes the mean velocity at 30 m height could be calculated from the 10 m mean velocity of the Met office historical record. Based on the wind velocities at 30 m around houses, the annual output energy of different wind turbines in U.K. regions is given. Comparing the annual energy production (AEP) of wind turbines sited at positions around houses and avoiding the positions with turbulence intensity larger than 18%, the optimal positions around house groups are given. The total AEP of wind turbines sited at the optimal positions are compared with the electricity requirement of households in the house group and the total amount of CO_2 emissions during the manufacture of the turbines; as a result of this compare, the economic payback time and carbon payback time of the turbines are given. Turbines with shortest economic and/or carbon payback time are suggested to be the most suitable turbines for different regions in U.K.

The optimal positions for different wind turbines in U.K. regions are largely decided by the frequency distribution of different wind velocity and the frequency distribution of input wind directions. For different regions in U.K., the optimal positions of each wind turbine around the houses are different. However, from the output energy analysis results, there are some general guidance can be given:

- Positions closer to the street side are more suitable than the area surrounded by houses.
- The building group with larger building density has fewer optimal positions for the siting of wind turbines.
- In order to produce enough energy, the rate power of wind turbines around semi-detached house should be larger than 2500 W; 30 m is an acceptable site height for most wind turbines. For terrace houses, the site position should be higher than 30 m from ground, and the rate power should be larger than 10,000 W.
- Horizontal Axis Wind Turbines are more suitable than Vertical Axis Wind Turbines because of the better economic payback time.
- Regions with larger Weibull scale parameter are more suitable for the setting of wind turbines. At 30m height, in order to produce enough energy for the electricity requirement of terrace households, the Weibull scale parameter of the region should be larger than 4.0.

8.2 Recommendations

In general, both energy output prediction method and shared wind system shown in this research could be proved if more funding is obtained. Further research could force on following directions:

The velocity and turbulence prediction method used in this research could be improved. In this research, they are based on the results from wind tunnel experiment and CFD models. In further research, the wind velocity and turbulence around real house could be measured and compared with wind tunnel and CFD results, which can

produce more accurate results. The results could also be improved by setting more details into the CFD and tunnel models.

The energy output prediction could be more accurate. The energy output is predicted from the hourly mean wind speed with manufacturer power curves, which shows the net output power of the turbines. This predicted energy output has a larger value than the actual energy output of the turbines due to the energy consumption of the turbine equipment and the tailing off trend in power production at high wind velocity. Energy output data from trials around real buildings could be used to construct more actual power output curves; with this output curve, the energy output prediction method could be improved.

For shared building wind energy system, the suitable wind turbines and optimal positions around houses in U.K. regions are shown in this research; and the energy output is proved to be enough for the electricity requirement of the houses. For further research, the practicalities of wind energy systems shared between households could be investigated.

The energy output analysis method introduced in this project could be used in wider contexts, e.g. terrain surface characteristics with different roughness class in U.K. or Europe. For terrain surface with lower roughness class than suburban areas, orography is an important influence factor of wind flow which should be considered in the CFD and tunnel experiments. While for other European countries, the wind turbines used to supply electricity for suburban households should be sited at positions higher than 30 m from ground and larger wind turbines shared by multiple households should be considered. This is because of the wind class in most other European countries are lower than the wind class in U.K.; if the wind turbines are sited at same height, the output energy of the wind turbines in these countries would be smaller than U.K. level. In order to produce enough energy, more powerful turbines should be selected and the sited positions of these turbines should be higher than U.K. level.

Appendix A

Appearance and power output curve of wind turbines

A- 1 the appearance and power output curve of Whisper 200[20]

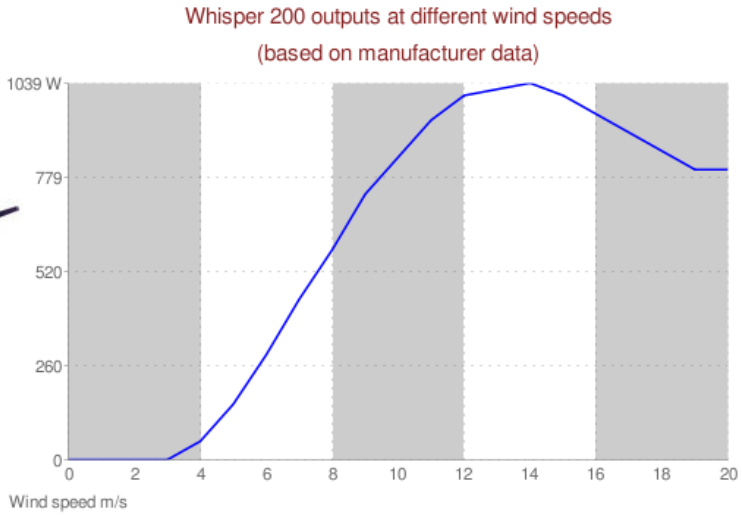

A- 2 the appearance and power output curve of Whisper 500[20]

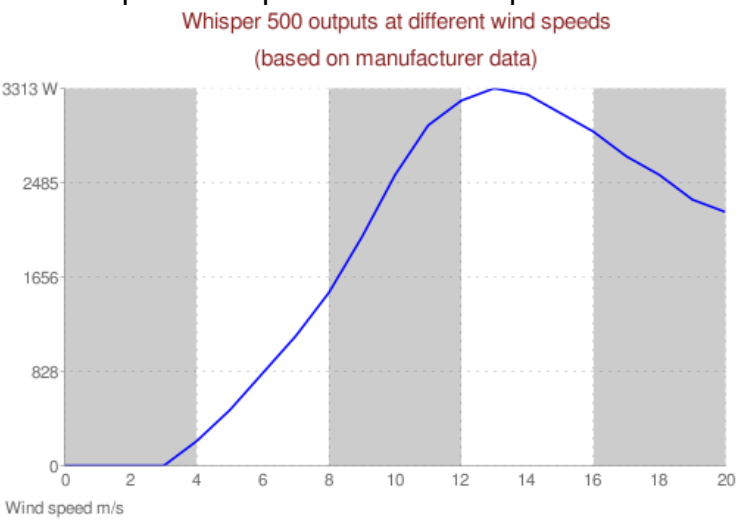

A- 3 the appearance and power output curve of Proven WT2500 [22]

A- 4 the appearance and power output curve of Proven 6KW [22]

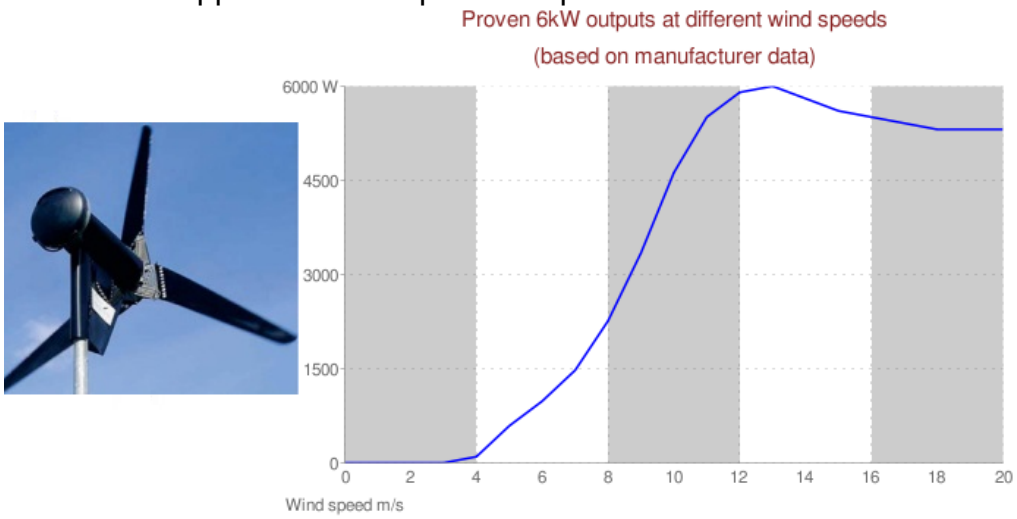

A- 5 the appearance and power output curve of Westwind 3KW [23]

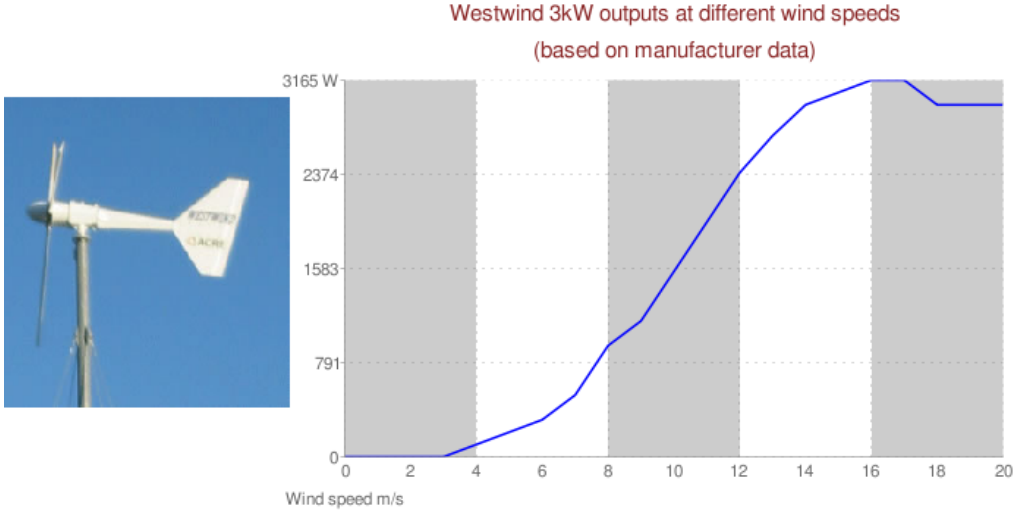

A- 6 the appearance and power output curve of Westwind 5.5KW [23]

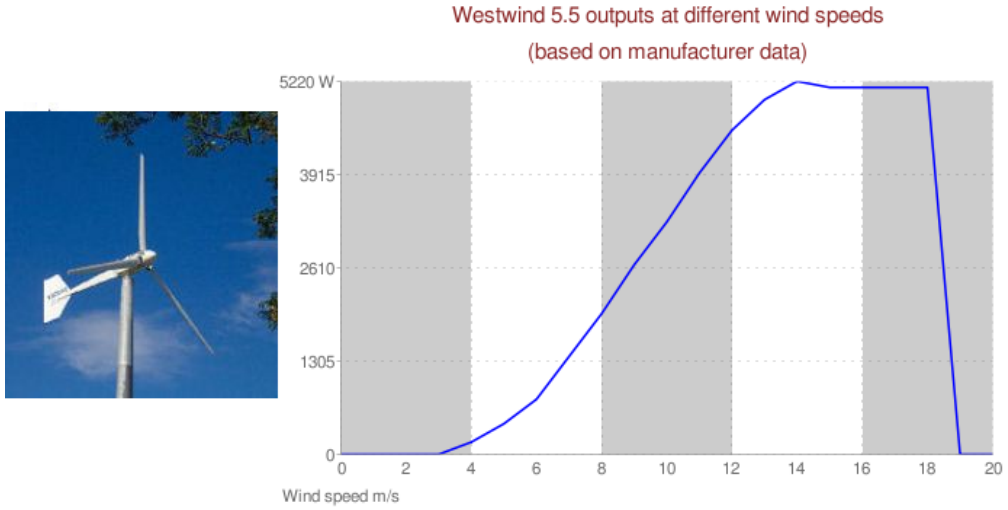

A- 7 the appearance and power output curve of Westwind 10KW [23]

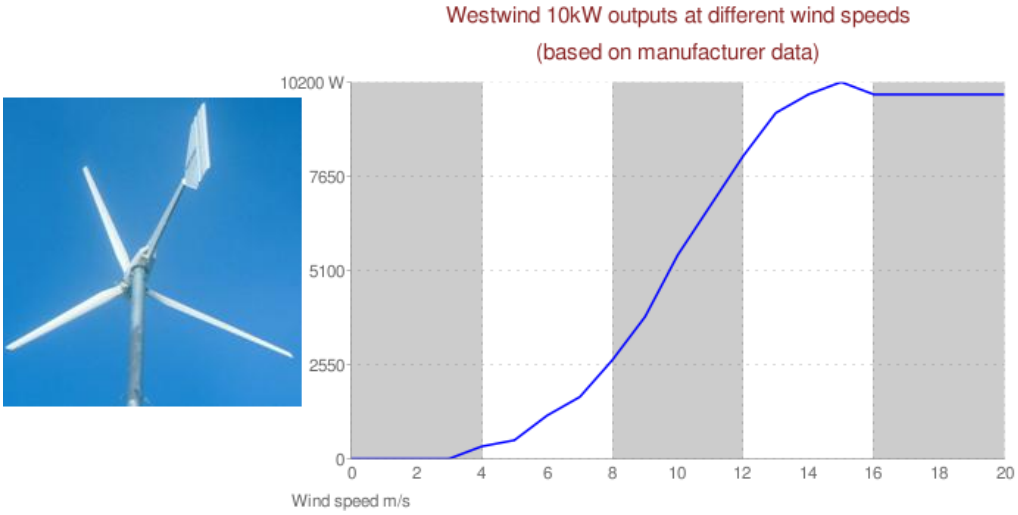

A- 8 the appearance and power output curve of Turby VAWT [24]

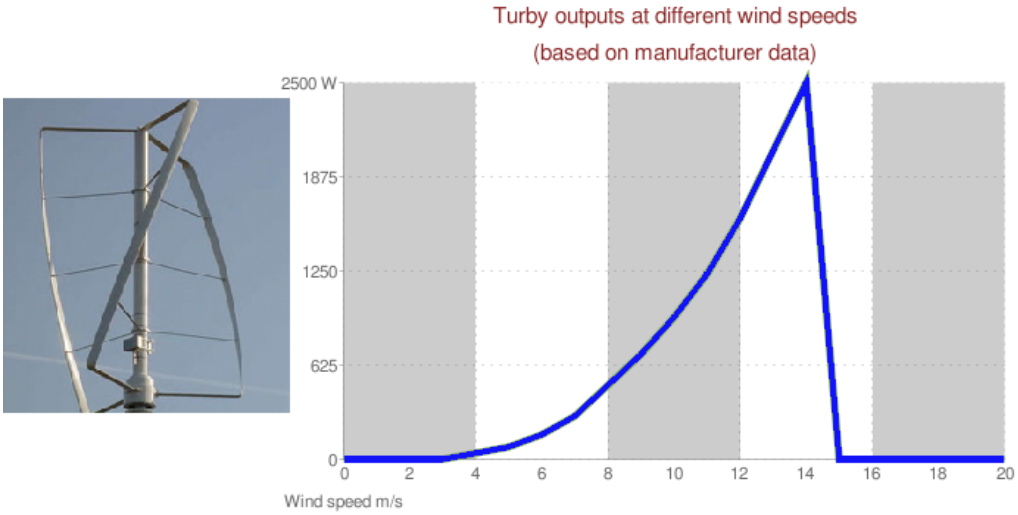

A- 9 the appearance and power output curve of Kestrel 1000 [25]

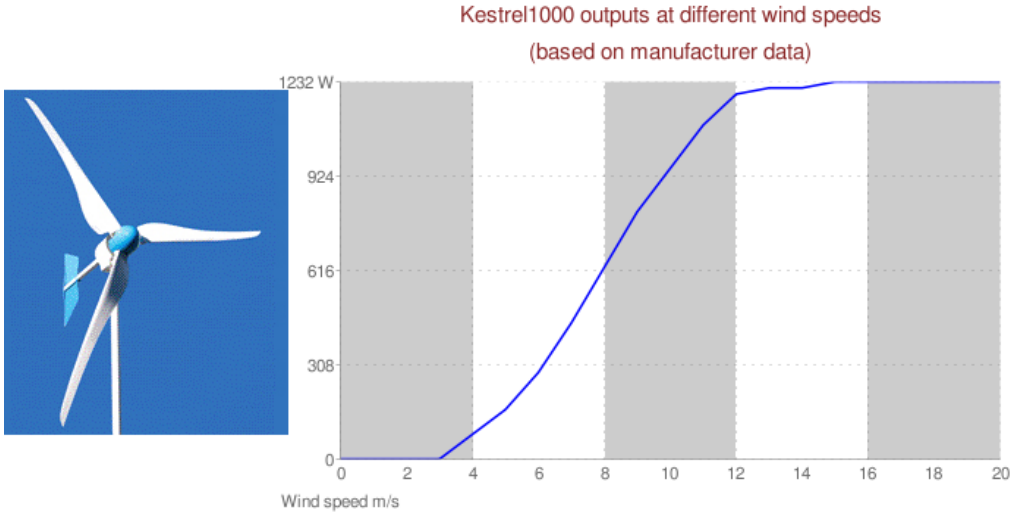

A- 10 the appearance and power output curve of Samrey Merline [26]

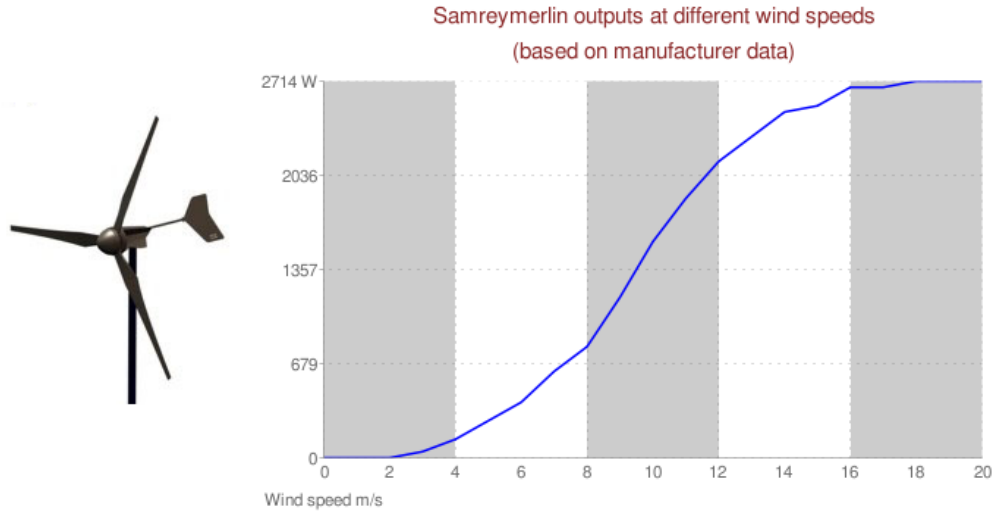

A- 11 the appearance and power output curve of Skystream 3.7 [20]

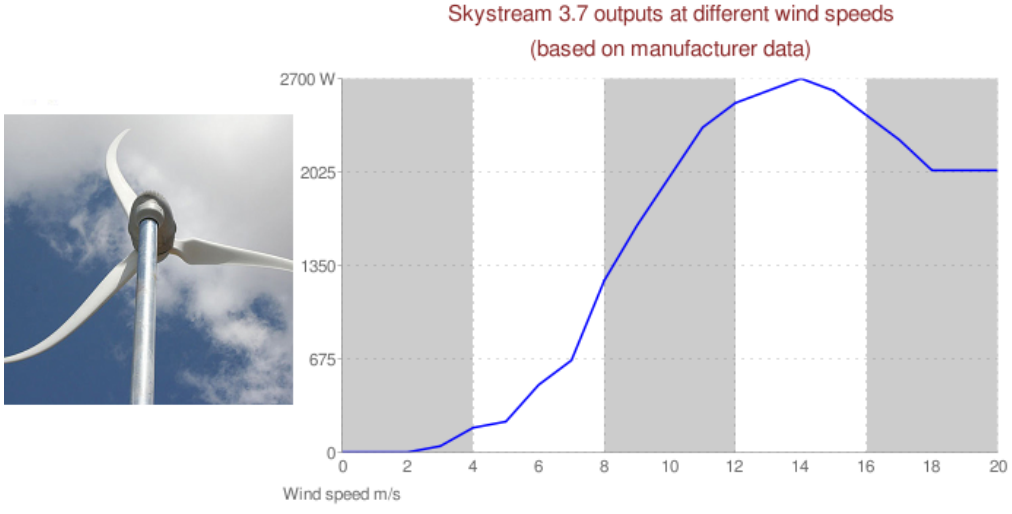

A- 12 the appearance and power output curve of Quiet Revolution [27]

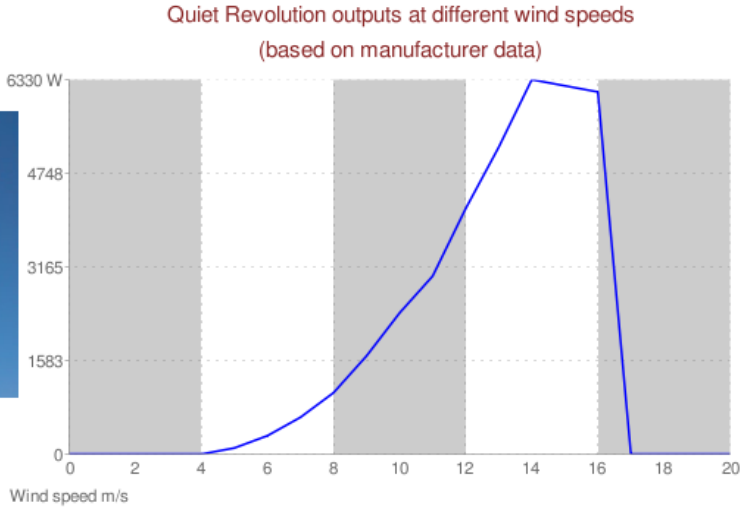

A- 13 the appearance and power output curve of Scirocco 6KW [28]

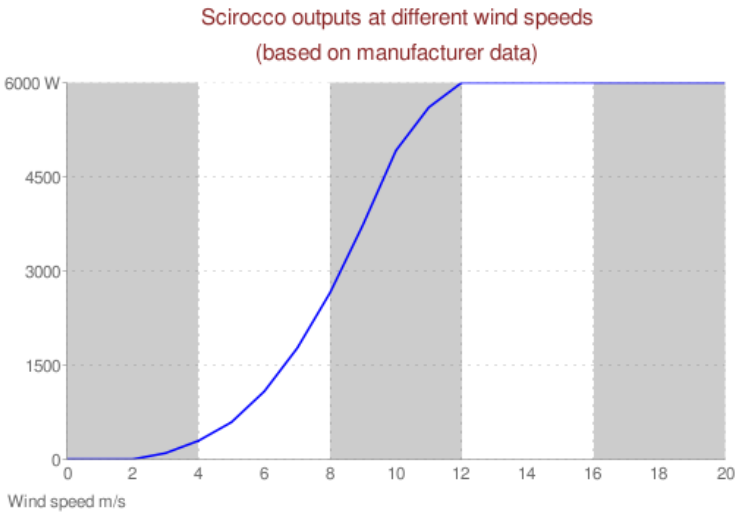

A- 14 the appearance and power output curve of Aerostar 6 [29]

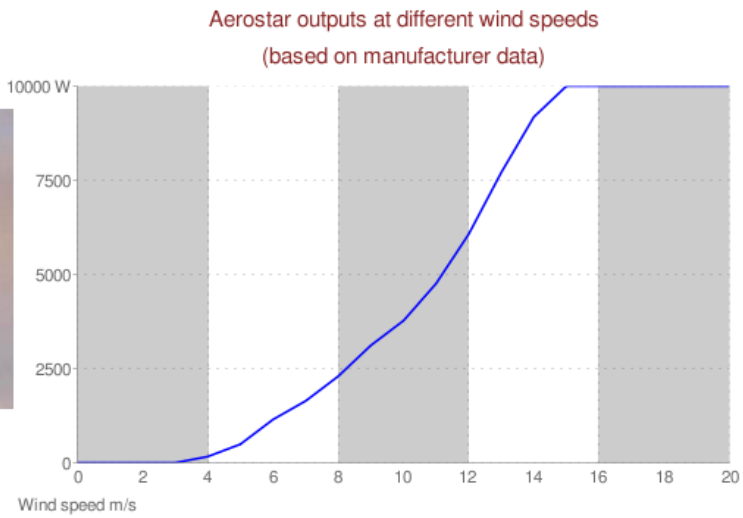

Appendix B

Frequency of 10 m height hourly mean wind velocity in U.K. cities

B- 1 frequency of 10 m height hourly mean wind velocity in London

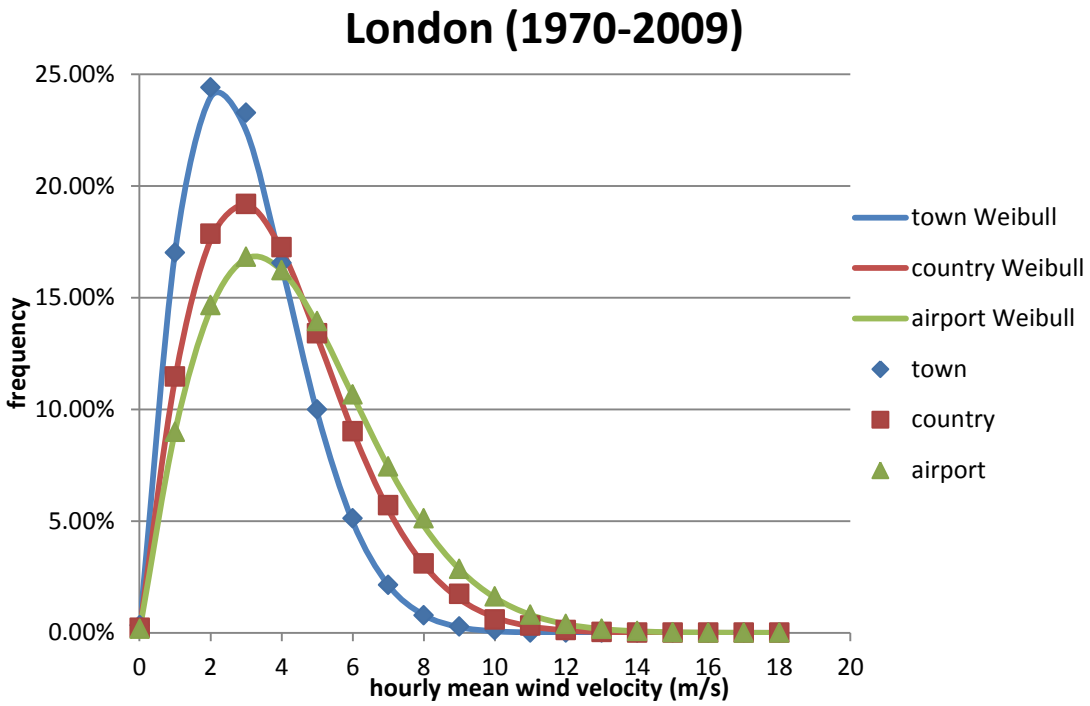

B- 2 frequency of 10 m height hourly mean wind velocity in Bristol

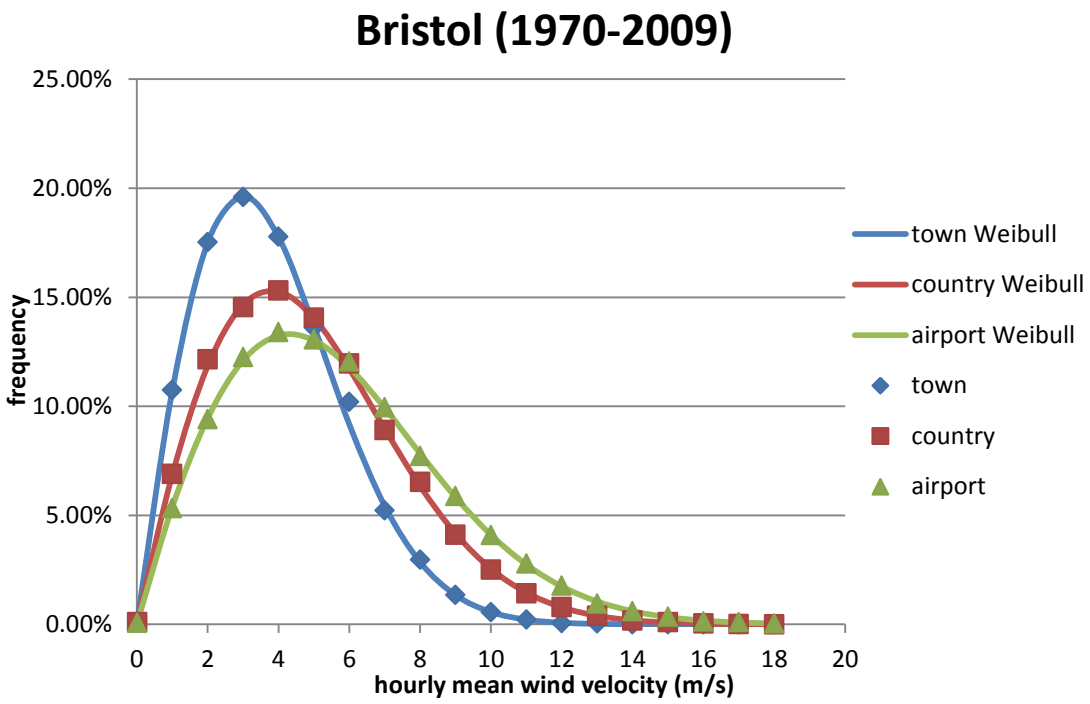

B- 3 frequency of 10 m height hourly mean wind velocity in Birmingham

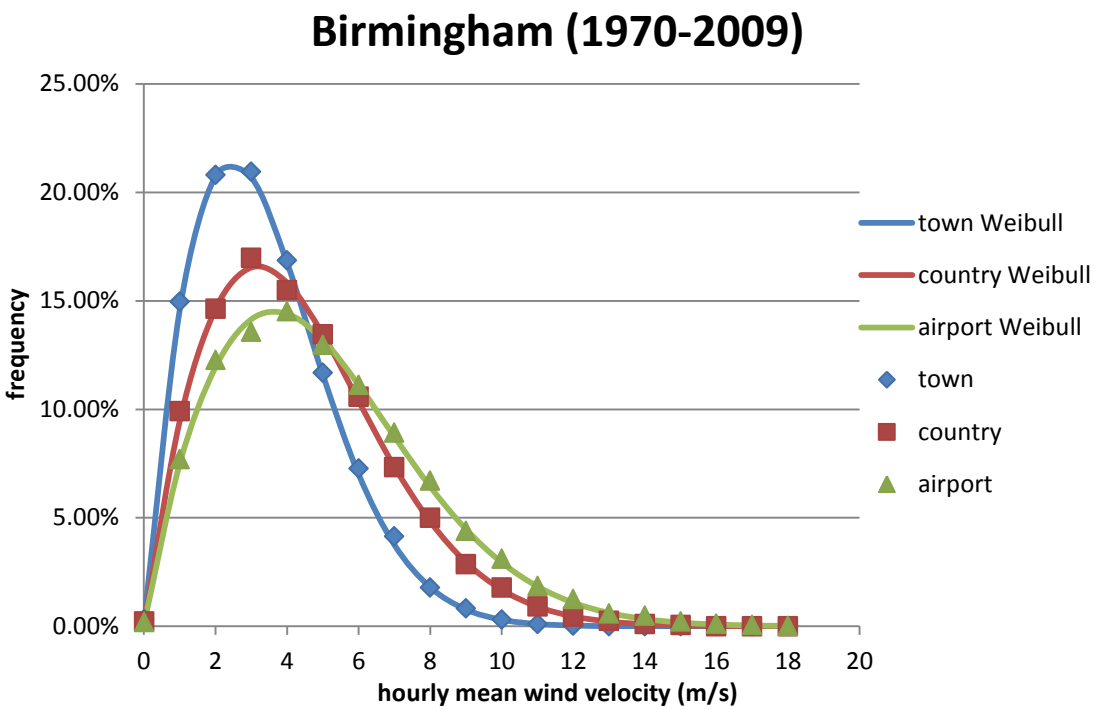

B- 4 frequency of 10 m height hourly mean wind velocity in Manchester

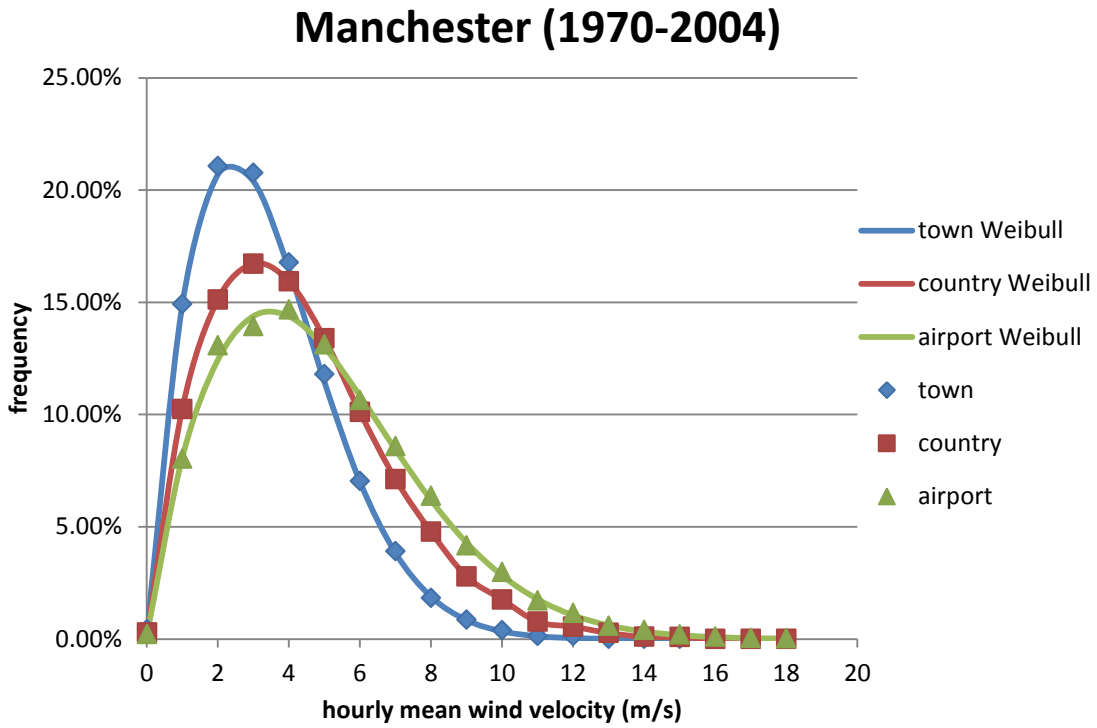

B- 5 frequency of 10 m height hourly mean wind velocity in Leeds

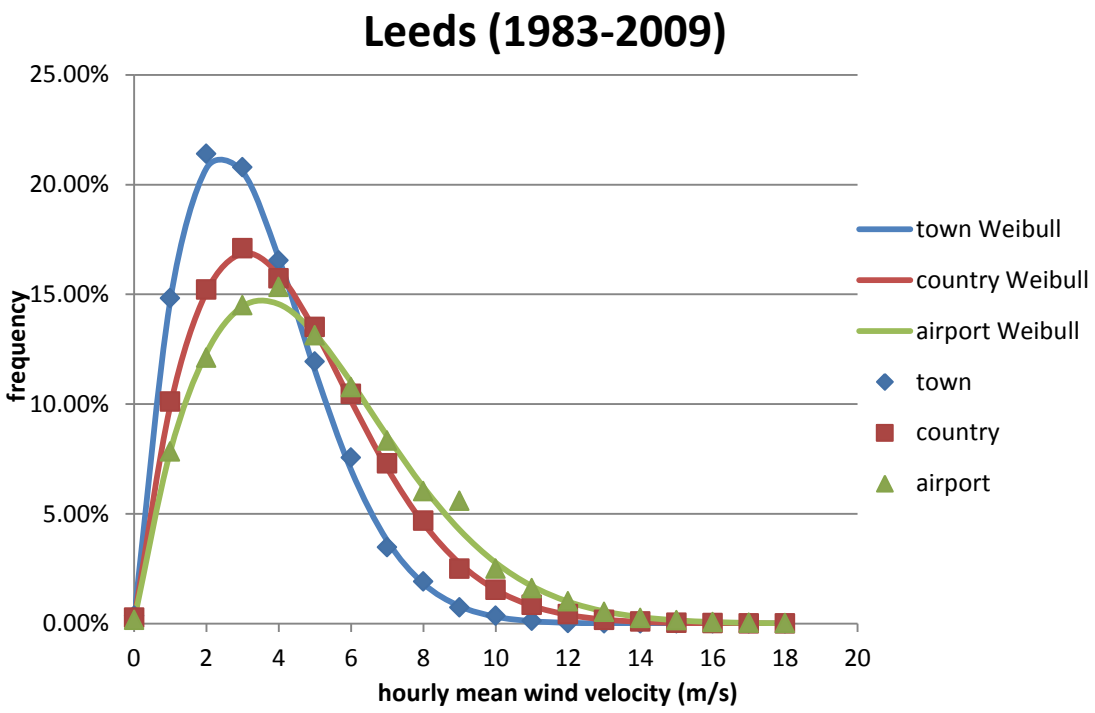

B- 6 frequency of 10 m height hourly mean wind velocity in Edinburgh

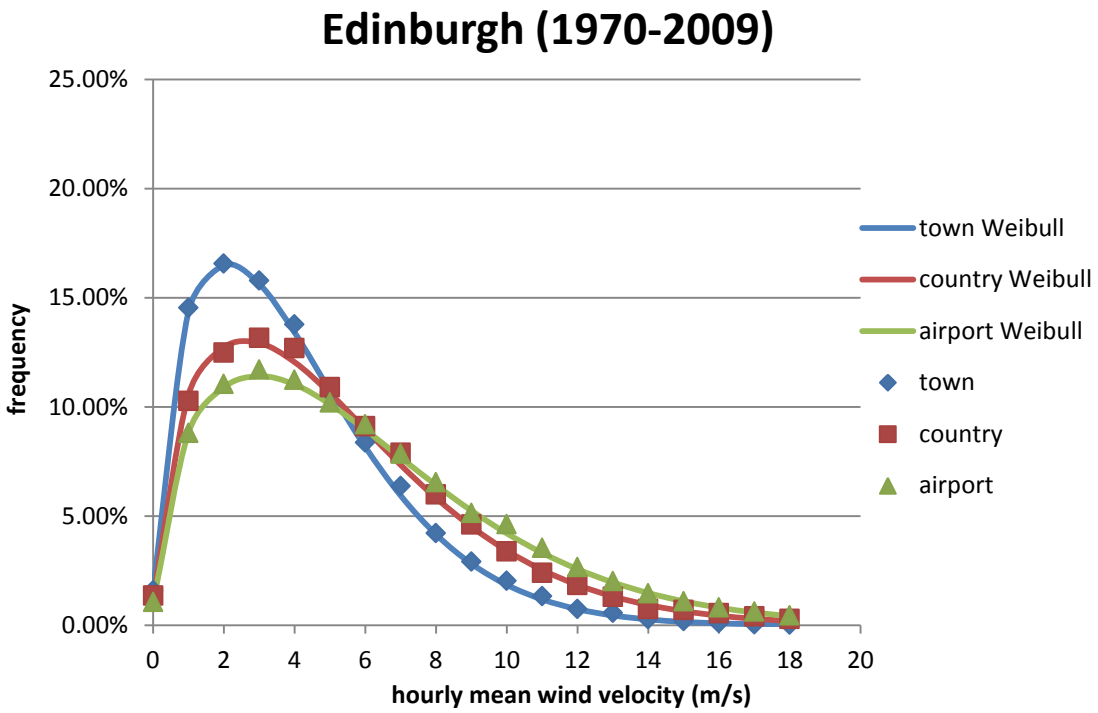

B- 7 frequency of 10 m height hourly mean wind velocity in Glasgow

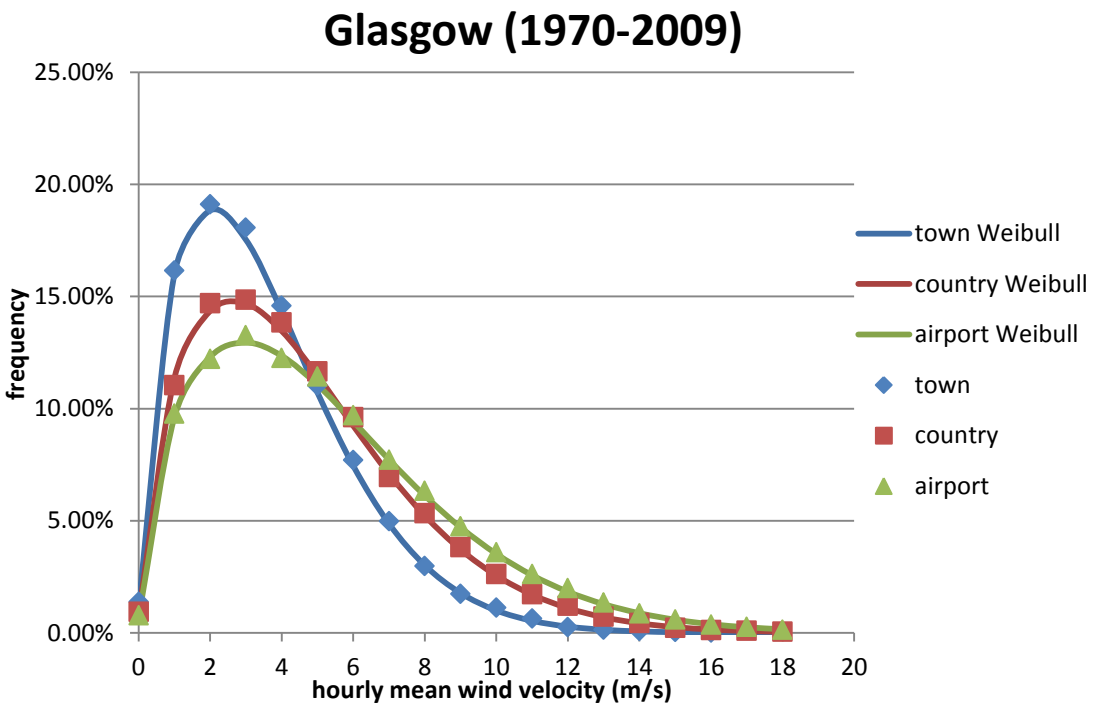

Appendix C

Wind direction frequency distribution in U.K. cities

C- 1 wind direction frequency distribution in London

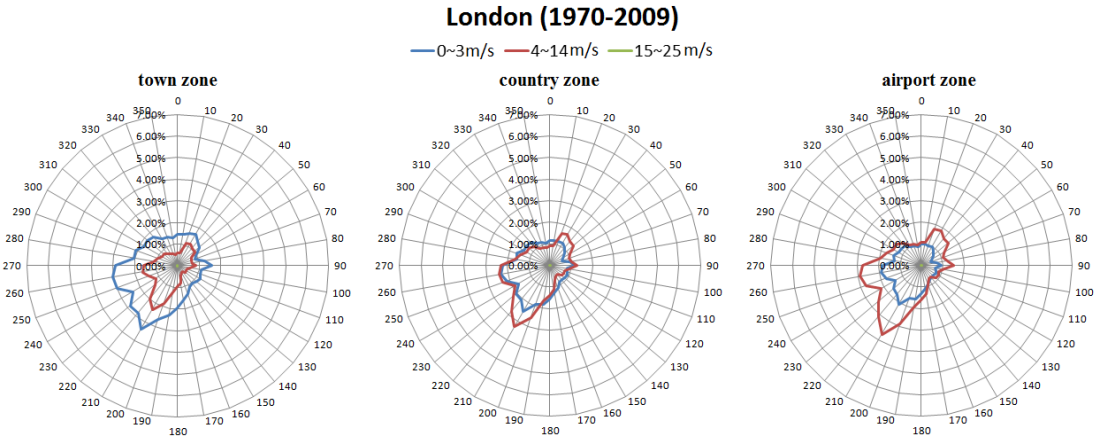

C- 2 wind direction frequency distribution in Bristol

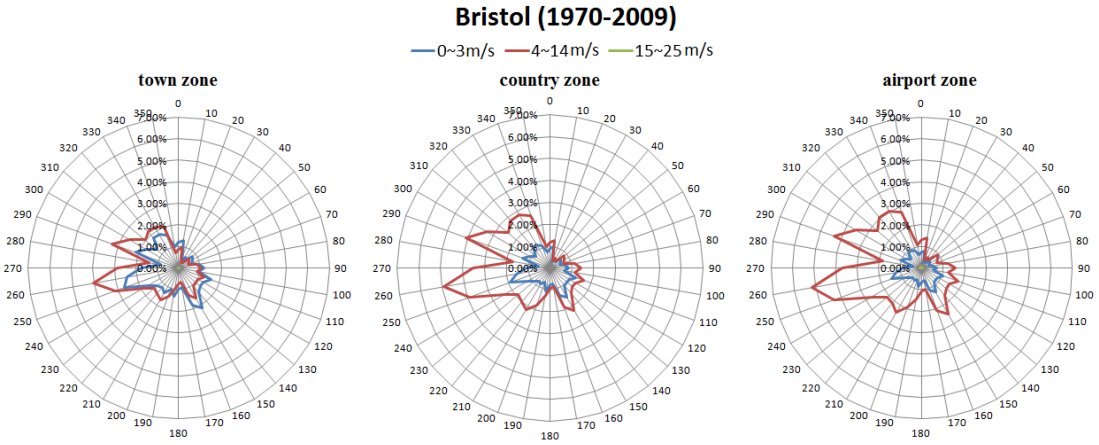

C- 3 wind direction frequency distribution in Birmingham

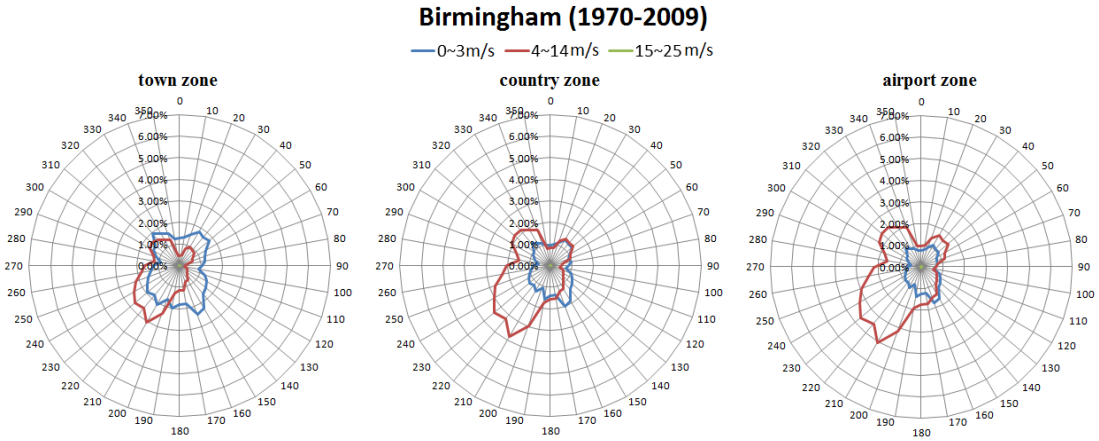

C- 4 wind direction frequency distribution in Manchester

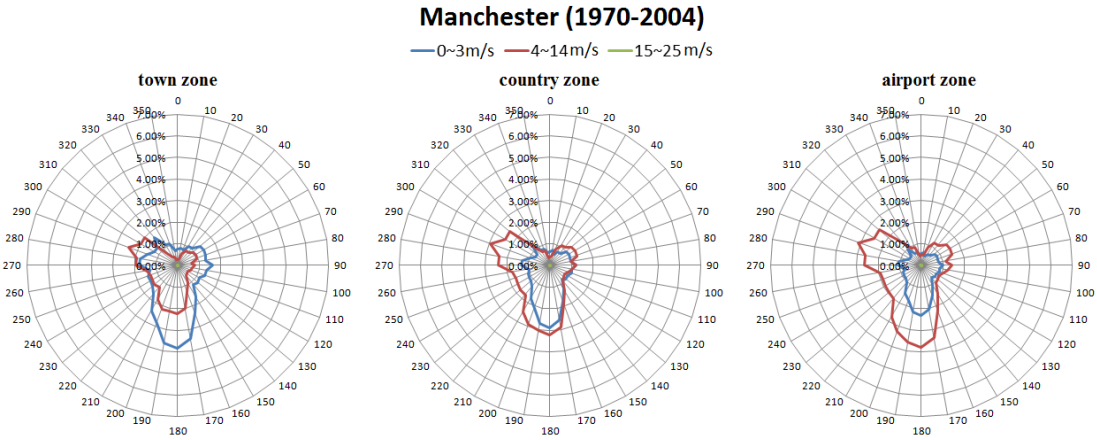

C- 5 wind direction frequency distribution in Leeds

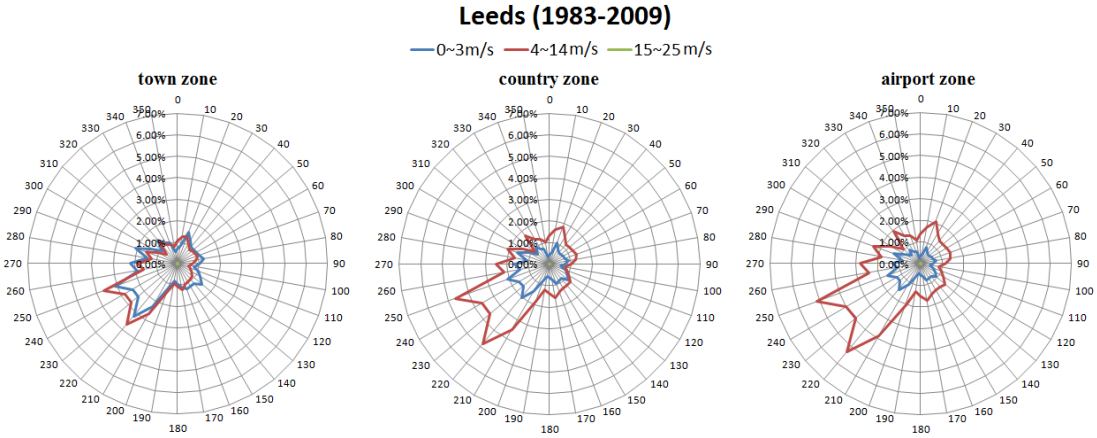

C- 6 wind direction frequency distribution in Edinburgh

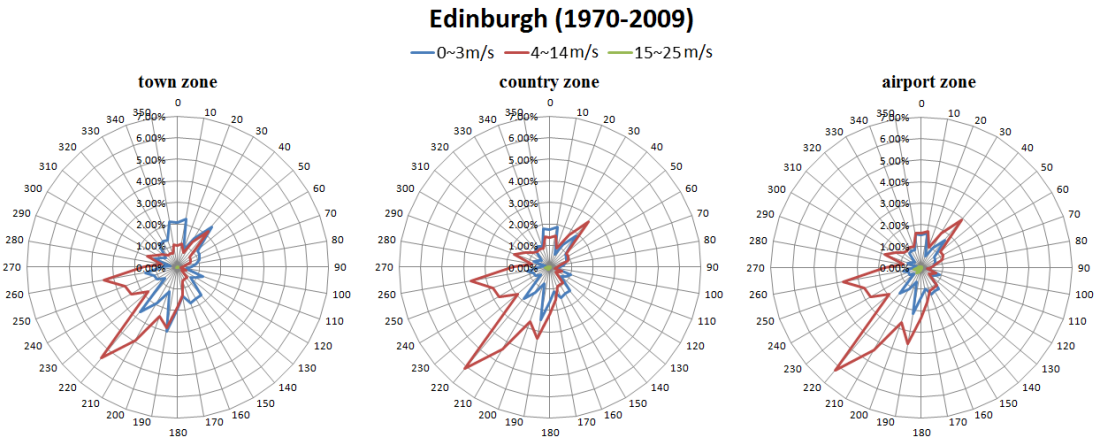

C- 7 wind direction frequency distribution in Glasgow

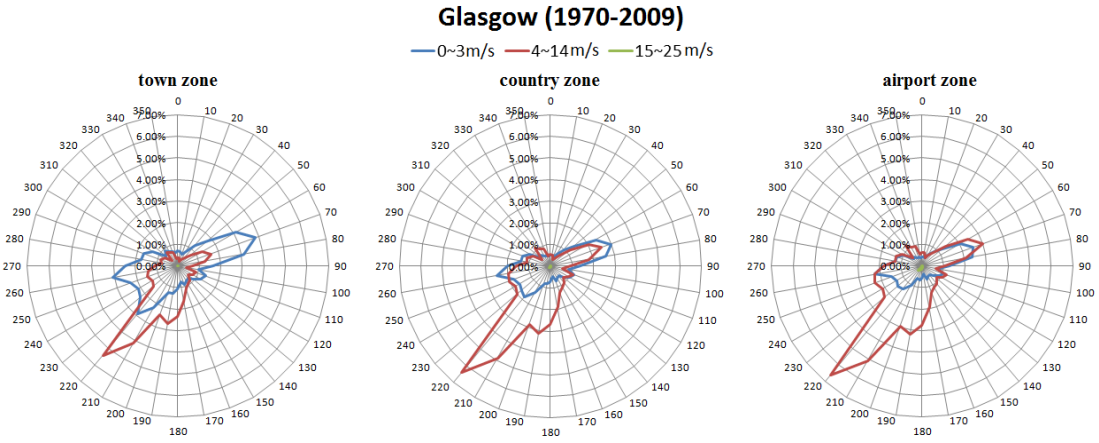

Appendix D

Wind power density distribution in U.K. cities

D- 1 wind power density distribution in London

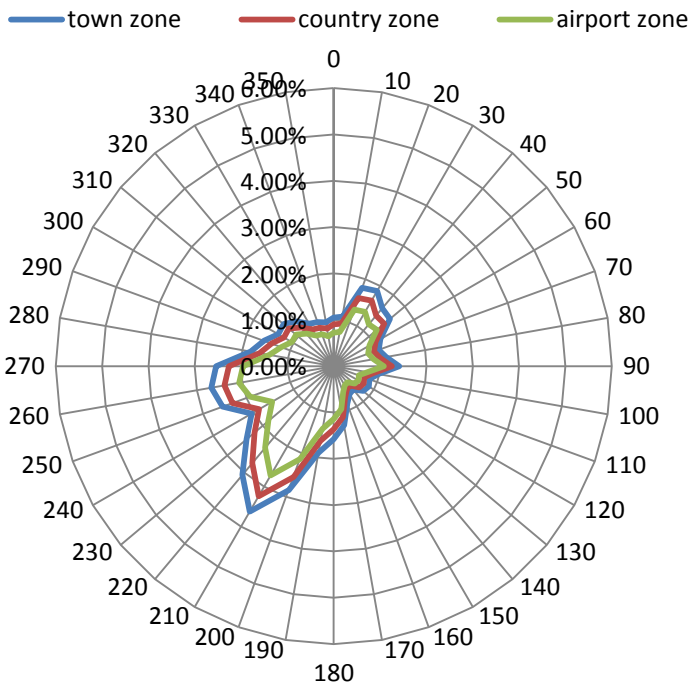

D- 2 wind power density distribution in Bristol

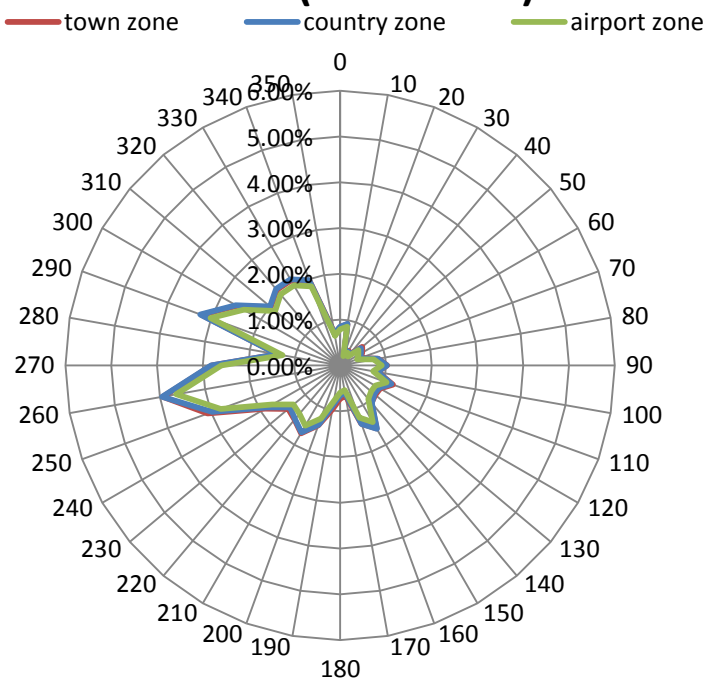

D- 3 wind power density distribution in Birmingham

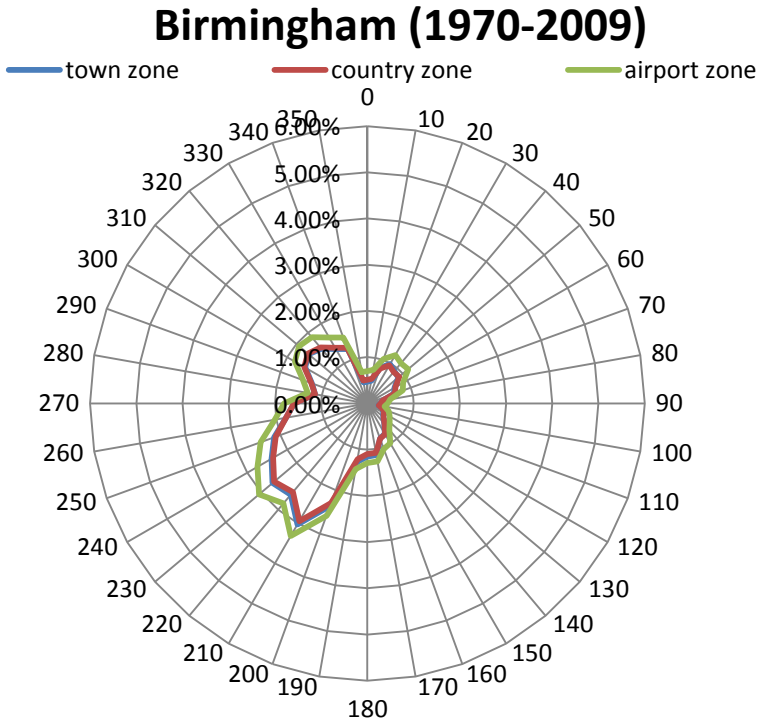

D- 4 wind power density distribution in Manchester

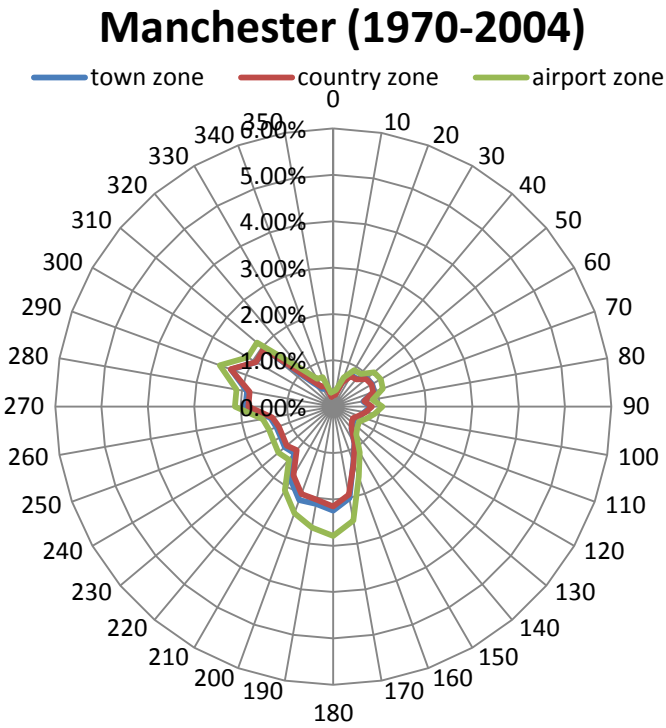

D- 5 wind power density distribution in Leeds

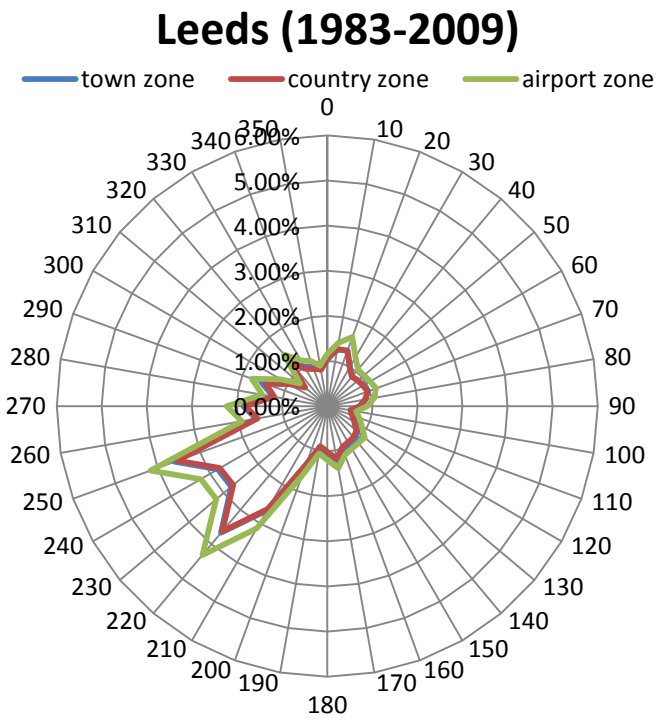

D- 6 wind power density distribution in Edinburgh

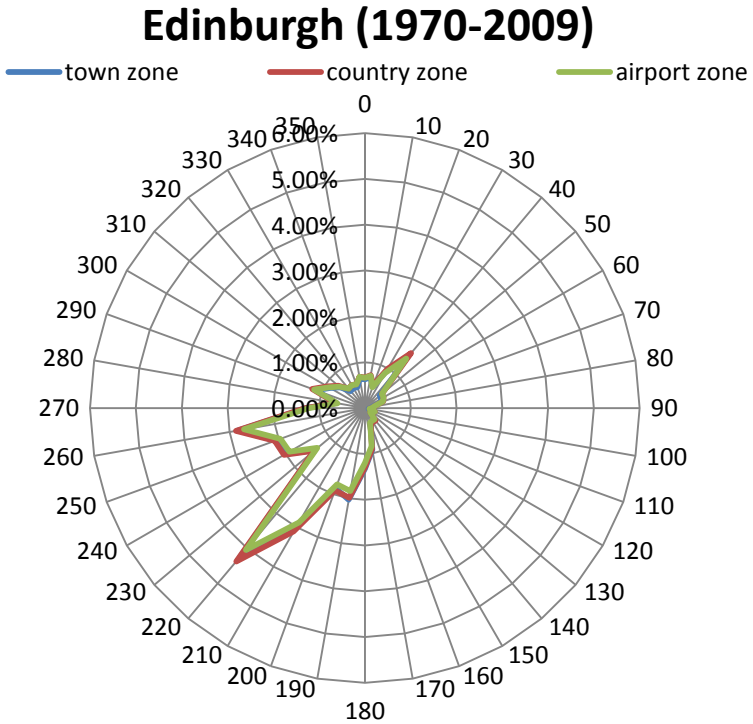

D- 7 wind power density distribution in Glasgow

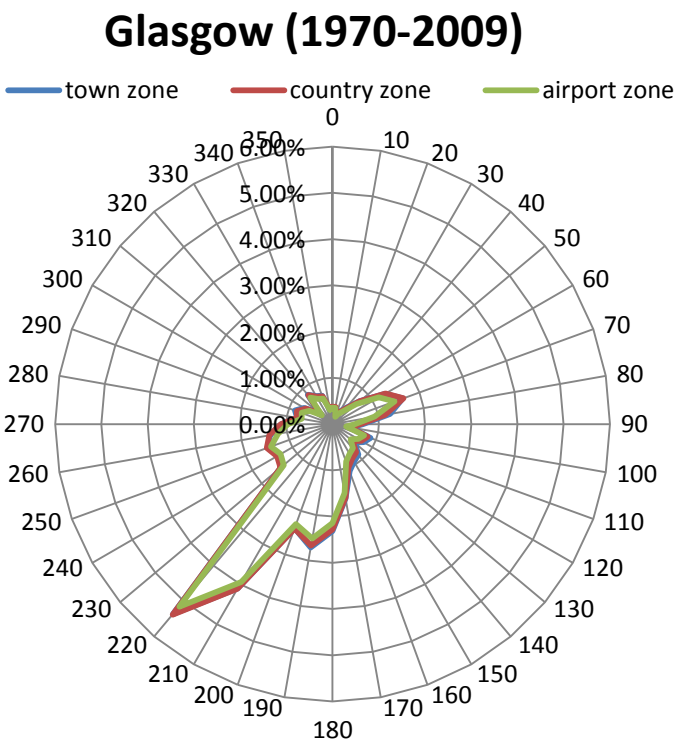

Appendix E

Required turbines number per householder in U.K. cities

required turbine number

Wind turbine	London			Bristol			Birmingham			Manchester			Leeds			Edinburgh			Glasgow		
	*T	C	A	T	C	A	T	C	A	T	C	A	T	C	A	T	C	A	T	C	A
Turby	13	5.9	3.9	6.0	2.8	2.0	8.6	3.7	2.6	8.3	3.9	2.6	8.5	4.0	2.7	3.7	2.2	1.7	5.6	2.8	2.1
Kestrel 1000	8.9	4.3	3.0	4.3	2.3	1.7	6.0	3.0	2.2	5.9	3.1	2.2	6.0	3.1	2.2	3.1	2.0	1.7	4.3	2.5	2.0
Whisper 200	9.8	4.6	3.2	4.6	2.5	1.9	6.5	3.2	2.4	6.4	3.3	2.4	6.4	3.3	2.4	3.4	2.2	1.8	4.7	2.7	2.1
Samrey Merline	5.2	2.7	1.9	2.7	1.5	1.1	3.7	1.9	1.4	3.6	2.0	1.4	3.7	2.0	1.4	1.9	1.2	0.9	2.7	1.5	1.2
Proven WT2500	4.4	2.1	1.5	2.1	1.1	0.8	2.9	1.4	1.1	2.9	1.5	1.1	2.9	1.5	1.1	1.5	0.9	0.8	2.1	1.2	0.9
Westwind 3kW	7.0	3.2	2.2	3.3	1.6	1.1	4.6	2.1	1.5	4.5	2.2	1.5	4.6	2.2	1.5	2.1	1.2	1.0	3.1	1.6	1.2
Skystream 3.7	4.6	2.3	1.6	2.3	1.2	0.9	3.2	1.6	1.1	3.2	1.6	1.2	3.2	1.7	1.2	1.6	1.0	0.8	2.3	1.3	1.0
Quiet Revolution	9.8	3.3	1.9	3.5	1.3	0.8	5.3	1.8	1.1	5.1	1.9	1.2	5.2	2.0	1.2	1.7	0.8	0.6	2.8	1.2	0.8
Whisper 500	3.2	1.6	1.1	1.6	0.9	0.6	2.2	1.1	0.8	2.2	1.1	0.8	2.2	1.2	0.8	1.2	0.7	0.6	1.6	0.9	0.7
Westwind 5.5kW	3.3	1.5	1.0	1.5	0.7	0.5	2.1	1.0	0.7	2.1	1.0	0.7	2.1	1.0	0.7	1.0	0.6	0.5	1.4	0.8	0.6
Proven 6kW	3.0	1.3	0.8	1.3	0.6	0.4	1.9	0.8	0.6	1.8	0.8	0.6	1.8	0.9	0.6	0.8	0.5	0.4	1.2	0.6	0.5
Scirocco 6kW	2.1	1.0	0.7	1.0	0.5	0.4	1.4	0.7	0.5	1.4	0.7	0.5	1.4	0.7	0.5	0.7	0.4	0.3	1.0	0.5	0.4
Westwind 10kW	2.3	1.0	0.7	1.0	0.5	0.3	1.5	0.7	0.4	1.5	0.7	0.5	1.5	0.7	0.5	0.6	0.4	0.3	1.0	0.5	0.4
Aerostar 6	2.6	1.2	0.8	1.2	0.6	0.4	1.7	0.8	0.5	1.6	0.8	0.5	1.7	0.8	0.6	0.8	0.4	0.3	1.1	0.6	0.4

* C:town zone; T: country zone; A: airport

Appendix F

Details of Wind Tunnel Experiment Measurement points

F-1 Semi-detached house model, wind flow from 0°

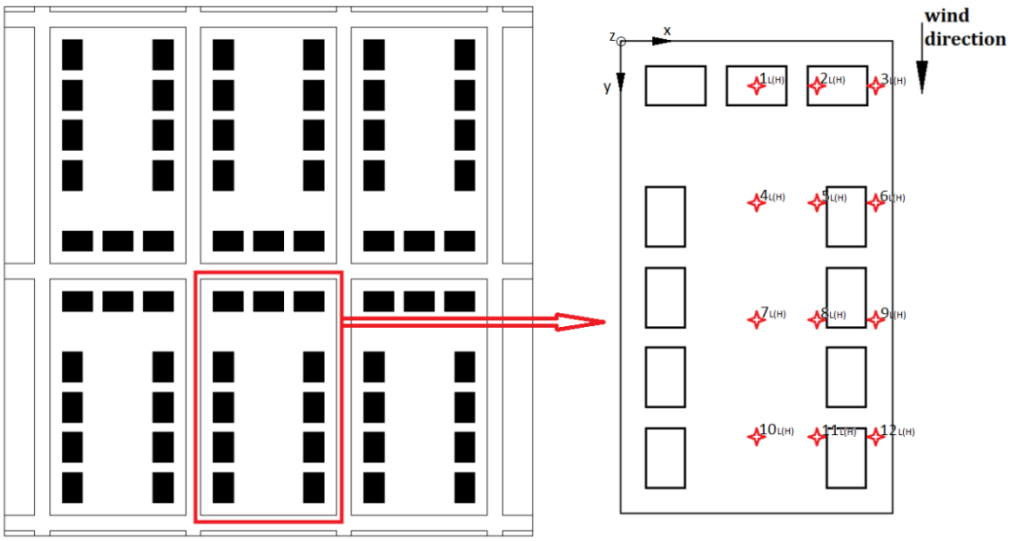

mark	coordinate, mm			velocity, m/s			
	x	*y*	*z*	$\bar{u}_x$	$\bar{u}_y$	$\bar{u}_z$	$\bar{u}$
1L	96	36	40	0.13	5.57	-0.06	5.57
2L	146	36	40	0.25	5.37	-0.13	5.38
3L	196	36	40	0.31	5.71	0.05	5.72
4L	96	136	40	0.17	5.43	0.36	5.45
5L	146	136	40	0.13	5.42	0.38	5.44
6L	196	136	40	0.12	5.58	0.25	5.59
7L	96	236	40	0.04	5.26	0.31	5.26
8L	146	236	40	0.05	5.50	0.18	5.50
9L	196	236	40	0.13	5.58	0.10	5.58
10L	96	336	40	0.11	5.86	0.51	5.89
11L	146	336	40	0.04	5.88	0.41	5.90
12L	196	336	40	0.17	5.94	0.39	5.96
1H	96	36	120	0.25	7.48	0.29	7.49
2H	146	36	120	0.33	7.44	0.28	7.45
3H	196	36	120	0.40	7.56	0.34	7.57
4H	96	136	120	0.26	7.55	0.61	7.58
5H	146	136	120	0.30	7.53	0.55	7.55
6H	196	136	120	0.33	7.47	0.43	7.49
7H	96	236	120	0.19	7.63	0.49	7.64
8H	146	236	120	0.24	7.47	0.52	7.50
9H	196	236	120	0.32	7.58	0.47	7.60
10H	96	336	120	0.17	7.70	0.71	7.74
11H	146	336	120	0.21	7.67	0.66	7.70
12H	196	336	120	0.26	7.72	0.68	7.75

F-2 Semi-detached house model, wind flow from 5°

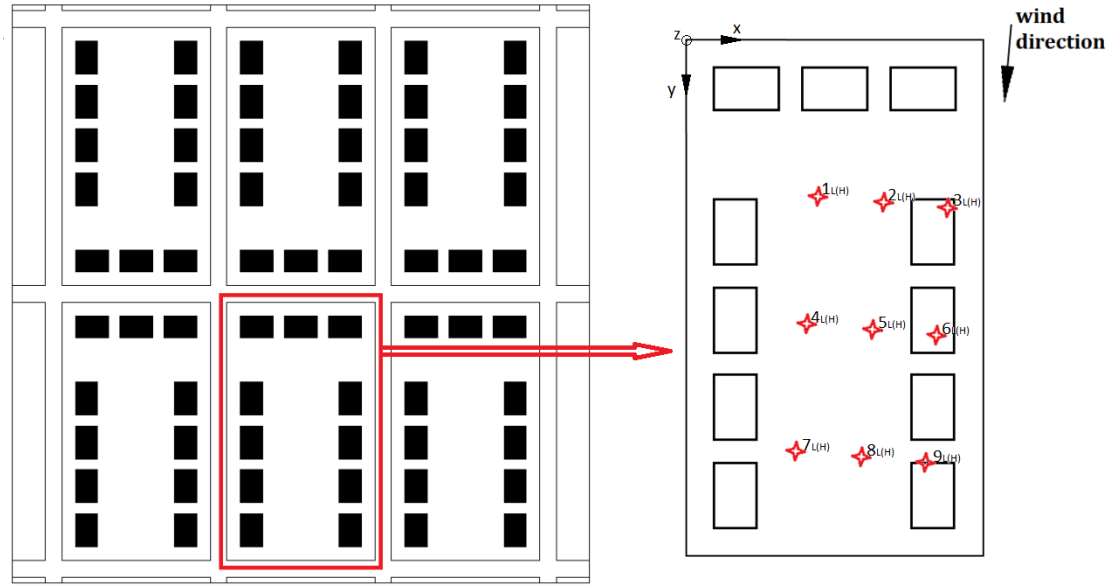

mark	coordinate, mm			velocity, m/s			
	x	*y*	*z*	$\bar{u}_x$	$\bar{u}_y$	$\bar{u}_z$	$\bar{u}$
1L	100	98	40	0.30	5.49	0.52	5.52
2L	150	102	40	0.25	5.42	0.37	5.44
3L	200	107	40	0.24	5.51	0.16	5.51
4L	91	197	40	0.27	5.38	0.30	5.39
5L	141	201	40	0.21	5.50	0.34	5.51
6L	191	206	40	0.16	5.45	0.02	5.46
7L	82	297	40	0.33	5.74	0.33	5.76
8L	132	301	40	0.21	5.92	0.38	5.94
9L	182	306	40	0.34	5.66	0.30	5.68
1H	100	98	120	0.45	7.65	0.52	7.68
2H	150	102	120	0.47	7.54	0.51	7.57
3H	200	107	120	0.54	7.50	0.46	7.54
4H	91	197	120	0.44	7.48	0.38	7.50
5H	141	201	120	0.50	7.60	0.37	7.63
6H	191	206	120	0.53	7.59	0.35	7.62
7H	82	297	120	0.37	7.73	0.60	7.76
8H	132	301	120	0.42	7.66	0.50	7.69
9H	182	306	120	0.51	7.59	0.48	7.62

F-3 Semi-detached house model, wind flow from 90°

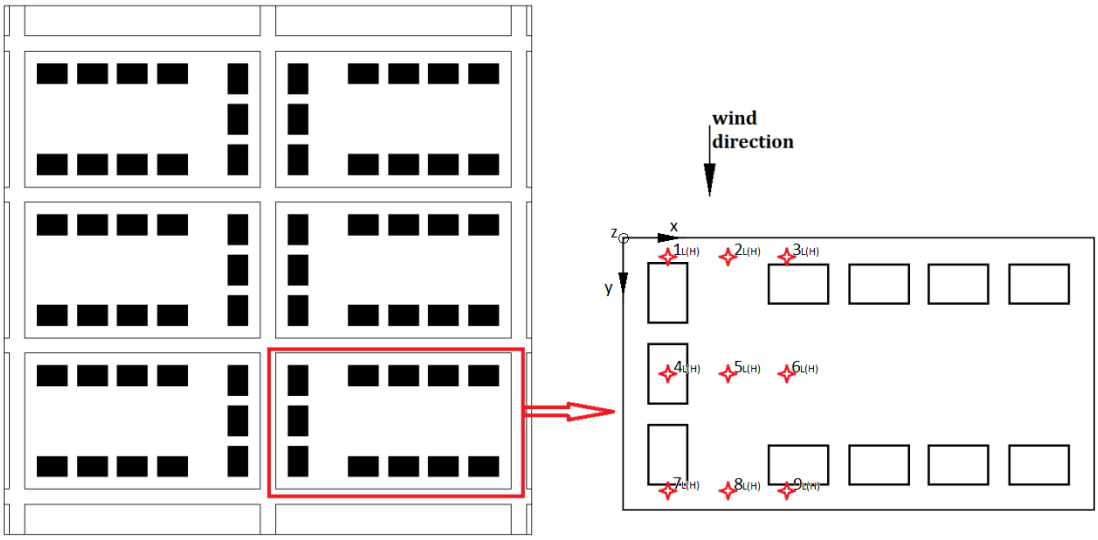

mark	coordinate, mm			velocity, m/s			
	x	*y*	*z*	$\bar{u}_x$	$\bar{u}_y$	$\bar{u}_z$	$\bar{u}$
1L	36	96	40	0.04	5.25	0.05	5.25
2L	86	96	40	0.18	5.38	0.15	5.38
3L	136	96	40	0.15	5.12	0.25	5.13
4L	36	196	40	0.15	5.48	0.23	5.48
5L	86	196	40	0.28	5.42	0.14	5.43
6L	136	196	40	0.32	5.37	0.37	5.40
7L	36	296	40	0.13	5.93	0.32	5.94
8L	86	296	40	0.20	5.89	0.35	5.90
9L	136	296	40	0.04	5.73	0.32	5.74
1H	36	96	120	0.27	7.38	0.36	7.40
2H	86	96	120	0.36	7.56	0.46	7.56
3H	136	96	120	0.40	7.42	0.45	7.45
4H	36	196	120	0.36	7.52	0.31	7.58
5H	86	196	120	0.45	7.60	0.35	7.60
6H	136	196	120	0.44	7.43	0.38	7.52
7H	36	296	120	0.32	7.63	0.41	7.60
8H	86	296	120	0.35	7.58	0.47	7.66
9H	136	296	120	0.36	7.53	0.48	7.66

F-4 terrace house model, wind flow from 0°

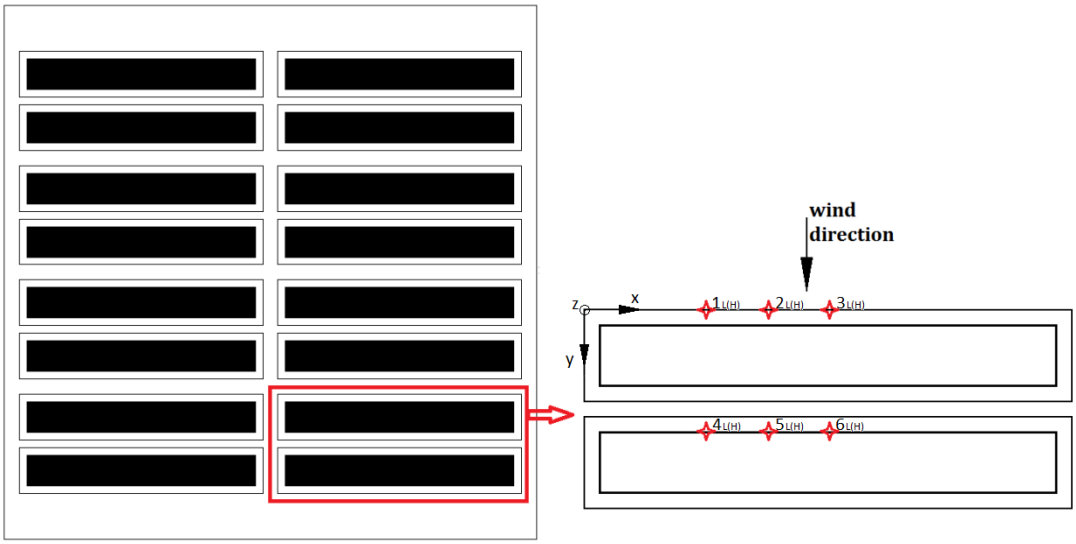

mark	coordinate, mm			velocity, m/s			
	x	*y*	*z*	$\bar{u}_x$	$\bar{u}_y$	$\bar{u}_z$	$\bar{u}$
1L	72	0	40	0.81	4.98	1.20	5.19
2L	122	0	40	1.07	4.71	0.95	4.92
3L	172	0	40	0.87	4.56	0.93	4.73
4L	72	100	40	0.91	5.51	1.21	5.71
5L	122	100	40	0.80	4.73	0.84	4.87
6L	172	100	40	1.22	5.02	0.94	5.25
1H	72	0	120	1.20	6.58	1.77	6.92
2H	122	0	120	1.13	6.88	1.91	7.23
3H	172	0	120	1.25	7.17	1.72	7.48
4H	72	100	120	1.25	6.97	1.67	7.28
5H	122	100	120	1.26	6.77	1.57	7.06
6H	172	100	120	1.16	6.95	1.54	7.21

F-5 terrace house model, wind flow from 5°

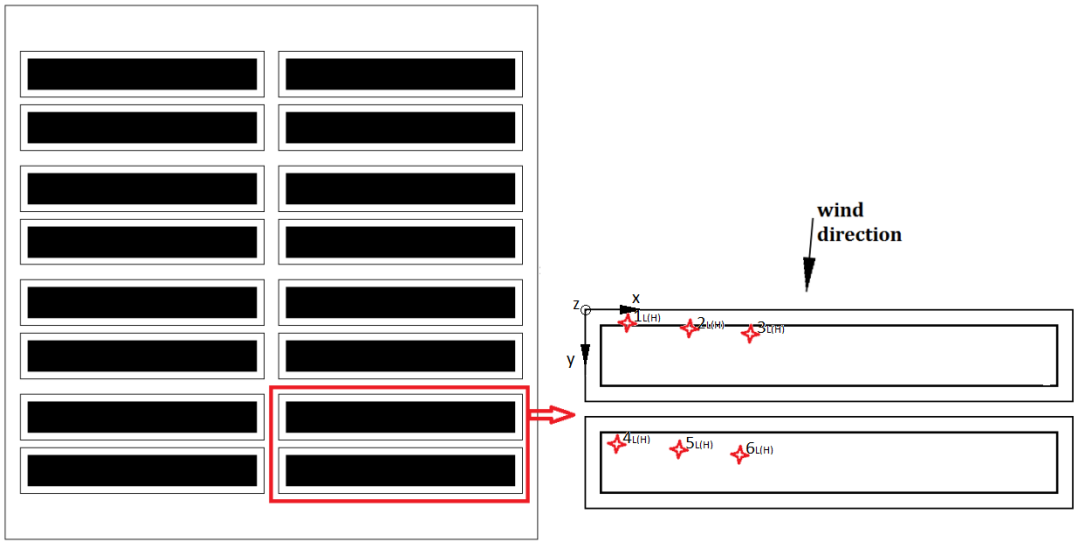

mark	coordinate, mm			velocity, m/s			
	x	*y*	*z*	$\bar{u}_x$	$\bar{u}_y$	$\bar{u}_z$	$\bar{u}$
1L	41	6	40	1.22	4.63	0.99	4.89
2L	91	10	40	0.80	4.66	0.89	4.82
3L	141	15	40	1.02	4.49	0.96	4.71
4L	32	106	40	0.92	5.33	1.06	5.51
5L	82	110	40	1.04	4.54	0.83	4.74
6L	132	115	40	0.93	4.58	0.89	4.76
1H	41	6	120	1.43	7.01	1.59	7.33
2H	91	10	120	1.30	7.30	1.71	7.61
3H	141	15	120	1.19	6.74	1.38	6.98
4H	32	106	120	1.37	7.34	1.52	7.62
5H	82	110	120	1.47	7.50	1.62	7.82
6H	132	115	120	1.24	7.18	1.32	7.40

F-6 terrace house model, wind flow from 85°

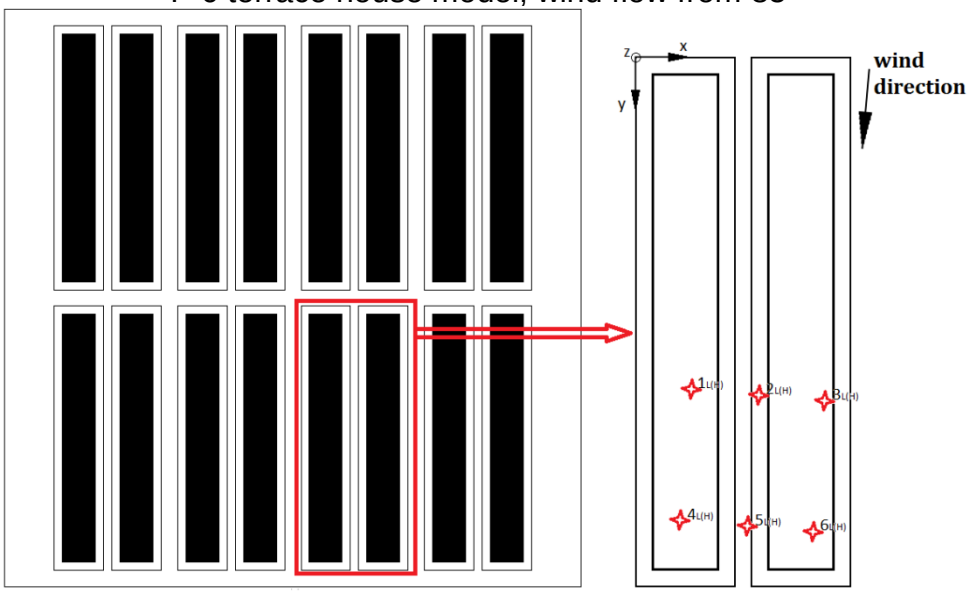

mark	coordinate, mm			velocity, m/s			
	x	*y*	*z*	$\bar{u}_x$	$\bar{u}_y$	$\bar{u}_z$	$\bar{u}$
1L	40	192	40	0.37	5.70	0.56	5.74
2L	90	196	40	0.59	6.10	0.61	6.16
3L	140	201	40	0.39	6.13	0.38	6.15
4L	32	292	40	0.32	6.12	0.49	6.15
5L	82	296	40	0.22	6.26	0.39	6.27
6L	132	301	40	0.34	6.11	0.44	6.13
1H	40	192	120	0.50	7.23	0.82	7.30
2H	90	196	120	0.51	7.49	0.79	7.55
3H	140	201	120	0.47	7.33	0.67	7.38
4H	32	292	120	0.40	7.62	0.83	7.67
5H	82	296	120	0.44	7.61	0.58	7.64
6H	132	301	120	0.44	7.25	0.64	7.29

F-7 terrace house model, wind flow from 90°

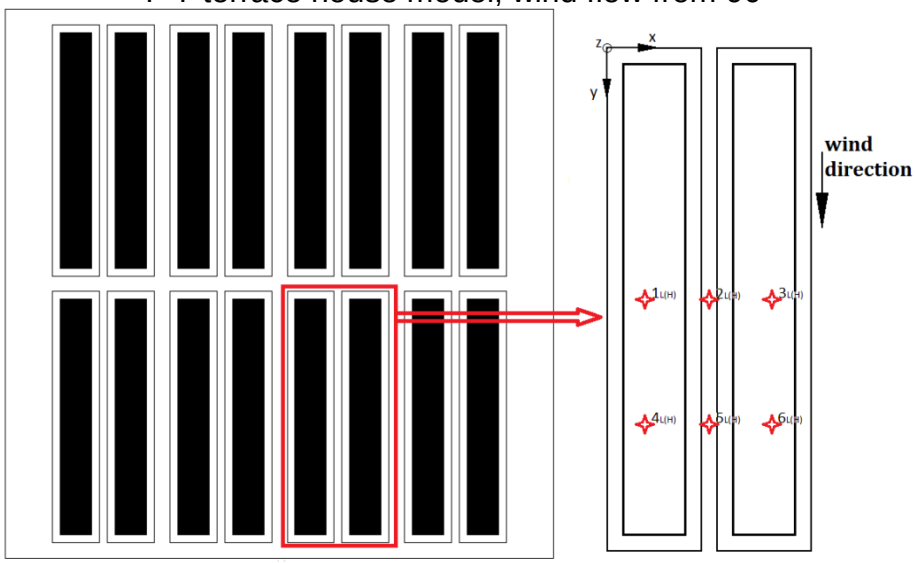

mark	coordinate, mm			velocity, m/s			
	x	*y*	*z*	$\bar{u}_x$	$\bar{u}_y$	$\bar{u}_z$	$\bar{u}$
1L	28	172	40	1.15	5.64	1.26	5.89
2L	78	172	40	0.83	5.22	1.17	5.42
3L	128	172	40	1.05	5.73	1.28	5.96
4L	28	272	40	0.92	5.62	1.20	5.82
5L	78	272	40	1.16	5.53	1.19	5.78
6L	128	272	40	1.02	5.73	1.08	5.92
1H	28	172	120	1.02	6.67	1.53	6.92
2H	78	172	120	1.13	6.80	1.70	7.10
3H	128	172	120	1.22	6.90	1.36	7.13
4H	28	272	120	1.28	7.10	1.60	7.39
5H	78	272	120	1.31	7.04	1.51	7.32
6H	128	272	120	1.11	7.21	1.72	7.49

Appendix G

Expectant payback time of turbines around building groups in U.K. cities

G- 1 expectant payback time of turbines used around houses; London

Semi-detached house groups					
Turbine name	**Require amount**	**Total AEP (kWh)**	**AEP per turbine (kWh)**	**Economic payback time (year)**	**Carbon payback time (year)**
Turby	46	108,612	2,361	8.7	1.6
Kestrel 1000	22	57,087	2,595	6.7	1.5
Whisper 200	22	52,914	2,405	3.1	1.6
Samrey Merline	23	96,609	4,200	4.2	0.9
Proven WT2500	20	106,703	5,335	6.9	0.7
Westwind 3kW	23	88,434	3,845	5.3	1.0
Skystream 3.7	21	108,353	5,160	5.1	0.7
Quiet Revolution	12	66,003	5,500	11.0	0.7
Whisper 500	16	112,364	7,023	2.6	0.5
Westwind 5.5kW	12	102,998	8,583	3.7	0.4
Proven 6kW	11	115,658	10,514	5.3	0.4
Scirocco 6kW	9	109,550	12,172	6.1	0.3
Westwind 10kW	8	108,398	13,550	3.9	0.3
Aerostar 6	7	78,530	11,219	2.5	0.3
Most Suitable Turbine: Whisper 500; Westwind 10kW					

Terrace house groups					
Turbine name	**Require amount**	**Total AEP (kWh)**	**AEP per turbine (kWh)**	**Economic payback time (year)**	**Carbon payback time (year)**
Turby	53	119,183	2,249	8.3	1.7
Kestrel 1000	23	57,700	2,509	6.5	1.5
Whisper 200	23	51,202	2,226	2.8	1.7
Samrey Merline	16	65,194	4,075	4.0	0.9
Proven WT2500	16	82,390	5,149	6.7	0.7
Westwind 3kW	16	59,677	3,730	5.1	1.0
Skystream 3.7	16	79,812	4,988	5.0	0.8
Quiet Revolution	9	48,024	5,336	10.6	0.7
Whisper 500	13	88,368	6,798	2.5	0.6
Westwind 5.5kW	9	74,941	8,327	3.6	0.5
Proven 6kW	9	91,852	10,206	5.2	0.4
Scirocco 6kW	9	105,606	11,734	5.9	0.3
Westwind 10kW	9	117,754	13,084	3.7	0.3
Aerostar 6	9	97,745	10,861	2.4	0.3
Most Suitable Turbine: none					

G- 2 expectant payback time of turbines used around houses; Bristol

Semi-detached house groups					
Turbine name	**Require amount**	**Total AEP (kWh)**	**AEP per turbine (kWh)**	**Economic payback time (year)**	**Carbon payback time (year)**
Turby	27	107,257	3,972	14.6	1.0
Kestrel 1000	22	83,765	3,808	9.9	1.0
Whisper 200	22	79,679	3,622	4.6	1.0
Samrey Merline	16	108,456	6,779	6.7	0.6
Proven WT2500	13	109,640	8,434	10.9	0.4
Westwind 3kW	17	111,453	6,556	9.0	0.6
Skystream 3.7	13	106,989	8,230	8.2	0.5
Quiet Revolution	11	112,576	10,234	20.4	0.4
Whisper 500	10	108,573	10,857	4.0	0.3
Westwind 5.5kW	8	112,387	14,048	6.1	0.3
Proven 6kW	6	106,668	17,778	9.0	0.2
Scirocco 6kW	6	117,128	19,521	9.8	0.2
Westwind 10kW	5	115,995	23,199	6.6	0.2
Aerostar 6	6	116,968	19,495	4.3	0.2
Most Suitable Turbine: Whisper 500; Aerostar 6					

Terrace house groups					
Turbine name	**Require amount**	**Total AEP (kWh)**	**AEP per turbine (kWh)**	**Economic payback time (year)**	**Carbon payback time (year)**
Turby	51	193,660	3,797	14.0	1.0
Kestrel 1000	23	85,108	3,700	9.6	1.0
Whisper 200	23	77,498	3,369	4.3	1.1
Samrey Merline	16	105,390	6,587	6.5	0.6
Proven WT2500	16	130,527	8,158	10.5	0.5
Westwind 3kW	16	101,713	6,357	8.7	0.6
Skystream 3.7	16	126,991	7,937	7.9	0.5
Quiet Revolution	9	89,599	9,955	19.8	0.4
Whisper 500	13	136,128	10,471	3.9	0.4
Westwind 5.5kW	9	122,474	13,608	5.9	0.3
Proven 6kW	9	153,227	17,025	8.6	0.2
Scirocco 6kW	9	169,693	18,855	9.5	0.2
Westwind 10kW	9	201,427	22,381	6.4	0.2
Aerostar 6	9	170,630	18,959	4.2	0.2
Most Suitable Turbine: Westwind 10kW					

G- 3 expectant payback time of turbines used around houses; Birmingham

Semi-detached house groups					
Turbine name	**Require amount**	**Total AEP (kWh)**	**AEP per turbine (kWh)**	**Economic payback time (year)**	**Carbon payback time (year)**
Turby	34	109,440	3,219	11.8	1.2
Kestrel 1000	22	70,742	3,216	8.4	1.2
Whisper 200	22	66,600	3,027	3.8	1.3
Samrey Merline	20	111,274	5,564	5.5	0.7
Proven WT2500	16	111,552	6,972	9.0	0.5
Westwind 3kW	21	110,759	5,274	7.2	0.7
Skystream 3.7	16	108,400	6,775	6.8	0.6
Quiet Revolution	14	95,988	6,856	13.7	0.6
Whisper 500	12	108,371	9,031	3.3	0.4
Westwind 5.5kW	10	114,471	11,447	5.0	0.3
Proven 6kW	8	113,886	14,236	7.2	0.3
Scirocco 6kW	7	111,764	15,966	8.0	0.2
Westwind 10kW	6	111,060	18,510	5.3	0.2
Aerostar 6	7	108,553	15,508	3.4	0.2
Most Suitable Turbine: Whisper 500; Aerostar 6					

-

Terrace house groups					
Turbine name	**Require amount**	**Total AEP (kWh)**	**AEP per turbine (kWh)**	**Economic payback time (year)**	**Carbon payback time (year)**
Turby	53	161,763	3,052	11.2	1.2
Kestrel 1000	23	71,681	3,117	8.1	1.2
Whisper 200	23	64,603	2,809	3.6	1.4
Samrey Merline	16	85,952	5,372	5.3	0.7
Proven WT2500	16	107,097	6,694	8.7	0.6
Westwind 3kW	16	81,592	5,100	7.0	0.7
Skystream 3.7	16	104,078	6,505	6.5	0.6
Quiet Revolution	9	69,984	7,776	15.5	0.5
Whisper 500	13	112,832	8,679	3.2	0.4
Westwind 5.5kW	9	99,559	11,062	4.8	0.3
Proven 6kW	9	123,660	13,740	7.0	0.3
Scirocco 6kW	9	138,680	15,409	7.7	0.2
Westwind 10kW	9	161,398	17,933	5.1	0.2
Aerostar 6	9	135,662	15,074	3.3	0.3
Most Suitable Turbine: none					

G- 4 expectant payback time of turbines used around houses; Manchester

Semi-detached house groups					
Turbine name	**Require amount**	**Total AEP (kWh)**	**AEP per turbine (kWh)**	**Economic payback time (year)**	**Carbon payback time (year)**
Turby	35	108,529	3,101	11.4	1.2
Kestrel 1000	22	68,471	3,112	8.1	1.2
Whisper 200	22	64,506	2,932	3.7	1.3
Samrey Merline	20	107,443	5,372	5.3	0.7
Proven WT2500	16	107,699	6,731	8.7	0.6
Westwind 3kW	21	106,666	5,079	7.0	0.7
Skystream 3.7	17	111,021	6,531	6.5	0.6
Quiet Revolution	12	92,210	7,684	15.3	0.5
Whisper 500	13	113,098	8,700	3.2	0.4
Westwind 5.5kW	10	110,307	11,031	4.8	0.3
Proven 6kW	8	109,923	13,740	7.0	0.3
Scirocco 6kW	7	108,443	15,492	7.8	0.2
Westwind 10kW	6	107,894	17,982	5.1	0.2
Aerostar 6	7	104,920	14,989	3.3	0.3
Most Suitable Turbine: Whisper 500; Westwind 10kW					

Terrace house groups					
Turbine name	**Require amount**	**Total AEP (kWh)**	**AEP per turbine (kWh)**	**Economic payback time (year)**	**Carbon payback time (year)**
Turby	53	155,334	2,931	10.8	1.3
Kestrel 1000	23	69,091	3,004	7.8	1.3
Whisper 200	23	62,321	2,710	3.4	1.4
Samrey Merline	16	82,863	5,179	5.1	0.7
Proven WT2500	16	103,260	6,454	8.3	0.6
Westwind 3kW	16	78,470	4,904	6.7	0.8
Skystream 3.7	16	100,321	6,270	6.2	0.6
Quiet Revolution	9	66,973	7,441	14.8	0.5
Whisper 500	13	108,805	8,370	3.1	0.5
Westwind 5.5kW	9	95,671	10,630	4.6	0.4
Proven 6kW	9	118,750	13,194	6.7	0.3
Scirocco 6kW	9	133,429	14,825	7.4	0.3
Westwind 10kW	9	154,976	17,220	4.9	0.2
Aerostar 6	9	130,437	14,493	3.2	0.3
Most Suitable Turbine: none					

G- 5 expectant payback time of turbines used around houses; Leeds

Semi-detached house groups					
Turbine name	**Require amount**	**Total AEP (kWh)**	**AEP per turbine (kWh)**	**Economic payback time (year)**	**Carbon payback time (year)**
Turby	35	108,244	3,093	11.4	1.2
Kestrel 1000	22	68,696	3,123	8.1	1.2
Whisper 200	22	64,528	2,933	3.7	1.3
Samrey Merline	20	107,023	5,351	5.3	0.7
Proven WT2500	16	107,399	6,712	8.7	0.6
Westwind 3kW	22	110,985	5,045	6.9	0.8
Skystream 3.7	17	110,739	6,514	6.5	0.6
Quiet Revolution	12	91,506	7,626	15.2	0.5
Whisper 500	13	113,033	8,695	3.2	0.4
Westwind 5.5kW	10	110,033	11,003	4.8	0.3
Proven 6kW	8	109,555	13,694	6.9	0.3
Scirocco 6kW	7	108,166	15,452	7.8	0.2
Westwind 10kW	6	107,357	17,893	5.1	0.2
Aerostar 6	7	104,054	14,865	3.3	0.3
Most Suitable Turbine: Whisper 500; Westwind 10kW					

Terrace house groups					
Turbine name	**Require amount**	**Total AEP (kWh)**	**AEP per turbine (kWh)**	**Economic payback time (year)**	**Carbon payback time (year)**
Turby	53	154,934	2,923	10.7	1.3
Kestrel 1000	23	69,318	3,014	7.8	1.3
Whisper 200	23	62,342	2,711	3.4	1.4
Samrey Merline	16	82,539	5,159	5.1	0.7
Proven WT2500	16	102,972	6,436	8.3	0.6
Westwind 3kW	16	78,050	4,878	6.7	0.8
Skystream 3.7	16	100,067	6,254	6.2	0.6
Quiet Revolution	9	66,462	7,385	14.7	0.5
Whisper 500	13	108,742	8,365	3.1	0.5
Westwind 5.5kW	9	95,432	10,604	4.6	0.4
Proven 6kW	9	118,352	13,150	6.7	0.3
Scirocco 6kW	9	133,088	14,788	7.4	0.3
Westwind 10kW	9	154,205	17,134	4.9	0.2
Aerostar 6	9	129,361	14,373	3.2	0.3
Most Suitable Turbine: none					

G- 6 expectant payback time of turbines used around houses; Edinburgh

Semi-detached house groups					
Turbine name	**Require amount**	**Total AEP (kWh)**	**AEP per turbine (kWh)**	**Economic payback time (year)**	**Carbon payback time (year)**
Turby	29	107,006	3,690	13.6	1.0
Kestrel 1000	22	72,415	3,292	8.6	1.2
Whisper 200	22	74,956	3,407	4.3	1.1
Samrey Merline	16	108,807	6,800	6.7	0.6
Proven WT2500	13	110,610	8,508	11.0	0.4
Westwind 3kW	17	111,411	6,554	9.0	0.6
Skystream 3.7	13	107,155	8,243	8.2	0.5
Quiet Revolution	11	111,574	10,143	20.2	0.4
Whisper 500	11	113,539	10,322	3.8	0.4
Westwind 5.5kW	8	107,646	13,456	5.8	0.3
Proven 6kW	7	121,391	17,342	8.8	0.2
Scirocco 6kW	6	114,894	19,149	9.6	0.2
Westwind 10kW	5	114,038	22,808	6.5	0.2
Aerostar 6	6	126,289	21,048	4.6	0.2
Most Suitable Turbine: Whisper 500; Aerostar 6					

Terrace house groups					
Turbine name	**Require amount**	**Total AEP (kWh)**	**AEP per turbine (kWh)**	**Economic payback time (year)**	**Carbon payback time (year)**
Turby	53	184,054	3,473	12.8	1.1
Kestrel 1000	23	73,082	3,177	8.3	1.2
Whisper 200	23	72,424	3,149	4.0	1.2
Samrey Merline	16	104,047	6,503	6.4	0.6
Proven WT2500	16	129,502	8,094	10.5	0.5
Westwind 3kW	16	100,475	6,280	8.6	0.6
Skystream 3.7	16	125,452	7,841	7.8	0.5
Quiet Revolution	9	88,075	9,786	19.5	0.4
Whisper 500	13	128,242	9,865	3.6	0.4
Westwind 5.5kW	9	115,828	12,870	5.6	0.3
Proven 6kW	9	149,365	16,596	8.4	0.2
Scirocco 6kW	9	164,842	18,316	9.2	0.2
Westwind 10kW	9	196,222	21,802	6.2	0.2
Aerostar 6	9	182,496	20,277	4.5	0.2
Most Suitable Turbine: Westwind 10kW					

G- 7 expectant payback time of turbines used around houses; Glasgow

Semi-detached house groups					
Turbine name	**Require amount**	**Total AEP (kWh)**	**AEP per turbine (kWh)**	**Economic payback time (year)**	**Carbon payback time (year)**
Turby	32	107,978	3,374	12.4	1.1
Kestrel 1000	22	69,540	3,161	8.2	1.2
Whisper 200	22	68,587	3,118	4.0	1.2
Samrey Merline	18	107,948	5,997	5.9	0.6
Proven WT2500	15	111,970	7,465	9.6	0.5
Westwind 3kW	19	109,299	5,753	7.9	0.7
Skystream 3.7	15	108,385	7,226	7.2	0.5
Quiet Revolution	12	106,289	8,857	17.7	0.4
Whisper 500	12	112,093	9,341	3.4	0.4
Westwind 5.5kW	9	108,741	12,082	5.2	0.3
Proven 6kW	7	107,396	15,342	7.8	0.2
Scirocco 6kW	7	119,388	17,055	8.6	0.2
Westwind 10kW	6	121,147	20,191	5.7	0.2
Aerostar 6	6	106,559	17,760	3.9	0.2
Most Suitable Turbine: Whisper 500; Aerostar 6					

Terrace house groups					
Turbine name	**Require amount**	**Total AEP (kWh)**	**AEP per turbine (kWh)**	**Economic payback time (year)**	**Carbon payback time (year)**
Turby	53	169,644	3,201	11.8	1.2
Kestrel 1000	23	70,563	3,068	8.0	1.2
Whisper 200	23	66,624	2,897	3.7	1.3
Samrey Merline	16	92,799	5,800	5.7	0.7
Proven WT2500	16	115,032	7,189	9.3	0.5
Westwind 3kW	16	89,145	5,572	7.6	0.7
Skystream 3.7	16	111,349	6,959	6.9	0.5
Quiet Revolution	9	77,694	8,633	17.2	0.4
Whisper 500	13	117,368	9,028	3.3	0.4
Westwind 5.5kW	9	105,263	11,696	5.1	0.3
Proven 6kW	9	132,951	14,772	7.5	0.3
Scirocco 6kW	9	147,796	16,422	8.2	0.2
Westwind 10kW	9	175,170	19,463	5.5	0.2
Aerostar 6	9	155,006	17,223	3.8	0.2
Most Suitable Turbine: none					

References

[1]. ML Schwartz; *Encyclopedia of coastal science*; pp.494-502; Springer; 2005; ISBN: 1402019033

[2]. HM Treasury; *Investing in Britain's potential: Building our long-term future*; chapter 7; pp. 168; TSO; 2006; ISBN: 0101698429

[3]. HM Treasury; *Building Britain's long-term future: Prosperity and fairness for families*; chapter 7; pp. 183; TSO; 2007; ISBN: 9780102944556

[4]. P.Torcellini, S.Pless, M.Deru; *Zero Energy Buildings: A Critical Look at the Definition*; National Energy Renewable Laboratory (NREL); USA; 2006

[5]. *Met Office: English Climate*. Met Office; U.K.; 2007.

[6]. HM Government; *Climate Change: The U.K. Programme 2006*; TSO; U.K.; 2006; ISBN: 9780215030726

[7]. Godfrey Boyle; *Renewable Energy*; 2nd Edn; Oxford: Oxford University Press; 2004; ISBN: 0199261784

[8]. T.I, E.L.Petersen; *European Wind Atlas*; Riso National Laboratory; Roskilde; Denmark; 1989; ISBN: 8755014828

[9]. I.MacLeay, K.Harris, A.Annut; *Digest of United Kingdom Energy Statistics 2011*; BERR; 2011; U.K.; ISBN: 9780115155277

[10]. M.Miller; *Using Google Maps and Google Earth*; Pearson Education, 2011; ISBN: 0132174766, 9780132174763

[11]. I.Hardill, D.T.Graham, E.Kofman; *Human Geography of the U.K.: An Introduction*; pp.201-203; Routledge; 2001; ISBN:0415214262, 9780415214261

[12]. SALFORD CITY COUNCIL SPD : House Extensions, SALFORD CITY COUNVIL

[13]. Cabinet office; *Helping to Shape Tomorrow: The 2011 Census of Population and Housing in England and Wales*; The Stationery Office, 2008; ISBN: 010175132X, 9780101751322

[14]. R.Chandler; *Building Type Basics for Housing*; pp.18, 89-94; John Wiley & Sons, INC. 2004; ISBN: 0471319309

[15]. B.C.Cochran, R.R.Damiani; *Harvesting Wind Power from Tall Building*;2008

[16]. N.Lazarus;.*Beddington Zero (Fossil) Development: Toolkit of Carbon Neutral Developments – Part II*; BioRegional; 2003

[17]. *Census 2011*; Office of National Statistics; 2011

[18]. *Fact Files: London Government Offices for the English Regions*; Government Office for London; U.K.; 2008.

[19]. T.R.Oke; *The energetic basis of the urban heat island*; Vol.108, Issue 455, pp. 1-24; Quarterly Journal of the Royal Meteorological Society; 1982

[20]. Southwest Windpower Renewable wind energy for homes and businesses: Skystream 3.7, Air Breeze, and Whisper wind turbines; http://www.windenergy.com/index_wind.htm; (accessed April 15, 2012)

[21]. J.F.Manwell, J.G.McGowan, A.L.Rogers; *Wind Energy Explained: Theory, Design and Application*; John Wiley & Sons, 2010; ISBN: 0470015004, 9780470015001
[22]. Proven Energy Wind Turbine Energy – small wind turbines; http://www.provenenergy.co.U.K./; (accessed April 15, 2012)
[23]. Westwind Wind turbines – Wind turbine Manufacturer Ireland; http://www.westwindturbines.co.U.K./index.asp; (accessed April 15, 2012)
[24]. Turby; http://www.turby.nl/; (accessed April 15, 2012)
[25]. Kestrel Small Wind Turbines for Remewable Energy. http://www.kestrelwind.co.za/; (accessed April 15, 2012)
[26]. Home – Samrey Wind Turbines; http://www.samrey.co.U.K./; (accessed April 15, 2012)
[27]. Quiet revolution; http://www.quietrevolution.co.U.K./; (accessed April 15, 2012)
[28]. Eoltec Wind Turbines; http://www.eoltec.com/; (accessed April 15, 2012)
[29]. Aerostar Wind Turbines; http://www.aerostarwind.com/; (accessed April 15, 2012)
[30]. BWEA: Delivering U.K. wind, wave and tidal energy; http://www.bwea.com/; (accessed April 15, 2012)
[31]. I.Paraschivoiu; *Wind Turbine Design: With Emphasis on Darrieus Concept*; Polytechnic international press; 2002; ISBN: 2553009313, 9782553009310.
[32]. S.Mertens; *Wind Energy in Built Environment*; Multi-science; U.K.; 2006; ISBN 0906522358.
[33]. G.K.Batchelor; *An Introduction to Fluid Dynamics*; Cambridge University Press; 2000; ISBN:0521663962
[34]. J.Happel, H.Brenner; *Low Reynolds Number Hydrodynamics: with Special Applications to Particulate Media*; Springer; 1965; ISBN: 9024728770.
[35]. Stationery Office; *Environmental Protection Act 1990 (c.43)*; 1990; ISBN: 0105443905, 9780105443902.
[36]. B.Turton., D.Sharper., N.Jenkins, E.Bossanyi; *Wind Energy Handbook*; John Wiley & Sons Ltd; 2001; ISBN: 0471489972, 978047489979.
[37]. Ellis; *CUR rapport, Dynamisch gedrag van hoge gebouwen,rapport 97-5*; 1997.
[38]. B.C.Cochran, R.R.Damiani. *Harvesting Wind Power from Tall Building*; CPP Wind Engineering; USA; 2008.
[39]. N.J.Cook *The Deaves and Harris ABL model applied to heterogeneous terrain*; Volume 66, Issue 3, March 1997, pp.197-214; Elsevier; 1997; ISBN: 01676105.
[40]. ESDU 82026; *Strong wind in the Atmospheric Boundary Layer*; ESDU international; 1993; ISBN: 9780856794070.
[41]. WAsP home page, DTU Wind Energy, http://www.wasp.dk/, (accessed September 20, 2012)
[42]. N.J.Cooks, *The designer's guide to wind loading of building structures*; Butterworths; 1985; ISBN: 0408008709, 9780408008709.
[43]. M.D.Perera, *Shelter behind two-dimensional solid and porous fences*, And Industrial Aerodyn. 8, pp.93-104; J. Wind engine. ; 1981.

[44]. P.A.Taylor, and H.W. Teunissen, *the Askervein Hill Project: Overview and background data*; 26, pp.169-189; Boundary-layer Meteorol; 1987.

[45]. W.Weibull; *A statistical distribution function of wide applicability*. 18, pp.293-297; J.Appl.Mesh; 1951.

[46]. M.B. Abbott, D.R.Basco; *Computational Fluid Dynamics – An Introduction for Engineers*; Longman Scientific & Technical; Harlow; England; 1989

[47]. *Households: by type of dwelling, 2000/01*: Regional Trends 37, Office for National Statistics; Northern Ireland Statistics and Research Agency; ONS/GSS: RT37605; 2000/01.

[48]. T.Cebeci, J. Cousteix; *Modelling and computation of boundary-layer flows : laminar, turbulent and transitional boundary layers in incompressible and compressible flows*; Berlin : Springer, 2005; ISBN: 354024459X

[49]. . W.B.Nelson; *Applied Life Data Analysis*; John Wiley & Sons; 2003; ISBN: 0471644625, 9780471644620

[50]. Great Britain. Parliament. House of Lords. Select Committee on Economic Affairs; *The Economics of Renewable Energy: Evidence*; The Stationery Office; 2008; ISBN: 0104013753, 9780104013755

[51]. DCEE; *Energy Trends March 2011*; National Statistics; ISSN: 2040-6029; 2011.

[52]. L.W.B.Browen, R.A.Antonia & L.P.Chua, *Calibration of X-probes for turbulent flow measurements*, Experiments in Fluids 7, 201-208, 1989.

[53]. K.Dawson; *Road Traffic Law Handbook*; A&C Black; 2010; ISBN: 1847667198, 9781847667199.

[54]. B.Blocken, T.Stathopoulos, J.Carmeliet; *CFD simulation of the atmospheric boundary layer: wall function problems*; Elsevier; Atmospheric Environment 41 (2007) 238-252; 2007.

[55]. Fluent Inc., Fluent User Defined Function Manual. Fluent Inc., 2003.

[56]. P.J Richards, R.P Hoxey; *Appropriate boundary conditions for computational wind engineering models using the k-ε turbulence model*; Journal of Wind Engineering and Industrial Aerodynamics 46&47; 145-153; 1993.

[57]. T.R.Ote; *Boundary layer Climates*; Methuen Ltd.; pp372; 1978

[58]. F.Durst; *Fluid Mechanics: An Introduction to the Theory of Fluid Flows*; Springer; 2008; ISBN: 3540713425, 9783540713425

[59]. C.Tropea, A.L.Yarin, J.F.Foss; *Springer Handbook of Experimental Fluid Mechanics, Volume 1*; Springer; 2007; ISBN: 3540251413, 9783540251415

[60]. N.J.Cook, *Wind-tunnel simulation of the adiabatic atmospheric boundary layer by roughness, barrier and mixing-device methods*, Journal of Industrial Aerodynamics, 3 157-176, 1978.

[61]. N.J.Cook, *Simulation of an adiabatic urban boundary layer in a wind tunnel*, Atmospheric Environment Pergamon Press 1973. Vol. 7, 691-705., 1973.

[62]. S.M.Mohsen & C.L.John *The decay power law in grid-generated turbulence*, J. Fluid Mech. Vol. 219 195-214, Great Britain, 1990.

[63]. E.M.Laws & J.L.Livesey, *Flow through screens*, Annual reviews Fluid Mech. 1978.10 247-266, 1978.

[64]. J.E. Bardina, P.G.Huang, T.J.Coakley, *Turbulence Modeling*

Validation, Testing, and Development, NASA Technical Memorandum 110446, 1997

[65]. T.J.Barth & D.Jespersen. *The design and application of upwind schemes on unstructured meshes.* Technical Report AIAA-89-0366, AIAA 27th Aerospace Sciences Meeting, Reno, Nevada, 1989

[66]. R.B.Stull; *An Introduction to Boundary Layer Meteorology*; Kluwer Academic Publishers, Dordrecht, 2003

[67]. J. Counihan; *Adiabatic atmospheric boundary layers: a review and analysis of data from the period 1880-1972*; Atmos. Environ,; 9; pp.871-905; 1975

[68]. H.Kozmar; *Scale effects in wind tunnel modelling of an urban atmospheric boundary layer*; Theor. Appl. Climatol.100(1-2); pp.153-162; 2010

[69]. T. Stathopoulos, C.C.Baniotopoulos; *Wind effects on buildings and design of wind sensitive structures*; CISM courses and lectures, vol.493, pp.31-65, 2007, DOI: 10.1007/978-3-211-73076-8_2

[70]. *Characteristics of wind velocity in the lower layer of the atmosphere near the ground: strong winds (neutral atmosphere)*; ESDU, 1972

[71]. *Characteristics of atmospheric turbulence near the ground: Part II: single point data for strong winds (neutral atmosphere)*; ESDU, 1985

[72]. J,D.Holmes; *Wind loading of structures*, 2nd Ed. Routledge, Taylor & Francis; U.K.; 2007

[73]. E.Simiu & R.H.Scanlan; *Wind Effects on Structures*, 3rd Ed. John Wiley & Sons; New York; 1996

[74]. C.Dyrbye & S.O.Hansen; *Wind loads on structures*; John Wiley & Sons; New York; 1997

[75]. H.Sockel; *Aerodynamik der Bauwerke*; Vieweg &Sohn; Braunschweig; 1984

[76]. J.Counihan; *Adiabatic atmospheric boundary layers: a review and analysis of data from the period 1880-1972*; Atmos.Environ; pp.871-905; 1975

[77]. J.D.Holmes; *Wind loading of structures*, 2nd Ed.; Routledge, Taylor & Francis, U.K.; 2007

[78]. IEC 61400-2; *Design requirements for small wind turbines*; IEC 2006

[79]. IEC 61400-1; *Site Assessment*; IEC 2006

[80]. N.Cai, J.Z.Xu; *Aerodynamic - Aero acoustic Experiment and design optimization of Reynolds Number Effect*; Journal of Engineering Thermophysics; P.R.China; 2000; ISSN: 0253-231X

[81]. *Encraft: Final Report Warwick Wind Trial* (2009), http://www.warwickwindtrials.org.uk/resources/Warwick+Wind+Trials+Final+Report+.pdf, (accessed April 15, 2012)

[82]. W.Chen; *Handbook of Structural Engineering*; Boca Raton: CRC press; pp.12-50; 1997; ISBN: 0849326745.

[83]. H.L.Harter, A.H.Moore; *Maximum likelihood estimation of the parameters of Gamma and Weibull populations from complete and from censored samples*; Technometrics; vol. 7; 1965

[84]. M.A.Al-Fawzan; *Methods for Estimating the Parameters of the Weibull Distribution*; King Abdulaziz City for Science and Technology; 2000

[85]. S.Rafailidis; *Influence of Building Areal Density and Roof Shape on*

the Wind Characteristic Above a Town; Hamburg, Germany; 1997

[86]. G.Theodoridis, N.Moussiopoulos; *Influence of Building Density and Roof Shape on the Wind and Dispersion Characteristics in an Urban Area: A Numerical Study*; Laboratory of Heat Transfer and Environmental Engineering; Greece; 2000

[87]. T.Kubota, M.Miura, Y.Tominaga, A.Mochida; *Wind Tunnel Tests on the Relationship between Building Density and Pedestrian-level Wind Velocity: Development of Guidelines for Realizing Acceptable Wind Environment in Residential Neighbourhoods*; Building and Environment 43; pp.1699–1708; 2008

[88]. J.Kim, D.Kim; *Effects of a Building's Density on Flow in Urban Areas*; Advances in Atmospheric Sciences, vol. 26, pp.45-56; 2009

[89]. B.E.Launder, D.B.Spalding; *Lectures in Mathematical Models of Turbulence; Academic Press; London*; 1972

[90]. T.H.Shih, W.W.Liou, A.Shabbir, Z.Yang, and J.Zhu; *A New Eddy-Viscosity Model for High Reynolds Number Turbulent Flows - Model Development and Validation*; Computers Fluids, 24(3): pp.227-238; 1995

[91]. B.E.Launder & D.B.Spalding; *the Numerical Computation of Turbulent Flows;* Computer Methods in Applied Mechanics and Engineering, 3: pp.269-289; 1974

[92]. *Wind turbines. Power performance measurements of electricity producing wind turbines*; BS EN 61400-12-1:2006; 2006

[93]. J.F.Graham; *Wind Turbine System for Buildings*; US 2009/0167025 A1; 2007

[94]. B.C.Krippene; *Vertical multi-phased wind turbine system*; US 20120288357 A1; 2012